

Proton NMR Studies of Intact Cells

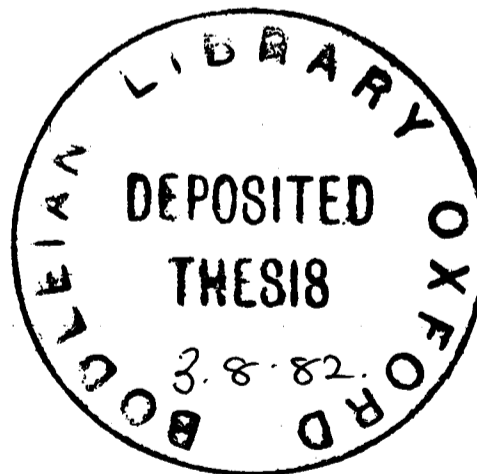
A thesis submitted in partial fulfilment
of the requirements for the degree
of Doctor of Philosophy.

by

Kevin M. Brindle

Wolfson College

Hilary 1982
Department of Biochemistry,
University of Oxford,
South Parks Road,
Oxford.



Abstract

The technique of ^1H spin echo n.m.r. has been used for the non-invasive study of enzyme catalysed $^1\text{H}/^2\text{H}$ equilibrium isotope exchange at the C-2 position of lactate in suspensions of human erythrocytes. The intracellular environment of the enzymes involved in this exchange has been investigated by comparing the exchange properties of the enzymes in the intact cell with the properties they display in vitro.

A study of the exchange of the lactate C-2 substituent with solvent, which is catalysed by a coupled system of four glycolytic enzymes, has been used to examine the kinetic properties of the individual enzymes in vitro. Measurements of the exchange in the intact cell have been used to investigate the in situ kinetic properties of one of these enzymes, glyceraldehydephosphate dehydrogenase. Contrary to the conclusions of previous studies with the isolated enzyme in vitro, these measurements have shown that the enzyme is not rate determining for glycolytic flux in the human erythrocyte and that it is unlikely that it is bound to the cell membrane in situ.

A study of $^1\text{H}/^2\text{H}$ exchange between the C-2 positions of methyl labelled lactate molecules, catalysed by lactate dehydrogenase, has been used to investigate the in situ kinetic properties of this enzyme. Comparison of these properties with those it displays in vitro indicate that the free intracellular NAD(H) concentration in the erythrocyte is only approximately 10% of the total extractable concentration. A considerable fraction of the coenzyme must be bound, therefore, in the intact cell. This type of experiment should be widely applicable to a variety of tissues and possibly to different dehydrogenases.

Theoretical aspects of bulk isotope exchange kinetics in

multi-enzyme systems are examined and the effects of chemical flux, and of isotope effects, on the measurement of isotopic flux are considered. The advantages of the n.m.r. method over conventional radioactive tracer techniques are described.

It is concluded that ^1H n.m.r. studies of $^1\text{H}/^2\text{H}$ isotope exchange may be used to obtain information about the kinetic properties of enzymes in intact cellular systems. The technique should be a useful complement, therefore, to the currently more widely used n.m.r. methods employing the ^{31}P and ^{13}C nuclei and to other methods used for the non-invasive study of metabolism.

Acknowledgements

I would like to thank my supervisor, Dr. Iain Campbell, for his help and advice over the past three years and for useful suggestions during the preparation of this thesis.

I would also like to thank Frank Brown, David Foxall and Bob Simpson for many valuable discussions during the course of the work described here. Thanks finally to Rod Porteous, Nick Soffe and Peter Styles for construction care and maintenance of the spectrometers.

I was supported by a Science Research Council postgraduate research studentship.

Abbreviations

- TIM - Triosephosphate isomerase.
GAPDH - Glyceraldehydphosphate dehydrogenase.
LDH - Lactate dehydrogenase.
ATPase - Adenosine triphosphatase
PFK - Phosphofruktokinase.
PGK - Phosphoglycerate kinase.
GAP - D-glyceraldehyde-3-phosphate.
DHAP - Dihydroxyacetone-phosphate.
FDP - D-fructose-1,6-diphosphate.
1,3-DPG - 1,3-diphosphoglycerate.
2,3-DPG - 2,3-diphosphoglycerate.

V - isotope exchange equilibrium velocity for the exchange of isotope between:

V_{C2X} - the C-2 position of lactate and solvent.

V_{ALD} - the pro-S C-3 position of DHAP and solvent.

$V_{ALD(RECON)}$ - the C-4 position of FDP and the aldehydic hydrogen of GAP.

V_{TIM} - the pro-S C-3 position of DHAP and the aldehydic hydrogen of GAP.

V_{GAPDH} - the aldehydic hydrogen of GAP and the 4B position of the nicotinamide ring of NADH.

V_{LDH} - the C-2 position of lactate and the 4A position of NADH

V_R - the reciprocal of the sum of the reciprocals of the equilibrium velocities of the non-varied enzymes in an equilibrium velocity determination (see page 54).

t_{null} - time at which peak inversion occurs during observation of C-2 exchange.

A_X - spectrophotometrically assayed activity of enzyme X.

Contents

	Page number
1	1
1.1	18
2	26
2.1	26
2.2	27
2.3	35
2.4	36
2.5	40
2.6	43
2.7	48
2.8	50
2.9	53
2.9.1	54
2.9.2	55
2.10	56
2.10.1	56
2.10.2	58
2.10.3	60
2.11	63
2.12	67
2.13	73

	Page number
2.14 Appendix 2 - Oxamate inhibition.	75
2.15 Appendix 3 - The effect of an isotope effect on an exchange time course.	77
2.16 Appendix 4 - Estimation of V_{C2X} in erythrocytes.	78
3 The properties of the C-2 exchange system <u>in vitro</u> .	84
3.1 Introduction.	84
3.2 Experimental.	85
3.3 The exchange system <u>in vitro</u> - a model for the system <u>in situ</u> ?	89
3.4 Isotope exchange measurements in the <u>in vitro</u> exchange system.	90
3.4.1 Data analysis.	90
3.4.2 Results.	94
3.5 Summary and conclusions.	97
3.6 References.	98
3.7 Appendix 1 - A computer program for calculating the specific equilibrium velocity of an enzyme.	101
3.8 Appendix 2 - Triosephosphate isomerase equilibrium velocity.	106
4 Development of a kinetic model to describe the properties of the C-2 exchange system in the erythrocyte.	108
4.1 Introduction.	108
4.2 Experimental.	108
4.3 Kinetic models to describe the effects of triose phosphate and FDP depletion on C-2 exchange.	109

	Page number	
4.4	A comprehensive kinetic model of the C-2 exchange system.	113
4.4.1	Derivation of the rate equations.	118
4.5	Uses of the kinetic model.	121
4.5.1	Validation of the double reciprocal relationship.	121
4.5.2	Simulation of the effects of chemical flux on isotopic flux.	123
4.5.3	Isotope leaks - the effect of side reactions on the exchange.	123
4.6	Summary and conclusions.	125
4.7	References.	126
4.8	Appendix 1 - A kinetic model to describe the effects of DHAP depletion on V_{C2X} .	127
4.9	Appendix 2 - Integration of polynomial and linear equations describing changes in V_{C2X} .	128
4.10	Appendix 3 - Computer programs for the numerical integration of the equations describing C-2 exchange.	131
5	A comparison of the kinetic properties expressed by glyceraldehydphosphate dehydrogenase in the intact erythrocyte and <u>in vitro</u> .	142
5.1	Introduction.	142
5.2	Experimental.	147
5.3	The method.	148
5.4	Determinations of the equilibrium velocity of glyceraldehydphosphate dehydrogenase <u>in situ</u> .	148
5.4.1	Effect of lactate production on estimates of V_{C2X} .	149

	Page number
5.4.2 Maintenance of a near equilibrium steady state during isotope exchange measurements.	151
5.4.3 Is the kinetic model an adequate description of the exchange system <u>in situ</u> ?	155
5.5 Apparent disequilibrium in the reaction catalysed by aldolase.	156
5.6 Conclusions.	159
5.7 Determinations of the equilibrium velocity of glyceraldehydphosphate dehydrogenase <u>in vitro</u> .	160
5.7.1 The effect of membrane binding.	162
5.8 Conclusions.	163
5.9 References.	171
6 A comparison of the kinetic properties expressed by lactate dehydrogenase in the intact erythrocyte and <u>in vitro</u> .	176
6.1 Introduction.	176
6.2 Experimental.	177
6.3 Measurement of the <u>in situ</u> equilibrium velocity of lactate dehydrogenase using oxamate inhibition.	180
6.4 Equilibration of isotope at the lactate C-2 position between methyl labelled lactate molecules - A direct method for obtaining the equilibrium velocity of lactate dehydrogenase.	182
6.4.1 Measurement of C-2 equilibration <u>in situ</u> and <u>in vitro</u> .	185
6.4.2 The concentrations of free NAD^+ plus NADH in the erythrocyte.	187

	Page number
6.4.3 The effect of pyruvate.	187
6.4.4 The effect of pH.	188
6.4.5 The effect of buffer composition.	190
6.4.6 The effect of enzyme concentration.	190
6.4.7 Isotope effects.	190
6.5 The total extractable NAD(H) concentration in the erythrocyte.	191
6.6 Conclusions.	192
6.7 References.	194
6.8 Appendix - Kinetic models for predicting the velocity of C-2 equilibration.	196
7 Some general comments on the application of ^1H n.m.r. to the study of isotope exchange and the kinetic properties expressed by enzymes in intact cells.	201
7.1 References.	205

1 General introduction

The basic concepts of metabolic regulation have evolved from a consideration of enzyme properties in vitro, in particular from studies of allosteric interactions with the metabolites and coenzymes of a metabolic pathway in which an enzyme is involved. The ultimate aim must be to relate the in vitro properties of the enzymes catalysing a metabolic pathway to a model which will predict the levels of, and changes in, the concentrations of metabolites observed in situ i.e. in the intact animal, cell or cellular organelle.

The kinetic properties of an enzyme may be regarded as an intrinsic function of its structure but their expression is determined by the pH, ionic strength, substrate and other effector concentrations in the enzyme's environment. If the kinetic properties of an enzyme determined in vitro are to have any relevance to its properties in situ then the conditions used in vitro should mimic those found in situ. This presupposes that the conditions in the latter case are known.

Two phenomena distinguish an enzyme's environment in situ from that in vitro: a) the living cell is in a metabolic steady state, an enzyme may be catalysing a reaction in the presence of both the reactants and products of the reaction. An enzyme is generally not saturated with substrate and may often be present at the same concentration as its substrates. In a conventional kinetic analysis in vitro, unidirectional flux across the enzyme is measured, usually at saturating concentrations of most of the substrates, in the absence of products (that is all the products together) and at enzyme concentrations much smaller than those of the substrates; b) the enzyme in situ is catalysing a reaction in a compartment. This compartment is

defined by a membrane and may be at the level of a cellular organelle, which localises the enzyme to a specific region(s) of a cell, or at the level of the cell itself which may localise an enzyme to a specific region of an organ (Sols & Marco, 1970). The transport properties and contents of the cell or organelle will dictate the in situ environment of the enzyme.

Another kind of compartmentation, which is a consequence of the high protein concentration found in situ, is that of "compartmentation by binding" (Sols & Marco, 1970). An enzyme or substrate may be localised to a specific region of a cell by virtue of binding to fixed structural proteins. In addition to possible localisation, binding may, in the case of an enzyme alter its catalytic properties and in the case of a substrate it will lower the concentration of the kinetically relevant free form (Masters, 1977). In skeletal muscle there is considerable evidence from histochemical and fluorescent antibody staining techniques that certain glycolytic enzymes are localised around the I bands of the myofibril (Ottaway & Mowbray, 1977). Sedimentation studies have shown that several of the glycolytic enzymes will bind to F actin (Arnold & Pette, 1970) and that the binding is enhanced by the presence of tropomyosin and troponin (Clarke & Masters, 1975). The enzymes show widely different affinities for the complex and modulation of affinity in the presence of different cellular metabolites (Clarke & Masters, 1975; Arnold & Pette, 1970). Binding of glyceraldehydephosphate dehydrogenase to a particulate fraction from chicken skeletal muscle has been shown to affect its kinetic properties (Dagher & Hultin, 1975). The binding of aldolase to F actin increases V_{max} and its K_m for FDP (Arnold & Pette, 1970). The changed kinetic properties of bound enzymes and modulation of binding by substrates have

led to suggestions that this may represent a new level of metabolic control which cannot be inferred from the kinetic properties of isolated enzymes in vitro (Masters, 1977). The human erythrocyte, which is the system studied here, is an attractive system to examine for this type of compartmentation since it has a simple, predominantly glycolytic, metabolism taking place in a single membrane bound compartment. The tight binding of the glycolytic enzymes; aldolase, glyceraldehydephosphate dehydrogenase (GAPDH) and phosphofructokinase, (PFK) to the cytoplasmic pole of the band 3 protein of the human erythrocyte membrane is well established (Kant & Steck, 1973; Strapazon & Steck, 1976; Strapazon & Steck, 1977; Yu & Steck, 1975; Higashi et al, 1979; Eby & Kirtley, 1979). Haemoglobin binding to this anion transporter, which is an integral membrane protein, has also been demonstrated (Salhany et al, 1980). The effect of substrate concentrations on binding, competition between the enzymes for binding and the effect of binding on catalytic activity have all been reported. There have been a number of reports on the binding of other glycolytic enzymes to the membrane of the human erythrocyte and to erythrocyte membranes from other species (Green et al, 1965; Wins & Schoffeniels, 1969; Tillmann et al, 1975; Duchon & Collier, 1971). Observation and degree of binding however appear to be dependent on the conditions of membrane isolation, in particular isolation in low ionic strength buffer. Indeed the well characterised binding of aldolase, GAPDH and PFK to band 3 protein is not observed at physiological ionic strengths (Strapazon & Steck, 1977; Yu & Steck, 1975; Higashi et al, 1979). This is also true of the binding of aldolase and other glycolytic enzymes to the particulate fraction from muscle and suggests that binding may be negligible in situ. However it has been shown that significant binding still occurs in muscle extracts at isotonic ionic strength provided that

the protein concentration is high (Clarke & Masters, 1974). This and the other muscle and erythrocyte studies mentioned above have examined membrane binding by separating the particulate and soluble fractions by centrifugation at 4°C. A discrepancy in the degree of salt elution of GAPDH from human erythrocyte membranes obtained by two different groups was attributed to different incubation times of the membrane preparations at 4°C (McDaniel et al, 1974). Failure to separate thermodynamic and kinetic effects and furthermore failure to truly simulate the in situ conditions (for example 37°C) may render many observed protein-protein interactions in vitro artefactual with regard to the true state in the intact cell. Using a much less drastic technique than cell disruption and fractionation, Kliman and Steck (Kliman & Steck, 1980) attempted to assess the extent of membrane binding of GAPDH by studying the kinetics of enzyme release from erythrocytes treated with the detergent saponin. Their results suggested that as much as 60% of the enzyme may be bound in the intact cell.

Direct associations of glycolytic enzymes in vitro have been reported although not always substantiated by subsequent investigations. In a ³¹P n.m.r. study very small shifts in the ³¹P resonances of 2,3-DPG were interpreted to indicate the existence of complexes involving the enzymes phosphoglycerate kinase, (PGK) glyceraldehydephosphate dehydrogenase and phosphoglycerate mutase. Shifts observed in spectra of human erythrocytes were thought to indicate enzyme complexation in situ (Fossel & Solomon, 1977). However a subsequent study showed that these shifts were within the noise level of the measurements and that the shifts observed in vitro are probably the result of small pH variations and not complex formation (Momsen et

al, 1979). Recently, however, Fossel and Solomon (1982) have replied to these criticisms by performing their experiments at higher magnetic field. The direct association of GAPDH and aldolase in vitro has been reported on the basis of physicochemical (Ovádi et al, 1978) and kinetic data (Ovádi & Keleti, 1978). In the latter case the K_m of GAPDH for GAP was found to be significantly lower in the presence of aldolase. A recent investigation however failed to detect any interaction (Masters & Winzor, 1981). An interaction proposed on theoretical grounds between PGK and GAPDH has not been observed experimentally (Vas & Batke, 1981).

The presence of enzyme concentrations similar to that of their substrates in situ ensures a high concentration of binding sites for intermediary metabolites (Sols & Marco, 1970; Ottaway & Mowbray, 1977; Masters, 1977)). For example in perfused liver it has been shown that most of the NADH is protein bound (Bücher, 1969). In rabbit skeletal muscle it has been estimated that the GAPDH concentration is 0.4mM and that there may be 0.5-1.0mM acylated active sites (Bloch et al, 1971). The concentrations of the enzymes substrates, GAP and 1,3-DPG, have been estimated at 80 and 50 μ M respectively. The acylated enzyme is thus a significant metabolic intermediate. In the human erythrocyte the GAPDH active site concentration is only about 12 μ M (Marshall & Omachi, 1974) yet this may represent a significant binding site for free NAD(H) (see chapter 6). A more subtle form of compartmentation is shown by the Mg^{2+} ion which binds to organic phosphates e.g. ATP. This is likely to have important consequences for metabolic control. For example in erythrocyte glycolysis; Mg^{2+} ATP is the substrate for both the control enzymes of this pathway i.e. hexokinase and PFK, while free ATP is an allosteric inhibitor of PFK and pyruvate kinase (Rapoport, 1974).

Consequently if free ATP were to increase at the expense of Mg^{2+} ATP, there would be inhibition of glycolysis. It has been suggested that inhibition of PFK at low pH may in part be due to a greater fraction of ATP present in the free form (Sols & Marco, 1970). For many kinases the Mg^{2+} bound form of the adenine nucleotide is an obligatory substrate and consequently the position of many kinase equilibria are dependent on the Mg^{2+} concentration (Veech et al, 1979).

The advantages of compartmentation of metabolites within enzyme complexes with regard to metabolic control and increased catalytic efficiency have been discussed (Ottaway & Mowbray, 1977; Masters, 1977; Rickey Welch, 1977). Despite demonstrations of enzyme binding to the erythrocyte membrane there is no firm evidence of a glycolytic complex although the following data has been used to suggest that enzyme complexes may exist. The apparent inaccessibility of DHAP and GAP to glycerol-3-phosphate dehydrogenase added to a concentrated hemolysate was thought to indicate possible compartmentation of these intermediates within an enzyme complex (Friedrich et al, 1977). It has been suggested that the ordered release of enzymes from erythrocytes suspended in hypotonic media reflects localisation of some enzymes near the membrane (Cseke et al, 1978). Studies of ^{14}C labelling of erythrocyte metabolites in the presence of $(1-^{14}C)$ glucose were interpreted as indicating compartmentation of the pentose phosphate pathway enzymes (Harvey & Kaneko, 1976). The difficulties involved in deducing compartmentation from tracer labelling studies have been discussed (Ottaway & Mowbray, 1977). The phosphorylation of adenosine at low adenosine concentrations and its deamination at high concentrations was interpreted as indicating compartmentation of adenosine kinase and adenosine deaminase activities. However this was subsequently shown to

be due simply to the kinetic properties of the enzymes (Fazio et al, 1980) and demonstrates that caution should be applied in attributing apparently anomalous kinetic behaviour of an enzyme in situ to compartmentation. Perhaps the best evidence for a glycolytic enzyme complex has come from studies of an enzyme complex isolated by differential centrifugation from E. Coli spheroplasts. Failure of an added intermediary glycolytic metabolite to dilute the flow of ^{14}C label through the glycolytic sequence catalysed by this complex was taken to indicate compartmentation of this particular intermediate within the complex (Mowbray & Moses, 1976). However a control experiment with the dissociated complex was not performed. To summarise, the high protein concentrations obtained in situ may result in; a) a free metabolite concentration much lower than the total concentration in the tissue and; b) protein-protein interactions which may localise an enzyme to specific regions of a cell or cellular organelle and which may modify the kinetic properties of the enzyme. In order to extrapolate the kinetic properties of an enzyme observed in vitro to the properties it expresses in situ, the free concentrations of its substrates and other effectors should be known as should the presence and effect of protein-protein interactions.

Inadequate knowledge of the in situ environments of enzymes makes it desirable to study the properties of the enzymes in the intact system. The methods available for the non-invasive study of enzymes in situ have recently been reviewed in an article by Sies (Sies, 1980). Fluorimetric and spectrophotometric methods have been employed at the level of the whole organ and the single cell to provide both spatial and temporal resolution of metabolic events. In the latter case electrophoretic microinjection into single cells has been used to induce

metabolic transients which have been followed by observing the fluorescence of NAD(P)H. Metabolic rates were evaluated topographically and heterogeneity was observed between nucleus and cytoplasm and within the cytoplasm itself (Kohen et al, 1979). Surface fluorescence from haemoglobin-free perfused liver has been used to study changes in NADH levels following anoxia and ethanol infusion (Bücher, 1969). From a correlation of these changes with the concentrations of lactate and pyruvate in the perfusate, with which the free NAD(H) concentration in the cytosol is in equilibrium, and with changes in the total extractable levels of these nucleotides it was deduced that over 90% of the NADH in the liver is bound. It was also concluded that the changes in NADH concentration observed occurred mainly in the cytosol. Surface fluorimetry has allowed observation of discrete regions of the liver's surface which display different metabolic behaviour (Ji et al, 1980). For a review of these optical techniques see Sies and Brauser (1980).

A comparison of an enzyme's substrate concentrations in situ with the equilibrium concentrations observed in vitro may be used to identify disequilibrium in the in situ reaction. This may be a true disequilibrium where the enzyme is rate limiting for flux or an apparent disequilibrium due to significant binding or compartmentation of the enzyme's substrates in situ. If an enzyme catalyses an equilibrium reaction of the form $A + B \rightleftharpoons C + D$ (i.e. its activity significantly exceeds the metabolic flux) then measurement of the concentrations of one reactant/product pair (e.g. A/C) may, if the equilibrium constant is known, give the ratio of the free concentrations of the other reactant/product pair (B/D) in situ. This forms the basis of the redox indicator metabolite method (Bücher & Sies, 1976). Applied non-invasively, this method involves the measurement of membrane

permeable oxidised and reduced substrates of a dehydrogenase in cell supernatants or organ perfusates. Knowledge of the dehydrogenase's equilibrium constant under the in situ conditions of pH and ionic strength permits calculation of the ratio of the free concentrations of NAD^+/NADH in the cellular compartment in which the dehydrogenase is located. In the example given above of the perfused liver, the concentrations of lactate and pyruvate, which freely and rapidly permeate the cell membrane, were used to calculate the free NAD^+/NADH ratio in the cytosol in which the enzyme lactate dehydrogenase is specifically located. The ratio of β -hydroxybutyrate to acetoacetate can be used to measure the intramitochondrial NAD^+/NADH ratio. Redox indicator metabolite couples also exist for the NADP(H) system.

In the human erythrocyte a discrepancy between the NAD^+/NADH ratio calculated from the lactate/pyruvate ratio in the extracellular fluid and the total extractable NAD^+ and NADH has been taken to indicate significant binding of NADH in the cell (Marshall & Omachi, 1974). This result is however contentious in view of the apparent difficulty of assaying total levels of NAD^+ and NADH (Burch et al, 1967) and the consequently wide range of values obtained for the levels of these nucleotides in the erythrocyte (Hasart et al, 1972). A fundamental problem with the measurement of any metabolite found only intracellularly is that changes in its concentration may occur during quenching of the tissue and extraction of the metabolite. A number of methods have been developed with a variety of tissues to try to overcome these problems (see for example Veech et al, 1979). The measurement of free and total NAD(H) in the erythrocyte is further discussed in chapter 6. The principle of the redox indicator method can also be applied to kinase equilibria although it now becomes a strictly invasive method

since kinase substrates are membrane impermeable and their assay requires cell disruption and extraction. For example, the tissue contents of the adenylate kinase and combined GAPDH and PGK reactions were measured in rapidly inactivated samples of blood, brain, muscle and liver (Veech et al, 1979). Comparison of the mass action ratios with the measured equilibrium constants of the enzymes in vitro indicated significant disequilibrium of the kinase reactions in those tissues containing mitochondria i.e. brain, muscle and liver. In muscle and brain the creatine kinase reaction was also apparently not at equilibrium. Since these kinases are located exclusively in the cytosol these results were taken to indicate significant compartmentation of ADP within the mitochondria. These calculations are critically dependent on accurate reproduction of the enzymes in situ environment in vitro when calculating the equilibrium constants, the pH being particularly important in the case of a dehydrogenase and the Mg^{2+} concentration in the case of a kinase.

It should be noted that the extraction and assay of metabolic intermediates in a cell may falsely identify an enzyme as being non-equilibrium, and thus rate limiting for flux, if a significant fraction of its substrate(s) are bound in situ. Apparent non-equilibrium of the substrates for aldolase in guinea pig brain slices may be due to binding of FDP (Rolleston & Newsholme, 1967).

Another approach to the study of enzymes and their environments in situ has involved the use of permeabilised cells. This technique has now been applied to a wide variety of cells including the erythrocyte (Aragón et al, 1980). The method involves cross-linking membrane proteins with bifunctional reagents in order to generate a protein

lattice. The membrane lipid is then removed making the cells permeable to intracellular metabolites. Conventional spectrophotometric enzyme kinetic studies can then be performed on these cell preparations. The rationale for this approach is that any protein-protein interactions which may exist in the cell are retained. Unfortunately the potential for artefact is considerable since the cross-linking reagents have been shown to modify the properties of some enzymes.

The application of n.m.r. to the non-invasive study of metabolism has expanded rapidly in recent years (reviewed in the following; Burt et al, 1979; Shulman et al, 1979; Gadian & Radda, 1981). The systems studied have ranged from the level of the isolated cellular organelle, the mitochondrion, to an intact animal.

In 1972 Eakin et al (1972) obtained ^{13}C n.m.r. spectra from yeast suspensions fed with glucose enriched at the C-1 position with ^{13}C . In 1973 Moon and Richards (1973) published ^{31}P n.m.r. spectra of human erythrocytes which showed resonances from 2,3-DPG, inorganic phosphate and ATP. The shifts of the 2,3-DPG and inorganic phosphate resonances were used to measure intracellular pH. Since then the majority of n.m.r. studies of metabolism have concentrated on these two nuclei.

Studies with the 100% abundant ^{31}P nucleus have involved the measurement of pH and the levels of phosphorylated metabolites in a range of systems including erythrocytes, yeast, E. Coli, mitochondria, hepatocytes, muscle, perfused organs such as rat heart and liver, rat heart and liver in situ in the intact animal and human limbs. The list is by no means exhaustive and the discussion of the results of relevance to the central theme of this thesis, the nature of an enzymes

environment in situ, can only be very limited.

The sensitivity of the chemical shift of a phosphate resonance, notably that of inorganic phosphate, to pH changes around neutrality, make ^{31}P n.m.r. a very powerful method for measuring intracellular and intraorganelle pH. In hepatocytes two inorganic phosphate resonances have been observed and assigned to the cytosolic and mitochondrial compartments (Cohen et al, 1978). The chemical shifts of these peaks give the pH in the two compartments. In skeletal muscle the anomalously large inorganic phosphate linewidth has been attributed to the distribution of phosphate between compartments of different pH. It is not certain, however, whether these phosphate pools reside within different regions of the muscle or in different compartments within individual muscle cells (Gadian et al, 1979). In human erythrocytes, as mentioned above, the 2,3-DPG phosphate resonances can be used to measure intracellular pH. However this is complicated by the fact that binding to haemoglobin also produces a shift in these resonances (Costello et al 1976). By comparing the chemical shifts of 2,3-DPG in model solutions approximating the pH, ionic strength and haemoglobin concentration found in the intact cell, estimates were made of the percentage of 2,3-DPG bound in situ. Binding of Mg^{2+} to ATP results in large downfield shifts of the α , β and γ phosphate resonances. Comparison of the relative shifts in these resonances obtained in model solutions in vitro with those obtained in the erythrocyte allowed estimation of the fraction of ATP bound to Mg^{2+} in the intact cell. From these data and from studies of the interactions of various phosphorylated metabolites with haemoglobin and Mg^{2+} under in situ conditions, simulated in vitro, the intracellular concentration of free Mg^{2+} was determined (Gupta et al, 1978). In kinetic studies on muscle the problems presented by the low

sensitivity of the n.m.r. technique have been elegantly circumvented by synchronising the electrical stimulation of contraction with collection of the n.m.r. data. By repeating the cycle of muscle excitation and data collection and by block averaging the signals obtained, the signal-to-noise ratio on resonances observed at specific times following muscle contraction is improved (Gadian et al, 1979). A similar method has been employed in examining the consequences of ischaemia in perfused kidney and heart (Burt et al, 1979). Using this method the fall in phosphocreatine in muscle has been used to calculate the total ATPase activity. It was found that the activity was tenfold lower in the intact muscle than in a myosin solution, indicating that the enzyme may be inhibited in situ. The capability of n.m.r. to continuously and non-invasively measure the levels of intracellular metabolites offers a considerable advantage over conventional methods which involve discrete sampling, tissue destruction and extraction of the compound. Loss of a metabolite during tissue quenching and extraction, as mentioned above, may seriously compromise the latter technique. N.m.r. methods, however, are confronted with the problem of calibration, the conversion of peak intensity into concentration (see Burt et al, 1979 for a discussion of this problem). Factors which affect peak intensity in the n.m.r. spectrum are discussed in the following chapter. Measurements of phosphocreatine/ATP ratios in skeletal muscle (Ackerman, et al, 1980) and (particularly in) brain have revealed higher ratios than previously observed using freeze extraction techniques. These results indicate that the extraction technique inevitably results in some phosphocreatine breakdown.

Studies with the ^{13}C nucleus, which has a low natural abundance, have involved injection of ^{13}C labelled metabolites into various cellular systems and monitoring the fate of the label in intermediary metabolites. Systems studied include many of those mentioned above for ^{31}P n.m.r. (reviewed in Shulman et al, 1979)

The "scrambling" of ^{13}C label between the C-1 and C-6 positions of FDP in yeast fed with (1- ^{13}C) or (6- ^{13}C) glucose showed that the aldolase and triosephosphate isomerase reactions are at equilibrium in situ (den Hollander et al, 1979). In E. Coli the absence of scrambling indicated that there is considerably more flux towards the trioses than in the reverse direction (Shulman et al, 1979). The labelling pattern observed in glucose in mouse liver perfused with ^{13}C labelled alanine indicated that the triosephosphate isomerase reaction is at equilibrium in this tissue (Cohen et al, 1979). In hepatocytes incubated with (3- ^{13}C) alanine comparison of the concentration of ^{13}C at the alanine C-2 position and the glucose C-5 position permitted assessment of the flux through pyruvate kinase relative to the gluconeogenic flux (Cohen et al, 1981). The labelling pattern in aspartate, it was thought, may indicate incomplete mixing of the mitochondrial oxaloacetate pool. Recently a comparison of ^{13}C n.m.r. and ^{14}C tracer studies of hepatic metabolism has been published (Cohen et al 1981a). The relative merits of radioactive tracer techniques and n.m.r. methods for studying cellular metabolism are discussed in a later chapter.

The intrinsically poor sensitivity of n.m.r., compared with other spectroscopic techniques, limits observation of cellular metabolites to compounds present in relatively high concentration. Even for those

compounds which are observed spectral accumulation times often of the order of minutes must be employed in order to obtain reasonable signal-to-noise ratios on the resonances of the compound in the n.m.r. spectrum. This limits the rates of change which can be monitored using n.m.r.. The technique of saturation transfer, however, which detects the transfer of magnetisation between two rapidly exchanging nuclei, allows measurements of rates in the range $1-10 \text{ s}^{-1}$ (Brown, 1980). The unidirectional rate constant for ATPase catalysed synthesis of ATP from ADP and Pi in E. Coli has been measured using this technique (Brown et al, 1977). The technique has also been applied to a study of creatine kinase in frog skeletal muscle where it was shown that the reaction catalysed by the enzyme is at equilibrium (Gadian et al, 1981). A study of adenylate kinase in human erythrocytes has also been reported (Gupta, 1979). The technique, which allows the direct measurement of an enzyme activity in situ, is however limited to a relatively narrow range of rates.

Compared to the ^{13}C and ^{31}P nuclei the ^1H nucleus has been little used in metabolic studies of whole cell systems. Although ^1H n.m.r. is more sensitive than either ^{31}P or ^{13}C n.m.r. it has the disadvantage that many resonances occur in a narrow frequency range which makes resolution a severe problem. The application of spin echo techniques, however, allows selection of resonances from small molecules such as cellular metabolites from a background envelope of protein resonances. Spectra were obtained initially from rat adrenal glands (Daniels et al, 1976) and from human erythrocytes (Brown et al, 1977). In the erythrocyte most of the resonances observed have been assigned (see chapter 2) and subsequent work has been concentrated on this cell. This has included measurement of lactate production and glutathione oxidation

and rereduction (Brown et al, 1977), transport across the cell membrane (Brindle et al, 1979) and isotope exchange in the metabolites lactate and pyruvate (Brindle et al, 1980; Simpson et al, 1981; Simpson et al 1982a&b; Brindle et al, 1982). The incorporation of ^2H labelled glycine into erythrocyte glutathione was used to measure the rate of glutathione synthesis (Isab & Rabenstein, 1979), however this has subsequently been shown to be an exchange reaction (Griffith, 1981).

The work presented here is a study of $^1\text{H}/^2\text{H}$ isotope exchange at the C-2 position of lactate in suspensions of human erythrocytes. The human erythrocyte has been an ideal vehicle for the development of the techniques presented here since it is an exceedingly well characterised system which has been used in the study of human genetics (Surgenor, 1975), in studies of membrane structure and transport (Marchesi et al, 1976; Ellory & Lew, 1977) and in studies of metabolism, in particular of glycolysis (Rapoport, 1968; Jacobasch et al, 1974; Rapoport, 1974). It is a readily available cell with no internal compartments and a predominantly glycolytic metabolism. There is no glycogenolysis or gluconeogenesis and, under normal conditions, flux of glucose through the pentose phosphate pathway is 10% or less than that flowing through glycolysis. The data available on the kinetic properties of erythrocyte enzymes and on the concentrations of metabolites are superior to those of most other cells. This wealth of in vitro kinetic data has permitted development of qualitative and semi-quantitative models (Rapoport, 1974) for the control of erythrocyte glycolysis. The ability of these models to predict changes in metabolite levels following specific metabolic perturbations suggests that the kinetic data obtained in vitro, at least for the non-equilibrium control enzymes of glycolysis, hexokinase and PFK, are similar to the kinetic properties displayed by these enzymes in

situ. It appears therefore that the intracellular environment in the erythrocyte is reasonably well characterised and can be simulated in vitro. Any discrepancies which may exist have not yet been detected in this sort of analysis.

The isotope exchanges studied here have been used to examine the properties of specific enzymes, catalysing reactions at equilibrium, in the human erythrocyte. The strategy employed has been to measure the equilibrium exchange properties of an enzyme in situ and to compare these with the properties of the enzyme in vitro. Simulation of the in situ environment in vitro has been used to investigate the free levels of enzyme substrates in situ and to determine the likelihood of possible enzyme-protein interactions in the cell.

1.1 References

Ackerman, J.J.H., Grove, T.H., Wong, G.G., Gadian, D.G. & Radda, G.K. (1980) *Nature* 283, 167-170

Aragón, J.J., Felíu, J.E., Frenkel, R.A. & Sols, A. (1980) *Proc. Natl. Acad. Sci.* 77, 6324-6328

Arnold, H. & Pette, D. (1970) *Eur. J. Biochem.* 15, 360-366

Bloch, W., Macquarrie, R.A. & Bernhard, S.A. (1971) *J. Biol. Chem.* 246, 780-790

Brindle, K.M., Brown, F.F., Campbell, I.D., Grathwohl, C. & Kuchel, P.W. (1979) *Biochem. J.* 180, 37-44

Brindle, K.M., Brown, F.F., Campbell, I.D., Foxall, D.L. & Simpson, R.J. (1980) *Biochem. Soc. Trans.* 8, 646-647

Brindle, K.M., Brown, F.F., Campbell, I.D., Foxall, D.L. & Simpson, R.J. (1982) *Biochem. J.* 202, 589-602

Brown, F.F., Campbell, I.D., Kuchel, P.W. & Rabenstein D.C. (1977) *FEBS Lett.* 82, 12-16

Brown, T.R. (1980) *Phil. Trans. R. Soc. Lond. B* 289, 441-444

Brown, T.R., Ugurbil, K. & Shulman, R.G. (1977) *Proc. Natl. Acad. Sci.* 74, 5551-5553

Bücher, Th. (1969) in "Pyridine nucleotide dependent dehydrogenases" (Sund, H. ed.), pp439-461, Springer Verlag, Berlin, Heidelberg & New York

Bücher, Th. & Sies, H. (1976) in "Use of isolated liver cells and kidney tubules in metabolic studies" (Tager, J.M., Söling, H.D. & Williamson, J.R. eds.) pp41-64 North-Holland Publ. Co., Amsterdam

Burch, H.B., Bradley, M.E. & Lowry, O.H. (1967) J. Biol. Chem. 242, 4546-4554

Burt, C., Cohen, S.M. & Bárány, M. (1979) Ann. Rev. Biophys. Bioeng. 8, 1-25

Clarke, F.M. & Masters, C.J. (1974) Biochim. Biophys. Acta. 358, 193-207

Clarke, F.M. & Masters, C.J. (1975) Biochim. Biophys. Acta. 381, 37-46

Cohen, S.M., Ogawa, S., Rottenberg, H., Glynn, P., Yamane, T., Brown, T.R. & Shulman, R.G. (1978) Nature 273, 554-556

Cohen, S.M., Shulman, R.G., & McLaughlin, A.C. (1979) Proc. Natl. Acad. Sci. 76, 4808-4812

Cohen, S.M., Glynn, P., & Shulman, R.G. (1981) Proc. Natl. Acad. Sci. 78, 60-64

Cohen, S.M., Rognstad, R., Shulman, R.G. & Katz, J. (1981a) J. Biol. Chem. 256, 3428-3432

Costello, A.J.R., Marshall, W.E., Omachi, A. & Henderson, T.O. (1976) Biochim. Biophys. Acta. 427, 481-491

Cseké, E., Váradi, A., Szabolcsi, G. & Biszku, E. (1978) FEBS Lett. 96, 15-18

Dagher, S.M. & Hultin, H.O. (1975) Eur. J. Biochem. 55, 185-192

Daniels, A., Williams, R.J.P., & Wright, P.E. (1976) Nature 261, 321-325

den Hollander, J.A., Brown, T.R., Ugurbil, K. & Shulman, R.G. (1979) Proc. Natl. Acad. Sci. 76, 6096-6109

Duchon, G & Collier, H.B. (1971) J. Membr. Biol. 6, 138-157

Eakin, R.T., Morgan, L.O., Gregg, C.T. & Matwiyoff, N.A. (1972) FEBS Lett. 28, 259-264

Eby, D. & Kirtley, M.E. (1979) Arch. Biochem. Biophys. 198, 608-613

Ellory, J.C. & Lew, V.L. (1977) "Membrane transport in red cells", Academic Press London, New York and San Francisco

Fazio, A., Kosic, J.P., Moir, R.D. & Bagnara, A.S. (1980) FEBS Lett. 113, 215-217

Fossel, E.T. & Solomon, A.K. (1977) *Biochim. Biophys. Acta.* 464, 82-92

Fossel, E.T. & Solomon, A.K. (1982) *Biochim. Biophys. Acta.* 649,
557-571

Friedrich, P., Apró-Kovács, V.A. & Solti, M. (1977) *FEBS Lett.* 84
183-186

Gadian, D.G., Radda, G.K., Richards, R.E. & Seeley, P.J. (1979) in
"Biological applications of magnetic resonance" (Shulman, R.G. ed.)
Academic Press

Gadian, D.G. & Radda, G.K. (1981) *Ann. Rev. Biochem.* 50, 69-83

Gadian, D.G., Radda, G.K., Brown, T.R., Chance E.M., Dawson, M.J.
& Wilkie, D.R. (1981) *Biochem. J.* 194, 215-228

Green, D.E., Murer, E., Hultin, H.O., Richardson, S.H., Salmon, B.,
Brierly, G.P. & Baum, H. (1965) *Arch. Biochem. Biophys.* 112, 635-647

Griffith, O.W. (1981) *J. Biol. Chem.* 256, 4900-4904

Gupta, R.K. (1979) *Biochim. Biophys. Acta.* 586, 189-195

Gupta, R.K., Benovic, J.L. & Rose, Z.B. (1978) *J. Biol. Chem.* 253,
6172-6176

Harvey, J.W. & Kaneko, J.J. (1976) *J. Cell. Physiol.* 89, 219-224

Hasart, E., Jacobasch, G. & Rapoport, S. (1972) *Acta. Biol. Med. Ger.* 28, 603-613

Higashi, T., Richards, C.S. & Uyeda, K. (1979) *J. Biol. Chem.* 254, 9542-9550

Isab, A.A. & Rabenstein, D.C. (1979) *FEBS Lett.* 106, 325-329

Jacobasch, G., Minikami, S. & Rapoport, S.M. (1974) in "Cellular and molecular biology of erythrocytes" (Yoshikawa, H. & Rapoport S.M. eds.) pp55-92 Urban & Schwarzenberg, Munich-Berlin-Wien

Ji, S., Lemasters, J.J. & Thurman, R.G. (1980) *FEBS Lett.* 113, 37-41

Kant, J.A. & Steck, T.L. (1973) *J. Biol. Chem.* 248, 8457-8464

Kliman, H.J. & Steck, T.L. (1980) *J. Biol. Chem.* 255, 6314-6321

Kohen, E., Kohen, C., Thorell, B. & Bartick, P. (1979) *Exp. Cell Res.* 119, 23-30

Marchesi, U.T., Furthmayr, H. & Tomita, M. (1976) *Ann. Rev. Biochem.* 45, 667-698

Marshall, W.E. & Omachi, A. (1974) *Biochim. Biophys. Acta.* 354, 1-10

Masters, C.J. (1977) *Curr. Top. Cell. Regul.* 12, 75-105

- Masters, C.J. & Winzor, D.J. (1981) Arch. Biochem. Biophys. 209, 185-190
- McDaniel, C.F., Kirtley, M.E. & Tanner, M.J.A. (1974) J. Biol. Chem. 255, 6478-6485
- Momsen G., Rose, Z.B. & Gupta, R.K. (1979) Biochem. Biophys. Res. Comm. 91, 651-657
- Moon, R.B. & Richards, J.H. (1973) J. Biol. Chem. 248, 7276-7278
- Mowbray, J. & Moses, V. (1976) Eur. J. Biochem. 66, 25-36
- Ottaway, J.A. & Mowbray, J. (1977) Curr. Top. Cell. Regul. 12, 107-208
- Ovádi, J. & Keleti, T. (1978) Eur. J. Biochem. (1978) 85, 157-161
- Ovádi, J. Salerno, C., Keleti, T. & Fasella, P. (1978) Eur. J. Biochem. 90, 499-503
- Rapoport, S.M. (1968) in "Essays in biochemistry" 4, 69-103 (Campbell, P.N. & Greville, G.D. eds.) Academic Press London and New York
- Rapoport, S.M. (1974) in "The human red cell in vitro" (Greenwalt, T.T. & Jamieson, G.A. eds.), pp153-188 Grune & Stratton, New York
- Rickey Welch, G. (1977) Prog. Biophys. Mol. Biol. 32, 103-191
- Rolleston, F.S. & Newsholme, E.A. (1967) 104, 524-533

Salhany, J.M., Cordes, K.A. & Gaines, E.D. (1980) *Biochemistry* 19, 1447-1454

Shulman, R.G., Brown, T.R., Ugurbil, K., Ogawa, S., Cohen, S.M. & den Hollander, J.A. (1979) *Science* 205, 160-166

Sies, H. (1980) *Trends. Biochem. Sci.* 5, 182-185

Sies, H. & Brauser, B. (1980) *Methods Biochem. Anal.* 26, 285-325

Simpson, R.J., Brindle, K.M., Brown, F.F., Campbell, I.D. & Foxall, D.L. (1981) *Biochem. J.* 193, 401-406.

Simpson, R.J., Brindle, K.M., Brown, F.F., Campbell, I.D. & Foxall, D.L. (1982a) *Biochem. J.* 202, 573-579

Simpson, R.J., Brindle, K.M., Brown, F.F., Campbell, I.D. & Foxall, D.L. (1982b) *Biochem. J.* 202, 581-587

Sols, A. & Marco, R. (1970) *Curr. Top. Cell. Regul.* 2, 227-270

Strapazon, E. & Steck, T.L. (1976) *Biochemistry* 15, 1421-1424

Strapazon, E. & Steck, T.L. (1977) *Biochemistry* 16, 2966-2970

Surgenor, D.M. (1975) "The red blood cell" (2nd edition) (Surgenor D.M. ed.) Academic Press New York San Francisco and London

Tillmann, W., Cordua, A. & Schröter, W. (1975) *Biochim. Biophys. Acta.* 382, 157-171

Vas, M. & Batke, J. (1981) *Biochim. Biophys. Acta.* 660 193-198

Veech, R.L., Lawson, J.W.R., Cornell, N.W. & Krebs, H.A. (1979) *J. Biol. Chem.* 254, 6538-6547

Wins, P. & Schoffeniels, E. (1969) *Biochim. Biophys. Acta.* 185, 287-296

Yu, J & Steck T.L. (1975) *J. Biol. Chem.* 250 9176-9184

2 Exchange of the C-2 hydrogen of lactate with solvent catalysed by glycolytic enzymes in the human erythrocyte

2.1 Introduction

The introductory chapter described the special features of an enzyme's in situ environment and examined the potential of the n.m.r. technique for the non-invasive investigation of this environment. The use of ^1H n.m.r. measurements of isotope exchange at the lactate C-2 position to investigate the in situ kinetic properties of human erythrocyte enzymes was briefly discussed. In this chapter the enzyme catalysed pathway which exchanges the C-2 hydrogen of lactate with solvent is described in detail. The n.m.r. method used to monitor the exchange is described and theoretical aspects of isotope exchange in multi-enzyme systems discussed. The measurement of exchange velocities in vitro and in erythrocyte suspensions is demonstrated and a method for measuring, in vitro, the specific equilibrium velocities of the enzymes involved in the exchange is described. The basic characteristics of the exchange in erythrocytes are demonstrated and the problems involved in using this technique to compare the in situ and in vitro isotope exchange properties of an individual enzyme discussed. The measurement of in situ enzyme equilibrium velocities is demonstrated in chapters 5 and 6.

2.2 Experimental

Most of the methods detailed in the following section have been used throughout the work presented in the following chapters. In subsequent experimental sections, therefore, only those methods peculiar to the particular chapter in which the section is found are described.

Materials

Biochemicals were obtained from Sigma (London), Chemical Co. (Poole, Dorset, U.K.) except for NAD^+ which was obtained from Boehringer (Lewes, East Sussex, U.K.). NADH was obtained in preweighed vials. Other chemicals were analytical grade. Aldolase, glyceraldehydophosphate dehydrogenase, lactate dehydrogenase and triosephosphate isomerase from rabbit muscle, lactate dehydrogenase from human erythrocyte and lipoamide dehydrogenase from porcine heart were obtained from Sigma. Ion exchange resins were obtained from BDH Chemicals Ltd. Activated, neutralised, charcoal was obtained from Sigma. 99.8% $^2\text{H}_2\text{O}$ was obtained from Fluorochem Ltd., Glossop, Derbyshire, U.K.. In $^2\text{H}_2\text{O}$ solutions, pH^* , the uncorrected pH meter reading is quoted.

Preparation of L-(2- ^2H)lactate

L-(2- ^2H) lactate was prepared essentially as described by Alizade et al (1975). Lithium lactate (250 mg) was dissolved in 25 mls of 0.1M sodium phosphate buffer, pH^* 6.0 in 99.8% $^2\text{H}_2\text{O}$, containing 50mg EDTA, 12mg dithiothreitol, 25mg NAD^+ (lithium salt), 1.25mg rabbit muscle lactate dehydrogenase and 2,500 units of porcine heart lipoamide dehydrogenase. The lipoamide dehydrogenase, obtained as an ammonium sulphate suspension, had been dialysed against 0.1% EDTA/1mM

2-mercaptoethanol (pH 7.0) and then lyophilised. The resulting solution was incubated at room temperature for approximately two weeks. A comparison of the ratio of p.m.r. peak intensities given by the methyl and C-2 protons in the resulting lactate with that given by L-(U-¹H)lactate showed that approximately 98% deuteration had been achieved at the C-2 position.

The deuterated lactate was isolated by first placing the enzyme solution on a boiling water bath for approximately 10 minutes. The precipitated protein was then centrifuged off and the supernatant loaded onto a 2 x 14 cm Dowex 1-X8 column in the chloride form (Bartlett, 1959). A linear gradient of 0-0.02M HCl was then applied at a flow rate of 1 ml/min and 5 ml fractions were collected. The total volume of the gradient was 400 ml. The lactate was detected using the assay system described below. Peak fractions were pooled, boiled for approximately 10 minutes with activated charcoal (this removed a slight yellow colour from the lactate preparation) and then neutralised by the addition of solid zinc carbonate. The resulting zinc lactate solution was brought back to the boil and then filtered on a Buchner funnel through hardened Whatman 50 filter paper to remove charcoal and excess zinc carbonate. The filtrate was lyophilised. The solid zinc lactate obtained was then dissolved to give approximately 10 mls of solution which was passed through a 2 x 14 cm column of Dowex 50-X8 in the lithium form (Brin, 1953). The eluate, containing lithium lactate, was lyophilised and the resulting solid stored in a dessicator. Lactate with a purity exceeding 90% could be prepared by this method. The yield was usually about 50%.

General Methods

Human erythrocytes were prepared from one day old blood (stored in citrate/phosphate/glucose) or from freshly drawn venous blood by washing once in 10 volumes of phosphate-buffered saline (5mM-sodium phosphate (pH 7.4)/0.15M NaCl in $^1\text{H}_2\text{O}$) and removing the buffy coat by aspiration. The cells were then washed five times in 1 volume of Krebs-Ringer buffer (Krebs & Henseleit, 1932) made in either $^2\text{H}_2\text{O}$ or $^1\text{H}_2\text{O}$ as appropriate. The buffers contained 10mM glucose (unless otherwise stated) and all washes were performed at room temperature. Erythrocyte lysates were prepared by freezing the cells twice in liquid nitrogen. Nicotinamide (20mM) was added to the cells prior to lysis in order to inhibit the NAD^+ glycohydrolase present on the external surface of the erythrocyte (Alivisatos & Denstedt, 1951). Cell densities were determined by the microhaematocrit method (Hawksley-microhaematocrit centrifuge).

The in vitro exchange system

Rabbit muscle aldolase, glyceraldehydophosphate dehydrogenase and triosephosphate isomerase, obtained as ammonium sulphate suspensions, were dialysed against 0.1% EDTA/1mM 2-mercaptoethanol before use. Human erythrocyte lactate dehydrogenase was used as a suspension in ammonium sulphate solution. In mixtures of the enzymes where the concentration of lactate dehydrogenase was varied the concentration of ammonium sulphate was also varied so that all the samples contained the same ammonium sulphate concentration. (Experiments showed that ammonium sulphate, at the concentrations used here, had no effect on the measured properties of the lactate dehydrogenase).

Enzyme Assays

These were performed according to Beutler (1975). In all of the assays described the assay system buffer contained 100mM Tris-HCl pH 7.4, 0.5mM EDTA and 0.2mM NADH. The assays were performed at 37°C in 1 ml volume, 1 cm path length cuvettes. These were acid washed prior to use. The enzyme catalysed reaction was observed by monitoring the oxidation of NADH at 340nm. The rate of reaction was calculated assuming an extinction coefficient for NADH of $6.22 \times 10^6 \text{ cm}^2 \text{ mol}^{-1}$ (Horecker & Kornberg, 1948). Enzyme activities are expressed in terms of units (μmol of substrate consumed/min).

The enzyme solutions to be assayed were diluted in 0.1% EDTA/1mM 2-mercaptoethanol so that the total activity added to the system resulted in an absorbance change of approximately 0.2 O.D. units in 20 minutes. Rates of reaction were calculated from the linear change in absorbance during this period. Cell preparations were diluted in 0.1% EDTA/1mM 2-mercaptoethanol as appropriate and freeze thawed twice in liquid nitrogen before addition to the assay system. The assay system was preincubated for 10 min before initiation of the reaction by addition of the enzyme's substrate. In all cases blank assays were performed where the added enzyme solution was replaced with H_2O . Only in the triosephosphate isomerase assay was the blank rate significant.

Absorbance measurements were made using a Hilger-Watts H700 Uvispek or Unicam SP800A UV spectrophotometer connected to a chart recorder. The full scale deflection on the recorder was set to 0.5 O.D. units.

Aldolase assay

The assay system contained approximately 0.2 unit/ml of triosephosphate isomerase and 0.2 units/ml of glycerol-3-phosphate dehydrogenase. The reaction was initiated by the addition of 1mM FDP. The FDP stock solution was assayed immediately prior to use by adding approximately 50 μ M FDP to the assay system and following the reaction to completion.

Triosephosphate isomerase assay

The assay system contained approximately 0.2 units/ml of glycerol-3-phosphate dehydrogenase. The reaction was initiated by the addition of 3mM DL-GAP. The GAP was prepared from the diethylacetal monobarium salt as described by Sigma and was assayed immediately prior to use by adding approximately 20 μ M to the assay system and then following the reaction to completion. It was found that the GAP solution could be stored frozen for a week without significant decomposition.

Glyceraldehydephosphate dehydrogenase assay

The assay system contained approximately 5 units/ml phosphoglycerate kinase, 10mM MgCl₂ and 8mM ATP (neutralised). The reaction was initiated by the addition of 10mM 3-phosphoglycerate (sodium salt).

Metabolite assays

Triose phosphate and FDP assays in erythrocytes

The assays were performed according to Beutler (1975). The principle of the assay is described in the legend to table 1.

Extraction

Perchloric acid extracts were prepared by adding 2 ml of the cell suspension (or lysate) to 8 ml of ice cold 4% PCA. Following centrifugation, 7 ml of the supernatant were neutralised with 1M K_2CO_3 and the volume adjusted to 10 ml. The resulting precipitate was centrifuged off and the supernatant filtered through a 0.22 μ m pore size Millipore filter in order to remove particulates. Throughout these operations the extract was maintained at 4°C.

Assay system

The assay system contained 100mM Tris-HCl pH 8.0, 0.5mM EDTA, 10mM NAD^+ , 4mM sodium arsenate, 1mM 2-mercaptoethanol and 2 ml of the extract in a total volume of 3.8 ml. The assay system buffer was filtered through a 0.22 μ m pore size Millipore filter prior to use. Fluorescence measurements were made using a Perkin-Elmer MPF-2A fluorescence spectrophotometer thermostatted at 37°C. The fluorescence was excited at 340nm and the emission observed at 460nm.

GAP plus DHAP were assayed by the addition of approximately 2 units/ml glyceraldehydephosphate dehydrogenase and 15 units/ml triosephosphate isomerase to the assay system. FDP was assayed by the addition of approximately 0.2 units/ml of aldolase. The fluorescence response was then calibrated by the addition of 0.5 μ M FDP followed by

1.0 μ M FDP. The total concentration of triose phosphates and FDP added to the system in the extract was usually between 0.5 and 2 μ M. Blank assays were also performed in which the extract was replaced with water. The FDP stock solution used to calibrate the fluorescence was assayed spectrophotometrically as described under "Aldolase assay".

Lactate assay

Protonated and deuterated lactate preparations were stored and assayed at a number of intervals during their use. Assays of concentration usually involved 5 determinations. The standard error on the mean was never greater than $\pm 5\%$ and determinations at intervals separated by 1-2 weeks gave values within this range.

The assay system contained a glycine buffer pH 9.2, containing hydrazine, (obtained from Sigma as part of a lactate assay kit) 10mg/ml NAD⁺ (lithium salt) and approximately 20 units/ml lactate dehydrogenase. To this was added approximately 25 μ M lactate and the resulting solution was incubated for 45-60 min in the dark at room temperature. The absorbance of this solution was then read against a blank at 340nm and the lactate concentration calculated assuming an extinction coefficient for NADH of $6.22 \times 10^6 \text{ cm}^2 \text{ mol}^{-1}$ (Horecker & Kornberg, 1948).

Proton Magnetic Resonance Methods

Spectra were obtained at 470 MHz using a spin echo sequence with $\tau=68\text{ms}$ (Brown et al, 1977, Brindle et al, 1979). Samples in $^1\text{H}_2\text{O}$ were run without a $^2\text{H}_2\text{O}$ lock since field drift during accumulation of a spectrum was negligible. Spectra were stored on disc by a computer controlled automatic data acquisition routine, which also provided

accurate timing for determination of exchange rates. Samples were run in 5mm diameter tubes containing 0.5 ml of solution or cell suspension. All samples were run at 37°C and preheated to this temperature before mixing. The pH values quoted were recorded at this temperature. All additions to the samples were of sufficiently small volume to have a negligible dilution effect. Concentrations in cell suspensions were calculated assuming that 72% of the cell volume is solvent water (Eilam & Stein, 1974).

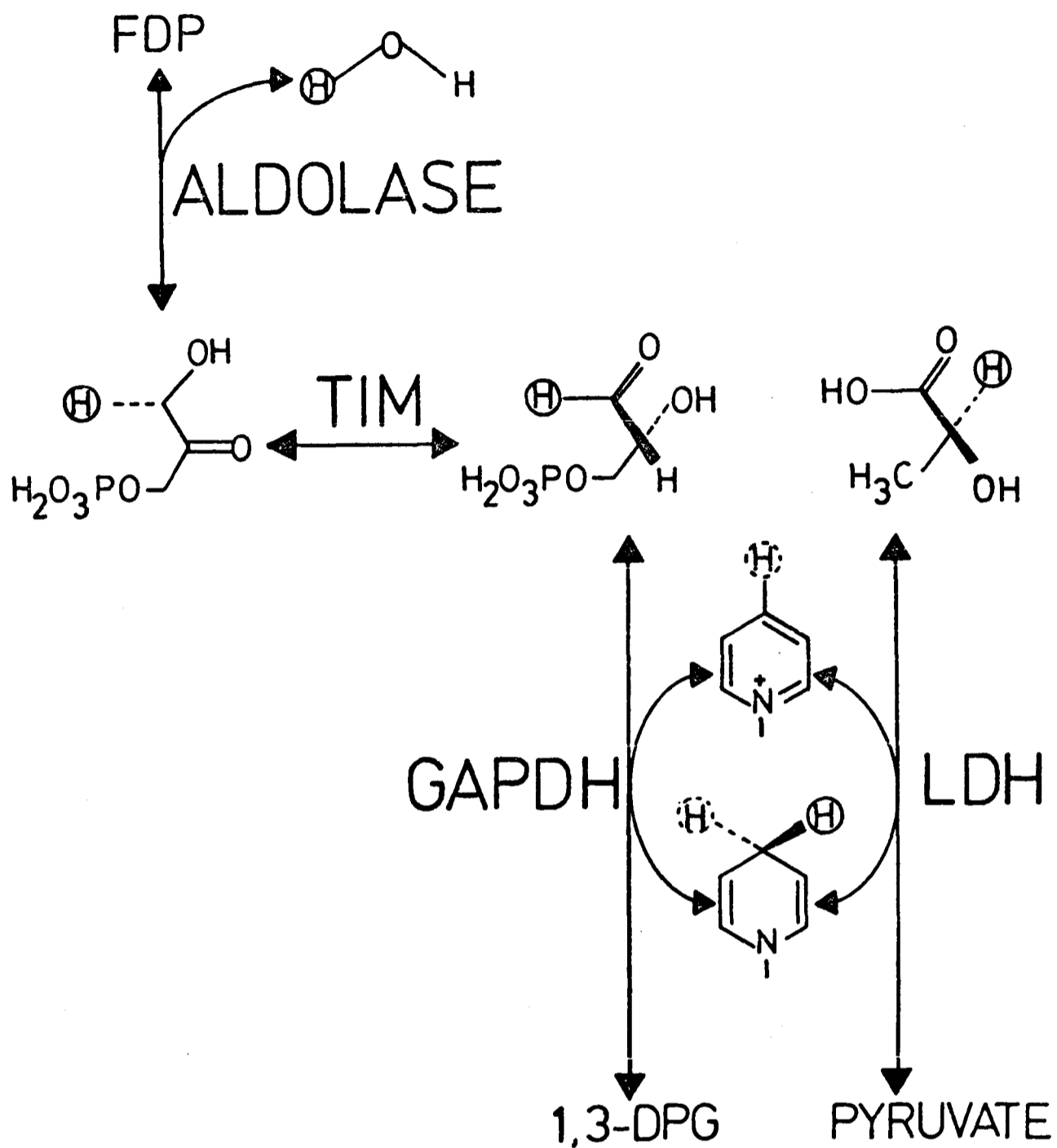


Figure 1

C-2 exchange pathway

Pathway taken by the label exchanging between the C-2 position of lactate and solvent. The exchanging isotope is ringed. Solvent isotope is stereospecifically incorporated into DHAP by aldolase (Rose & Warms, 1969). The abbreviations for the enzymes are; LDH, lactate dehydrogenase; GAPDH, glyceraldehydphosphate dehydrogenase and TIM, triosephosphate isomerase.

2.3 The C-2 exchange system

The pathway for the exchange of hydrogen between the C-2 position of lactate and solvent in human erythrocytes, as proposed by Rose and Warms (1969), is shown in figure 1. Four enzymes are involved; aldolase, triosephosphate isomerase, glyceraldehydophosphate dehydrogenase and lactate dehydrogenase. This pathway has also been invoked to explain production of solvent labelled ethanol (labelled at the C-2 position) from D glucose and D mannose fermented by the yeast *Saccharomyces cerevisiae* (Saur et al, 1968) and as a contributor to solvent labelling observed in liver infused with L-(2-³H)lactate (Bücher, 1969). A possible pathway for exchange not considered by Rose and Warms in the erythrocyte is shown in figure 2. Solvent label is introduced into the pentose phosphate pathway intermediates by the enzyme ribulosephosphate 3-epimerase (Maxwell, 1961) and can exchange with the aldehydic hydrogen of GAP via the reactions catalysed by transaldolase and transketolase (Hue & Hers, 1972). There is considerable transaldolase activity in the human erythrocyte but transketolase is present in only low activity (Freidemann & Rapoport, 1974). The epimerase has been shown to be present in horse erythrocytes (Dickens & Williamson, 1956) and in human erythrocytes as well, although again in low activity (see chapter 4). The quantitative significance of this pathway to the solvent exchange of hydrogen at the C-2 position of lactate is not known. It is felt, however, in view of the low activities of the enzymes involved, that its contribution is unlikely to be large (see chapter 4). A possible contribution of this pathway to the exchange at the C-2 position of lactate will not affect any of the conclusions reached in the work presented here.

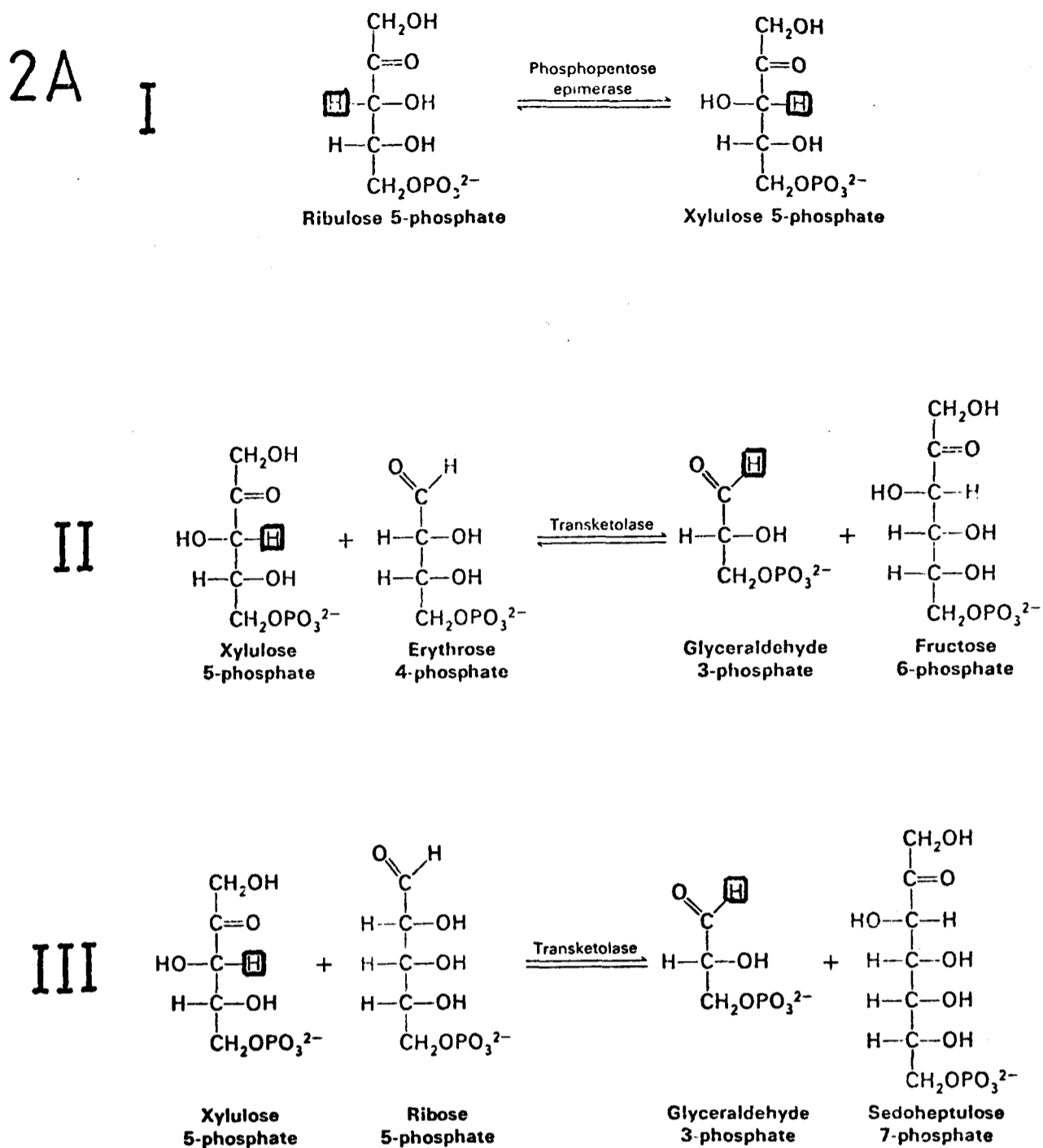


Figure 2

The ribulosephosphate 3-epimerase pathway for the solvent exchange of the aldehydic hydrogen of GAP.

2A

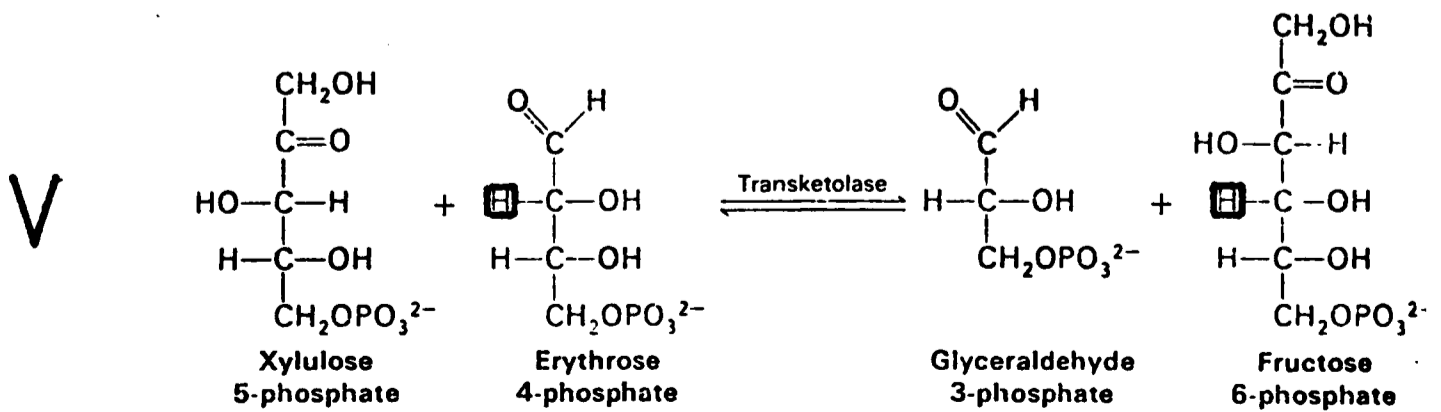
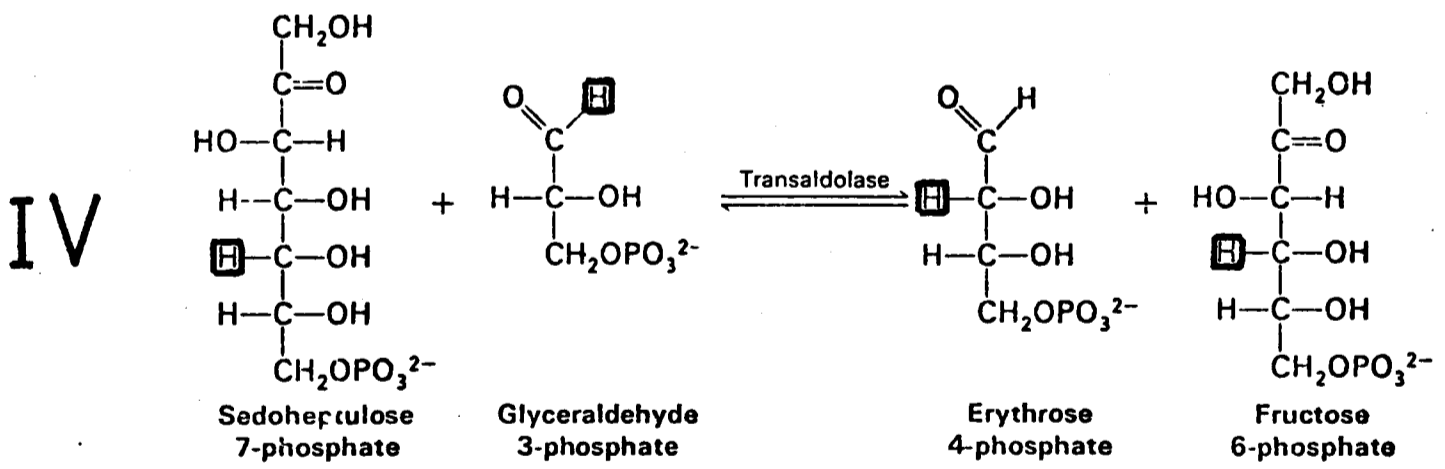
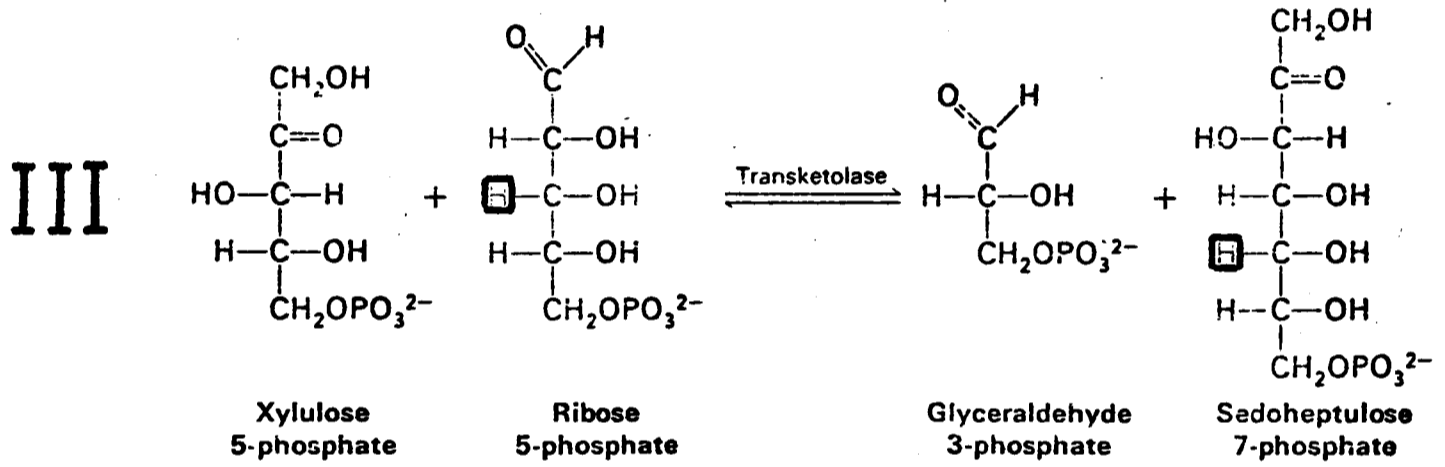
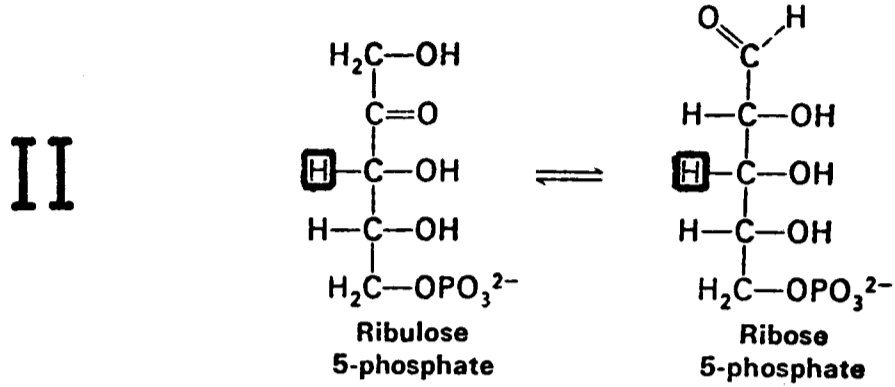
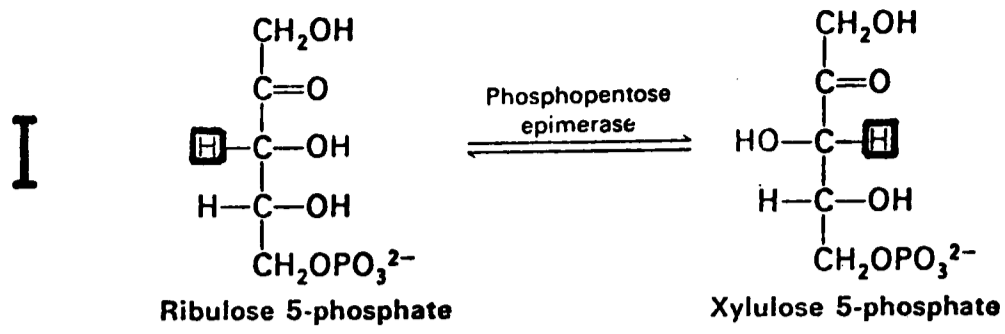
The epimerase introduces solvent label into the 3 position of the pentose phosphate pathway intermediates, ribulose-5-phosphate and xylulose-5-phosphate (reaction I). The solvent label can then exchange with the aldehydic hydrogen of GAP in either of the two reactions catalysed by transketolase (reactions II and III).

2B

The solvent label introduced by the epimerase can exchange with the 3 position of ribose-5-phosphate in the reaction catalysed by phosphopentoseisomerase (reaction II). The label introduced into ribose-5-phosphate can subsequently exchange with the hydrogen at the 5 position of sedoheptulose-7-phosphate in the reaction catalysed by transketolase (reaction III). Reaction of this intermediate with GAP in the reaction catalysed by transaldolase (reaction IV) results in labelling of erythrose-4-phosphate at the 2 position. Labelled erythrose-4-phosphate can react with xylulose-5-phosphate in the reaction catalysed by transketolase (reaction V) to label fructose-6-phosphate at the 4 position. Fructose-6-phosphate can also be labelled in this position by reaction of labelled GAP with sedoheptulose-7-phosphate in the reaction catalysed by transaldolase (reaction IV).

The label at the 4 position of fructose-6-phosphate can subsequently exchange with the aldehydic hydrogen of GAP via the reaction catalysed by transaldolase (reaction IV) and the reactions catalysed by phosphofructokinase and aldolase.

2B



2.4 Theoretical aspects of isotope exchange kinetics
in the multi-enzyme C-2 exchange system

Equilibrium velocity

The equilibrium velocity for the exchange of label between two pools of concentration, A and B, may be calculated from the fractional progress toward equilibrium, f_e , using the following equation (Boyer, 1959).

$$v = \frac{-2.3 (A) \cdot (B) \cdot 1 \cdot \log(1 - f_e)}{(A) + (B) \text{ time}} \dots \dots \dots (1)$$

For C-2 hydrogen exchange where one of these pools is solvent and is thus much larger than the lactate pool, the equilibrium velocity v can be calculated by multiplying the first order rate constant for the exchange by the lactate concentration.

Relationship of the observed equilibrium velocity to the equilibrium velocities of the individual enzyme catalysed steps in C-2 exchange

For trace isotope exchange, the exchange rate of steps in series add reciprocally (Yagil & Hoberman, 1969). Under certain conditions this also applies to bulk isotope exchange. In the C-2 exchange system, if the concentration of lactate is significantly greater than that of the intermediate substrates involved in the exchange, the individual isotope exchange equilibrium velocities of the enzymes can be related to the overall equilibrium velocity by the following equation (see chapter 3 and Foxall, 1981).

$$\frac{1}{V_{C2X}} = \frac{1}{V_{ALD}} + \frac{1}{V_{TIM}} + \frac{2}{V_{GAPDH}} + \frac{2}{V_{LDH}} \dots\dots\dots(2)$$

V_{C2X} is the measured overall equilibrium velocity for the system and V_{ALD} , V_{TIM} , V_{GAPDH} and V_{LDH} are the equilibrium velocities of aldolase, triosephosphate isomerase, glyceraldehydophosphate dehydrogenase and lactate dehydrogenase respectively. The factors of two arise for the dehydrogenases because lactate dehydrogenase reacts stereospecifically with the A face of the coenzyme NADH, whereas glyceraldehydophosphate dehydrogenase reacts stereospecifically with the B face. In order for the solvent isotope introduced onto the B face of the coenzyme by glyceraldehydophosphate dehydrogenase to get to the C-2 position of the lactate molecule it must pass twice through the reactions catalysed by glyceraldehydophosphate dehydrogenase and lactate dehydrogenase. The influence of steric specificity on the rates of hydrogen exchange between substrates of NAD-coupled dehydrogenases has been discussed (Hung & Hoberman, 1972).

The effect of enzyme activity and substrate concentration on the exchange rate

The interactions between metabolic flux, substrate concentrations and enzyme activities in multi-enzyme systems have been extensively discussed. See for example, Kacser and Burns (1979). In the following discussion Kacser and Burns's definitions of sensitivity and elasticity have been used in discussing the effect of enzyme and substrate concentrations on the rate of C-2 exchange. The sensitivity coefficient Z_i is defined as:

$$Z = \frac{\delta F/F}{\delta E_1/E_1}$$

where F is metabolic flux and E is the catalytic activity of any one enzyme. Z describes the fractional change in flux due to a fractional change in enzyme activity. For a system in steady state the sum of the sensitivity coefficients for all the enzymes in the pathway is unity.

The sensitivity coefficient of an enzyme in the C-2 exchange system is the partial derivative of the overall equilibrium velocity (V_{C2X}) with respect to that enzyme's equilibrium velocity. For example, for aldolase this is V_{C2X}/V_{ALD} . From equation 2 it can be seen that the sum of the sensitivity coefficients for the enzymes involved in C-2 exchange is unity. The value of an individual sensitivity coefficient will depend on the equilibrium velocity of the enzyme in relation to others in the pathway. The equilibrium velocity of an enzyme is dependent on its concentration and turnover number and on the concentrations of its substrates.

If a substrate concentration is changed in the C-2 exchange system then the equilibrium velocity of one or more of the enzymes will also change. The fractional change in enzyme rate which occurs on a fractional change in substrate concentration has been designated the elasticity coefficient (Kacser & Burns, 1979).

$$\frac{\delta v_i / v_i}{\delta S_i / S_i} = \epsilon_{S_i}^{v_i}$$

where v_i is the enzyme rate for the enzyme E_i , S_i is substrate concentration and $\epsilon_{S_i}^{v_i}$ is the elasticity coefficient. For C-2 exchange this coefficient describes the fractional change in an enzyme's equilibrium velocity due to a fractional change in the concentration of one of its substrates. The coefficient will be large if a large change in an enzyme's equilibrium velocity occurs following a small change in substrate concentration. This may be the case, for example, if the concentration changes occur at or around the apparent K_m of the enzyme for this particular substrate.

Elasticity coefficients can also be applied to the effects of inhibitors and other factors in an enzyme's environment such as pH and ionic strength which will also affect the equilibrium velocity of the enzyme.

For equilibrium isotope exchange, where an enzyme's reactants are at or near chemical equilibrium, flux of isotope in both directions across the enzyme is measured. If a substrate concentration is varied in order to determine an apparent isotope exchange K_m , then there will also be changes in the concentrations of the enzyme's other substrates. In conventional enzyme kinetic studies unidirectional rates are measured with the reactants usually present in excess. Initial rates are measured before there is significant build up of product. An apparent K_m obtained from isotope exchange measurements cannot be equated, therefore, with a K_m obtained from conventional enzyme kinetic studies

(Boyer, 1959).

In addition if a substrate concentration is changed in the C-2 exchange system then it will not just affect the equilibrium velocity of a single enzyme but all those enzymes for which it is a common substrate or have a substrate with which it is in chemical equilibrium. However using the method shown in figure 14 the effect of substrate concentration on a single enzyme can be measured.

2.5 Isotope effects

Equation 2 assumes that there are no kinetic isotope effects, that is that the equilibrium velocities of the enzymes are fixed for a given set of substrate concentrations and environmental conditions and are independent of the fractional labelling state of the substrates. If there were significant kinetic isotope effects then the equilibrium velocities would be time dependent functions which change as the fractional labelling of the substrates change.

The C-2 exchange system is potentially sensitive to both primary and secondary isotope effects since the transfer of hydrogen label between the lactate C-2 position and solvent requires the breakage and reformation of a number of C-H bonds and changes in hybridisation of carbon atoms bonded to the hydrogen label. Deuterium isotope effects on C-H bond breaking show a wide range of values with k_H/k_D ranging from essentially unity to values as high as 45 (Kresge, 1977). Most primary kinetic isotope effects lie in the range, $k_H/k_D=2-10$. Secondary kinetic isotope effects are much smaller and usually have limiting values of 1.02-1.40 (Kirsch, 1977).

There are two types of isotope effect which must be considered in the C-2 exchange system, these are; a) equilibrium isotope effects which will cause displacement of equilibria and b) kinetic isotope effects. Equilibrium isotope effects have been extensively studied (Cleland, 1980; Cook et al, 1980) and rules have been formulated for predicting their magnitude. These effects are in general small. For example, for lactate deuterated at the C-2 position the lactate dehydrogenase equilibrium is displaced by a factor of 1.19 towards lactate and NAD^+ . This is the result of deuterium having a higher affinity for the carbon atom at the C-2 position of lactate than at the 4 position of the nicotinamide ring of NADH. Changes in equilibrium positions due to changes in fractional labelling of the substrates involved in C-2 exchange are expected, therefore, to have a negligible effect on the equilibrium velocities of the enzymes.

A primary kinetic isotope effect, if fully expressed, would have a marked effect on the observed equilibrium velocity of an enzyme. The full expression of a primary or secondary kinetic isotope effect in an enzyme catalysed reaction is, however, rarely if ever observed (Northrop, 1977). For example, an isotope effect on C-H bond cleavage would only be fully observed in the velocity of an enzyme reaction if this cleavage step were rate limiting for the overall enzymic reaction and if all the other steps such as substrate binding and product release were infinitely fast.

For the enzymes involved in C-2 exchange significant expression of a kinetic isotope effect is unlikely. The oxidation of C-2 deuterated lactate catalysed by lactate dehydrogenase shows a kinetic isotope effect with $k_H/k_D = 1.6$ at lactate concentrations below approximately 5mM but this effect disappears at higher concentrations with k_H/k_D

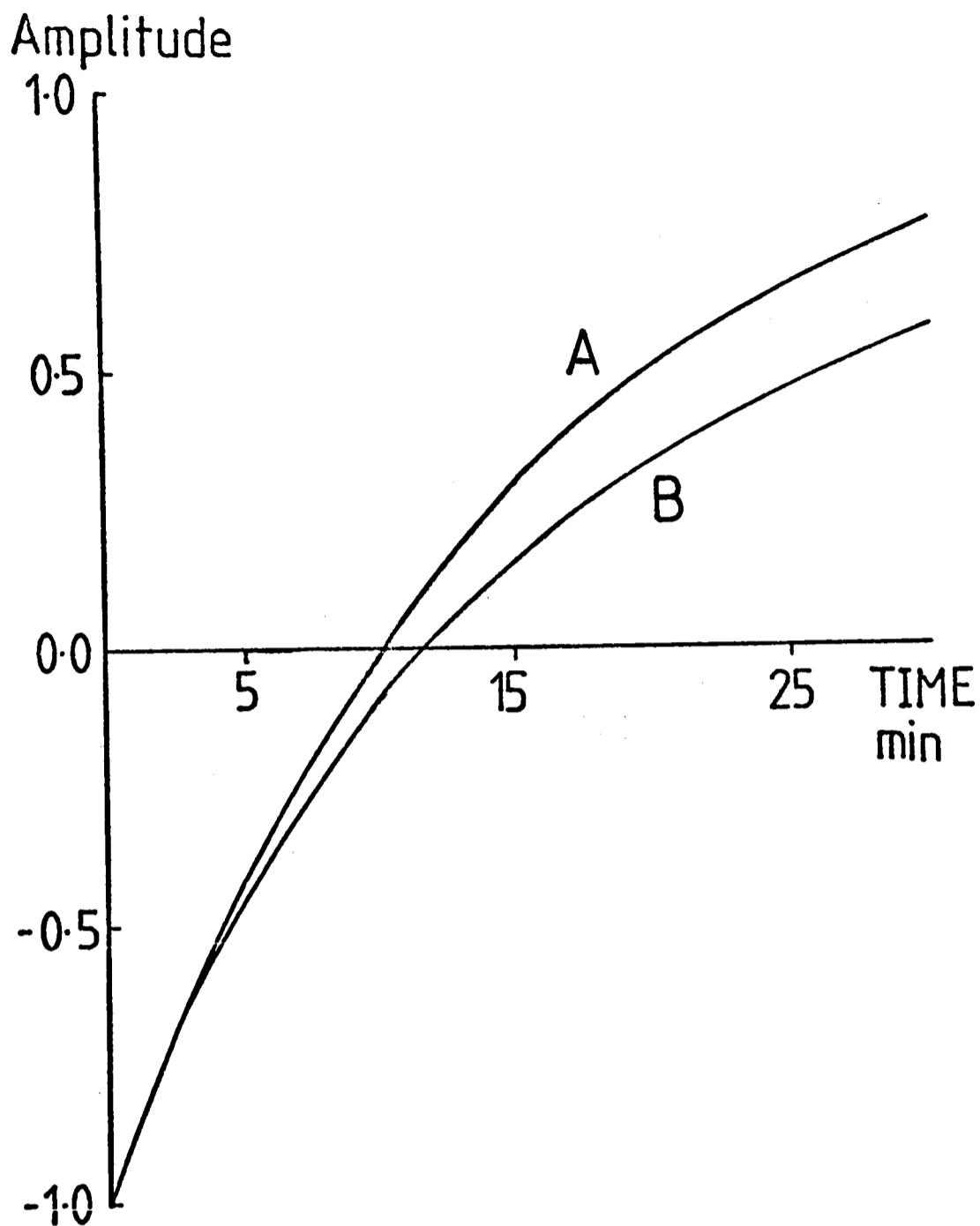


Figure 3

Theoretical exchange time courses demonstrating an isotope effect on the rate constant for the exchange.

The exchange has an amplitude of 2, the $t_{1/2}$ for an exchange time course is given by the intersection of the curve with the abscissa. Curve A shows an exchange time course where there are no isotope effects. The exchange has a $t_{1/2}$ of 10 minutes. Curve B shows an exchange time course where the rate constant for the exchange shows an isotope effect of 2. At the start of the exchange, where the fractional labelling of the exchanging species is close to zero, the rate constant for curve B has the same value as that for A. At $t = \infty$ however when the exchanging species is completely labelled, the rate constant for exchange has a value half that of the rate constant for curve A and half that of its original value at $t=0$ (see appendix 3). Thus as the fractional labelling of the exchanging compound increases so too does the expression of the kinetic isotope effect.

approaching unity (Cantwell & Dennis, 1970). Studies of glyceraldehydophosphate dehydrogenase (Trentham, 1971) have shown that the rate determining step of oxidative phosphorylation is NADH release at high pH and phosphorylysis of the acyl enzyme at low pH. For the reverse reaction the rate determining step at high pH is a process associated with NADH binding, probably a conformational change and GAP release at low pH. The steady state rate of NADH oxidation was shown to be the same for NADH deuterated or protonated at the C-4 position. The rate of exchange of the pro-S hydrogen at the C-3 position of DHAP with solvent, catalysed by aldolase, has been shown to be unaffected by isotopic substitution (Rose & Rieder, 1958). In the case of triosephosphate isomerase there will be no primary kinetic isotope effect since the solvent label stereospecifically incorporated into DHAP by aldolase is not subsequently exchanged during isomerisation (Rieder & Rose, 1959). For any enzyme the effect of a kinetic isotope effect on the overall exchange velocity of the C-2 exchange system will be minimal if the sensitivity coefficient of the enzyme is small.

In the work presented here isotope effects on enzyme equilibrium velocities have not been measured since the effects are likely to be small and their effect on the overall exchange can be reduced by making estimates of the rate constant for the exchange from the apparent half time or from the exchange time course prior to this point. This is demonstrated in figure 3. Isotope effects on enzyme equilibrium velocities could be measured using the techniques shown here if the exchange were performed in a 50:50 mixture of $^1\text{H}_2\text{O}$ and $^2\text{H}_2\text{O}$ and the exchange of L-(2- ^2H) and L-(U- ^1H) lactate were compared. By using an $^1\text{H}_2\text{O}/^2\text{H}_2\text{O}$ mixture the effect of non-specific solvent effects on the enzyme and thus on the rate of exchange are removed (Schowen, 1977).

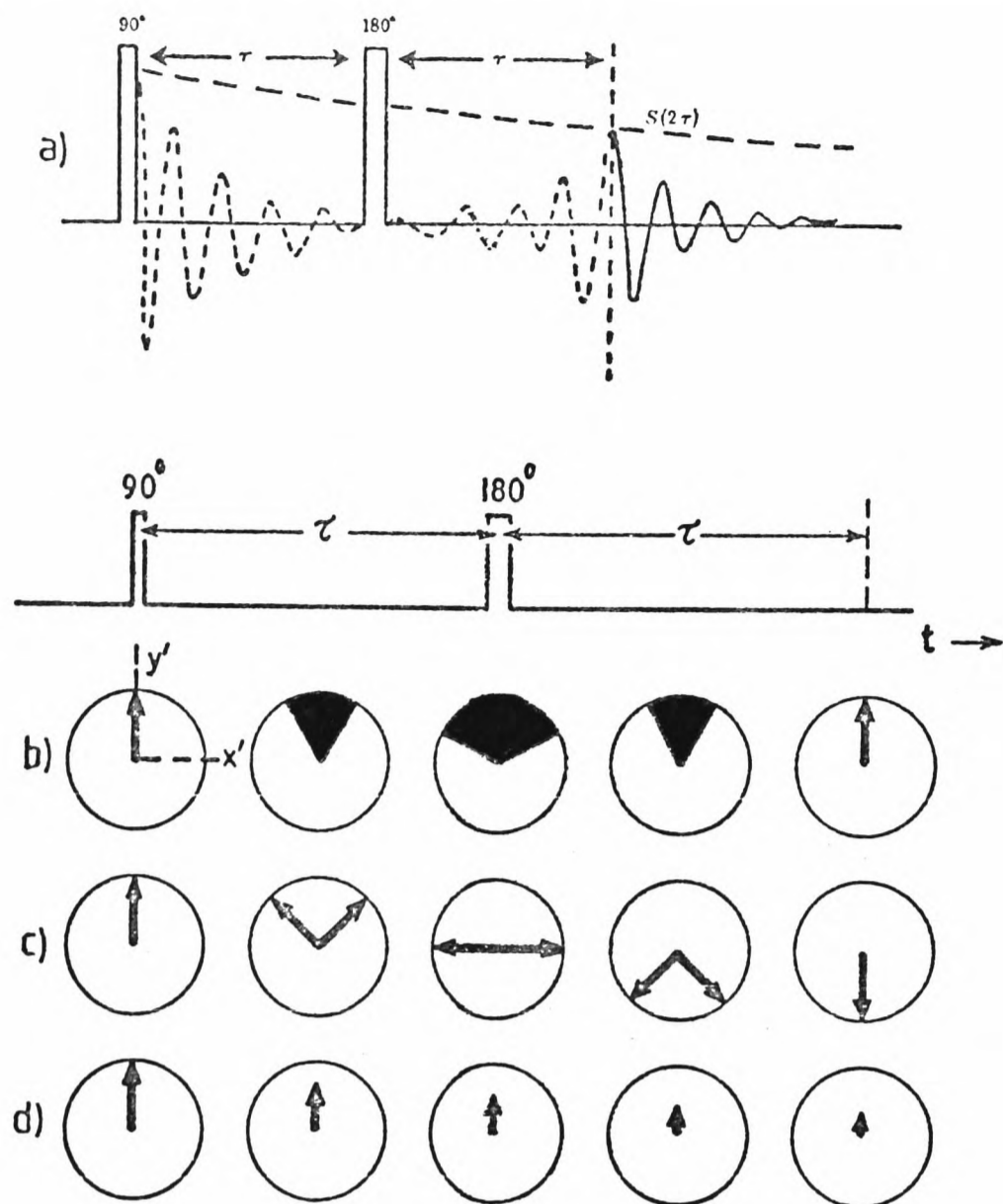


Figure 4

Spin echoes - refocussing of the magnetisation at time 2τ following a 180° pulse at time τ .

a) The signal detected in the x,y plane as the magnetisation vector rotates around the z axis.

Illustration of the effects in the x,y plane.

The 90° pulse introduces the magnetisation, which was previously along the z axis, into the y' direction at $t=0$. This magnetisation is then influenced by the field inhomogeneity, the coupling J , and T_2 . For illustrative purposes these three effects have been separated, but of course they happen simultaneously. b) The effects of field inhomogeneity: different parts of the sample resonate at slightly different frequencies, and fanning out of the magnetisation is observed. A 180° pulse reverses this process and all the components are in phase again forming an echo at $t=2\tau$. c) The effect of a 180° pulse on a doublet in a first order spectrum where both A and X are equally affected by the 180° pulse. Field inhomogeneity and chemical shift effects are still refocussed at time 2τ but the phase of each component in the doublet deviates from that of a singlet by an angle $\phi = +2\pi J\tau$. Thus for a first order spectrum refocussed when $2\tau = 1/J$, a doublet will be 180° out of phase with respect to the phase of a singlet. d) The T_2 decay.

2.6 The spin echo method

The intention here is to briefly outline the principles of the method. A basic understanding of n.m.r. is assumed and the reader is referred to the following texts for further information (Wuthrich, 1976; Campbell & Dobson, 1979).

A simple two pulse sequence $90^\circ - \tau - 180^\circ$ produces an echo at time 2τ after the 90° pulse (Carr & Purcell, 1954), (see figure 4). The amplitude of the echo is given by;

$$S(2\tau) = S(0) \exp(-2\tau/T_2 - 2D\gamma^2 G^2 \tau^3/3) F(J) \dots \dots \dots (3)$$

where γ is the magnetogyric ratio, G is the magnetic field gradient experienced by a molecule diffusing with coefficient D and $S(0)$ is the echo amplitude after the 90° pulse. The $F(J)$ term leads to modulation of the signal if there is homonuclear spin-spin coupling in the system. For a singlet $F(J)=1$ at all values of τ , but for a first order doublet, $F(J)$ is of the form $\cos(2\tau J)$ (see Campbell & Dobson, 1979 and references cited therein, see also figure 5). $S(2\tau)$ is thus a function of three variables: a) the intrinsic T_2 of the observed nuclear resonance, a parameter that depends largely on the mobility of the molecule observed; b) the spin-spin coupling patterns of the resonances and c) a term arising if the molecule diffuses to a region of different applied magnetic field during the refocussing period 2τ .

The dependence of echo amplitude on T_2 allows the selective observation of resonances on the basis of their T_2 s. At relatively long τ values the resonances of those molecules with short T_2 values are eliminated from the spectrum. This is illustrated in figure 6 which shows erythrocyte spectra collected at progressively longer τ values. For the single pulse experiment and at short τ values the spectrum is

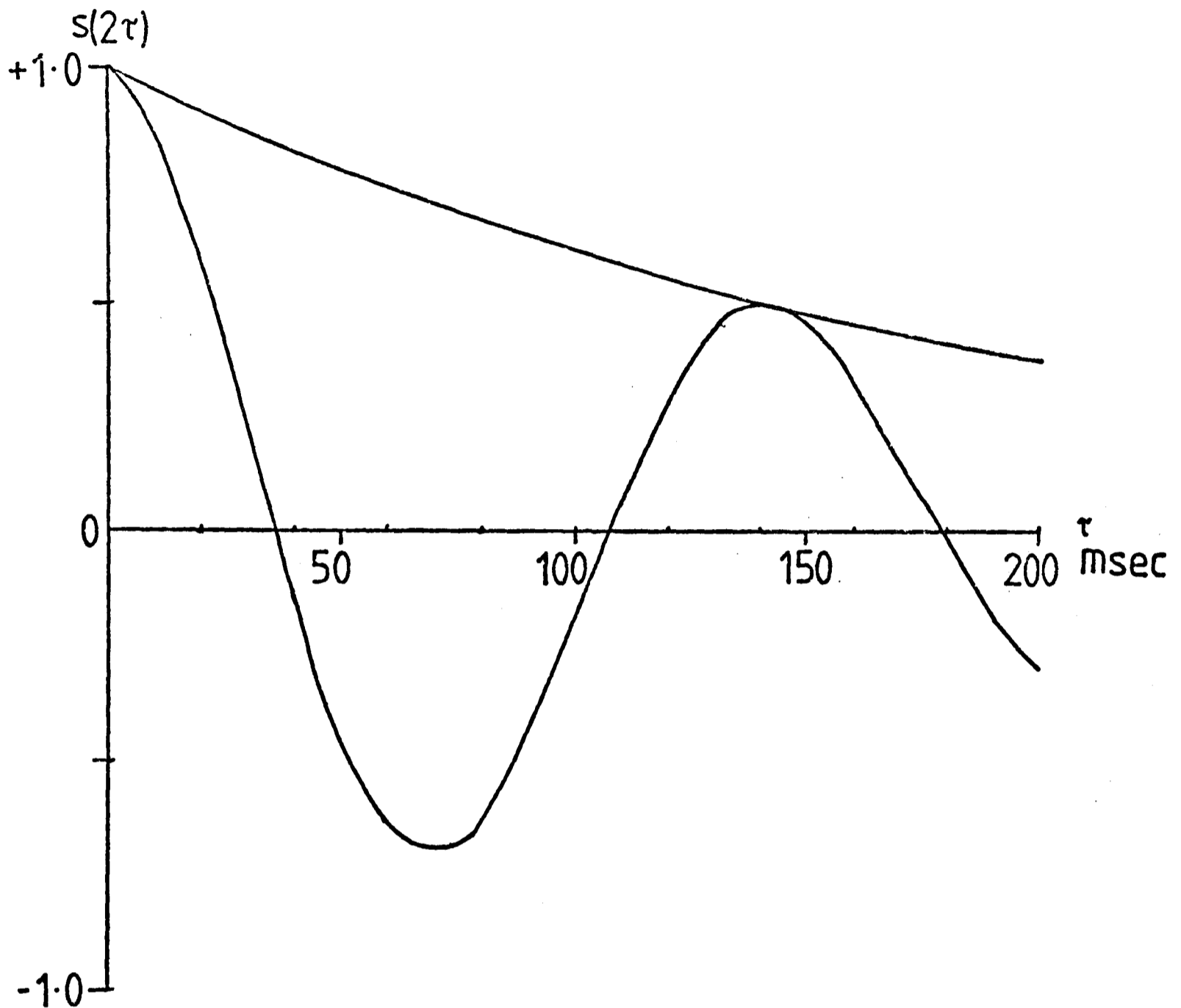


Figure 5

Phase modulation of echoes.

Line A shows the phase modulation of a doublet, $J=7$ Hz, as a function of τ in the spin echo experiment. The line was plotted using equation 3 although the diffusion term containing $DG^2\tau^3$ was omitted. $S(0)$ was arbitrarily given a value of 1 and T_2 a value of 200 ms. It should be noted that with diffusion the decay of the signal would be significantly faster. Line B shows the echo amplitude of a singlet under the same conditions. It can be seen that the doublet and singlet have an opposite phase at around 70 ms.

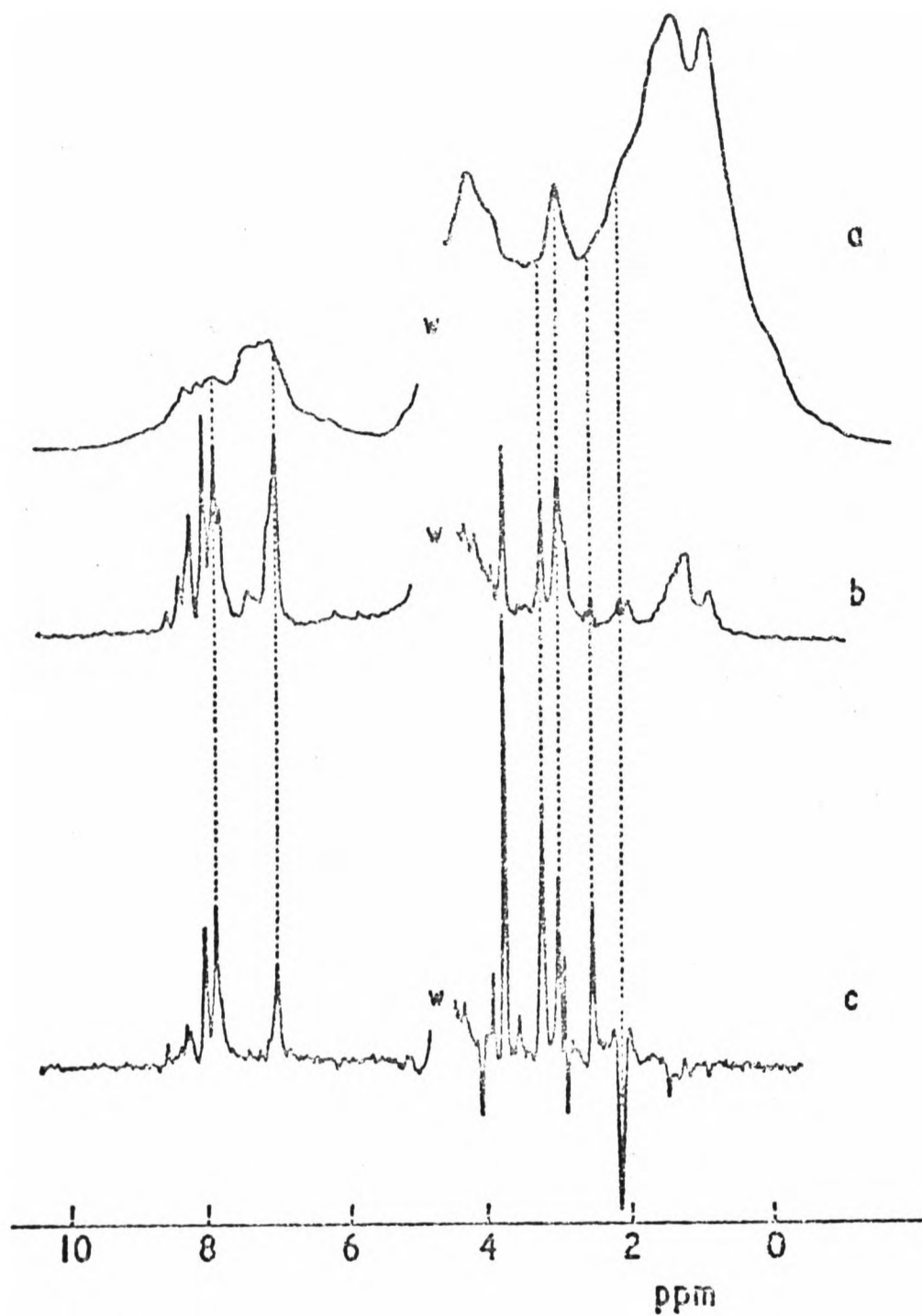


Figure 6

Proton spectra of human erythrocytes at 270 MHz

270 MHz spectra of glucose depleted erythrocytes at 37°C. a) Normal Fourier transform spectrum. b) Spectrum obtained using a $90^\circ - \tau - 180^\circ - \tau$ pulse sequence, with $\tau = 20$ ms. c) Spin echo spectrum with $\tau = 60$ ms.

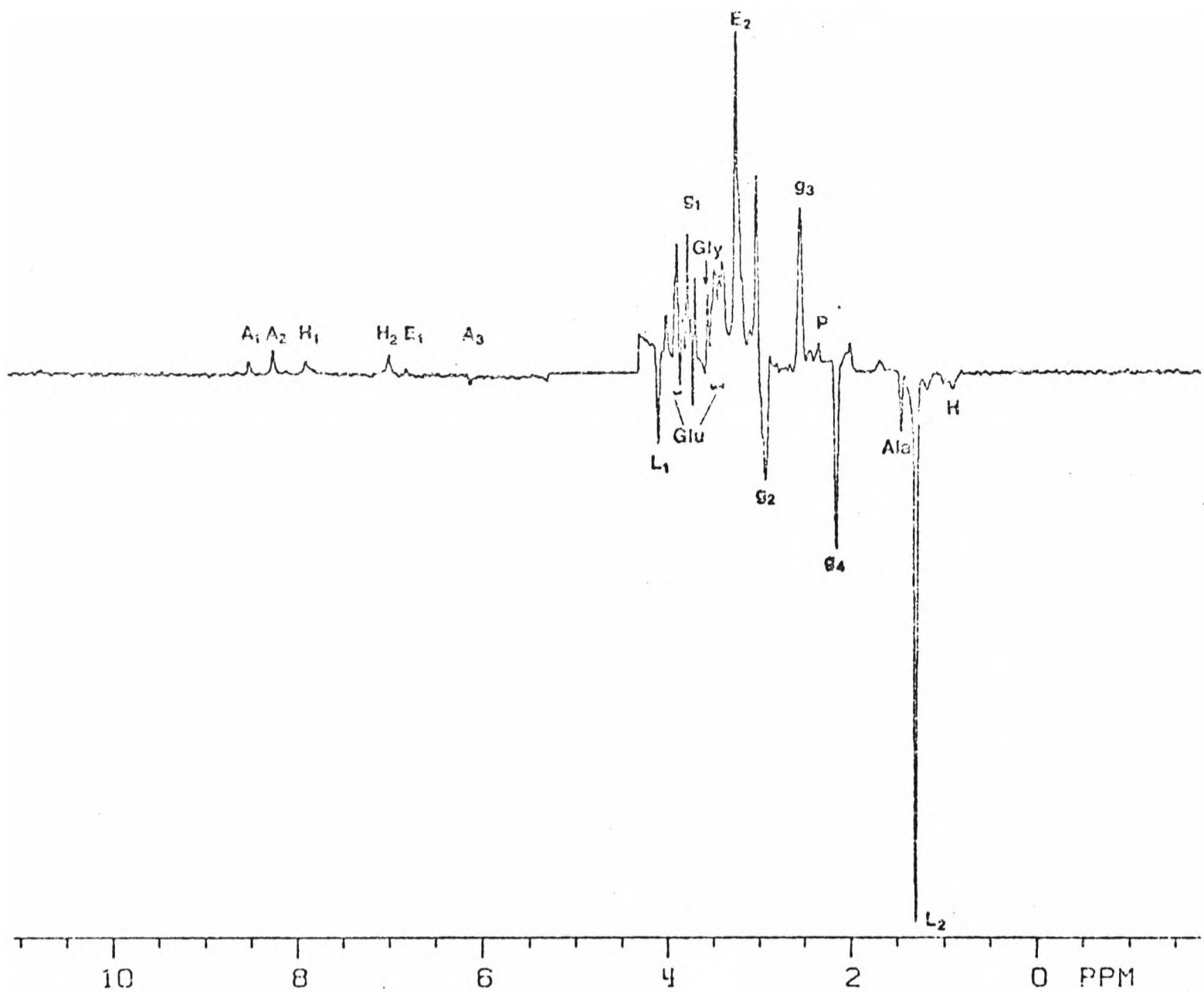


Figure 7

Spin echo proton spectrum of human erythrocytes at 470 MHz.

Spin₁ echo spectrum obtained at 470 MHz ($\tau=68$ ms) of packed erythrocytes in H_2O , Krebs Ringer buffer (containing 10mM glucose). The water resonance was suppressed by applying a saturating pulse at the water resonance frequency between successive repetitions of the $90^\circ-\tau-180^\circ-\tau$ pulse sequence. 168 scans were accumulated in 3 minutes. Chemical shifts (ppm) are with respect to sodium (2,3- H_2)-3-trimethylsilylpropanoate. The resonance assignments are as follows:

- A1,A2; from the purine ring of the adenine nucleotides, predominantly ATP (A1 C(8) of purine, A2 C(2) of purine).
- A(3); from the ribose moiety of the nucleotides, predominantly ATP (C(1') of ribose)
- Ala; alanine methyl
- E1, E2; ergothioneine
- gl-g4; glutathione
- Glu; glucose
- Gly; glycine
- H; methyl resonances from aliphatic amino acid residues of haemoglobin (e.g. valine, leucine, isoleucine)
- H1, H2; haemoglobin surface histidines (H1 C(2) ring proton, H2 C(4) ring proton).
- L1; lactate C-2 proton (coincident with an unassigned resonance).
- L2; lactate methyl
- P; pyruvate methyl

dominated by haemoglobin resonances. At longer τ values resonances from the relatively immobile nuclei of haemoglobin are lost due to their short T_2 s. This leaves resonances from the more mobile nuclei which have longer T_2 s e.g. from the metabolites lactate and pyruvate and the surface histidines of haemoglobin. Figure 7 shows an erythrocyte spectrum obtained at 470 MHz ($\tau=68$ ms) in which the resonance assignments are shown.

At longer τ values it may be observed that there is inversion of some peaks. This is due to the $F(J)$ term in equation 3, see also figure 5. Modulation in an observed resonance may be used to detect the properties of another resonance to which it is spin coupled. This is employed here to measure isotope exchange at the lactate C-2 position by monitoring peak inversion of the spin coupled C-3 protons. When a C-2 proton is exchanged for a deuteron the homonuclear coupling between the C-2 and C-3 proton resonances is removed and at 68ms $F(J)$ changes from -1 to +1 (see section on observation of the exchange).

The term involving $G^2 D$ in equation 3 is important if the observed molecule diffuses to a region of different field during the period 2τ . Under these circumstances the magnetisation does not refocus at 2τ and significant damping of echo amplitude can result. In cell suspensions field gradients may exist due to differences in magnetic susceptibility between the intra and extracellular compartments. In human erythrocyte suspensions the extracellular field inhomogeneity can be enhanced by the addition of a complexed paramagnetic ion. The resulting difference in echo intensity from molecules in the intra and extracellular compartments has been used to measure transport of small molecules into the cells (Brindle, et al 1979).

In addition to its dependence on γ , T_2 , J and magnetic susceptibility, echo amplitude will also depend on the T_1 of the resonance. Apart from the dependence on γ and J , T_2 and T_1 are factors which will affect the peak intensity of a resonance in any n.m.r. experiment and are not just peculiar to the spin echo experiment. (although T_2 is much more important in this case). The problems involved in quantitating a peak intensity in an n.m.r. spectrum in terms of concentration were mentioned in the introduction. The problem is to convert the peak intensity observed from an intracellular metabolite into concentration. If rapid pulsing is employed in order to maximise the signal-to-noise ratio then this inevitably results in saturation. In such a situation the peak intensity(ies) given by a standard solution of the metabolite in vitro will only be comparable to that given by the metabolite in situ if the T_1 s in the two cases are similar. T_1 s of metabolites in situ and in vitro may differ because of differences in ionic strength, pH and the occurrence of binding interactions. The problem can be avoided by pulsing more slowly in order to prevent saturation and a calibration protocol based on this approach has been described for ^{31}P n.m.r. studies (Dawson et al, 1977). The general problem of quantitation has been discussed by Burt et al (1979).

Fast exchange, on an n.m.r. timescale, of molecules between free and bound states will result in a spectrum showing contributions from both the free and bound forms. The relative contribution will depend on the lifetime of the molecule in each state. The fast exchange of ATP between a free solution form and haemoglobin bound form results in broadening of the ATP phosphate resonances in the n.m.r. spectrum (Gupta et al, 1978). In the limit of tight binding to a large protein (and

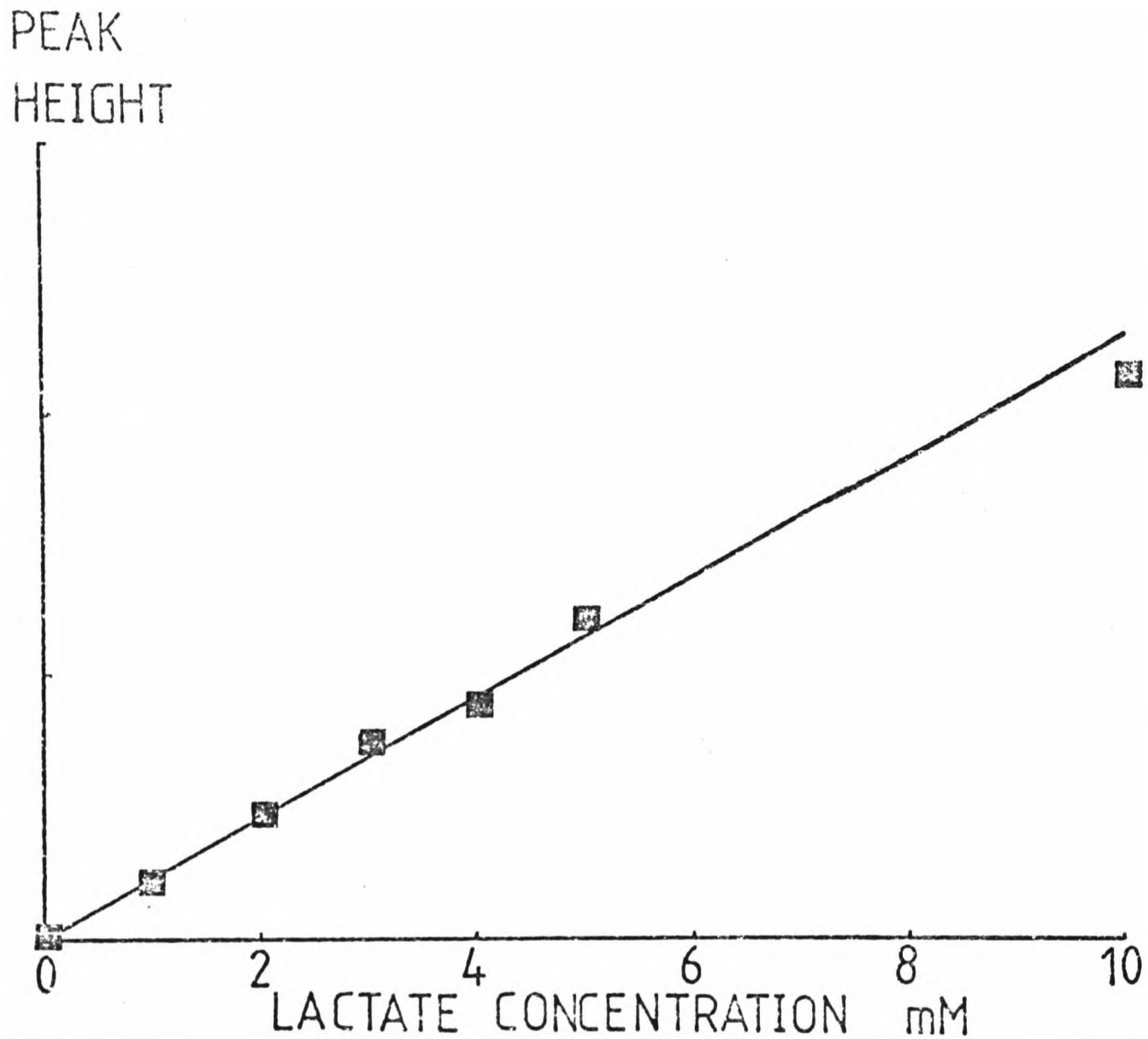


Figure 8

Dependence of methyl peak height on added lactate concentration in an erythrocyte suspension.

The cells were washed, in the absence of glucose, in Krebs-Ringer buffer made with $^2\text{H}_2\text{O}$. They were then packed and treated with 0.5mM iodoacetate to prevent endogenous lactate production. Aliquots of lactate were added to this cell suspension and spin echo spectra ($T = 68\text{ms}$) were recorded at 270 MHz (112 scans in 2 minutes) following each addition. The figure shows the dependence of the observed lactate methyl peak height on added lactate concentration.

consequently slow exchange) the resonances of a small molecule may disappear completely from the n.m.r. spectrum. For example ADP is not observed in muscle where it is tightly bound to actin (Gadian & Radda, 1981). Poor resolution, often found in ^1H spectra, may result in overlapping resonances. If peaks do overlap and this is not recognised then measurement of concentration from peak intensity will clearly be in error. Considerations such as these highlight the problems involved in relating peak intensity to the concentration, free or bound, of a molecule in an intact cellular system.

In the isotope exchange experiments to be described these problems are largely avoided since measurements of absolute concentration are not required. Furthermore the molecule observed, lactate, is not bound to any significant extent in the erythrocyte at the concentrations used here. This is demonstrated in figure 8 which shows the dependence of peak height on lactate concentration in an erythrocyte suspension. Lactate production, observed to occur at a linear rate by conventional assay procedures is also observed to be linear in the n.m.r. experiment, which again indicates that there can be no significant lactate binding in the cell. When measurements of absolute lactate concentration were required the lactate peak intensity in the n.m.r. spectrum was calibrated by adding a known amount of lactate to the cells. Lactate is rapidly transported across the cell membrane (Deuticke et al, 1978; Brindle et al, 1979).

In order to obtain estimates of isotope exchange rates at the lactate C-2 position the only n.m.r. requirements are that the T_1 and T_2 of the lactate methyl resonance should be unaffected by isotopic substitution at the C-2 position and thus that the relationship between

peak height and concentration should remain constant. The invariance of the lactate methyl resonance T_1 and T_2 is demonstrated in a later section.

Changes in magnetic susceptibility in an erythrocyte suspension could also change the proportionality between peak intensity and concentration. Although changes in susceptibility during measurement of an exchange time course are not generally observed the absence of fluctuations is not essential if estimates of the rate constant for the exchange are made from a single point. This point is the apparent $t_{1/2}$ for the exchange given by the point of peak inversion (see later). Since lactate is rapidly transported across the cell membrane the isotopic composition of the lactate in all regions of differing susceptibility will be essentially the same. A variable contribution of these regions to the peaks observed at the point of inversion, or null point, is obviously of no consequence.

Fluctuations in machine stability, like changes in susceptibility, are unimportant if the null point is used to estimate exchange rates. Small fluctuations in probe sensitivity and magnet homogeneity, however, can be corrected for by normalising peak intensities to an internal standard. The intensity of which should, in the absence of machine effects, remain constant. In erythrocytes the standard used has been provided by the coincident resonances from the quaternary methyls of intracellular ergothioneine and choline. In the in vitro studies lactate peak heights were usually normalised to a resonance from the buffer.

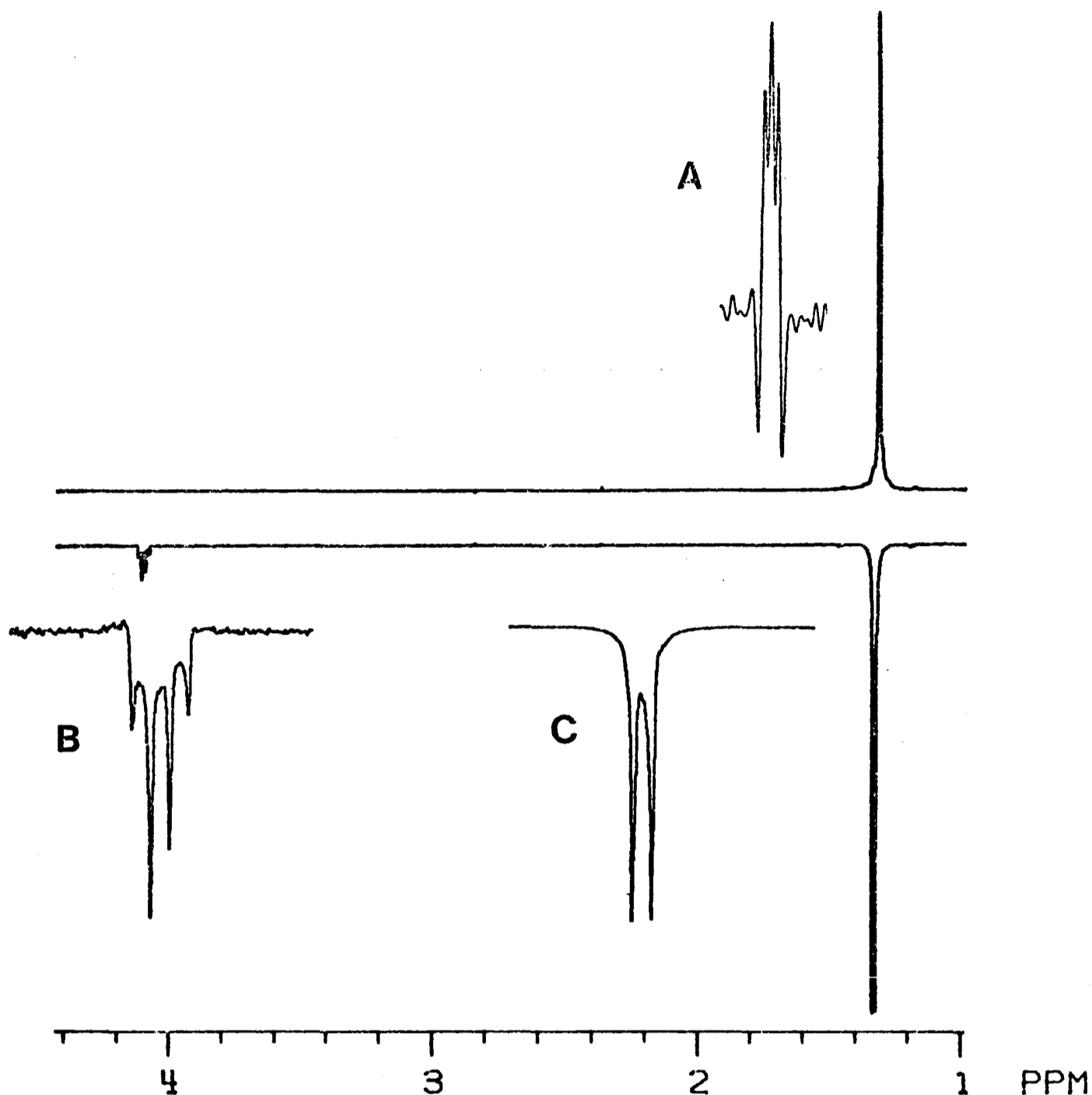


Figure 9

Spin echo spectra ($\tau = 68$ ms) of L-(U-¹H) lactate and L-(2-²H) lactate.

The spectra were obtained at 470 MHz with the exception of the expansion of the peak labelled A which was obtained at 300 MHz. The negative excursions in this spectrum are the result of the resolution enhancement procedure applied to the free induction decay. The top spectrum is of L-(2-²H) lactate and the bottom spectrum of L-(U-¹H) lactate. The peaks marked A and C are expansions of the methyl groups. The peak marked B is an expansion of the C-2 proton quartet.

The protonated and deuterated lactates were dissolved in 10mM phosphate buffer pH 7.2, 0.05 mM EDTA in ²H₂O.

2.7 Observation of the exchange

The spectrum obtained from L-(U-¹H) lactate using a $90^\circ - \tau - 180^\circ - \tau$ pulse sequence with τ set at 68ms is shown in the lower half of figure 9. It consists of a single proton (the C-2 proton) quartet at 4 ppm (labelled B in the figure) and a three proton (C-3 methyl) doublet at 1.3 ppm (labelled C). The coupling constant J between the C-2 proton and the protons of the methyl is approximately 7 Hz. Thus in a spin echo spectrum $F(J) = -1$ when $\tau = 68$ ms and the methyl resonance is inverted, (see figure 5). If the C-2 proton is exchanged for a deuteron the homonuclear coupling between the C-3 and C-2 proton resonances is lost and at $\tau = 68$ ms $F(J)$ changes from -1 to +1. This illustrated by the top spectrum shown in figure 9. The methyl resonance (labelled A) now has a positive phase. Heteronuclear coupling with the C-2 deuteron leads to splitting of the methyl resonance. Since the deuteron has a spin quantum number of 1 this coupling results in a triplet which has components of equal intensity. The coupling is very weak with a coupling constant of 1 Hz.

The rate of isotope exchange at the lactate C-2 position can thus be monitored by observing inversion of the methyl resonance. This has three major advantages over direct observation of the C-2 proton, these are; a) by observing inversion of the signal from the three protons of the methyl the effect of the exchange of the single proton or deuteron at the C-2 position is amplified. Since the T_2 of the C-2 proton resonance is shorter than that of the methyl resonance this results in an amplification factor in excess of 6 in the spin echo experiment; b) direct observation of the C-2 proton is difficult due to its close proximity to the water resonance and c) at the point of peak inversion

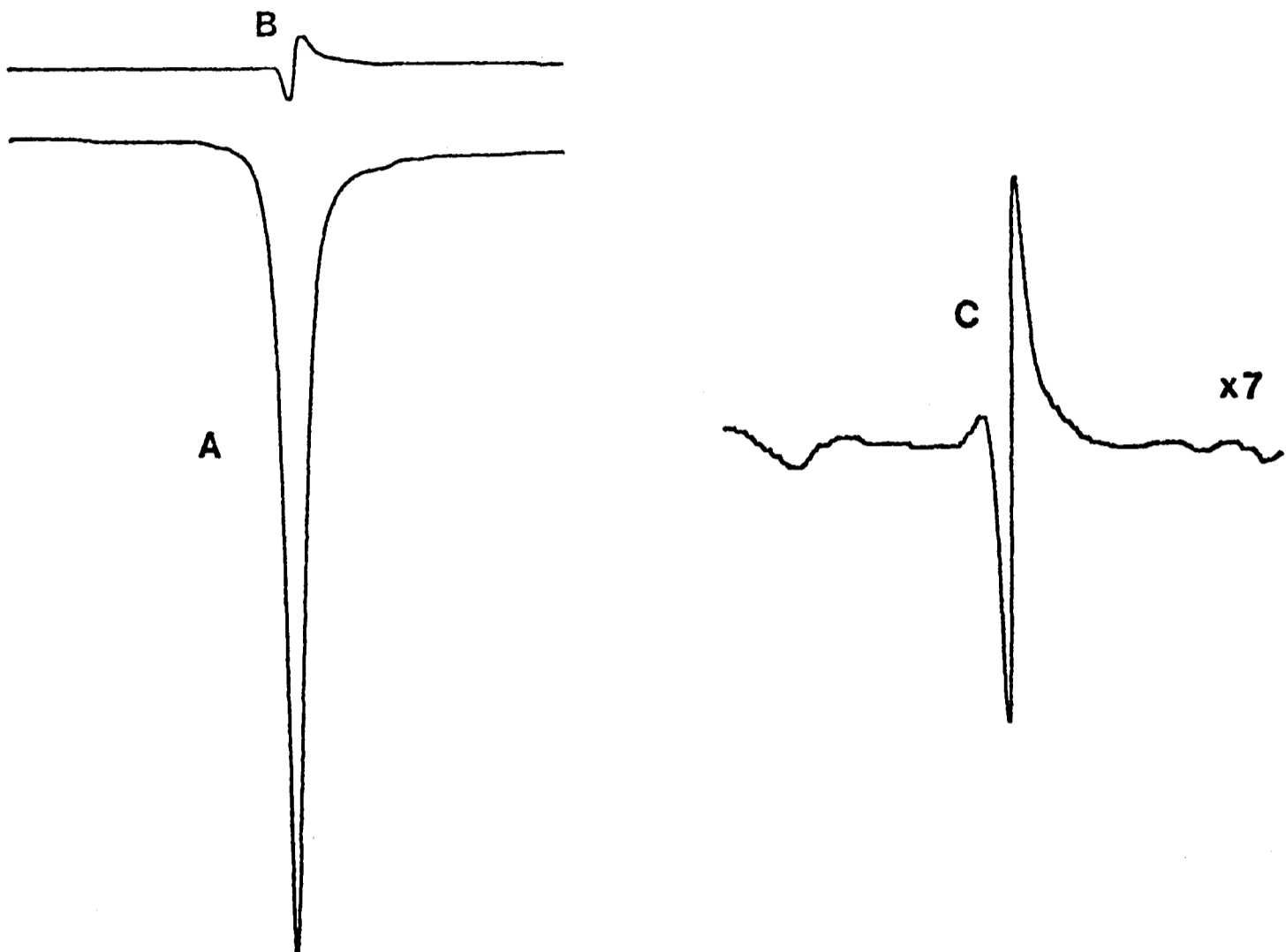


Figure 10

Spin echo proton spectra demonstrating that deuterium substitution at the C-2 position of lactate results in symmetrical inversion of the methyl resonance about the baseline. Observation of a null point.

A The methyl region of a spin echo spectrum ($\tau = 68$ ms) of 10mM $\overline{\text{L}}\text{-(U-}^1\text{H)}\text{lactate}$. B The methyl region of the spectrum obtained following the addition of 10mM $\text{L-(2-}^2\text{H)}\text{lactate}$, C shows an expansion of this region.

The lactates were dissolved in 100mM imidazole-glycylglycine buffer pH 7.4, 0.5mM EDTA in $^1\text{H}_2\text{O}$. The water resonance was suppressed by applying a saturating pulse at the water resonance frequency between successive repetitions of the $90^\circ - \tau - 180^\circ - \tau$ pulse sequence. The free induction decays were multiplied by an exponential with a time constant which resulted in a 30 Hz line broadening.

a "null point" is obtained (illustrated in figure 10) which represents the point at which 50% of the lactate present is deuterated at the C-2 position. Such a point is obtained because unlike with conventional radioactive labelling techniques and the ^{13}C n.m.r. labelling technique described in the first chapter both the labelled and unlabelled forms of the lactate are observed. The "null point" or point of 50% labelling has important implications for the measurement of exchange rates in erythrocytes where there is endogenous lactate production (see later).

The equivalence of the positive and negative lactate methyl resonances at $\tau = 68$ ms is demonstrated by the spectrum, shown in figure 10, of an equimolar mixture of L-(2- ^2H) lactate and L-(U- ^1H) lactate. The observed "null point" results from the summation of the positive methyl peak of the C-2 deuterated lactate with the negative methyl peak of equal intensity from the C-2 protonated lactate. Symmetry of inversion and consequently a null point at 50% labelling would not be observed if deuteration/protonation at the C-2 position affected the relaxation properties of the methyl protons. For example partial deuteration of the lactate methyl group has been shown to affect the T_1 s of the remaining protons (Simpson et al, 1982a). The incomplete cancellation of the methyl peaks at the null point is due to a small upfield shift of the methyl protons in the lactate deuterated at the C-2 position. This, however, has a negligible effect on the observed inversion of the methyl peak and estimations of the rate constant for the exchange from the time course of this inversion. Changes in the multiplicity of the methyl resonance have a negligible effect on the observed methyl peak height (and thus symmetry of inversion) due to the large linewidths in the observed spectra. Intrinsic linewidths were further increased by exponential multiplication of the free induction

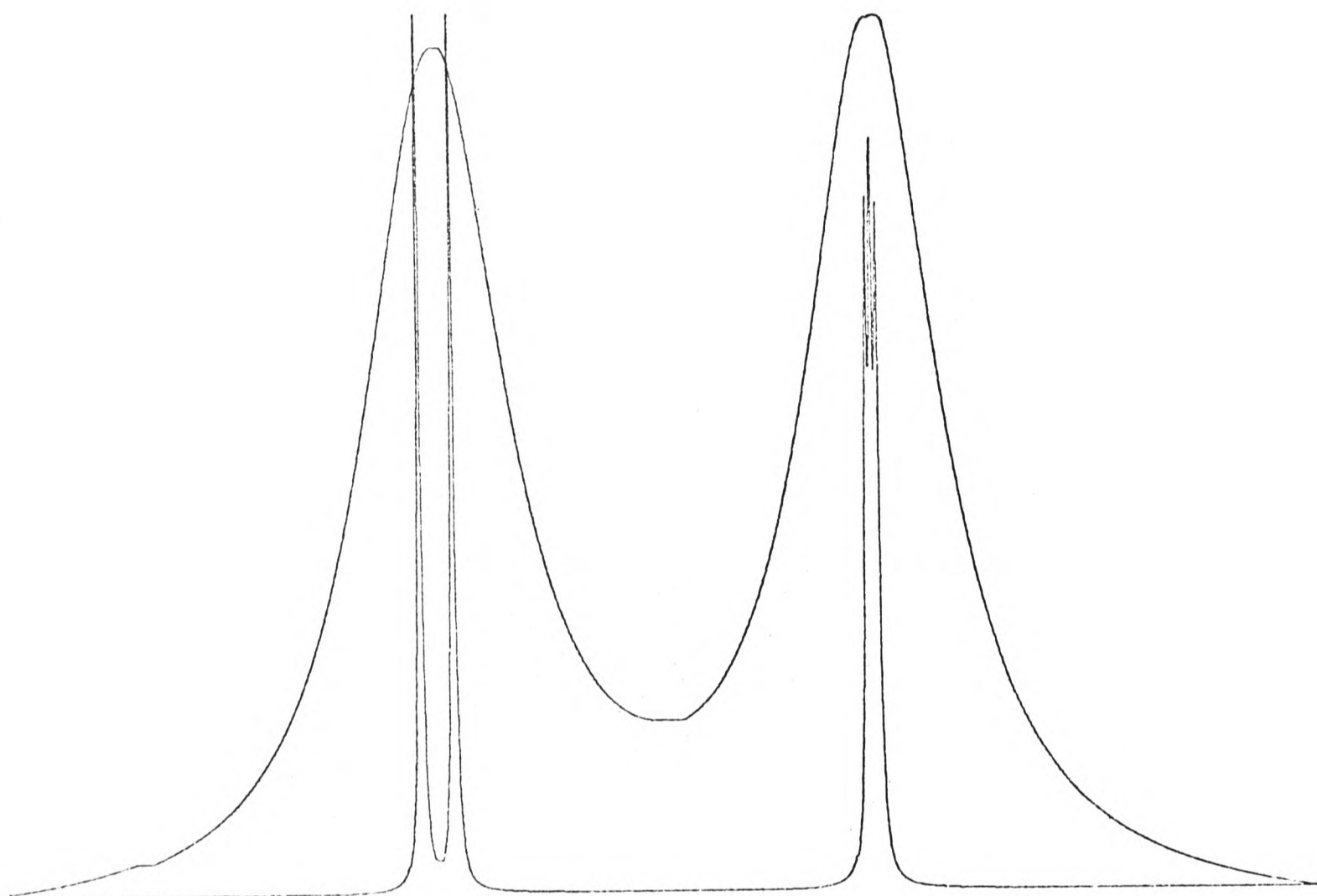


Figure 11

Simulated spectra showing the effect of linewidth on peak height.

A simulated spectrum (lower trace) showing a doublet and triplet of equal intensity. If the linewidths are assumed to be 1 Hz then the doublet has a coupling constant of 7 Hz. When the lines are broadened to give linewidths in excess of $4J$ the peak heights of the doublet and triplet become equal (upper trace). The spectra were generated using commands available in the Nicolet 1180 computer software.

decays with time constants which resulted in a 16 or 30 Hz line broadening (A 16 Hz line broadening was applied to cell spectra and 30 Hz to spectra obtained from in vitro preparations where the intrinsic line widths were much smaller). This is illustrated in the simulated spectra shown in figure 11. When the linewidths are less than or comparable to J there is a significant difference in the peak height of a doublet and triplet of equal intensity. However when the linewidths are in excess of 4J (where J is the coupling constant of the doublet, which for lactate is approximately 7 Hz) then the peak heights of the doublet and triplet become equal. (A similar result is obtained with a doublet and singlet of equal intensity.)

Figures 12A and 12B show exchange time courses which demonstrate lactate peak inversion in erythrocyte suspensions in buffer made with $^2\text{H}_2\text{O}$ and $^1\text{H}_2\text{O}$ and incubated with L-(U- ^1H)lactate and L-(2- ^2H)lactate respectively.

2.8 Estimation of isotope exchange equilibrium velocities

Equilibrium velocities in vitro were calculated by multiplying the lactate concentration by a first order rate constant obtained from a least squares fit of the exchange timecourse. (The fitting procedure used is a standard routine available in the Nicolet 1180 computer software).

In cells, because of endogenous lactate production, the time at which peak inversion occurs, referred to subsequently as t_{null} , is used to calculate V_{C2X} , the overall equilibrium velocity. Endogenous lactate production during an exchange time course has a number of effects; a) it dilutes the added lactate, b) it affects the peak heights observed

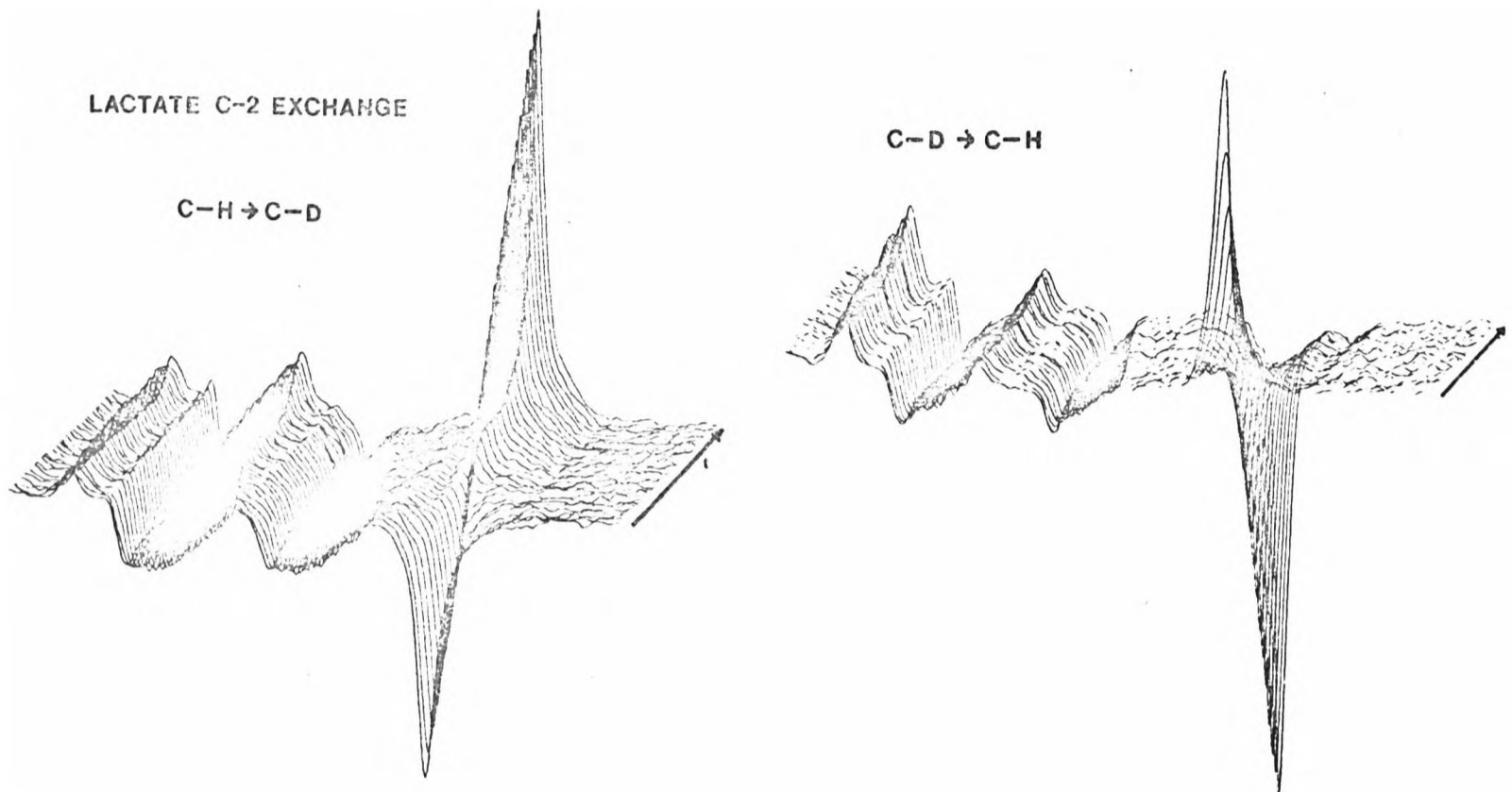


Figure 12

Stacked plots of lactate₂ C-2 isotope exchange time courses in erythrocyte suspensions in ²H₂O and ¹H₂O.

A
Inversion of the lactate methyl resonance following the addition of 12mM L-(2-¹H) lactate to erythrocytes in Krebs-Ringer buffer made with ²H₂O (75% haematocrit). Sequential 2 min (112 scan) spin echo ($\tau = 68\text{ms}$) spectra were accumulated following the addition of the lactate.

B
Inversion of the lactate methyl resonance following the addition of 12mM L-(2-²H) lactate to erythrocytes in Krebs-Ringer buffer made with ¹H₂O (75% haematocrit). Sequential 2 min (112 scan) spin echo ($\tau = 68\text{ms}$) spectra were accumulated following the addition of the lactate.

during the exchange time course of the added lactate and c) it represents a source of lactate labelled with solvent isotope in addition to that produced by exchange.

At the point of peak inversion the positive and negative components of the lactate methyl peak effectively cancel out and a null point is obtained. This point (t_{null}) represents the point at which 50% of all the lactate present is solvent labelled at the C-2 position. V_{C2X} can be calculated from t_{null} as follows.

If endogenous lactate production during an exchange time course is negligible and if L_0 and L_e are the concentrations of added and solvent labelled lactate respectively at $t=0$, then:

$$V_{\text{C2X}} = \frac{(L_0 + L_e)}{t_{\text{null}}} \ln \left[\frac{2L_0}{L_0 + L_e} \right] \dots\dots\dots(4)$$

L_e is calculated by taking a spectrum prior to addition of the labelled lactate and from knowledge of the percentage labelling at the C-2 position of the added lactate.

If there is endogenous lactate production and the rate of this is small compared to V_{C2X} , then the following equation can be used to give an approximate correction for this effect.

$$V_{\text{C2X}} = k_L \frac{\ln \left[\frac{2L_0}{Lt_{\text{null}}} \right]}{\ln \left[\frac{Lt_{\text{null}}}{L_0 + L_e} \right]} \dots\dots\dots(5)$$

This equation was derived from an integrated rate equation which allowed for dilution of the lactate pool by endogenous lactate production and which assumed that solvent label was introduced into this pool at a constant rate, k_L , independent of that introduced by exchange.

Calculation of V_{C2X} from the point of peak inversion, where the fractional labelling state at the C-2 position is known, avoids the necessity of fitting the exchange time course to the integrated rate equation. This simplification would not be possible if the exchange were observed by monitoring the peak intensity of the C-2 proton directly. Furthermore the t_{null} method does not require knowledge of the endpoint for the exchange only the degree of labelling of the lactate present at $t=0$ which is readily obtained. The derivation of these equations is shown in appendix 4.

C-2 Exchange in vitro

An in vitro exchange system was produced by mixing aldolase, glyceraldehydephosphate dehydrogenase and triosephosphate isomerase from rabbit muscle and human erythrocyte lactate dehydrogenase. NAD^+ , FDP and lactate were the only substrates added. The other substrates necessary for the exchange, GAP, DHAP, NADH and pyruvate are produced by equilibration of FDP and lactate across the reactions catalysed by aldolase and lactate dehydrogenase respectively. Exchange time courses were initiated by adding 12mM L-(U- 1 H)lactate to the enzyme mixture. The mixtures were preincubated with FDP for approximately five minutes prior to lactate addition in order to ensure that the FDP had come to chemical and isotopic equilibrium. Both of these processes are expected to be rapid. Loss of protons from FDP to solvent 2H_2O , in the reaction

$1/V_{C2X}$ (UMOL/MIN/ML)⁻¹

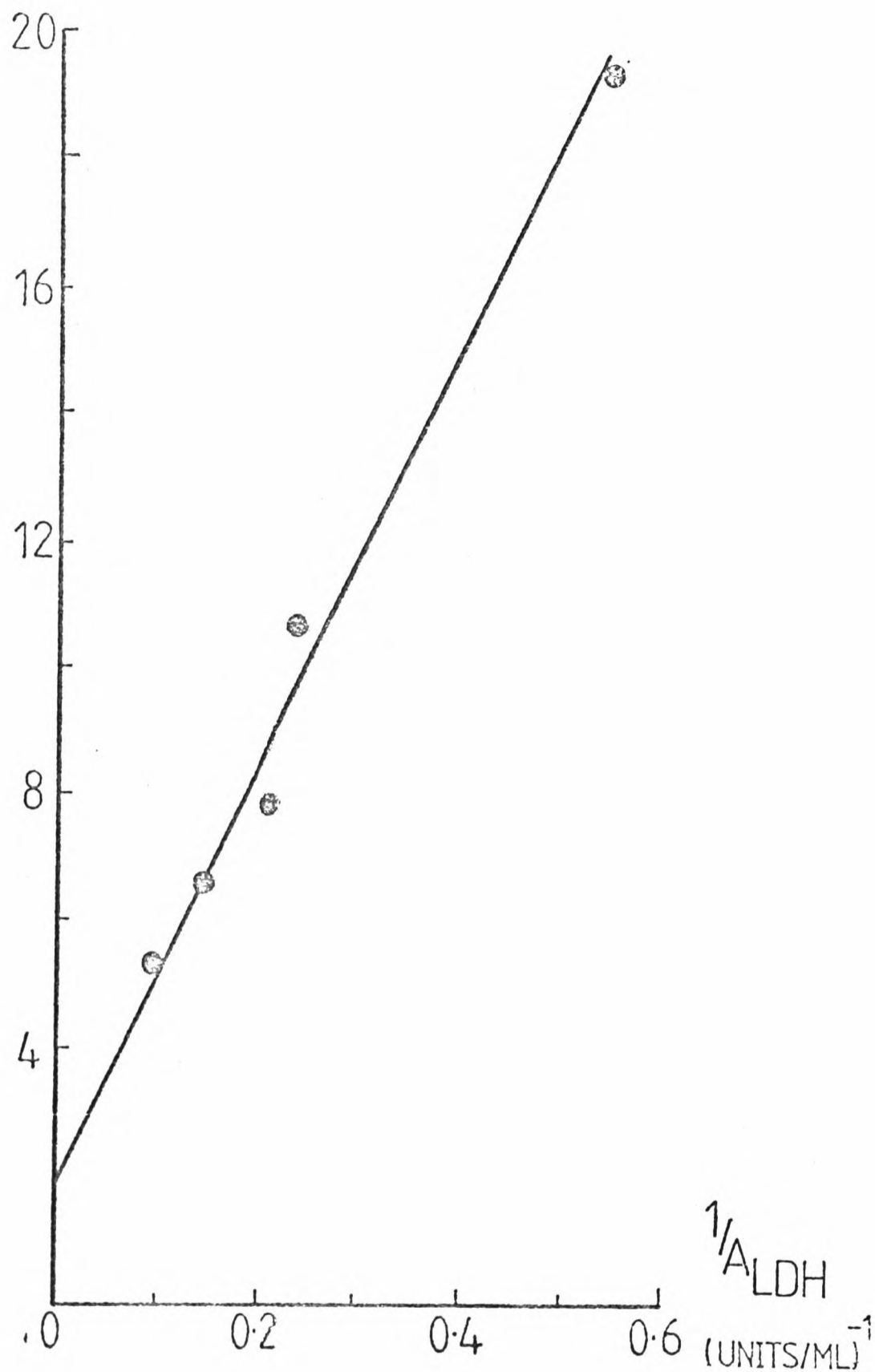


Figure 13

Plot of $1/V_{C2X}$ versus $1/A_{LDH}$ obtained in an in vitro C2 exchange system.

The mixture of enzymes contained approximately 3 units/ml glyceraldehyde phosphate dehydrogenase, 200 units/ml triosephosphate isomerase and 0.3 units/ml aldolase in 100mM Tris - HCl pH 7.4, 3mM dithioerythritol and 0.5mM EDTA. NAD⁺, 100μM and FDP, 200μM, were added approximately 5 min prior to the start of a time course which was initiated by the addition of 12mM L-(2-¹H) lactate. The exchange was monitored by collecting spectra (112 scans each) every 2 min for 40 min. Lactate dehydrogenase assays were performed at 37°C in 100mM Tris - HCl pH 7.4, 0.5mM EDTA. The oxidation of 0.2mM NADH was monitored at 340nm following the addition of 1mM pyruvate.

catalysed by aldolase, is considerably faster than the exchange of isotope at the lactate C-2 position. More important, however, is that the concentration of DHAP and the other intermediate substrates involved in the exchange are present at much lower concentrations than the lactate. Relaxation of the FDP/DHAP/GAP system to chemical equilibrium is rapid since only 200 μ M FDP was added to mixtures containing approximately 0.3 units/ml of aldolase (which has a very low K_m for FDP (Mehler, 1963) and approximately 200 units/ml triosephosphate isomerase. Relaxation of the lactate/pyruvate system to chemical equilibrium is also rapid, attainment of equilibrium requiring an estimated conversion of 17 μ M lactate and NAD^+ to pyruvate and NADH respectively. Although the in vitro experiments shown in this chapter were performed in $^2\text{H}_2\text{O}$ they can also be performed in $^1\text{H}_2\text{O}$ with L-(2- ^2H) lactate (see chapters 3,5 and 6).

2.9 Determination of an individual enzyme equilibrium velocity in vitro

Measurement of V_{C2X} in enzyme mixtures, where the concentrations of three of the four enzymes involved in the exchange are held constant and the fourth varied, allows the equilibrium velocity of the varied enzyme to be determined. The equilibrium velocity of human erythrocyte lactate dehydrogenase was determined by holding the concentrations of aldolase, triosephosphate isomerase and glyceraldehydophosphate dehydrogenase constant while the lactate dehydrogenase concentration was varied. Fig.13 shows a plot of $1/V_{\text{C2X}}$ versus $1/A_{\text{LDH}}$, where A_{LDH} is lactate dehydrogenase activity measured spectrophotometrically. The linearity of the plot demonstrates that the velocity of C-2 exchange can be related to enzyme activity by the following equation,

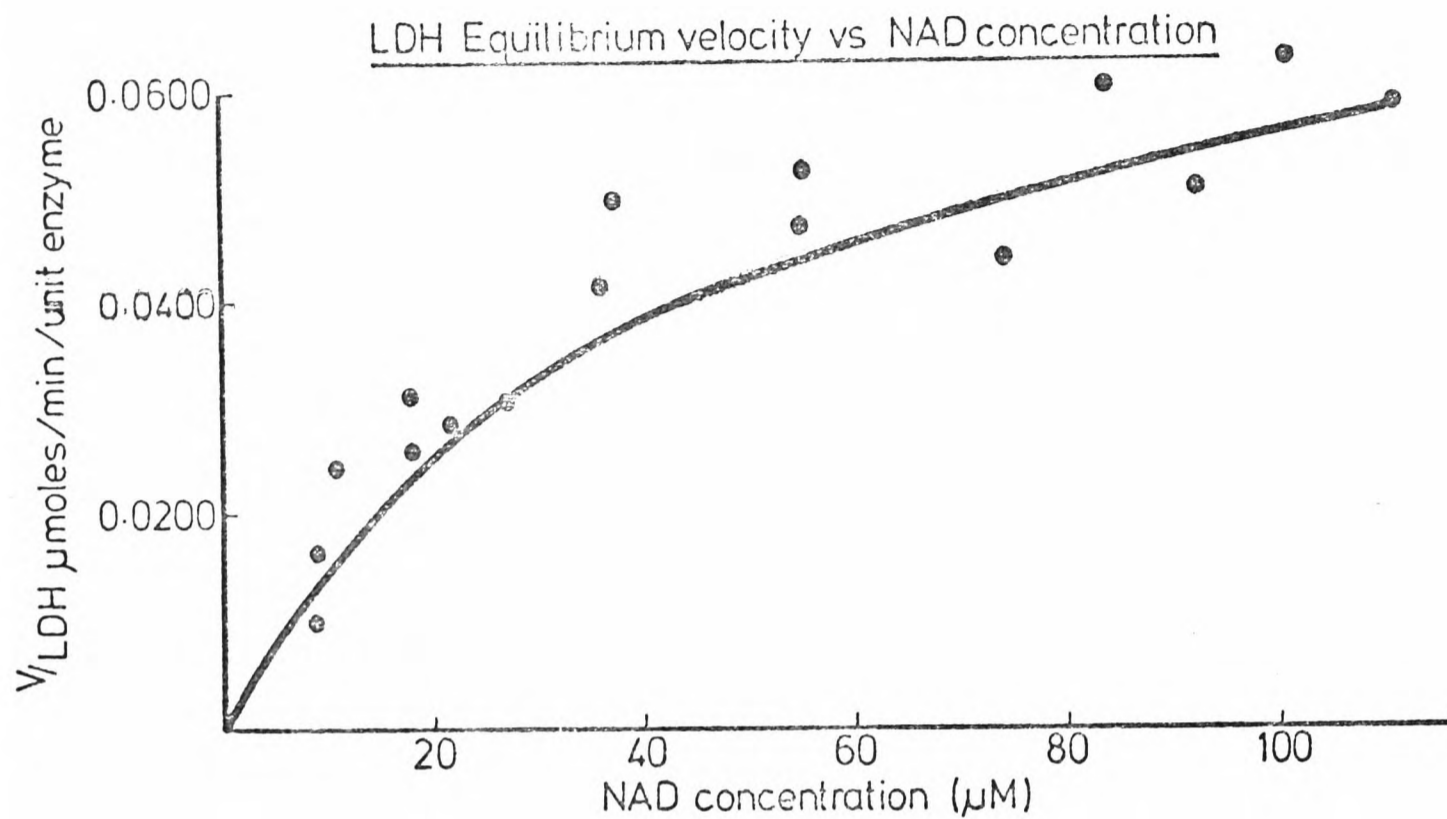


Figure 14

Dependence of the lactate dehydrogenase isotope exchange equilibrium velocity on NAD^+ concentration in an in vitro C-2 exchange system.

The conditions of the experiment were similar to those described in the legend to Fig.13. This experiment was repeated at various NAD^+ concentrations and the lactate dehydrogenase equilibrium velocity obtained at each NAD^+ concentration. The NAD^+ concentrations quoted are those of the NAD^+ added to the enzyme mixture. The slopes of the double reciprocal plots, which were determined by logarithmic linear regression, were used to calculate lactate dehydrogenase equilibrium velocities. A better method for obtaining equilibrium velocities from the exchange data is discussed in the next chapter.

$$\frac{1}{V_{C2X}} = \frac{1}{(V_R)} + \frac{2}{\alpha A_{LDH}} \dots\dots\dots(6)$$

The term $(1/V_R)$ is the sum of the reciprocals of the equilibrium velocities for aldolase, triosephosphate isomerase and glyceraldehydophosphate dehydrogenase. The term $2/\alpha A_{LDH}$ is equivalent to $1/V_{LDH}$, the reciprocal of the lactate dehydrogenase equilibrium velocity. Thus the plot shown in Fig. 13 has a slope of $2/\alpha$ and an intercept on the ordinate of $1/V_R$. The term α is the specific equilibrium velocity of the lactate dehydrogenase. The value obtained for α , 0.064umols lactate exchanged/min/unit of enzyme activity, can be compared with a value of 0.057 calculated using an equation derived by the method of Yagil and Hoberman (1969) for lactate dehydrogenase and using the kinetic constants of the beef heart enzyme (Borgmann et al, 1974) (see appendix 1 for equation). It should be pointed out, however, that the level of agreement may be coincidental since the kinetic constants, in addition to being for the beef heart enzyme, were obtained in 1H_2O rather than 2H_2O and in phosphate buffer, in which lactate dehydrogenase displays a higher affinity for NAD^+ and NADH than in Tris buffer (Winer & Schwert, 1958). Deuterium substitution also affects the binding of these coenzymes (Thomson et al, 1964).

2.9.1 Effect of substrate concentration

The effect of the concentration of a substrate on an individual enzyme can be determined by measuring the specific equilibrium velocity of the enzyme at a variety of concentrations of the particular substrate. For example the dependence of the lactate dehydrogenase equilibrium velocity on NAD^+ concentration is shown in Fig.14. The solid line is a theoretical curve derived from the equation shown in appendix 1 and the kinetic constants of the beef heart enzyme.

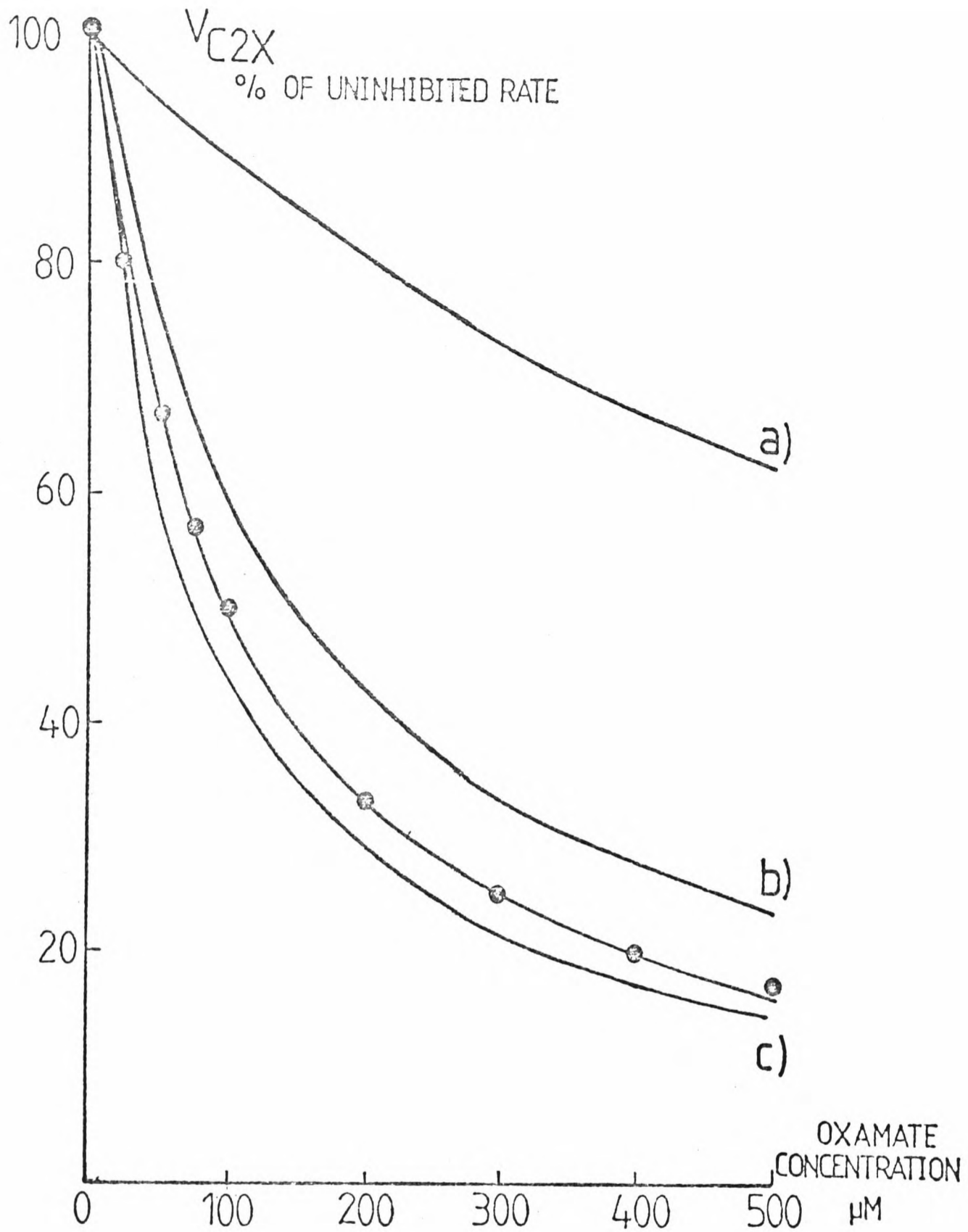


Figure 15

Effect of oxamate on V_{C2X} observed in an in vitro C-2 exchange system.

The conditions of the experiment were similar to those described in the legend to Fig.13. The solid line drawn through the experimental points is a theoretical curve constructed by assuming that there is simple competitive inhibition of lactate dehydrogenase by added sodium oxamate (see appendix 2). The other lines are theoretical curves which show the effect of changing the ratio of the lactate dehydrogenase equilibrium velocity to that of the other enzymes, (a) $V_{LDH}/V_R = 20$, (b) $V_{LDH}/V_R = 2.0$, (c) $V_{LDH}/V_R = 0.2$.

2.9.2 Effect of an inhibitor

Fig. 15 shows the effect of oxamate, an inhibitor of lactate dehydrogenase (Novoa et al, 1959), on V_{C2X} in vitro. The line drawn through the experimental points is a theoretical curve constructed with the assumption that oxamate is a simple competitive inhibitor of lactate dehydrogenase (see appendix 2). The other curves plotted in Fig.15 show how the sensitivity of the exchange to inhibition of lactate dehydrogenase is altered by changing the sensitivity coefficient of the enzyme. If the coefficient is decreased by increasing the lactate dehydrogenase concentration then the exchange becomes less sensitive to inhibition of the enzyme. The figure demonstrates the relationship between elasticity and sensitivity with regard to the overall rate of exchange. A similar plot showing the effect of a substrate concentration on the exchange would be more complex since it will change the equilibrium velocity of more than one enzyme.

The close fit of the experimental data to the theoretical curve demonstrates the precision of the n.m.r. technique for measuring the rate of isotope exchange. In this experiment the only variable was the oxamate concentration.

This inhibition experiment can be carried out with erythrocytes and used to estimate the sensitivity coefficient of the enzyme in situ. A comparison of this coefficient, with that expected from the enzymes activity in the cell and its known isotope exchange properties in vitro, yields information regarding the free concentrations of its substrates NAD^+ and NADH in the intact cell (see chapter 6).

2.10 C-2 exchange in situ

In erythrocytes the glycolytic system is not at equilibrium but in a steady state. However the enzymes involved in C-2 exchange; aldolase, triosephosphate isomerase, glyceraldehydophosphate dehydrogenase and lactate dehydrogenase are all near equilibrium in the erythrocyte (Minikami & Yoshikawa, 1966). That is, the mass action ratios of their substrates are similar to the equilibrium constants measured for these enzymes in vitro. It is this near equilibrium condition which permits exchange of isotope. A further consideration in the intact cell is that of lactate transport across the cell membrane. This however is rapid at 37°C (Deuticke et al, 1978; Brindle et al, 1979) and thus V_{C2X} will be relatively insensitive to the rate of transport. This demonstrates a general point that in order to study the isotope exchange properties of enzymes in intact cells a labelled molecule must be used which rapidly penetrates the cell membrane.

If the effect of substrate concentrations on the exchange in situ are to be examined then these must be changed without destroying cellular integrity. In the case of substrates transported across the cell membrane, for example lactate and pyruvate, this can be achieved by simple addition of these substrates to the cell suspension. For substrates to which the membrane is impermeable then these must be changed indirectly, for example the triosephosphate concentrations can be raised by incubation at 40°C.

2.10.1 The effect of DHAP concentration on the exchange

The relatively rapid rate of exchange at the lactate C-2 position, observed in intact cells, is dependent on the presence of high levels of DHAP. For example, blood stored in citrate/phosphate/glucose shows no

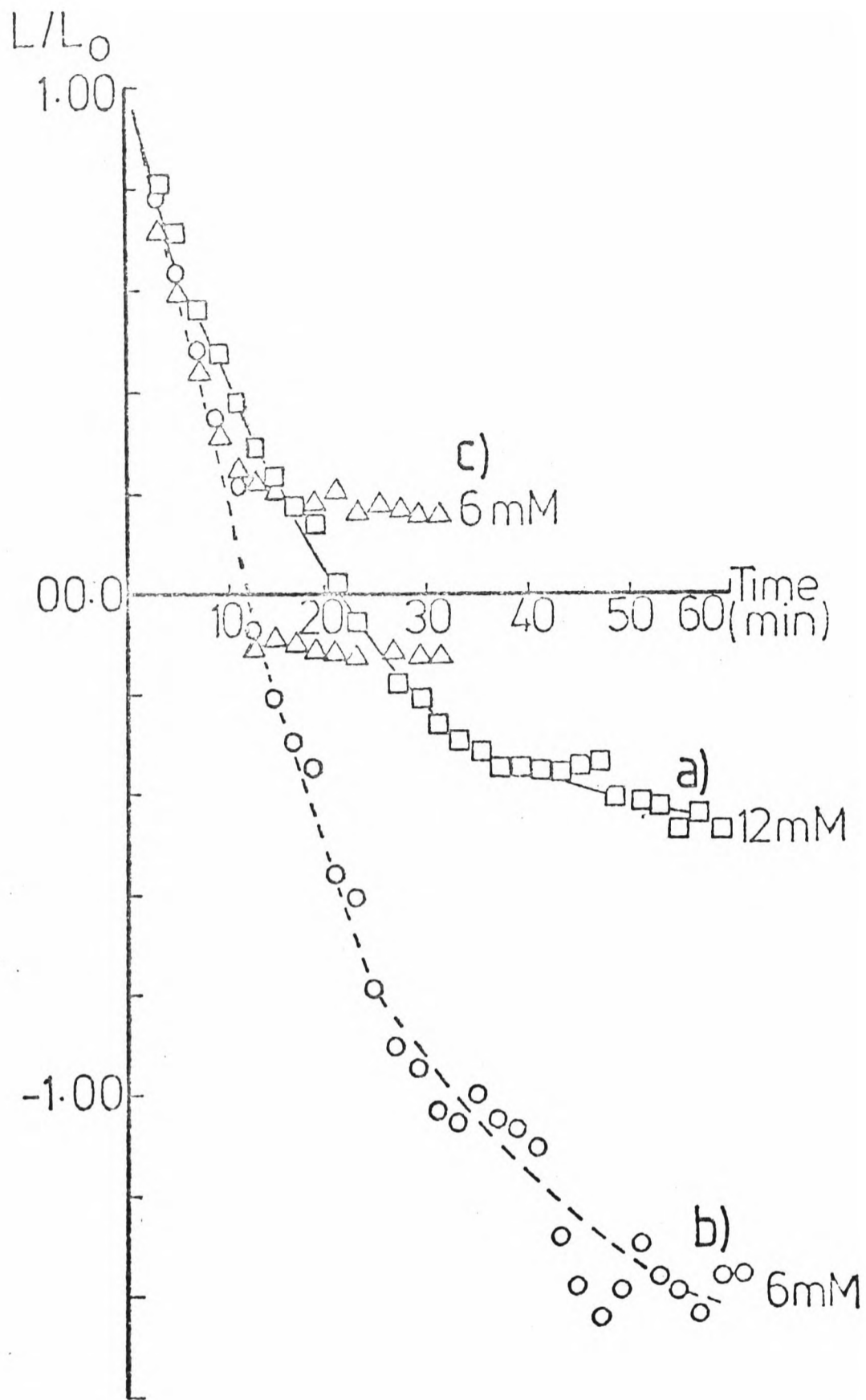


Figure 16

Effect of triosephosphate depletion on the exchange in erythrocytes.

Plot of the ratio of peak height at time t (L) to peak height at $t=0$ (L_0) for L -(2 - 2 H)lactate incubated with intact erythrocytes and a lysate in 0 Krebs-Ringer buffer made with 1 H $_2$ O.

a) Erythrocytes (76% haematocrit) with 12mM lactate; b) erythrocytes (68% haematocrit) with 6mM lactate; c) lysate prepared from erythrocytes with an haematocrit of 71%, with 12mM lactate.

observable exchange and very low levels of the triose phosphates and FDP (Bartlett & Barnet, 1960; Table 1). However, if erythrocytes are washed in Krebs-Ringer buffer at pH 7.4 and stored subsequently at 4°C for 24 h or more then the triose phosphates and FDP can rise to very high levels (Eckel et al., 1966; Table 1). These cells catalyse rapid isotope exchange at the C-2 position of added lactate. Freshly drawn erythrocytes have very low levels of the triosephosphates. If the cells are cooled, however, the triosephosphate levels rapidly rise (Beutler, 1975) and lactate added to these cells again shows rapid isotope exchange at the C-2 position. Fig.16 shows exchange time courses for L-(2-²H)lactate incubated with intact cells and a lysate in ¹H₂O. The 12mM lactate time course in the whole cells terminates before peak inversion is complete. This effect is even more marked in the case of the lysate. When 6mM lactate was added to the same batch of cells however there was complete exchange. DHAP assays showed that before the addition of lactate to the intact cells there was 0.74µmols DHAP/ml cell water. This had dropped to 0.04µmols DHAP/ml cell water after incubation for 60 min at 37°C. The decrease in DHAP concentration in the lysate is faster and a lysate incubated for 30 min at 37°C showed no detectable DHAP. These results imply that the premature termination of the exchange observed in Fig.16 is due to a decrease in the level of DHAP and the other metabolites involved in the exchange with which it is in equilibrium e.g. GAP. The peak heights shown in Fig.16 are quoted as ratios of the peak height at t=0 (obtained by extrapolation). Values in excess of -1.00 obtained for 6mM lactate are due to endogenous lactate production and incomplete deuteration at the C-2 position of the added lactate. In the case of the lysate the exchange has terminated at the null point where the positive and negative lactate methyl peaks are observed simultaneously.

Table 1

Comparison of triose phosphate and FDP concentrations in erythrocytes stored in citrate/phosphate/glucose and in cells washed and stored for 24 h at 4°C in Krebs-Ringer buffer, pH 7.4.

Concentrations were determined in neutralised perchloric acid extracts. GAP was determined by measuring the increase in fluorescence as NAD^+ is reduced to NADH in the reaction catalysed by glyceraldehydephosphate dehydrogenase. Arsenate was substituted for phosphate to make the reaction irreversible. DHAP was determined by adding triosephosphate isomerase which converts DHAP to GAP and leads to a further production of NADH. FDP concentration was determined by the addition of aldolase which cleaves FDP to GAP and DHAP (Beutler, 1975).

Conditions of storage	Concentrations ($\mu\text{mols/ml}$ cell water)		
	GAP	DHAP	FDP
citrate/phosphate/glucose at 4°C	0	2	2
Krebs-Ringer buffer, pH 7.4 at 4°C	54	572	743

The effect of changes in the triosephosphate concentrations on estimates of V_{C2X} are discussed in the next section.

2.10.2 The effect of lactate concentration on the exchange

The effect of lactate concentration on V_{C2X} is shown in Table 2. This shows V_{C2X} corrected for the effect of solvent labelled lactate present at $t=0$, (corrected using equation 4) and corrected for both solvent labelled lactate present at $t=0$ and for lactate production occurring between lactate addition at $t=0$ and the observed t_{null} , (corrected using equation 5). This latter correction is small since the rate of lactate production is small compared to V_{C2X} . In these cells a rate of lactate production of approximately 4mM/hr/ml cells was observed. The correction for solvent labelled lactate present at $t=0$ (L_e) can be minimised by thorough washing of the cells prior to lactate addition and by using lactate which has a high degree of labelling at the C-2 position.

These experiments were performed in 1H_2O . In 2H_2O they are complicated by deuteration of the lactate methyl which occurs because of equilibration of the lactate and pyruvate methyls in the reaction catalysed by lactate dehydrogenase. The pyruvate methyl undergoes hydrogen exchange with solvent in a reaction catalysed by the α amino groups of haemoglobin (see Simpson et al, 1981 & 1982a & b).

The observed t_{null} for the exchange and thus the calculated V_{C2X} is a function of the equilibrium velocities of all four enzymes involved and their substrate concentrations. If there are changes in the concentrations of these substrates during measurement of an equilibrium

Table 2

	Added lactate concentration	Observed t_{mull} (min)	DHAP concentration at observed t_{mull} ($\mu\text{moles/ml}$ cell water)	V_{G2X} corrected for solvent labelled lactate at $t=0$ ($\mu\text{moles/min/ml}$ cells)	V_{G2X} corrected for solvent labelled lactate at $t=0$ and and for lactate growth ($\mu\text{moles/min/ml}$ cells)
A	4.6	5	0.22	0.448	0.401
	6.9	10	0.16	0.398	0.355
	9.2	10	0.16	0.507	0.463
	11.5	12	0.14	0.545	0.502
	13.8	17	0.11	0.484	0.443
	16.1	18	0.10	0.529	0.487
	18.4	23	0.07	0.486	0.445
	23.0	31	0.03	0.457	0.417
B	4.5	7	1.08	0.357	0.288
	4.5	6	1.09	0.375	0.304
	9.0	12	1.04	0.469	0.406
	9.0	12	1.04	0.455	0.389
	13.6	18	0.98	0.495	0.434
	13.6	17	0.99	p.505	0.442
	18.1	23	0.94	0.520	0.459
	18.1	22	0.94	0.522	0.439
	22.6	27	0.90	0.551	0.491

Table 2

Effect of L-(2-²H)lactate concentration on the overall equilibrium velocity in erythrocytes in Krebs-Ringer buffer made with ¹H₂O.

Equilibrium velocities were measured in packed erythrocyte suspensions (84% haematocrit for the erythrocytes used in part A of the table and 79% for part B). The quoted lactate concentrations were those added to the samples and were corrected for the excluded volume of the samples by assuming that 72% of the intracellular volume is solvent water (Eilam & Stein, 1974). The added lactate was 98% deuterated at the C-2 position as judged by proton n.m.r.. The cells were washed just prior to use in order to lower the endogenous lactate concentration. This was approximately the same in all samples at about 1mM. Equilibrium velocities were calculated from the observed t_{null} (see text). DHAP assays were performed on a parallel incubation according to the method described in the legend to Table 1.

velocity and if these significantly affect the individual equilibrium velocities of the enzymes, then the observed t_{null} and the calculated overall equilibrium velocity will be affected. The magnitude of these substrate concentration effects will depend on the individual sensitivity and elasticity coefficients of the enzymes.

We have already shown that the exchange depends on relatively high concentrations of the triose phosphates and that these decline at 37°C. The results in Table 2 show, however, that above a certain level, changes in the concentrations of the triose phosphates, which are represented here by the DHAP concentration, have a negligible effect on the calculated overall equilibrium velocity. In part A of the table the DHAP concentration decreases by approximately 90% between the observed t_{null} at low lactate concentration and that observed at high lactate concentration and yet there is no significant difference in the calculated equilibrium velocity. In part B the DHAP concentration decreases by only 20% between the t_{null} observed at high and low lactate concentrations respectively and again there is no decrease in the calculated equilibrium velocity and in fact there is an increase. The results in parts A and B also show that there is no significant dependence of the overall equilibrium velocity on lactate concentration, particularly at higher lactate concentrations. The lower values for V_{C2X} observed at lower added lactate concentrations in part B of the table may be due to a lower equilibrium velocity of, for example, lactate dehydrogenase.

Since there is no significant dependence of V_{C2X} on lactate concentration (at relatively high concentrations of lactate) and on the concentrations of the triose phosphates (over the concentration ranges

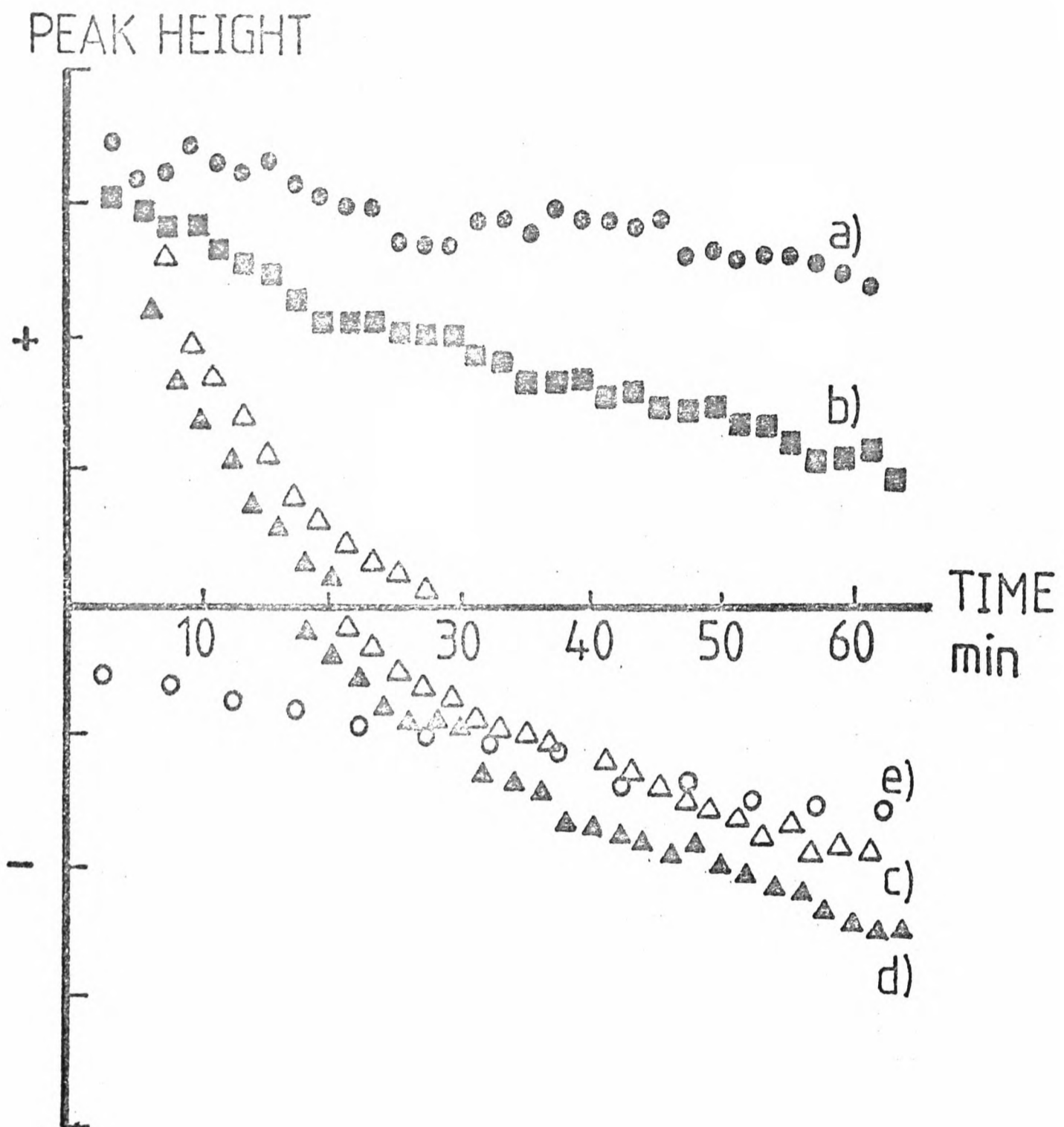


Figure 17

Inhibition by pyruvate of the exchange in erythrocytes.

Plot of lactate methyl peak height versus time following the simultaneous addition to erythrocytes (70% haematocrit) of 12mM lactate and a) 5mM pyruvate, b) 1mM pyruvate, c) 0.5mM pyruvate, d) no pyruvate and e) no addition of lactate or pyruvate.

The cells were suspended in Krebs-Ringer buffer made with $^1\text{H}_2\text{O}$.

shown) then V_{C2X} will remain effectively constant during an exchange time course.

In order to compare, using this technique, the properties of glyceraldehydephosphate dehydrogenase in situ and in vitro (see chapter 5) it is essential that the substrate equilibrium which exists in vitro approximates the near equilibrium steady state that exists in situ. At relatively high concentrations of lactate and the triose phosphates the percentage changes in their concentrations in situ during measurement of V_{C2X} are small. Furthermore the elasticity coefficients of the enzymes for these substrates are small in this concentration range. The effects of concentration changes occurring prior to observation of a null point are further reduced if the time taken to obtain a null is reduced. For example, in 1H_2O , the time taken to reach a null point can be reduced by decreasing the percentage deuteration of the added lactate.

2.10.3 The effect of pyruvate concentration on the exchange

Figure 17 shows the effect of pyruvate addition on the exchange of L-(2- 2H)lactate added to an erythrocyte suspension in 1H_2O , the rate of exchange is decreased at higher pyruvate concentrations.

Addition of pyruvate to these cells will have a number effects, that is; a) it will rapidly increase the $NAD^+/NADH$ ratio; b) it will accelerate the long term depletion of the triose phosphates (Rose & Warms, 1966) and c) it will lead to a transient increase in the 1,3-DPG concentration (Rose & Warms, 1970). Each of these events can be expected to affect the equilibrium velocities of the enzymes involved in C-2 exchange as outlined below.

An increase in the NAD^+/NADH ratio will affect the equilibrium velocities of both lactate dehydrogenase and glyceraldehydephosphate dehydrogenase. An increase in the 1,3-DPG concentration may inhibit glyceraldehydephosphate dehydrogenase by formation of an enzyme-1,3-DPG complex which is inactive in the exchange (the enzyme has a high affinity for 1,3-DPG (Furfine & Velick, 1965)). It should be noted that if the currently accepted mechanism for the enzyme is correct (Fersht, 1977) then both P_i and 1,3 DPG are not essential for the exchange of isotope between GAP and NAD(H). This is supported by the results shown here for an in vitro exchange system which contained no added phosphate and thus very little (if any) 1,3-DPG. The observed inhibition of the exchange at high concentrations of pyruvate is not simply due to a total depletion of the triosephosphates. DHAP assays of the cells used in the experiment of Fig.17 showed that before incubation at 37°C there were $0.71\mu\text{mols}$ DHAP/ml cell water and that following incubation for 15 min at 37°C in the presence of 5mM added pyruvate there were still $0.16\mu\text{mols}$ DHAP/ml cell water present. At this added pyruvate concentration there was no detectable exchange (Fig.17). In this case the decrease in intensity of the methyl peak of added lactate, which has a positive phase since the lactate is deuterated at the C-2 position, is due to an increase in endogenous lactate which is protonated at the C-2 position and thus has an inverted methyl peak.

In addition to its indirect effects, pyruvate will also directly inhibit exchange of isotope across lactate dehydrogenase. This has been observed experimentally by Silverstein & Boyer (1964) and is predicted by an equation (shown in appendix 1) which relates the kinetic parameters of lactate dehydrogenase to its isotope exchange equilibrium velocity. Pyruvate will also inhibit the exchange by the formation of

abortive complexes with the enzyme, (see for example Simpson et al, 1982b).

N.m.r. analysis of pyruvate inhibition of the exchange can only readily be demonstrated in $^1\text{H}_2\text{O}$. Deuteration of the pyruvate methyl, which was mentioned previously, is accelerated in the presence of high pyruvate concentrations and this leads to increased lactate methyl deuteration and loss of lactate methyl peak intensity (see Simpson et al, 1982a&b)

2.11 Conclusions

It has been shown that the technique is capable of precise measurements of isotope exchange at the C-2 position of lactate and that these measurements can be used to investigate the kinetic properties of the enzymes involved in the exchange. In chapters 5 and 6 it will be shown that measurements of lactate C-2 exchange can be used to compare the in vitro and in situ properties of the erythrocyte enzymes glyceraldehydophosphate dehydrogenase and lactate dehydrogenase respectively.

Isotope exchange at the lactate C-2 position has been studied previously using radiolabelled L-(2-³H)lactate in the erythrocyte (Rose & Warms, 1969) and in the liver (Hoberman, 1965; Bücher, 1969). The n.m.r. technique presented here has permitted a much more detailed study of the exchange in the erythrocyte since it is both non-invasive and provides rapid and continuous assessment of the isotopic composition of the exchanging species. The repeated sampling, extractions and separations required by radioactive labelling techniques are eliminated and the errors and labour involved are consequently reduced.

A disadvantage of the n.m.r. technique is its inherent lack of sensitivity. With the 470 MHz instrument used here a reasonable threshold of detection in intact erythrocytes is approximately 0.5mM for the methyl group of lactate in a sample volume of approximately 0.5 ml and a sampling time of 2 min. However it has been demonstrated that isotope exchange at the C-2 position of lactate can be employed to give, in an indirect manner, some assessment of isotope exchange in metabolites present in micromolar concentrations, (for example, NAD(H) and GAP).

The measurement of equilibrium isotope exchange allows investigation of the kinetic properties of an enzyme catalysing a reaction at equilibrium at the physiological equilibrium concentrations of the enzyme's substrates both in vitro (as demonstrated above) and in situ (as demonstrated in chapters 5 and 6). With conventional enzyme kinetic investigations spectrophotometric and fluorimetric methods are employed to study the time course of a chemical reaction. Under these circumstances it is not normally possible to use physiological concentrations of an enzyme's reactants and the reaction is usually far displaced from equilibrium. At high enzyme concentration the initial rate phase of most systems away from equilibrium is too short to be examined except by stopped flow methods. With the exchanges studied here, although chemical relaxation is exceedingly rapid, the isotopic relaxation is very much slower and its first order nature enhances the accuracy of rate measurements.

Although enzymes catalysing reactions at equilibrium are, a priori, uninteresting from the point of view of metabolic control, they may be used, as will be shown in subsequent chapters, as probes of the intracellular environment. This is achieved by measuring the isotope exchange properties of an enzyme in situ and comparing these properties with those the enzyme displays in vitro under conditions simulating the in situ conditions.

To summarise much of what has been said in this chapter; the following are a set of basic conditions which ideally should be fulfilled if the n.m.r. technique described is to be successfully applied to the study of equilibrium isotope exchange.

1) The relationship between peak intensity and fractional labelling must be known. This will usually require knowledge of the start and endpoints for the exchange, in the case of C-2 exchange it requires knowledge only of the start point for the exchange. A simple linear relationship between peak intensity and fractional labelling will not exist if a change in labelling affects the relaxation properties of the observed protons.

2) The exchange should be described by a simple kinetic model which relates observed changes in n.m.r. peak intensities to the equilibrium velocity of a system or the equilibrium velocity of an individual enzyme within that system. Under certain circumstances where the aim is to compare the exchange properties of an enzyme in situ and in vitro it is not essential that this model be a complete description of the exchange system and its manifestation in the n.m.r. experiment (see chapter 6). This qualifier can also apply to condition 1.

3) The equilibrium velocity of an individual enzyme should be directly proportional to its concentration. A non-linear relationship will be realised if the enzyme and one or more of its substrates are of comparable concentration and if there is significant binding of these substrates to the enzyme. The effect of mutual depletion of free enzyme and substrate concentrations is considered in chapters 5 and 6.

4) The reaction(s) must be at chemical equilibrium or in a near equilibrium steady state. The steady state rate of chemical transformation should be smaller than that of the isotope exchange rate. There should be no time dependent changes in an enzyme's substrate concentrations, during exchange measurements, which significantly affect the enzyme's equilibrium velocity.

5) Isotope effects on the equilibrium velocity of the enzyme of interest should be small. Where a comparison is being made, however,

between the in vitro and in situ properties of an enzyme then this may not be essential (see chapter 6).

6) A labelled probe molecule which rapidly penetrates the compartment containing the enzyme under observation should be used. Transport limitation of the rate of isotope exchange will produce double (or even multi) exponential kinetics and the extraction of an isotope exchange rate will require accurate knowledge of the rate of transport of the exchanging species. If the rate of transport is much slower than the exchange rate then the latter will obviously not be measurable. In a multi-compartmented system interpretation of isotope exchange data will be considerably more complex.

2.12 References

Alivisatos, S.G.A. & Denstedt, O.F. (1951) *Science* 114, 281-283

Alizade, M.A., Dessau, W. & Simon, H. (1975) *Hoppe-Seyler's Z. Physiol. Chem.* 356, 73-82

Bartlett, G.R. (1959) *J. Biol. Chem.* 234, 459-465

Bartlett, G.R. & Barnet, H.N. (1960) *J. Clin. Invest.* 39, 56-61

Beutler, E. (1975) "Red Cell Metabolism", 2nd edn., Grune & Stratton, New York.

Borgmann, U., Moon, T.W. & Laidler, K.J. (1974) *Biochemistry* 13, 5152-5158

Boyer, P.D. (1959) *Arch. Biochem. Biophys.* 82, 387-410

Brin, M (1953) *Biochemical Preparations* 3, 61-66

Brindle, K.M., Brown, F.F., Campbell, I.D., Grathwohl, C. & Kuchel, P.W. (1979) *Biochem. J.* 180, 37-44

Brindle, K.M., Brown, F.F., Campbell, I.D., Foxall, D.L. & Simpson, R.J. (1982) *Biochem. J.* 202, 589-602

Brown, F.F., Campbell, I.D., Kuchel, P.W. & Rabenstein, D.C. (1977) *FEBS Lett.* 82, 12-16

Bücher, T. (1969) in "Pyridine Nucleotide Dependent Dehydrogenases" (Sund, H. ed.), pp 439-461, Springer Verlag, Berlin, Heidelberg & New York.

Burt, C.T., Cohen, S.M. & Bárány, M. (1979) Ann. Rev. Biophys. Bioeng. 8, 1-25

Campbell, I.D. & Dobson, C.M. (1979) Methods. Biochem. Anal. 25, 1-133

Cantwell, A.M. & Dennis, D. (1970) Biochem. Biophys. Res. Commun. 41, 1166-1170

Carr, H.Y. & Purcell, E.M. (1954) Phys. Rev. 94, 630-638

Cleland, W.W. (1980) Methods. Enzymol. 64, 104-125

Cook, P.F., Blanchard, J.S. & Cleland, W.W. (1980) Biochemistry 19, 4853-4858

Dawson, M.J., Gadian, D.G. & Wilkie, D.R. (1977) J. Physiol. (London) 267, 703-735

Deuticke, B., Rickert, I. & Beyer, E. (1978) Biochim. Biophys. Acta. 507, 137-155

Dickens, F. & Williamson, D.H. (1956) Biochem. J. 64, 567-578

- Eckel, R.E., Salvatore, C.R., Lodish, H. & Berggren, A.B. (1966)
Amer. J. Physiol. 210, 737-743
- Eilam, Y. & Stein, W.D. (1974) Methods. Membr. Biol. 2, 283-354.
- Fersht, A. (1977) "Enzyme Structure and Mechanism", pp. 298-299, W.H.
Freeman & Co., Reading and San Francisco.
- Foxall, D.L. (1981) D. Phil. Thesis Oxford University
- Friedemann, H. & Rapoport, S.M. (1974) in "Cellular and Molecular
Biology of Erythrocytes" (Yoshikawa, H. & Rapoport, S.M. eds.) pp
181-259 Urban and Schwarzenberg, Munich, Berlin, Wien
- Furfine, C.S. & Velick, S.F. (1965) J. Biol. Chem. 240, 844-855
- Gadian, D.G., & Radda, G.K. (1981) Ann. Rev. Biochem. 50, 69-83
- Gupta, R.K., Benovic, J.L. & Rose, Z.B. (1978) J. Biol. Chem. 253,
6165-6171
- Hoberman, H.D. (1965) Ann. N. Y. Acad. Sci. 119, 1070-1083
- Horecker, B.L. & Kornberg, A. (1948) J. Biol. Chem. 175, 385-390
- Hue, L. & Hers, H. (1972) Eur. J. Biochem. 29, 268-275
- Hung, H.C. & Hoberman, H.D. (1972) Biochem. Biophys. Res. Commun. 46,
399-405

Kacser, H. & Burns, J.A. (1979) *Biochem. Soc. Trans.* 7, 1149-1160

Kirsch, J.F. (1977) in "Isotope Effects on Enzyme-Catalysed Reactions"
(Cleland, W.W., O'Leary, M.H. & Northrop, D.B.) pp 100-121
University Park Press, Baltimore, London, Tokyo

Krebs, H.A. & Henseleit, K. (1932) *Hoppe-Seyler's Z. Physiol. Chem.*
210, 33-66

Kresge, A.J. (1977) in "Isotope Effects on Enzyme-Catalysed Reactions"
(Cleland, W.W., O'Leary, M.H. & Northrop, D.B.) pp 37-63 University
Park Press, Baltimore, London, Tokyo

Maxwell, E.S. (1961) *Enzymes* 2nd edn. 5, 443-453

Mehler, A.H., (1963) *J. Biol. Chem.* 238, 100-104

Minikami, S. & Yoshikawa, H. (1966) *J. Biochem. (Tokyo)* 59, 139-144

Northrop, D.B. (1977) in "Isotope Effects on Enzyme-Catalysed Reactions"
(Cleland, W.W., O'Leary, M.H. & Northrop, D.B.) pp 122-152
University Park Press, Baltimore, London, Tokyo

Novoa, W.B., Winer, A.D., Glaid, A.J. & Schwert, G.W. (1959) *J. Biol.
Chem.* 234, 1143-1148

Rieder, S.V. & Rose, I.A. (1959) *J. Biol. Chem.* 234, 1007-1010

Rose, I.A. & Rieder S.V. (1958) *J. Biol. Chem.* 231, 315-329

- Rose, I.A. & Warms, J.V.B. (1966) *J. Biol. Chem.* 241, 4848-4854
- Rose, I.A. & Warms, J.V.B. (1969) *J. Biol. Chem.* 244, 1114-1117
- Rose, I.A. & Warms, J.V.B. (1970) *J. Biol. Chem.* 245, 4009-4015
- Saur, W.K., Crespi, H.L., Halevi, E.A. & Katz J.J. (1968)
Biochemistry 7, 3529-3546
- Schowen, R.L. (1977) in "Isotope Effects on Enzyme-Catalysed Reactions"
(Cleland, W.W., O'Leary, M.H. & Northrop, D.B.) pp 64-99 University
Park Press, Baltimore, London, Tokyo
- Silverstein, E. & Boyer, P. (1964) *J. Biol. Chem.* 239, 3901-3907
- Simpson, R.J., Brindle, K.M., Brown, F.F., Campbell, I.D. & Foxall,
D.L. (1981) *Biochem. J.* 193, 401-406
- Simpson, R.J., Brindle, K.M., Brown, F.F., Campbell, I.D. & Foxall,
D.L. (1982a) *Biochem. J.* 202, 573-579
- Simpson, R.J., Brindle, K.M., Brown, F.F., Campbell, I.D. & Foxall,
D.L. (1982b) *Biochem. J.* 202, 581-587
- Thomson, J.F., Darling, J.J. & Bordner, L.F. (1964) *Biochim. Biophys.*
Acta. 85, 177-185
- Trentham, D.R. (1971) *Biochem. J.* 122, 71-77

Winer, A.D. & Schwert, G.W. (1958) J. Biol. Chem. 231, 1065-1083

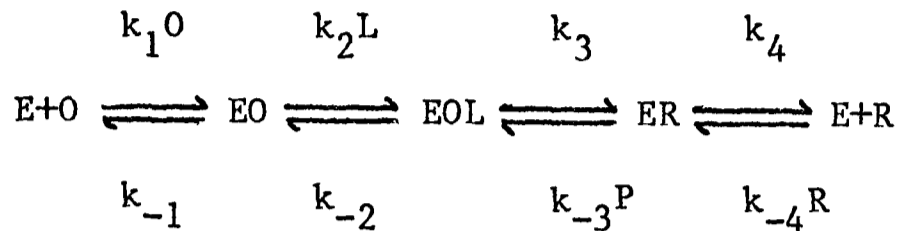
Wuthrich, K. (1976) "NMR in Biological Research: Peptides and Proteins"
North Holland/American Elsevier

Yagil, G. & Hoberman, H.D. (1969) Biochemistry 8, 352-360

2.13 Appendix 1

Lactate dehydrogenase equilibrium velocity

The reaction mechanism for lactate dehydrogenase can be represented as follows, (Borgmann et al, 1974):



where O and L are NAD^+ and lactate, or their concentrations, and R and P are NADH and pyruvate or their concentrations. It is assumed that EOL and ERP are rapidly interconverted and, for simplicity, EOL is written for EOL-ERP.

The equilibrium velocity of an enzymatic reaction can be related to the kinetic parameters of the reaction as shown by Yagil and Hoberman (1969). These workers derived the following relationship for an equilibrium velocity of a reaction proceeding by n consecutive steps:

$$1/V_e = \sum_1^n 1/V_i$$

Thus the equilibrium velocity of lactate dehydrogenase for the exchange of isotope between the C-2 position of lactate and NADH can be related to the kinetic parameters of the enzyme by the following equation:

$$1/V_e = 1/(E)_t \left[\frac{1}{k_{-4}(R)} + \frac{k_4}{k_{-3} k_{-4} (R)(P)} + \frac{k_3 k_4}{k_{-2} k_{-3} k_{-4} (R)(P)} \right]$$

$$\left[1 + \frac{k_{-4}(R)}{k_4} + \frac{k_{-3} k_{-2} k_{-4} (R)(P)}{k_3 k_2 k_4 (L)} + \frac{k_{-3} k_{-4} (R)(P)}{k_3 k_4} \right]$$

where $(E)_t$ is the total enzyme concentration. This was calculated by dividing the measured activity for lactate dehydrogenase (assayed spectrophotometrically) by k_{-1} . This and the other kinetic constants used here were calculated for the beef heart enzyme at 37°C and are from the data of Borgmann et al, (1974).

NAD dependence

The line shown in Fig. 14 was calculated using the equation shown above. The lactate, pyruvate, NAD^+ and NADH concentrations were estimated using an equilibrium constant of 1.11×10^{-11} (Williamson et al, 1967). Fluorimetric and spectrophotometric measurements of variation in the NADH concentration in the enzyme mixture with varying lactate and pyruvate concentrations (see next chapter) confirmed that the NAD^+ and NADH concentrations were determined by the lactate dehydrogenase equilibrium.

References

Borgmann, U., Moon, T.W. & Laidler, K.J. (1974) *Biochemistry* 13, 5152-5158

Williamson, D.H., Lund, P. & Krebs, H.A. (1967) *Biochem. J.* 103, 514-527

Yagil, G. & Hoberman, H.D. (1969) *Biochemistry* 8, 352-360

Appendix 2

2.14 Oxamate inhibition

Kinetic and binding studies (Novoa et al, 1959b; Novoa & Schwert, 1961) have shown that oxamate binds to both the NAD⁺ and NADH bound forms of lactate dehydrogenase, although it has a higher affinity for the latter form.

The dissociation constant for NADH binding to bovine heart lactate dehydrogenase has been estimated at 2.5×10^{-7} M in Tris buffer, pH 7.08 at an ionic strength of 0.2, (Novoa et al, 1959a). The dissociation constant for NAD⁺ binding has been estimated at 3.9×10^{-3} M in 0.1M sodium phosphate buffer, pH 6.8, (Takenaka & Schwert, 1956). The NAD⁺ and NADH concentrations present in the experiment depicted in Fig. 15 were estimated to be 83 and 17 μ M respectively. Thus under the conditions of this experiment and assuming human erythrocyte lactate dehydrogenase has similar kinetic properties to the bovine heart enzyme then the enzyme will be predominantly in the NADH bound form. Oxamate inhibition of the exchange can thus be regarded as a case of simple competitive inhibition where oxamate competes with pyruvate for binding to the NADH bound form of the enzyme.

For competitive inhibition

$$v = \frac{V S}{S + K(1 + I/K_i)}$$

where v is the rate of the enzyme catalysed reaction, V is the rate of the reaction at infinite concentration of substrate, S is substrate concentration, I is inhibitor concentration, K_i is the dissociation constant for the enzyme inhibitor complex and K is the dissociation constant for the substrate. By equating v with the isotope exchange equilibrium velocity this equation was used to calculate the percentage

reduction in the lactate dehydrogenase equilibrium velocity at various oxamate concentrations and using various values for K_i . A pyruvate concentration of $17\mu\text{M}$ was used in the calculations since this is the concentration estimated to be present when 12mM lactate is added to an enzyme mixture containing $100\mu\text{M}$ NAD^+ , which were the conditions of the experiment shown in Fig.15. A value of $71\mu\text{M}$ was chosen for the dissociation constant of pyruvate by equating a reported K_m value, for human erythrocyte lactate dehydrogenase (Wang, 1977), with K_i . The effect of a percentage decrease in the lactate dehydrogenase equilibrium velocity on the overall exchange of isotope at the C-2 position of lactate can be calculated using equation 2 (see text). If oxamate only inhibits lactate dehydrogenase then the effect of a percentage decrease in the lactate dehydrogenase equilibrium velocity can be expressed as a percentage decrease in V_{C2X} . The experimental data shown in Fig. 15 were fitted using a K_i value of $60\mu\text{M}$, which is similar to that obtained for the bovine heart enzyme by steady state kinetic analysis and from binding studies (Novoa et al, 1959b; Novoa & Schwert, 1961).

References

Novoa, W.B. & Schwert, G.W. (1961) J. Biol. Chem. 236, 2150-2153

Novoa, W.B., Winer, A.D., Glaid, A.J. & Schwert, G.W. (1959a) J. Biol. Chem. 234, 1143-1148

Novoa, W.B., Schwert, G.W. & Millar, D.B.S. (1959b) J. Biol. Chem. 234, 1149-1154

Takenaka, Y & Schwert, G.W. (1956) J. Biol. Chem. 223, 157-170

Wang, C. (1977) Eur. J. Biochem. 78, 569-574

2.15 Appendix 3

The effect of an isotope effect on an exchange time course

If there is a kinetic isotope effect on the equilibrium velocity of a reaction then its expression in the observed rate of exchange will change as the fractional labelling of the reactants changes.

Let

$$dX/dt = -kX$$

where X is the fractional labelling of the reactant and k is the first order rate constant for the exchange.

Let

$$\alpha = (k_1 - k_2)/k_2$$

where k_1 is the first order rate constant for the exchange observed at $t=0$ and k_2 is the rate constant at $t=\infty$.

$$dk/dt = k_2 (1 + \alpha X)$$

so when $t=0$ $X=1$ and $k=k_1$ and when $t=\infty$ $X=0$ and $k=k_2$.

$$dX/dt = -k_2 (1 + \alpha X) X$$

$$\frac{dX}{X(1 + \alpha X)} = -k_2 dt$$

Integrating both sides of this equation and rearranging we obtain;

$$X = \frac{e^{-k_2 t}}{1 + \alpha (1 - e^{-k_2 t})}$$

when $k_1=k_2$ i.e. when there is no isotope effect and $\alpha =0$ the above equation reduces to

$$X = e^{-kt}$$

2.16 Appendix 4

Estimation of V_{C2X} in erythrocytes

Equations for calculating the overall equilibrium velocity, V_{C2X} , from the observed $t_{1/2}$ for the exchange in erythrocytes.

The equations allow corrections to be made for the effect of solvent labelled lactate present at $t=0$ and for the effect of lactate production occurring between $t=0$ and the observed point of 50% labelling.

Solvent labelled lactate has two effects: a) The solvent labelled lactate present at $t=0$, (endogenous or added) significantly reduces the observed $t_{1/2}$ if it represents a significant fraction of the total lactate and b) it dilutes the added labelled lactate.

Endogenous lactate production occurring during an exchange time course represents a source of solvent labelled lactate in addition to that produced by exchange. This endogenous lactate will not be entirely solvent labelled in the presence of added labelled lactate. Under these circumstances its fractional labelling will be dictated by the fractional labelling of the glycolytic intermediates involved in the exchange through which it is produced. This is discussed more fully in the next two chapters. However in the correction shown below endogenous lactate production is regarded as a source of solvent labelled lactate, produced at a constant rate, in addition to that formed by exchange, which is produced at an exponentially declining rate. The correction is therefore an over correction which becomes a better approximation as the ratio of the exchange rate to the rate of lactate production decreases.

Correction for solvent labelled lactate present at t=0

Let X_L represent the fraction of labelled lactate

$$dX_L/dt = -k X_L$$

where k is the first order rate constant for the exchange.

$$dX_L/dt = -V X_L/(L_0+L_e)$$

where t is time

V is the overall equilibrium velocity, V_{C2X}

L_0 is the labelled lactate concentration at $t=0$

L_e is the solvent labelled lactate concentration at $t=0$

At $t=0$, $X_L=1$ and at $t=\infty$, $X_L=0$. On integration of the above we obtain;

$$\ln X_L = -V t/(L_0+L_e) + c$$

where c is a constant of integration.

$$\text{when } t=0 \quad X_L = L_0/(L_0+L_e)$$

$$\text{and therefore } c = \ln L_0/(L_0+L_e)$$

$$X_L = \frac{L_0 e^{-V t/(L_0+L_e)}}{(L_0+L_e)}$$

At the point of 50% labelling $X_L=0.5$ and therefore;

$$V = \frac{-(L_0+L_e)}{t} \ln ((L_0+L_e)/2L_0)$$

where t is the time at which peak inversion occurs.

Correction for solvent labelled lactate present at t=0 and lactate production occurring during an exchange time course

From the above it can be seen that;

$$dX_L/dt = -V X_L / (L_0 + L_e + k_L t)$$

where k_L is the rate of lactate production. On integration we obtain;

$$X_L = \frac{L_0 e^{-V \ln(1 + k_L t / (L_0 + L_e)) / k_L}}{(L_0 + L_e)}$$

For C-2 exchange where there is inversion of the methyl resonance the methyl peak height at time t ($h(t)$) in the spin echo spectrum can be described by the following equation.

$$h(t) = \rho (L_0 + L_e) (1 + 2X_L)$$

Where ρ is a conversion factor for converting lactate concentration into peak height. It should be noted that a simple proportionality between peak height and concentration is lost in $^2\text{H}_2\text{O}$ where there is deuteration of the methyl group of endogenous lactate due to solvent isotope exchanges occurring at the phosphoglucoisomerase and pyruvate kinase steps of glycolysis (Rose & Rose, 1969). In addition both the endogenous and added lactates can undergo deuteration in the methyl group by equilibration with deuterated pyruvate formed in an exchange reaction catalysed by haemoglobin (Simpson et al, 1982).

Adding a constant linear term for lactate production to the above

equation and omitting ρ we obtain;

$$h(t) = (L_0 + L_e) (1 - 2X_L) + k_L t$$

At the point of 50% labelling and peak inversion $h(t)=0$ and therefore;

$$V = -k_L \ln \left[\frac{(L_0 + L_e + k_L t)}{2 L_0} \right] \frac{1}{\ln \left[\frac{(1 + k_L t)}{L_0 + L_e} \right]}$$

where t is given by the point of peak inversion.

Observation of the exchange at the C-2 position

If the C-2 proton is observed directly then the following equations can be derived relating changes in C-2 proton peak intensity to the overall equilibrium velocity. Estimation of an equilibrium velocity from observation of the C-2 proton would require fitting of the exchange time course to these equations.

The exchange in $^1\text{H}_2\text{O}$; L-(2- ^2H)lactate \rightarrow L-(U- ^1H)lactate

In this experiment there will be zero C-2 proton peak intensity at $t=0$. As the exchange proceeds the C-2 proton peak intensity will increase. Thus the time over which the peak intensity is changing most rapidly and which is thus the most sensitive area for estimation of a rate constant is the least well observed part of the time course. In this experiment the only C-2 substituent observed is the proton, contrast this with observation of the methyl where the effects of both proton and deuterium substitution at the C-2 position are observed.

The equation describing the exchange has the following form

$$h(t) = A e^{-kt} + Bt + c$$

where A is the amplitude of the exchange and B a constant linear term representing lactate production. The exponential term will have the same form as shown above. Thus we can write that

$$h(t) = A \left(1 - e^{-V \ln(1 + k_L t / (L_0 + L_e)) / k_L} \right) + k_L t + c$$

The amplitude for the exchange of added labelled lactate is proportional to L_0 , the concentration of added C-2 deuterated lactate. The value for L_0 is only obtained following completion of the exchange when there is complete protonation of the lactate. At $t=0$ the peak observed is proportional to the concentration of solvent labelled (protonated) lactate, L_e . Thus we obtain that

$$h(t) = (L_0 + L_e + k_L t) - L_0 e^{-V \ln(1 + k_L t / (L_0 + L_e)) / k_L}$$

The exchange in $^2\text{H}_2\text{O}$; L-(U- ^1H)lactate \rightarrow L-(2- ^2H)lactate

Solvent labelled lactate (deuterated) present at $t=0$ is not observed, its concentration can only be estimated from the methyl resonance (even this is complicated by methyl deuteration). A value for L_e is thus not directly obtainable from observation of the C-2 proton resonance. Since L_e has no effect on the C-2 proton peak intensity the following equation is obtained.

$$h(t) = L_0 e^{-V \ln(1 + k_L t / (L_0 + L_e)) / k_L} + c$$

At $t=0$ the peak intensity observed is proportional to the concentration of added protonated lactate L_0 and therefore $c=0$. In this exchange the value of L_0 can only be obtained by extrapolation of the time course to $t=0$.

In summary, by monitoring the exchange by observation of the methyl resonance both the labelled and unlabelled lactate species are observed. The corollary of this is that a unique point is observed in an exchange time course, the null point or point of peak inversion, which indicates the point at which 50% of the lactate is labelled. With direct observation of the C-2 proton fractional labelling can only be assessed retrospectively when the amplitude of the exchange has been determined, this will normally entail following the exchange to completion. Estimation of an exchange equilibrium velocity from the exchange time course of the C-2 proton will require fitting of the time course to the appropriate equation. The other advantages of observing the methyl have been discussed in the text.

References

Rose, I.A. & Rose, Z.B. (1969) in Compr. Biochem. 17, 93-161

Simpson, R.J., Brindle, K.M., Brown, F.F., Campbell, I.D. & Foxall, D.L. (1982) Biochem. J. 202, 573-579

3 The properties of the C-2 exchange system in vitro

3.1 Introduction

In the previous chapter the basic characteristics of the C-2 exchange system in the intact erythrocyte were described and a method for obtaining, in vitro, the isotope exchange equilibrium velocities of the individual enzymes involved in the exchange was demonstrated.

In this chapter the properties of the in vitro system and its use in determining individual enzyme equilibrium velocities are examined. The measured equilibrium velocities are used in the following chapter in a model of the exchange system in situ.

3.2 Experimental

Materials

Sephadex was obtained from Pharmacia (Great Britain) Ltd. Middlesex. Carboxymethylcellulose (CM-22) was obtained from Whatman Ltd. Kent. Ultrafiltration membranes were from Amicon Ltd., Surrey and Millipore filters from Millipore (U.K.) Ltd. Middlesex.

Triose phosphate and FDP assays in the in vitro exchange system

Extracts of the in vitro system were prepared by withdrawing 0.5 ml aliquots and adding these to 4.5 ml of ice cold 8% PCA. After standing for 10-15 min the samples were placed on a boiling water bath for approximately 5 min and then neutralised with 1M K_2CO_3 and made up to 10 ml with H_2O . Boiling following neutralisation resulted in a marked loss of FDP. The resulting precipitates were centrifuged off and the supernatants stored frozen overnight.

The extracts were assayed for triose phosphates and FDP as described in chapter 2. Despite the conditions used for extraction a stable fluorescence reading following addition of glyceraldehydephosphate dehydrogenase to the assay system could not be obtained. This indicated that either the added glyceraldehydephosphate dehydrogenase was contaminated with triosephosphate isomerase, or that some triosephosphate isomerase activity had survived the extraction procedure.

Spectrophotometric assays of NADH in the in vitro exchange system

Aliquots of the exchange system were placed in 1 ml cuvettes (1 cm path length) in a double beam Unicam SP800A UV spectrophotometer

thermostatted at 37°C. NADH concentrations in the system were calculated from the measured increase in absorbance at 340nm following the addition of NAD⁺ to the system.

Fluorimetric assays of NADH in the in vitro exchange system

The fluorescence measurements were made using 3 ml aliquots of the in vitro system thermostatted at 37°C in a Perkin-Elmer MPF-2A fluorescence spectrophotometer. The buffer used was filtered through a 0.22µm pore size Millipore filter before use in order to remove particulates. The fluorescence was excited at 340nm and the emission observed at 460nm.

Preparation of human erythrocyte enzymes

Aldolase

Aldolase was prepared according to Strapazon and Steck (1977). Approximately 250 ml of day old cells (stored in citrate/phosphate/glucose) were washed 4 times in 2 volumes of phosphate buffered saline (0.15M NaCl, 5mM sodium phosphate pH 7.0) and the buffy coat removed by aspiration. The cells were then lysed by diluting 50 ml aliquots of packed cells in 2 l of 5mM sodium phosphate buffer, pH 7.0, containing 1mM EDTA and 1mM dithiothreitol. The buffer was prewarmed to 37°C and the hypotonically lysed cells were incubated for 30 min at 37°C. The membranes, containing bound aldolase and GAPDH, were collected by centrifuging the lysate at 13,000 r.p.m. for 20 min at 37°C in a Sorvall RC-5 centrifuge (GSA rotor). The supernatants and debris buttons were aspirated off and the membrane fractions pooled and washed 3-5 times in the phosphate buffer. These membranes can be stored for several days at 0-5°C with no loss of enzyme activity (Strapazon &

Steck, 1977).

The membrane pellets from 250 ml of cells were resuspended in 500 ml of the sodium phosphate buffer and mixed with 500 ml of 2mM FDP. The resulting suspension was brought to pH 7.8 with 1M NaOH and stirred in an ice water bath for 1hr. The membranes were then centrifuged off by spinning at 13,000 r.p.m. for 1hr at 0°C. The supernatant was collected and recentrifuged to remove the last traces of membrane material.

The supernatant, containing aldolase, was adjusted to pH 6.5 with 10% acetic acid and then passed through a 1.2 x 12 cm column of carboxymethylcellulose (CM-22 from Whatman) at a maximum flow rate of 5 ml/min. The column had been prewashed with 1.5M NaCl then 100mM sodium phosphate, pH 6.5 and finally 5mM sodium phosphate, pH 6.5. This column absorption step removed the remaining haemoglobin contaminant. The effluent from this column was adjusted to pH 5.5 with 10% acetic acid and applied to a second CM-22 column prepared as above, except at pH 5.5. The loaded column was washed with 25 ml of 5mM sodium phosphate, pH 5.5 and then developed with a 30 ml gradient of 0-300mM NaCl in the same buffer. One ml fractions were collected and the aldolase detected by its absorbance at 280nm and by its enzymic activity. Peak fractions were pooled and concentrated in an Amicon ultrafiltration cell with a PM-30 membrane to give a solution containing 3-4 units/ml. The total activity recovered was approximately 10 units representing a yield of approximately 5%. The concentrated enzyme preparation was stored frozen at -70°C where it was stable for at least 2 weeks.

Glyceraldehydophosphate dehydrogenase

Glyceraldehydophosphate dehydrogenase was prepared according to Eby and Kirtley (1979). The aldolase free membrane pellet was resuspended in 500 ml of sodium phosphate buffer, pH 7.0 containing 1mM EDTA, 3mM dithiothreitol and 0.5M NaCl. The resulting suspension was incubated for 30 min at 4°C. The membranes were then centrifuged off by spinning at 13,000 r.p.m. for 1 hr at 4°C. The supernatant containing the enzyme was concentrated in an Amicon ultrafiltration cell using a PM-30 membrane to give 5-10 ml of enzyme solution. This was applied to a Sephadex G-100 column (4 x 70 cm) previously equilibrated with 5mM sodium phosphate buffer pH 7.0 containing 1mM EDTA and 1mM dithiothreitol. Three ml fractions were collected and the glyceraldehydophosphate dehydrogenase detected by its absorbance at 280nm and by its enzymic activity. Peak fractions were pooled and concentrated in an Amicon ultrafiltration cell with a PM-30 membrane. The enzyme was resuspended in 2.6M ammonium sulphate to give a solution containing approximately 200 units/ml. The total activity recovered was approximately 1000 units. The enzyme was stable as an ammonium sulphate suspension for at least 3 months.

Chromatography in both the aldolase and glyceraldehydophosphate dehydrogenase preparations was performed at 4°C.

3.3 The exchange system in vitro - a model for the system in situ ?

It has been shown that in the erythrocyte the metabolites involved in C-2 exchange are present at near equilibrium concentrations (Minikami & Yoshikawa, 1966). The in vitro system, which is at equilibrium as opposed to a near equilibrium steady state, was expected therefore to be a good model system. In this section the measured equilibrium concentrations of metabolites found in the in vitro system are compared with the values expected from published values for the equilibrium constants of the enzyme catalysed reactions. The aim of this investigation was to show that the in vitro system is at chemical equilibrium and that the final equilibrium concentrations of the substrates can be predicted from the added substrate concentrations. This avoids the requirement of having to assay for the varied substrate each time its concentration is changed.

Table 1 shows the results of triose phosphate and FDP assays performed on an in vitro exchange system. The table also shows the expected equilibrium values based on the known equilibrium constants for the reactions catalysed by aldolase and triosephosphate isomerase, (see also table 4). The reaction catalysed by glyceraldehydophosphate dehydrogenase, which has an equilibrium constant of 5×10^{-8} (Cori et al, 1950), will not significantly perturb these equilibria at the NAD^+ , P_i , GAP and hydrogen ion concentrations encountered in these studies. The table shows good agreement between the expected and observed values.

The equilibrium NAD^+ and NADH concentrations in the in vitro enzyme system were measured spectrophotometrically (table 2) and

Table 1

Assays of FDP, DHAP and GAP in the in vitro C-2 exchange system.

A	Time (min) following the addition of 150 μ M FDP to the <u>in vitro</u> system	Measured FDP concentration (μ M)	Measured DHAP plus GAP concentration (μ M)
	0	27	238
	5	26	252
	10	30	297
	30	13	262
	40	17	276

The expected equilibrium concentrations are 255 μ M DHAP + GAP and 23 μ M FDP (see table 4).

B	Time (min) following the addition of 700 μ M FDP to the <u>in vitro</u> system	Measured FDP concentration (μ M)	Measured DHAP plus GAP concentration (μ M)
	60	281	843

The expected equilibrium concentrations are 873 μ M DHAP + GAP and 264 μ M FDP (see table 4).

Table 1

A - The in vitro system contained 12mM lactate, 100 μ M NAD⁺ and approximately 40 units/ml triosephosphate isomerase, 0.4 units/ml aldolase, 1 unit/ml glyceraldehydophosphate dehydrogenase and 35 units/ml lactate dehydrogenase. The buffer was 100mM Tris-HCl pH^{*} 7.4 in ²H₂O containing 3mM dithiothreitol and 0.5mM EDTA.

B - The buffer was the same as in A except that the solvent was ¹H₂O. In addition it contained 80mM KCl which gives a total chloride concentration of approximately 0.15M. The system contained 20 μ M NAD⁺, 12mM lactate, 0.5mM Pi and 0.25mM MgCl₂. The concentration of Mg⁺⁺ and Pi are equivalent to the estimated free concentrations in the erythrocyte (Veech et al, 1979; Marshall & Omachi, 1974; Gupta et al, 1978).

Details of the extraction procedure and assay for the triose phosphates and FDP are given in the Experimental section.

Table 2

Spectrophotometric assays of NADH in the in vitro C-2 exchange system.

	Additions to the <u>in vitro</u> system	Absorbance change at 340 nm	NADH concentration (μ M)
A	1mM FDP	-	-
	15 μ M NAD ⁺	0.009	1.5
	12mM lactate	0.033	5.3
B	1mM FDP	-	-
	15 μ M NAD ⁺	-	-
	12mM lactate	0.030	4.8
C	15 μ M NAD ⁺	-	-
	1mM FDP	-	-
	12mM lactate	0.035	5.6

Table 2

The NADH concentrations were calculated using an extinction coefficient of $6.22 \times 10^6 \text{ cm}^2 \text{ mole}^{-1}$ (Horecker & Kornberg, 1948). The expected equilibrium concentration of NADH following the addition of 1mM FDP to the system containing $15\mu\text{M NAD}^+$ is $0.6\mu\text{M}$, this assumes an equilibrium constant for the reaction catalysed by glyceraldehydophosphate dehydrogenase of 5×10^{-8} (Cori et al, 1950). The expected equilibrium concentration in the presence of 12mM lactate and ignoring the glyceraldehydophosphate dehydrogenase equilibrium is $5.6\mu\text{M}$, this assumes an equilibrium constant of 1.11×10^{-11} for the lactate dehydrogenase reaction (Williamson et al, 1967).

A, B and C are three separate experiments, the specified additions to the system were made sequentially. The system also contained 0.5mM Pi, 0.25mM MgCl_2 and approximately 100 units/ml lactate dehydrogenase, 100 units/ml triosephosphate isomerase, 1 unit/ml aldolase and 10 units/ml glyceraldehydophosphate dehydrogenase. The buffer was 100mM Tris-HCl pH 7.4 in $^1\text{H}_2\text{O}$ containing 3mM dithiothreitol, 0.5mM EDTA and 80mM KCl.

The concentration of the NAD^+ stock solution, from which additions to the in vitro system were made, was determined by measuring the absorbance at 260nm and using an extinction coefficient of $17.6 \times 10^6 \text{ cm}^2 \text{ mole}^{-1}$ (Dalziel, 1963). The lactate and FDP stock solutions were assayed as described in chapter 2.

Table 3

Fluorimetric assays of NADH in the in vitro C-2 exchange system.

Total added NAD ⁺ concentration (μM)	Observed NADH concentration (μM)	Expected NADH concentration (μM)
26	14	9
53	19	13
79	25	16
105	27	19
132	32	22
158	34	24
184	36	26
211	38	28
Total added pyruvate concentration (μM)		
0.33	5	2.6
0.66	2	1.3
1.00	2	0.9

Table 3

The expected NADH equilibrium concentration was calculated by assuming that the reaction catalysed by glyceraldehydophosphate dehydrogenase makes a negligible contribution to the production of NADH and that the equilibrium constant for the lactate dehydrogenase reaction is 1.11×10^{-11} (Williamson et al, 1967).

The fluorescence response was calibrated by adding aliquots of a standard NADH solution to an in vitro system containing no enzymes. The NADH solution used was assayed spectrophotometrically by measuring the absorbance at 340nm.

The in vitro system contained 12mM lactate, 400uM FDP and approximately 0.2 units/ml aldolase, 0.5 units/ml glyceraldehydophosphate dehydrogenase, 40 units/ml lactate dehydrogenase and 80 units/ml triosephosphate isomerase. The buffer was 100mM Tris-HCl, pH 7.4 in $^1\text{H}_2\text{O}$ containing 3mM dithiothreitol and 0.5mM EDTA.

Table 4

The expected equilibrium concentrations of FDP, DHAP and GAP following the addition of FDP to the in vitro C-2 exchange system.

Added FDP concentration (μM)	Equilibrium FDP concentration (μM)	Equilibrium DHAP concentration (μM)	Equilibrium GAP concentration (μM)
50	3.1	90	4.1
100	11	170	7.4
150	23	244	11
200	37	312	14
250	54	376	17
300	72	436	20
350	92	493	22
400	114	548	25
450	136	600	27
500	160	650	30
550	185	699	32
600	210	745	34

The expected equilibrium concentrations were calculated using an equilibrium constant for the reaction catalysed by aldolase of 1.2×10^{-4} (Herbert et al, 1940) and an equilibrium constant for the reaction catalysed by triosephosphate isomerase of 22 (Veech et al, 1979). The reaction catalysed by glyceraldehydophosphate dehydrogenase is not expected to significantly perturb these equilibria at the NAD^+ and Pi concentrations used here.

fluorimetrically (table 3).

The spectrophotometric measurements show levels of NADH which compare favourably with those expected if the reaction catalysed by lactate dehydrogenase and the added lactate and NAD^+ concentrations solely determine the final NAD^+ and NADH concentrations. The levels of NADH measured fluorimetrically (table 3) also show reasonable agreement with the expected values. However the apparent NADH concentration is slightly higher than expected. This may in part be due to fluorescence enhancement of NADH bound to lactate dehydrogenase (Velick, 1958). The concentration of lactate dehydrogenase in this system was approximately $2\mu\text{M}$. The enzyme was absent from the NADH solutions used to calibrate the fluorescence. Addition of pyruvate to the system results in a marked loss of NADH consistent with the lactate dehydrogenase equilibrium determining the NAD(H) concentration.

3.4 Isotope exchange measurements in the in vitro exchange system

3.4.1 Data analysis

By measuring the dependence of the isotope exchange rate on the concentration of a particular enzyme in the in vitro system the specific equilibrium velocity of the enzyme can be measured. In chapter 2 the specific equilibrium velocity of lactate dehydrogenase was determined at different NAD^+ concentrations using a double reciprocal plot analysis of the exchange data. Double reciprocal plots are however unreliable for extracting kinetic parameters from data which show a hyperbolic relationship (see Dowd & Riggs, 1965). In this sort of analysis, using figure 13 chapter 2 as an example, points at very low enzyme

concentration make a disproportionate contribution to the determination of the slope of the double reciprocal plot. These points are frequently the least accurately measured points. Other types of linear plot are available but most are statistically objectionable on the grounds that errors in the measured parameters can seriously affect estimates of kinetic constants made from these plots. Non-linear least squares regression analysis is a much sounder procedure (Eisenthal & Cornish-Bowden, 1974b) although it assumes that the errors are normally distributed, that the independent variable (enzyme concentration in the case of the isotope exchange analysis) is known exactly and that the correct weighting factors are known. It is usual to assume that the weighting factor equals one for every observation, an assumption which implies, in the case of isotope exchange, that the errors in all of the measured equilibrium velocities are of equal variance. This may not be justified. All of these methods rely heavily on assumptions about the distribution of errors. The analysis which will be used here, the so called "direct plot" (Eisenthal & Cornish-Bowden, 1974a), makes few assumptions about error. The principal assumption that remains is that the error in any observation is as likely to be positive as it is to be negative (Eisenthal & Cornish-Bowden, 1974b).

For C-2 exchange the activity (A) of an enzyme (X) can be related to the overall equilibrium velocity (V_{C2X}) of the exchange system by the following equation;

$$V_{C2X} = \frac{A_X}{n/\alpha + A_X/V_R} \dots\dots\dots(1)$$

where V_R is the reciprocal of the sum of the reciprocals of the

equilibrium velocities of the other enzymes involved in the exchange, α is the specific equilibrium velocity of the enzyme X and n has a value of 1 if X is aldolase or triosephosphate isomerase and 2 if X is one of the dehydrogenases. This equation can be rearranged to give;

$$1 = \frac{V_R}{V_{C2X}} - \frac{nV_R}{\alpha A_X} \dots\dots\dots(2)$$

which is of the general form;

$$x/a + y/b = 1$$

the equation of a line in xy space with intercepts a on the x axis and b on the y axis. Thus V_R and nV_R/α are linearly related for given values of V_{C2X} and A_X , even though V_{C2X} and A_X are not. Equation 2 defines a straight line plotted in $V_R, nV_R/\alpha$ space. In general any point in V_{C2X}, A_X space can be represented as a line in $V_R, nV_R/\alpha$ space. So for each observation (A_X, V_{C2X}) there exists a straight line in $V_R, nV_R/\alpha$ space with intercepts $-A_X$ on the nV_R/α axis and V_{C2X} on the V_R axis. This line relates all the values of V_R and nV_R/α that satisfy equation 1 exactly for the particular values of V_{C2X} and A_X . It follows that the coordinates of the point where the lines intersect provide the only values of V_R and nV_R/α that satisfy equation 1 for every observation. Thus in a plot of V_{C2X} versus A_X a series of lines are obtained, the coordinates of intersection of these lines give V_R on the y axis and nV_R/α on the x axis from which α can be calculated. Because of error, these lines do not intersect at a unique point, but the points of intersection can be used to estimate V_R and nV_R/α . This procedure is described in appendix 1 together with a computer program which

calculates the coordinates of the line intersections and from these α and V_R . The program also contains an error analysis which uses the method of Cleland (1967). This is based on a least squares approach and assumes that the error in measurements of enzyme concentration or activity are much less than the error in determinations of V_{C2X} . This is probably untrue, so although equilibrium velocities are quoted with standard errors, these are not true standard errors but are provided as an index of the relative accuracy of the measurement. More general statistical analyses are available which recognise that there may be error in both of the experimentally measured parameters (see Cleland, 1967). These methods were not used because; a) their validity has been questioned (Eisenthal & Cornish-Bowden, 1974b); b) in any equilibrium velocity determination there were usually only four determinations of V_{C2X} at different enzyme concentration and it was felt that a better idea of the real error in a determination would be obtained by repeating the experiment a number of times.

A prerequisite for the above analysis is that the equilibrium velocity of an enzyme should be linearly dependent on its concentration. The dependence of equilibrium velocity on enzyme concentration is discussed in chapter 5 and examined in some detail in chapter 6 where the dependence of the lactate dehydrogenase equilibrium velocity on enzyme concentration is measured and compared with theoretical expectations.

Tables 5,6,7 and 8 show the results of equilibrium velocity determinations performed on aldolase, triosephosphate isomerase, glyceraldehydophosphate dehydrogenase and lactate dehydrogenase respectively. In all equilibrium velocity determinations the overall

PEAK HEIGHT

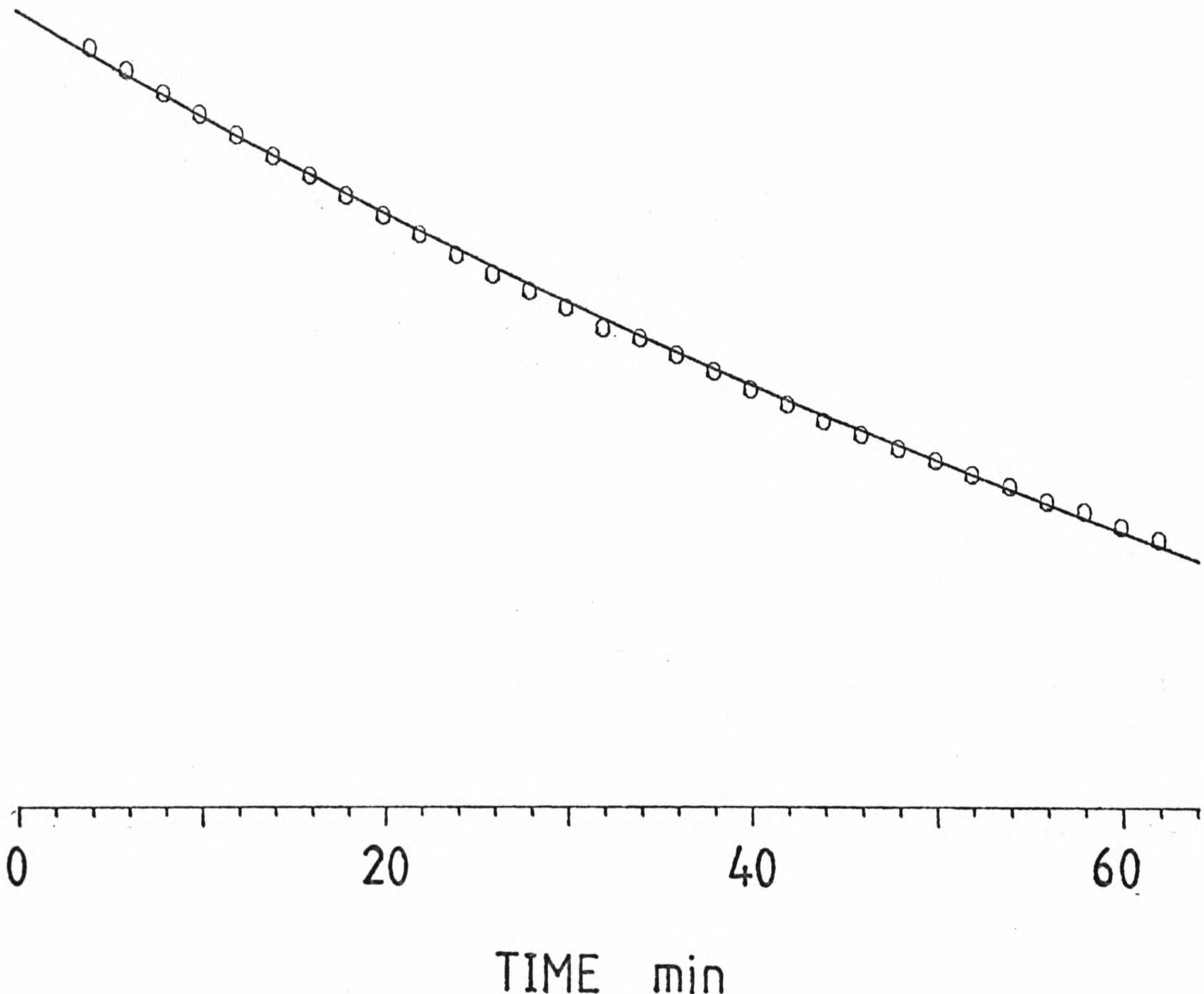


Figure 1

A typical in vitro exchange time course.

The figure shows a plot of lactate peak height versus time during an exchange time course. The solid line is that obtained from a least squares fit of the data to the following equation;

$$h(t) = A(1 - 2e^{-kt})$$

$h(t)$ is peak height at time t , A is the amplitude of the exchange and k the first order rate constant for the exchange. The values of A and k are calculated from the least squares fit. V_{C2X} is calculated by multiplying the added lactate concentration by k . The fitting procedure used is a routine available in the Nicolet 1180 computer software.

The figure shows an exchange time course ₁ obtained when 12mM L-(2-²H)lactate was added to an in vitro system in ₂ H₂O.

exchange equilibrium velocity was measured at four or more enzyme concentrations by following the exchange in 12mM lactate (unless otherwise stated). The exchange was monitored until between 30–50% of the lactate had exchanged. A first order rate constant was obtained from a least squares fit of the exchange time course as described in the legend to figure 1. The computed standard error on these rate constants was never greater than $\pm 5\%$. Subsequent analysis of exchange rate versus enzyme concentration was as described above.

3.4.2 Results

The results for lactate dehydrogenase are those initially presented in figure 14 in chapter 2. They show the dependence of the enzyme's equilibrium velocity on NAD^+ concentration. Also shown is a preliminary study of the dependence on lactate concentration. The results agree well with the predictions of the model, described in appendix 1 of chapter 2, which relates the known kinetic parameters of lactate dehydrogenase to the equilibrium velocity for the exchange of isotope between the lactate C-2 position and the C-4 position of the nicotinamide ring of NADH. This study was performed at an ionic strength lower than that present in the cell. If the properties displayed by the enzyme in vitro are to be compared with the properties it displays in situ then the effects of salt concentration should be considered. The measured kinetic parameters of the enzyme have been shown to be affected by salt concentration (Winer & Schwert, 1958; Silverstein & Boyer, 1964; Anderson, 1981; Rivedal & Sanner, 1979). The effect of buffer composition on the activity of the enzyme is considered in chapter 6.

Table 5

Aldolase equilibrium velocity determinations in the in vitro C-2 exchange system.

Concentration of FDP added to the <u>in vitro</u> system (μM)	Aldolase equilibrium velocity ($\mu\text{mol}/\text{min}/\text{unit}$)
A - Rabbit muscle enzyme	
37	0.52 $\begin{matrix} + \\ - \end{matrix}$ 0.09
102	2.04 $\begin{matrix} + \\ - \end{matrix}$ 0.08
204	1.25 $\begin{matrix} + \\ - \end{matrix}$ 0.19
306	1.41 $\begin{matrix} + \\ - \end{matrix}$ 0.05
408	1.17 $\begin{matrix} + \\ - \end{matrix}$ 0.06
B - Human erythrocyte enzyme	
60	1.27 $\begin{matrix} + \\ - \end{matrix}$ 0.13
73	1.54 $\begin{matrix} + \\ - \end{matrix}$ 0.24
200	1.30 $\begin{matrix} + \\ - \end{matrix}$ 0.13
400	1.01 $\begin{matrix} + \\ - \end{matrix}$ 0.08

Table 5

A - The exchange system contained 100mM Tris-HCl pH* 7.4, 0.5mM EDTA, 3mM dithiothreitol, 80mM KCl, 100 μ M NAD⁺ and 12mM lactate in ²H₂O. Samples containing 0.5 ml of the exchange system in a 5 mm diameter n.m.r. tube were prewarmed for approximately 5 minutes before initiation of an exchange time course by the addition of 12mM lactate to an otherwise complete exchange system. Exchange at the lactate C-2 position was usually monitored for 45-90 min (see text) depending on the velocity of the exchange. At the end of the exchange measurement the samples were assayed for aldolase activity as described in chapter 2. The aldolase activity was varied between 0.2 and 1.0 units/ml. There were fixed but unknown concentrations of the other enzymes involved in the exchange. The FDP stock solution from which additions to the exchange system were made was assayed immediately prior to use.

B - The conditions were the same as in A except that 6mM lactate was used and the aldolase activity was varied between 0.02 and 0.1 units/ml.

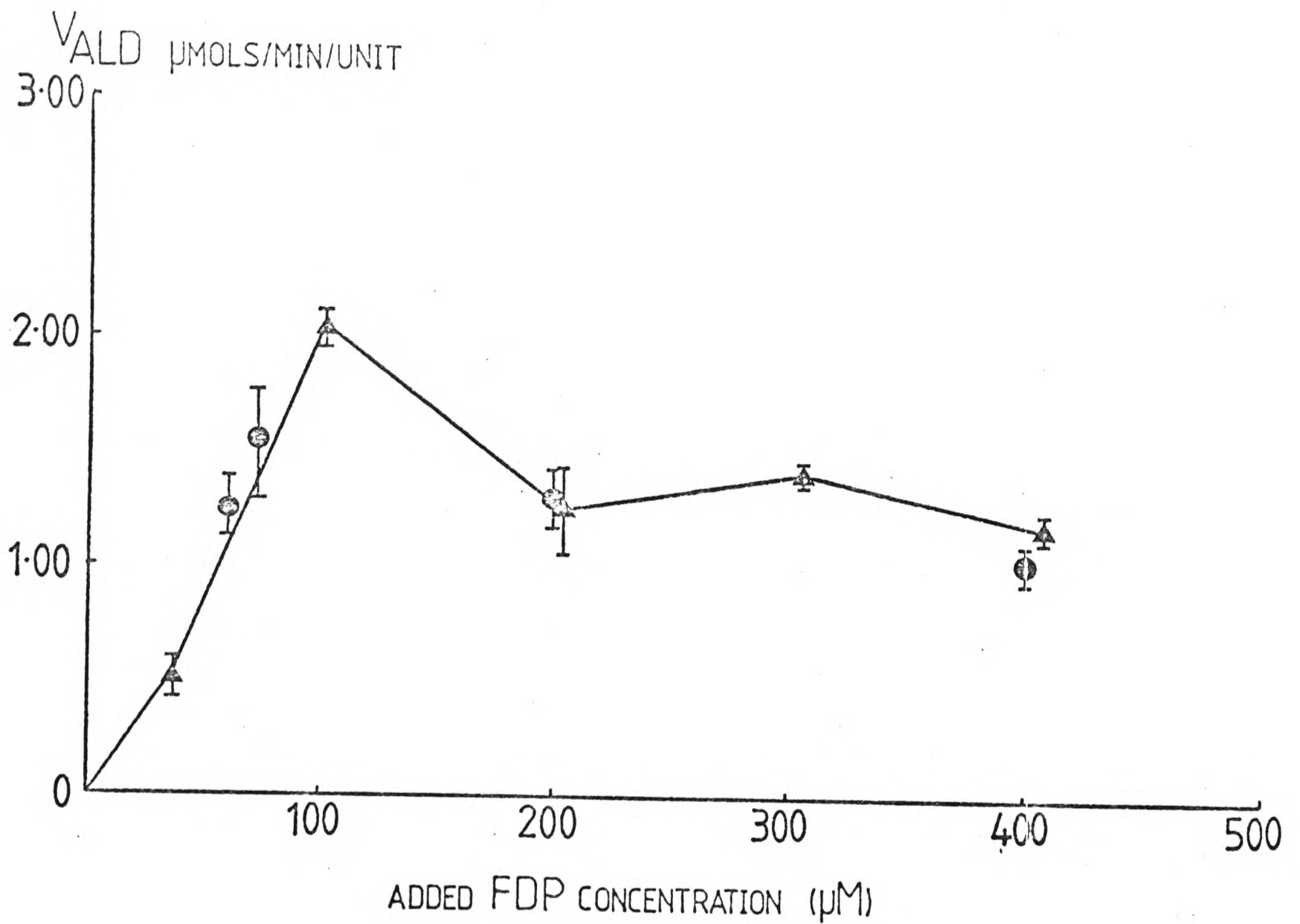


Figure 2

The dependence of the aldolase equilibrium velocity on the added FDP concentration in the in vitro C-2 exchange system.

The points marked (●) were obtained with the human erythrocyte enzyme and those marked (▲) with the rabbit muscle enzyme.

Table 5 shows the dependence of the aldolase equilibrium velocity on the added FDP concentration in the in vitro system. Both the human erythrocyte and rabbit muscle enzymes were studied, preparation of the erythrocyte enzyme is described in the Experimental section. Aldolase catalyses the stereospecific exchange of the pro-S hydrogen at the C-3 position of DHAP with solvent (Rose, 1958). The concentration of the enzyme bound DHAP intermediate, which is active in the exchange, is influenced by a number of factors. For example increasing the ionic strength has been shown to inhibit FDP cleavage (Mehler, 1963) and to increase the dissociation constant of the enzyme-DHAP complex (Grazi & Trombetta, 1974; Mehler & Bloom, 1963). For this reason the equilibrium velocities were determined in the presence of physiological chloride concentrations. A rate of DHAP detritiation of 1.1 μ mol exchanged/min/unit enzyme has been measured at pH 7.0 in the absence of FDP and GAP by Rose and coworkers (Rose et al, 1965). The concentration of DHAP was 96 μ M and the temperature was 35 $^{\circ}$ C. The spectrophotometric enzyme assay used in that study was virtually identical to that used here. Lowe and Pratt (1976) measured a deuteration rate of 1.5 μ mol/min/unit enzyme at pH 7.5 and 25 $^{\circ}$ C, the DHAP concentration was 6.1mM. The spectrophotometric assay of enzyme activity was similar to that used here although it was performed at 25 $^{\circ}$ C. These results show good agreement with the results presented in table 5 and figure 2. Rose et al (1965) showed however that as the GAP concentration is increased there is a marked decrease in the exchange rate. This was shown to be due to an enhanced recondensation reaction at higher GAP concentrations. As demonstrated in table 4 the equilibrium DHAP concentration is far higher than the concentrations of GAP and FDP when the added FDP concentration is low. This is due to the equilibria catalysed by both aldolase and triosephosphate isomerase. It has been

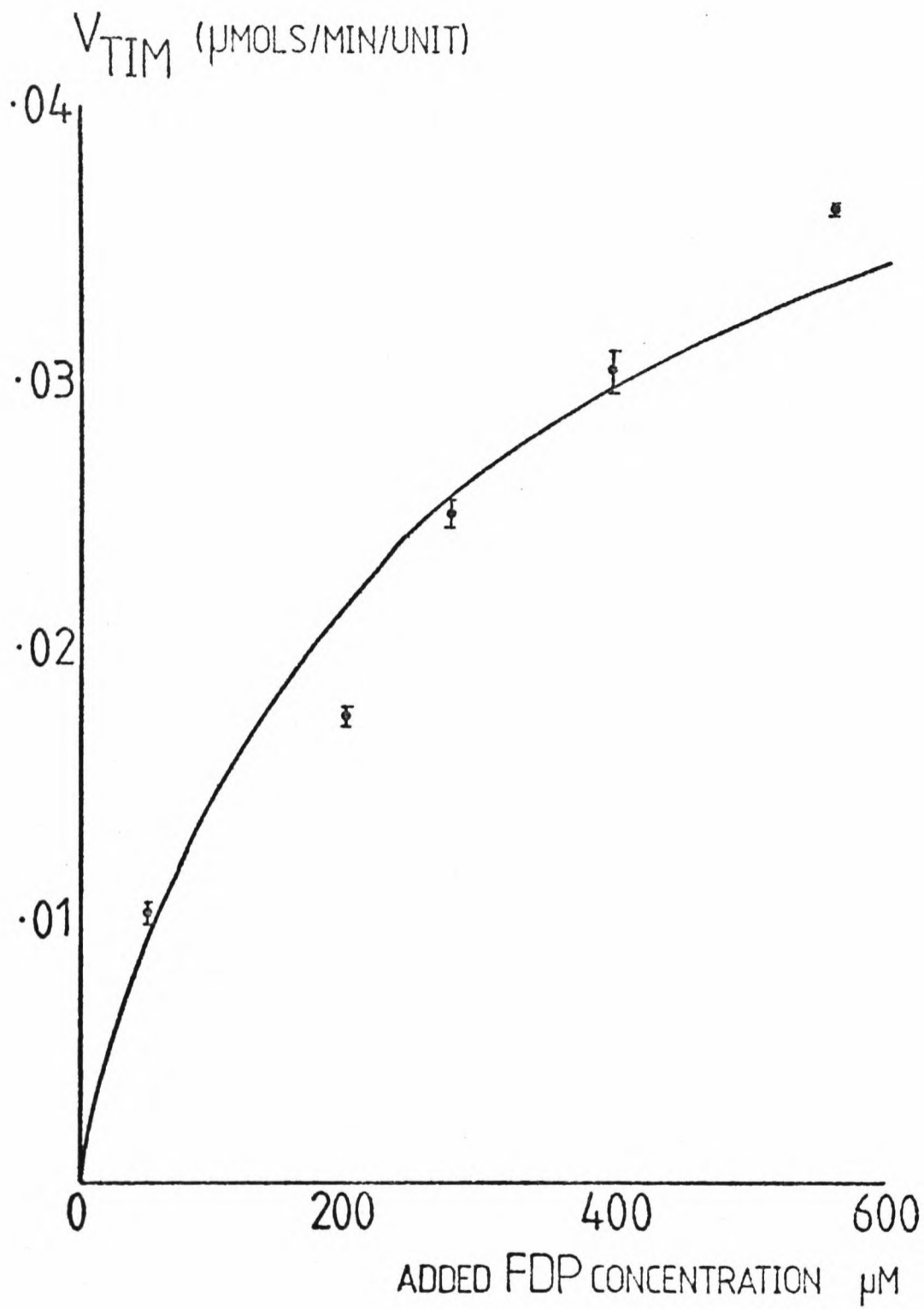


Figure 3

The dependence of the triosephosphate isomerase equilibrium velocity on the added FDP concentration in the in vitro C-2 exchange system. The solid line drawn through the experimental points was calculated as described in appendix 2.

shown that under these conditions the aldolase-DHAP complex is the prevalent enzyme-substrate complex (Grazi & Trombetta, 1980; Ottaway, 1979). As the concentration of FDP added to the system is increased the equilibrium FDP concentration forms an increasing proportion of the total triosephosphate and FDP pool. The slight depression therefore in the observed exchange velocity observed at higher added FDP concentrations (see figure 2) may be the result of a decreased fraction of the enzyme in a DHAP bound form due to increased competition with FDP for binding to the enzyme.

Figure 3 shows the dependence of the triosephosphate isomerase equilibrium velocity on the concentration of FDP added to the in vitro exchange system (see also table 6). The solid line is a theoretical curve constructed using the equation shown in appendix 2. This equation relates the kinetic parameters of the enzyme to the expected equilibrium velocity for the exchange of hydrogen between the pro-S C-3 position of DHAP and the aldehydic hydrogen of GAP. The equation was derived using the method of Yagil and Hoberman (1969) which was described in appendix 1 of chapter 2. The kinetic constants used in this model are those of Albery and Knowles (1976). The absolute values for the equilibrium velocity predicted by the model depend on the turnover number chosen for the enzyme. In order to draw the theoretical curve shown in figure 3 an arbitrary value was chosen for this number so that the predicted and observed velocities had the same range of values (see appendix 2). This is considered justified since it is the shape and not the amplitude of this curve which is important.

The dependence of the equilibrium velocity of human erythrocyte glyceraldehydophosphate dehydrogenase on the concentration of FDP added

Table 6

Triosephosphate isomerase equilibrium velocity determinations in the in vitro C-2 exchange system.

Concentration of FDP added to the <u>in vitro</u> system (μM)	Triosephosphate isomerase equilibrium velocity ($\mu\text{mol}/\text{min}/\text{unit}$)
50	0.010 $\begin{matrix} + \\ - \end{matrix}$ 0.004
200	0.017 $\begin{matrix} + \\ - \end{matrix}$ 0.003
200 + 0.25mM Mg^{++}	0.015 $\begin{matrix} + \\ - \end{matrix}$ 0.001
280	0.025 $\begin{matrix} + \\ - \end{matrix}$ 0.005
400	0.030 $\begin{matrix} + \\ - \end{matrix}$ 0.008
560	0.036 $\begin{matrix} + \\ - \end{matrix}$ 0.002

Conditions in the in vitro system were similar to those described in the legend to table 5 except that 6mM lactate was used. The triosephosphate isomerase activity was varied between 2 and 20 units/ml. Details of the enzyme assay are given in chapter 2. The determinations were performed as described in the text and in the legend to table 5.

Table 7

Glyceraldehydphosphate dehydrogenase equilibrium velocity
determinations in the in vitro C-2 exchange system.

Concentration of FDP added to the <u>in vitro</u> system (μM)	Glyceraldehydphosphate dehydrogenase equilibrium velocity ($\mu\text{mol}/\text{min}/\text{unit}$)
120	0.040 $\begin{matrix} + \\ - \end{matrix}$ 0.005
160	0.034 $\begin{matrix} + \\ - \end{matrix}$ 0.007
200	0.042 $\begin{matrix} + \\ - \end{matrix}$ 0.005
400	0.062 $\begin{matrix} + \\ - \end{matrix}$ 0.018
600	0.072 $\begin{matrix} + \\ - \end{matrix}$ 0.012

The conditions in the in vitro system were similar to those described in the legend to table 5 except that there was no KCl present. The glyceraldehydphosphate dehydrogenase activity was varied between 1 and 6 units/ml. The determinations were performed as described in the text and in the legend to table 5.

Table 8

Lactate dehydrogenase equilibrium velocity determinations in the in vitro C-2 exchange system.

A	Concentration of NAD^+ added to the <u>in vitro</u> system (μM)	Lactate dehydrogenase equilibrium velocity ($\mu\text{mol}/\text{min}/\text{unit}$)
	9	0.017 $\begin{matrix} + \\ - \end{matrix}$ 0.003
	9	0.009 $\begin{matrix} + \\ - \end{matrix}$ 0.002
	11	0.024 $\begin{matrix} + \\ - \end{matrix}$ 0.004
	18	0.027 $\begin{matrix} + \\ - \end{matrix}$ 0.010
	18	0.031 $\begin{matrix} + \\ - \end{matrix}$ 0.004
	22	0.030 $\begin{matrix} + \\ - \end{matrix}$ 0.011
	27	0.031 $\begin{matrix} + \\ - \end{matrix}$ 0.003
	28	0.042 $\begin{matrix} + \\ - \end{matrix}$ 0.015
	36	0.043 $\begin{matrix} + \\ - \end{matrix}$ 0.012
	37	0.050 $\begin{matrix} + \\ - \end{matrix}$ 0.010
	43	0.056 $\begin{matrix} + \\ - \end{matrix}$ 0.006
	55	0.049 $\begin{matrix} + \\ - \end{matrix}$ 0.001
	59	0.059 $\begin{matrix} + \\ - \end{matrix}$ 0.006
	74	0.046 $\begin{matrix} + \\ - \end{matrix}$ 0.003
	83	0.065 $\begin{matrix} + \\ - \end{matrix}$ 0.019
	92	0.052 $\begin{matrix} + \\ - \end{matrix}$ 0.008

Table 8 (contd.)

B

Concentration of lactate added to the <u>in vitro</u> system (μM)	Lactate dehydrogenase equilibrium velocity ($\mu\text{mol}/\text{min}/\text{unit}$)
12	0.056 \pm 0.006
8	0.042 \pm 0.004
4	0.024 \pm 0.004

A - Conditions in the in vitro system were similar to those described in the legend to table 5. The FDP concentration however was fixed at $200\mu\text{M}$. The lactate dehydrogenase activity was varied between 2 and 15 unit/ml, details of the assay are given in the Experimental section.

B - Conditions were the same as in A except that the NAD^+ concentration was fixed at $40\mu\text{M}$.

The NAD^+ concentration in the stock solution, from which additions to the in vitro system were made, was determined by measuring absorbance at 260nm. Equilibrium velocity determinations were performed as described in the text and in the legend to table 5.

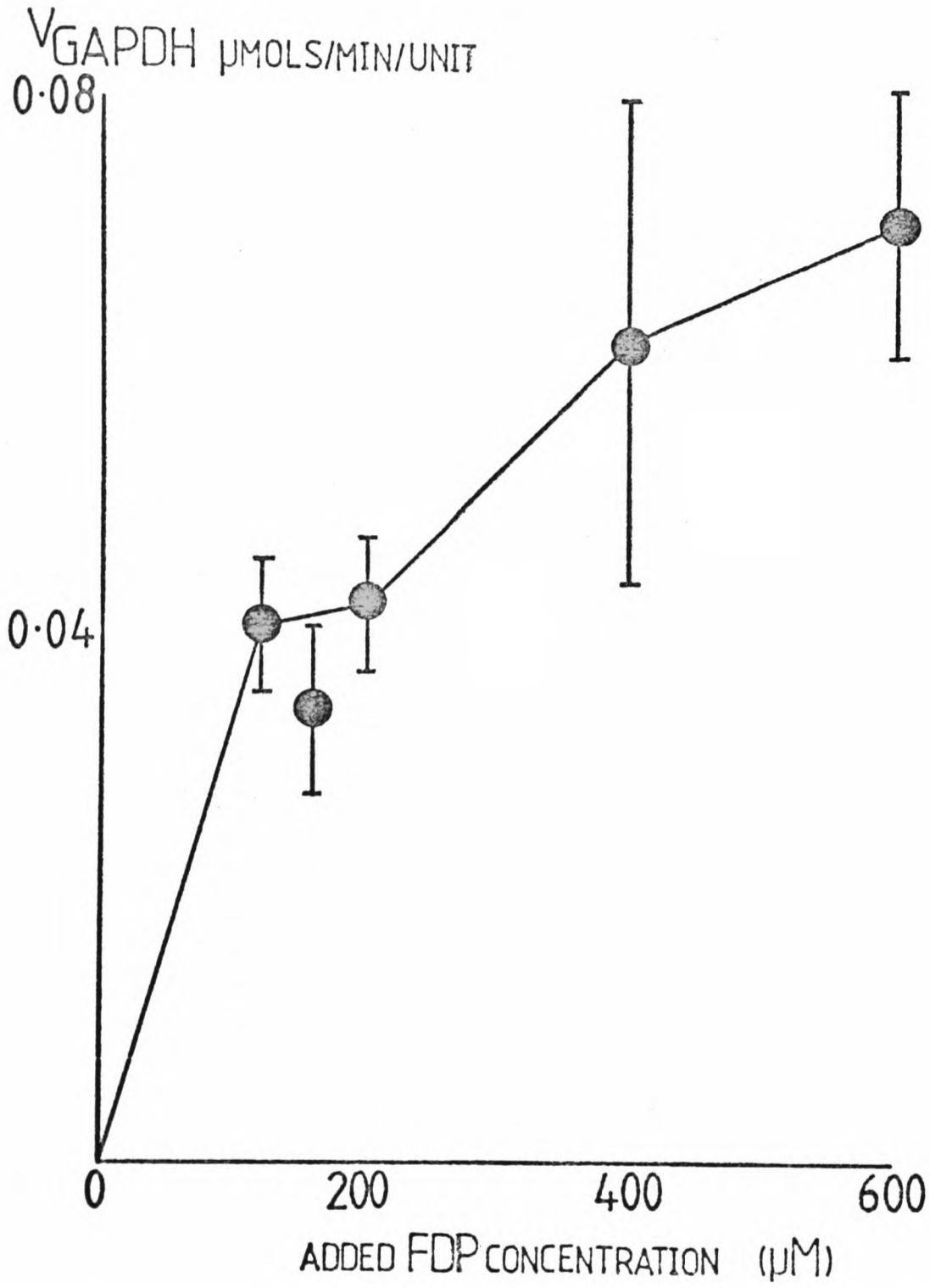


Figure 4

The dependence of the glycerinaldehydophosphate dehydrogenase equilibrium velocity on the added FDP concentration in the in vitro C-2 exchange system.

to the in vitro system is shown in figure 4 and table 7. Preparation of the enzyme is described in the Experimental section. The enzyme catalyses the exchange of isotope between the B face C-4 position of the nicotinamide ring of NADH and the aldehydic hydrogen of GAP. Further equilibrium velocity determinations on this enzyme are presented in chapter 5.

3.5 Summary and conclusions

The in vitro exchange system has been shown to be at chemical equilibrium. The concentrations of the exchanging intermediates in the system can be calculated from the known equilibrium constants for the reactions involved. This avoids the necessity of having to assay for the concentration of an intermediate each time the concentration of a substrate added to the system is changed. A method for analysing the exchange rate versus enzyme concentration was presented and the advantages of this direct plot analysis over the double reciprocal plot were described.

In conclusion the in vitro system has been shown to be a well defined reproducible system in which the expected in situ conditions can be simulated and which can be used to measure the isotope exchange equilibrium velocities of the individual enzymes involved in C-2 exchange.

3.6 References

- Albery, W.J. & Knowles, J.R. (1976) *Biochemistry* 15, 5627-5631
- Anderson, S.R. (1981) *Biochemistry* 20, 464-467
- Cleland, W.W. (1967) *Adv. Enzymol.* 29, 1-32
- Cori, C.F., Velick, S.F. & Cori, G.T. (1950) *Biochim. Biophys. Acta* 4, 160-169
- Dalziel, K. (1963) *J. Biol. Chem.* 238, 1538-1543
- Dowd, J.E. & Riggs, D.S. (1965) *J. Biol. Chem.* 240, 863-869
- Eby, D. & Kirtley, M.E. (1979) *Arch. Biochem. Biophys.* 198, 608-613
- Eisenthal, R. & Cornish-Bowden, A. (1974a) *Biochem. J.* 139, 715-720
- Eisenthal, R. & Cornish-Bowden, A. (1974b) *Biochem. J.* 139, 721-730
- Grazi, E. & Trombetta, G. (1974) *Biochim. Biophys. Acta* 364, 120-127
- Grazi, E. & Trombetta, G. (1980) *Eur. J. Biochem.* 107, 369-373
- Gupta, R.K., Benkovic, J.L. & Rose, Z.B. (1978) *J. Biol. Chem.* 253, 6172-6176

Herbert, D., Gordon, H., Subramanyan, V. & Green, D.E. (1940)

Biochem. J. 34, 1108-1123

Horecker, B.L. & Kornberg, A. (1948) J. Biol. Chem. 175, 385-390

Lowe, G. & Pratt, R.F. (1976) Eur. J. Biochem. 66, 95-104

Marshall, W.E. & Omachi, A (1974) Biochim. Biophys. Acta 354, 1-10

Mehler, A.H. (1963) J. Biol. Chem. 238, 100-104

Mehler, A.H. & Bloom, B. (1963) J. Biol. Chem. 238, 105-107

Minikami, S. & Yoshikawa, H. (1966) J. Biochem. (Tokyo) 59, 139-144

Ottaway, J.H. (1979) Biochem Soc. Trans. 7, 398-402

Rivedal, E. & Sanner, T. (1979) Biochim. Biophys. Acta 567, 60-65

Rose, I.A. (1958) J. Am. Chem. Soc. 80, 5835-5836

Rose, I.A., O'Connell, E.L. & Mehler, A.H. (1965) J. Biol. Chem. 240,
1758-1765

Silverstein, E. & Boyer, P.D. (1964) J. Biol. Chem. 239, 3901-3907

Strapazon, E. & Steck, T.L. (1977) Biochemistry 16, 2966-2970

Veech, R.L., Raijman, L., Dalziel, K. & Krebs, H.A. (1969) *Biochem. J.* 115, 837-842

Veech, R.L., Lawson, J.W.R., Cornell, N.W. & Krebs, H.A. (1979) *J. Biol. Chem.* 254, 6538-6547

Velick, S.F. (1958) *J. Biol. Chem.* 233, 1455-1467

Williamson, D.H., Lund, P. & Krebs, H.A. (1967) *Biochem. J.* 103, 514-527

Winer, A.D. & Schwert, G.W. (1958) *J. Biol. Chem.* 231, 1065-1083

Yagil, G. & Hoberman, H.D. (1969) *Biochemistry* 8, 352-360

3.7 Appendix 1

A computer program for calculating the specific equilibrium velocity of an enzyme.

The program estimates a specific equilibrium velocity for an enzyme using a direct plot analysis (Eisenthal & Cornish-Bowden, 1974a) which was described in the text. The program also estimates a "standard error" for this value using the method of Cleland (1967). The program is written in BASIC and was run on a CTL MOD1 computer. The following is a description of the program.

Lines 30 to 130 constitute a command module. The user is invited to enter a command which then transfers control to a specified part of the program. The initial command will be, E, enter points. This transfers control to line 140 and the user is shown the format in which data should be input (line 160). The number of each input is printed (line 170) prior to entry. Input is terminated with the entry 0,0. Control returns to the command module at line 80. On entering C, calculate, control is transferred to line 400. The coordinates of the intersection points of lines drawn according to the direct plot analysis are calculated and stored in the E matrix (lines 450 and 460) and printed (line 470). These lines are drawn between V_{C2X} (plotted on the y or V_R axis) and $-A_X$ (plotted on the x or V_R/α axis), (see text). There will be $1/2 n(n-1)$ intersections, where n is the number of data points entered. Following printing of the coordinates of intersection the user is invited to delete outliers. These are aberrant data points, the lines drawn through them do not intersect the other lines in the region in which most intersections are found. Outliers are readily

seen in the data display which prints the coordinates of intersection between specified data points. If the user types, Y, to the question "discard outliers Y/N", then control is transferred to line 280. The number of the data point to be deleted is input and the point is subsequently deleted. Control is then transferred to the command module. The command C will result in calculation of the coordinates for intersection of those data points remaining. If no further outliers are to be discarded then N is typed to the "discard outliers" question and the user is then asked if the enzyme is a dehydrogenase. If the answer to this question is yes then the y coordinates of the line intersections are assigned values corresponding to $2V_R/\alpha$ instead of V_R/α (see text). The median values of the coordinates of the line intersections on the x and y axes are then estimated in the subroutine beginning at line 800. It has been shown that these values represent the best estimates of V_R and V_R/α (Eisenthal & Cornish-Bowden, 1974b). The subroutine initially sorts, in ascending order, the x or y coordinates in the E matrix. The value of Z at the call of the subroutine specifies whether the matrix values are sorted according to the values of the x or y coordinates). The program then searches for intersection points which have negative x and y coordinates i.e. the points lie in the third quadrant (lines 950 and 960). In a reappraisal of the direct plot Eisenthal and Cornish-Bowden (1978) pointed out that these intersections should be assigned large positive values. This is accomplished in lines 970 to 1160 in which these coordinates are given positive values and are assigned large values in the analysis simply by shuffling them to the other end of the E matrix i.e. above the largest positive values found during the sorting process implemented at the start of the subroutine. If there are an even number of points in the E matrix then the median value is the average value of the two middle points. This is calculated

at line 1180. If there are an odd number of points then the median value is that of the middle point. This is calculated at line 1210. The subroutine returns to the main program the median values for V_R and nV_R/α (where $n=2$ for a dehydrogenase). The value for α , the specific equilibrium velocity for the enzyme, is then calculated and the "standard error" estimated using the subroutine beginning at line 1250. At lines 1300 and 1310 the squares of the deviations of the experimental points from the values expected with the computed values for α and V_R are calculated. At completion of the loop at line 1380 the variable Q has the value of the sum of the squares of the deviations. The elements of the F matrix are assigned the following values;

$$\begin{bmatrix} \sum_i \left[\frac{dV_{C2Xi}}{d\alpha} \right]^2 & \sum_i \frac{dV_{C2Xi}}{d\alpha} \frac{dV_{C2Xi}}{dV_R} \\ \sum_i \frac{dV_{C2Xi}}{d\alpha} \frac{dV_{C2Xi}}{dV_R} & \sum_i \left[\frac{dV_{C2Xi}}{dV_R} \right]^2 \end{bmatrix}$$

The derivatives $dV_{C2X}/d\alpha$ and dV_{C2X}/dV_R are calculated at lines 1320 and 1330. Multiplication of the inverse of this matrix (H in the program) by σ^2 , which is equal to the sum of the squares of the deviations (Q) multiplied by $1/(C-2)$ where C is the number of experimental points, gives a matrix containing the following values.

$$\begin{bmatrix} \text{Variance}(\alpha) & \text{Covariance}(\alpha, V_R) \\ \text{Covariance}(\alpha, V_R) & \text{Variance}(V_R) \end{bmatrix}$$

The square root of the variance gives the standard error, for α this is calculated at line 740. (It should be noted that the derivatives were

obtained for an equation in which α was the reciprocal of the specific equilibrium velocity). The specific equilibrium velocity, α and its "standard error" are then printed as is V_R and its standard error. Control is then returned to the command module. The program run is terminated by typing Z.

It will be noted that outliers are considered to be those points that give line intersections outside the region of the majority of intersections. These intersections lie in the first quadrant. It was mentioned above, however, that intersections in the third quadrant are considered as having large positive values. These points are not automatically considered as outliers (see Eisinger & Cornish-Bowden 1978). The reason for this becomes apparent if an isotope exchange analysis is considered in which the equilibrium velocities of the non-varied enzymes vastly exceed that of the varied enzyme on which the equilibrium velocity determination is being made. In this case the approximately linear part of the hyperbola relating V_{C2X} to the concentration of the varied enzyme is being observed. A direct plot of the data obtained in this region tends to be a set of nearly parallel lines. If there were no error the line intersections would occur at large positive x and y coordinates. However very small errors in the measured parameters can result in the lines intersecting in the third quadrant. These points however are not outliers. Thus the user of the analysis must exercise some discretion when using it. In the isotope exchange analysis points which give line intersections in the third quadrant are regarded as outliers unless the conditions described above exist. Under these circumstances the sensitivity coefficient of the varied enzyme approaches unity and the specific equilibrium velocity is obtained simply by taking the ratio of V_{C2X} to the activity of the

enzyme. The value of the "standard error" tends to indicate whether the correct decision has been made in regarding a third quadrant intersection as an outlier. If it is an outlier then its deletion should result in a significant reduction in the apparent error on χ^2 .

References

Eisenthal, R. & Cornish-Bowden, A. (1974a) *Biochem. J.* 139, 715-720

Eisenthal, R. & Cornish-Bowden, A. (1974b) *Biochem. J.* 139, 721-730

Eisenthal, R. & Cornish-Bowden, A. (1978) *Biochim. Biophys. Acta* 523,
268-272

```

10 DIM D(10, 3), E(45, 3), F(2, 2), H(2, 2), L(45, 2)
20 MAT L = ZER(45, 2)
30 PRINT "ENTER COMMAND"
40 PRINT "E ENTER POINTS"
50 PRINT "B DELETE POINT"
60 PRINT "C CALCULATE"
70 PRINT "Z END"
80 PRINT "ENTER COMMAND"
90 INPUT DS
100 IF DS = "E" THEN 140
110 IF DS = "C" THEN 400
120 IF DS = "B" THEN 280
130 IF DS = "Z" THEN 1420
140 LET C = 1
150 PRINT "INPUT DATA"
160 PRINT "VC2X,AX,RETURN"
170 PRINT C
180 LET D(C, 3) = C
190 INPUT D(C, 1), D(C, 2)
200 IF D(C, 1) = 0 THEN 250
210 LET C = C + 1
220 IF C = 10 THEN 240
230 GOTO 170
240 PRINT "ONLY 10 DATA POINTS ALLOWED"
250 LET C = C - 1
260 GOTO 80
270 REM POINT DELETION
280 PRINT "DATA POINT NUMBER"
290 INPUT J
300 FOR P = 1 TO C
310 IF D(P, 3) = J THEN 330
320 NEXT P
330 LET C = C - 1
340 FOR P1 = P TO C
350 LET D(P1, 1) = D(P1 + 1, 1)
360 LET D(P1, 2) = D(P1 + 1, 2)
370 LET D(P1, 3) = D(P1 + 1, 3)
380 NEXT P1
390 GOTO 80
400 PRINT "DATA POINTS X INTERCEPT Y INTERCEPT"
410 MAT F = ZER(45, 3)
420 LET R = 1
430 FOR A = 1 TO (C - 1)
440 FOR B = (A + 1) TO C
450 LET E(R, 2) = -1 * (D(A, 1) - D(B, 1)) / (D(A, 1) / D(A, 2) - D(B, 1) / D(B, 2))
460 LET E(R, 3) = (D(A, 1) / D(A, 2)) * E(R, 2) + D(A, 1)
470 PRINT D(A, 3); "-"; D(B, 3), E(R, 2), E(R, 3)
480 LET R = R + 1
490 NEXT B
500 NEXT A
510 LET R = R - 1
520 PRINT "DISCARD OUTLIERS Y/N"
530 INPUT DS
540 IF DS = "Y" THEN 280
550 IF DS = "N" THEN 560
560 PRINT "DEHYDROGENASE ? Y/N"
570 LET T = 1
580 INPUT DS
590 IF DS = "N" THEN 620
600 IF DS = "Y" THEN 610
610 LET T = 2
620 REM ESTIMATE MEDIAN VALUES
630 PRINT "MEDIAN X VALUE"; " ("; T; "VR/ALPHA)"
640 LET Z = 2
650 GOSUB 810
660 LET M = X
670 PRINT "MEDIAN Y VALUE (VR)"
680 LET Z = 3
690 GOSUB 810
700 LET N = X
710 LET O = M / N
720 LET O1 = T * N / M
730 GOSUB 1250
740 LET R1 = (SQR(F(1, 1)) / O) * O1
750 PRINT "SPECIFIC EQUILIBRIUM VELOCITY"
760 PRINT O1; "+/-"; R1; " U MOLES/MIN/UNIT ENZYME"
770 LET R1 = SQR(F(2, 2))
780 PRINT "VR="; N; "+/-"; R1; "UMOLES/MIN"
790 GOTO 80

```

```

800 REM SUBROUTINE TO FIND MEDIAN VALUE
810 LET K = 0
820 FOR P = 2 TO R
830 IF E(P, Z) >= E(P - 1, Z) THEN 910
840 LET Q = 2
850 LET W = E(P, Q)
860 LET E(P, Q) = E(P - 1, Q)
870 LET E(P - 1, Q) = W
880 LET Q = Q + 1
890 IF Q = 3 THEN 850
900 LET K = 1
910 NEXT P
920 IF K > 0 THEN 810
930 LET A = 1
940 FOR P = 1 TO R
950 IF E(P, 2) < 0 AND E(P, 3) < 0 THEN 970
960 IF E(P, 2) > 0 OR E(P, 3) > 0 THEN 1000
970 LET L(A, 1) = -1 * E(P, 2)
980 LET L(A, 2) = -1 * E(P, 3)
990 LET A = A + 1
1000 NEXT P
1010 FOR P = 1 TO R
1020 IF E(P, 2) < 0 AND E(P, 3) < 0 THEN 1050
1030 NEXT P
1040 GOTO 1110
1050 FOR J = P TO R
1060 LET E(J, 2) = E(J + 1, 2)
1070 LET E(J, 3) = E(J + 1, 3)
1080 NEXT J
1090 GOTO 1010
1100 PRINT E(1, 2), E(2, 2), E(3, 2)
1110 IF A = 1 THEN 1170
1120 LET A = A - 1
1130 FOR W = 1 TO A
1140 LET E((R - W) + 1, 2) = L(W, 1)
1150 LET E((R - W) + 1, 3) = L(W, 2)
1160 NEXT W
1170 IF INT(R / 2) <> R / 2 THEN 1210
1180 LET X = (E(R / 2, Z) + E(R / 2 + 1, Z)) / 2
1190 PRINT X
1200 GOTO 1240
1210 LET R1 = INT(R / 2) + 1
1220 LET X = E(R1, Z)
1230 PRINT X
1240 RETURN
1250 REM SUBROUTINE TO ESTIMATE ERRORS
1260 MAT F = ZER(2, 2)
1270 MAT H = ZER(2, 2)
1280 LET Q = 0
1290 FOR P = 1 TO C
1300 LET D(P, 3) = D(P, 2) / (Q + D(P, 2) / N)
1310 LET Q = Q + (D(P, 3) - D(P, 1)) ↑ 2
1320 LET S1 = ((D(P, 2) * ((Q / D(P, 2) + 1 / N) ↑ 2)) ↑ -1) * -1
1330 LET S2 = ((N ↑ 2) * ((Q / D(P, 2) + 1 / N) ↑ 2)) ↑ -1
1340 LET F(1, 1) = F(1, 1) + S1 ↑ 2
1350 LET F(1, 2) = F(1, 2) + S1 * S2
1360 LET F(2, 1) = F(1, 2)
1370 LET F(2, 2) = F(2, 2) + S2 ↑ 2
1380 NEXT P
1390 MAT H = INV(F)
1400 MAT F = (Q / (C - 2)) * H
1410 RETURN
1420 STOP
1430 END

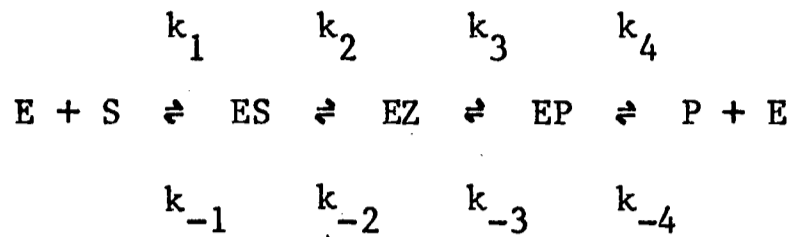
```

***F

3.8 Appendix 2

Triosephosphate isomerase equilibrium velocity

The kinetic mechanism of triosephosphate isomerase can be represented as;



where S is DHAP and P is GAP (Albery & Knowles, 1976). The equilibrium velocity of a reaction proceeding by n consecutive steps can be described by the following equation, (Yagil & Hoberman, 1969).

$$1/v_e = \sum_{i=1}^n 1/v_i$$

Thus the equilibrium velocity for the exchange of isotope between the pro-S C-3 position of DHAP and the aldehydic hydrogen of GAP, can be described by the following equation;

$$1/v_e = \frac{1}{(E)t(S)} \left[\frac{1}{k_1} + \frac{1}{\frac{k_2 k_1}{k_{-1}}} + \frac{1}{\frac{k_3 k_2 k_1}{k_{-2} k_{-1}}} + \frac{1}{\frac{k_4 k_3 k_2 k_1}{k_{-3} k_{-2} k_{-1}}} \right]$$

$$1 + (S) \left[\frac{k_1}{k_{-1}} + \frac{k_2 k_1}{k_{-2} k_{-1}} + \frac{k_3 k_2 k_1}{k_{-3} k_{-2} k_{-1}} \right]$$

where S is the DHAP concentration and (E)t is the total enzyme concentration. In calculating the specific equilibrium velocity of the enzyme the concentration of enzyme equivalent to 1 unit of activity was arbitrarily assigned a value of 2.3×10^{-9} M. This resulted in the experimentally observed and predicted equilibrium velocities having the same range of values.

The rate constants used to construct the theoretical curve shown in figure 3 in the main text were those of Alberty and Knowles (1976) who estimated the rate constants from isotope exchange measurements performed at 30°C and pH 7.5. The rate constants used in the model were as follows:

$$\begin{array}{ll}
 k_1 = 10^8 \text{ M}^{-1} \text{ s}^{-1} & k_{-1} = 8 \times 10^4 \text{ s}^{-1} \\
 k_2 = 2 \times 10^3 \text{ s}^{-1} & k_{-2} = 6 \times 10^3 \text{ s}^{-1} \\
 k_3 = 7 \times 10^4 \text{ s}^{-1} & k_{-3} = 9 \times 10^4 \text{ s}^{-1} \\
 k_4 = 4 \times 10^3 \text{ s}^{-1} & k_{-4} = 1 \times 10^7 \text{ M}^{-1} \text{ s}^{-1}
 \end{array}$$

The equilibrium concentrations of GAP and DHAP were calculated assuming an equilibrium constant for triosephosphate isomerase of 22 (Veech et al, 1969) and an equilibrium constant for aldolase of 1.2×10^{-4} (Herbert et al, 1940).

References

Alberty, W.J. & Knowles, J.R. (1976) *Biochemistry* 15, 5627-5631

Herbert, D., Gordon, H., Subramanyan, V. & Green, D.E. (1940)
Biochem. J. 34, 1108-1123

Veech, R.L., Raijman, L., Dalziel, K. & Krebs, H.A. (1969) *Biochem. J.* 115, 837-842

Yagil, G. & Hoberman, H.D. (1969) *Biochemistry* 8, 352-360

4 Development of a kinetic model to describe the properties of the C-2 exchange system in the erythrocyte

4.1 Introduction

In the previous chapter the properties of the in vitro exchange system and its suitability as a model of the system in situ were discussed. In this chapter models are developed which relate the observed in vitro properties of the enzymes to the properties expressed by the system of enzymes in situ.

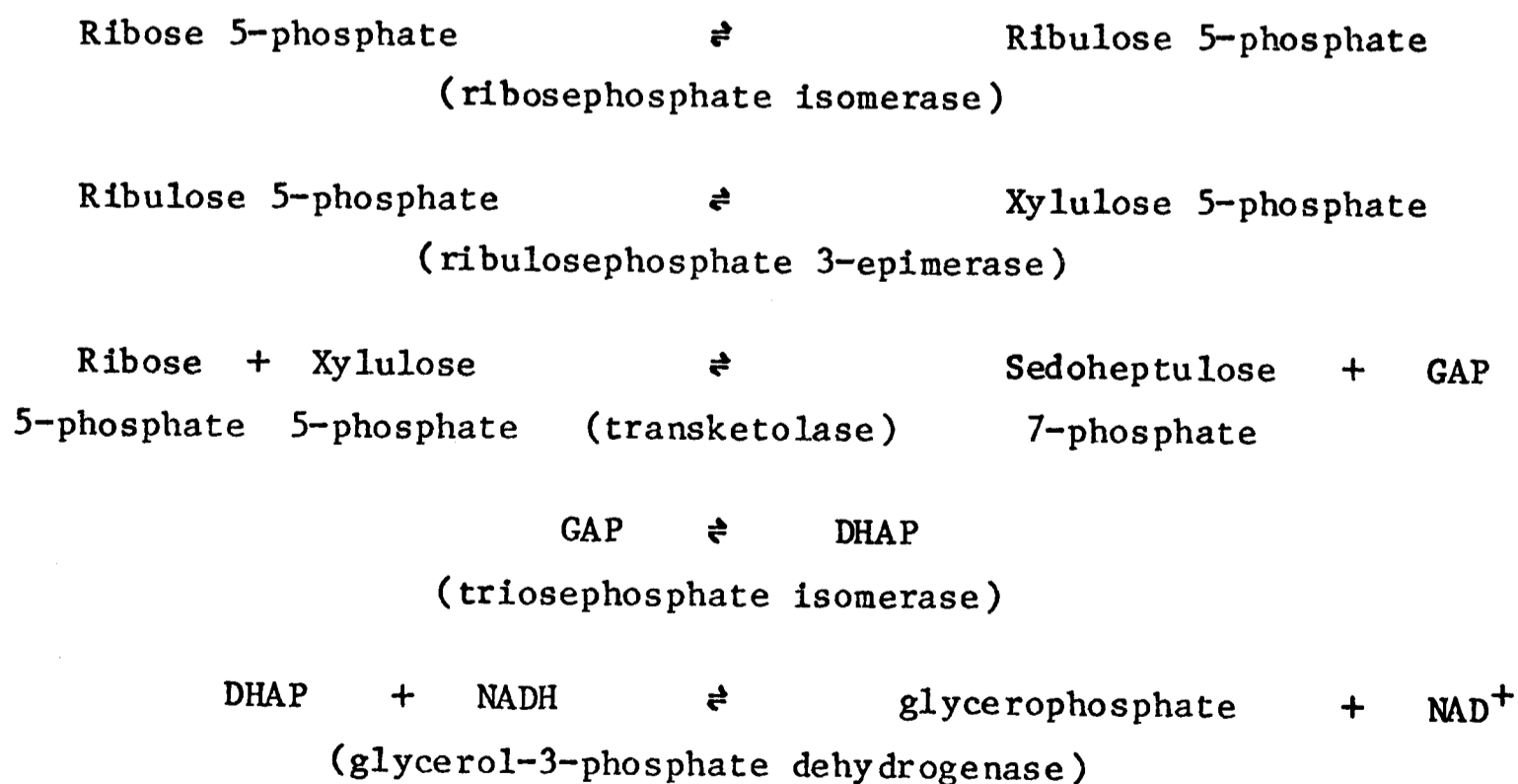
4.2 Experimental

Materials

Transketolase, ribulosephosphate 3-epimerase and ribosephosphate isomerase from yeast were obtained from Sigma.

Ribulosephosphate 3-epimerase assay

The assay system is based on that described by Horecker et al (1956). The reactions involved are:



The reaction was initiated by the addition of 0.4mM ribose 5-phosphate

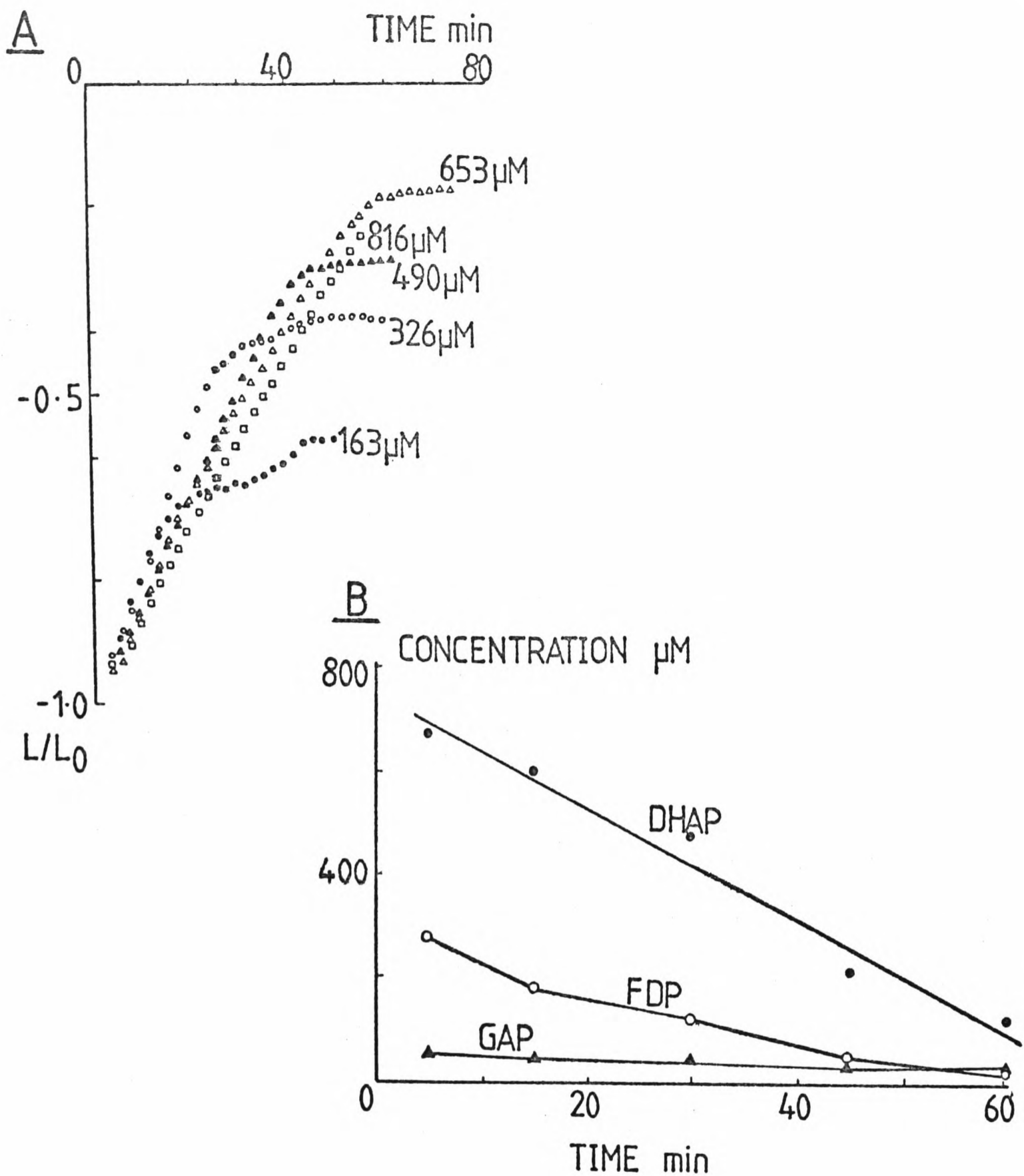


Figure 1

The effect of triosephosphate and FDP depletion on the exchange in a glucose depleted erythrocyte lysate.

A The effect of added FDP concentration on the rate and extent of the exchange. The concentrations of FDP added to the lysate are shown. The figure shows plots of lactate methyl peak height expressed as the ratio L/L_0 , where L is peak height at time t and L_0 is peak height at $t=0$. Exchange time courses were initiated by adding 12mM lactate and the specified FDP concentration to a sample of the lysate containing 100 μM NAD^+ and 20mM nicotinamide. The lysates were prepared by freeze thawing packed glucose depleted erythrocytes twice in liquid nitrogen. The erythrocytes were suspended in Krebs-Ringer buffer pH 7.4 made with $^2\text{H}_2\text{O}$ and the lysates were diluted by 1:2 in this buffer before use in exchange determinations.

B The results of FDP assays on a lysate to which 580 μM FDP had been added. Details of the assay are given in the Experimental section in chapter 2.

and monitored by observing the oxidation of NADH at 340nm. The assay system contained 100mM Tris-HCl pH 7.4, 0.5mM EDTA, 0.2mM NADH, 0.2mM thiamine pyrophosphate (neutralised), 3mM dithiothreitol and approximately 0.2 units of transketolase, 0.2 units of ribosephosphate isomerase, 5 units of triosephosphate isomerase and 5 units of glycerol-3-phosphate dehydrogenase. Assays were performed essentially as described in chapter 2. It was noted that the yeast ribosephosphate isomerase preparation showed some capacity to oxidise NADH. However at the concentration present in the assay system this activity was small and could be corrected for by using a blank.

4.3 Kinetic models to describe the effects of triose phosphate and FDP depletion on C-2 exchange

It was shown in chapter 2 that observation of the exchange is dependent on relatively high levels of the triose phosphates and FDP and that following depletion of these intermediates in the erythrocyte there is termination of the exchange. Figure 1 shows the same effect in a glucose depleted erythrocyte lysate to which various concentrations of FDP had been added. As the concentration of FDP was increased so too was the extent of the exchange. The correlation between loss of the exchange and depletion of the triose phosphates indicated that the exchanges catalysed by aldolase, triosephosphate isomerase and glyceraldehydophosphate dehydrogenase had ceased. The behaviour of the exchange prior to total depletion reflects changes in the individual equilibrium velocities of these enzymes as their substrate concentrations change. The predictions of a very simple model which could qualitatively describe this system are shown in figure 2. This model was derived on the assumption that aldolase is wholly rate limiting for the C-2 exchange system (i.e. it has a sensitivity

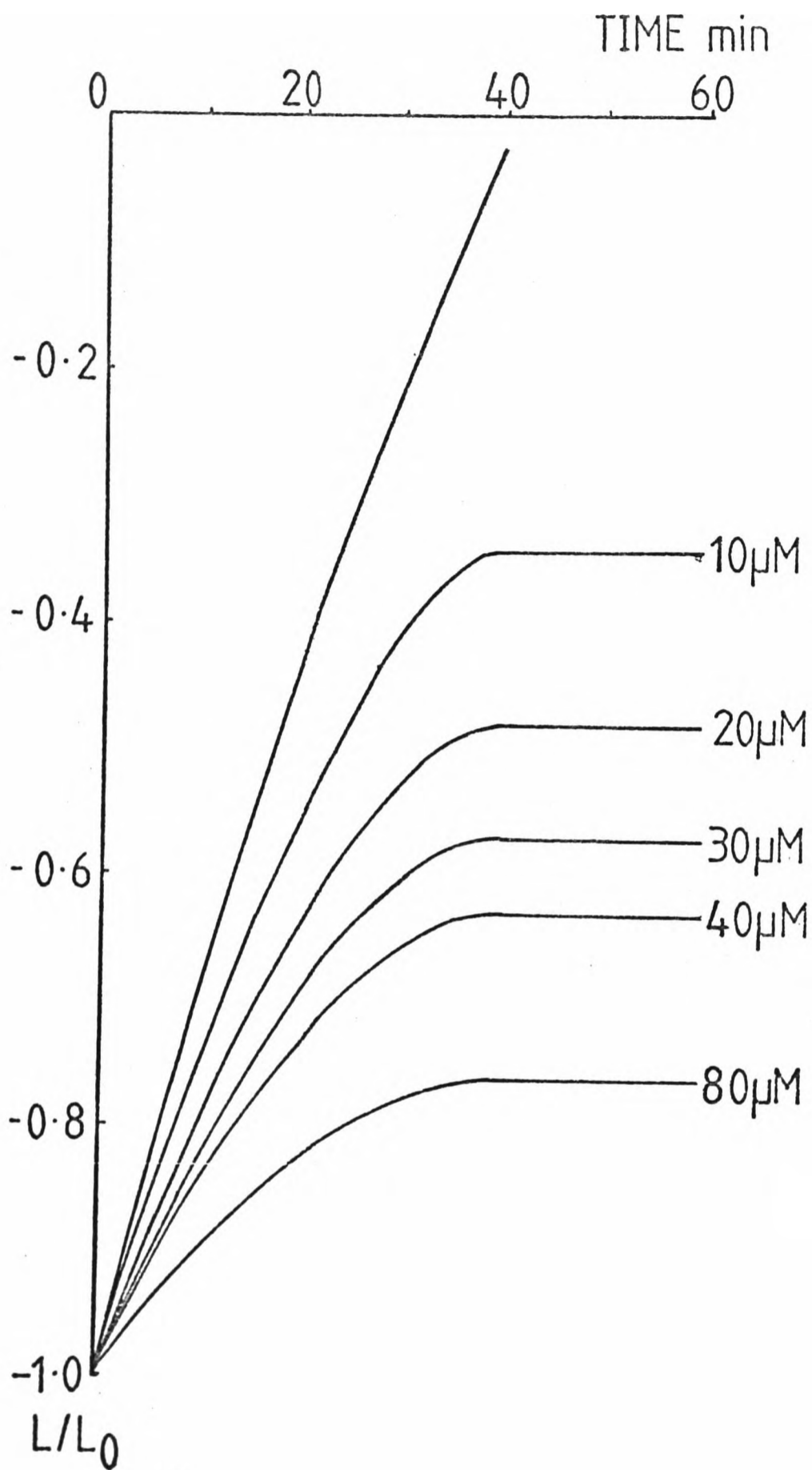


Figure 2

Theoretical time courses predicted by a model in which the exchange catalysed by aldolase is assumed to be rate limiting for C-2 exchange.

The figure shows a plot of peak height versus time where peak height is expressed as the ratio L/L_0 , L is the peak height at time t and L_0 is the peak height at $t=0$. The conditions used in the model were as follows, (see appendix 1). $V_{C2X} = 0.1\text{mM}/\text{min}$, $D_0 = 40\mu\text{M}$, $k_D = 1\mu\text{M}/\text{min}$. The value for K_m was varied as shown in the figure.

coefficient of 1) and that its equilibrium isotope exchange velocity is a Michaelis-Menten function of the DHAP concentration (see appendix 1 for the derivation). The exchange time courses, shown in figure 1, show abrupt termination of the exchange at low triose phosphate and FDP concentrations. This behaviour is reproduced in the model when a low aldolase "Km" for DHAP is used. This is illustrated in figure 2, as the "Km" is decreased the extent of the exchange is increased and the exchange rate changes more rapidly near the point of total DHAP depletion and termination of the exchange. This model is however very limited, it cannot for example predict the faster rate of exchange observed at lower added FDP concentrations (see figure 1). In the following section a more sophisticated model is developed to describe the effects of triose phosphate depletion. This model is based on the observed in vitro exchange properties of the enzymes for which these intermediates are substrates.

The dependencies of the aldolase, triosephosphate isomerase and glyceraldehydophosphate dehydrogenase equilibrium velocities on the concentrations of DHAP and GAP can be calculated from the results shown in chapter 3. Examination of these results show that the aldolase equilibrium velocity is not a simple Michaelis-Menten function of the DHAP concentration but is in fact a more complex function of the enzyme's substrate concentrations. Consider the effect of triose phosphate depletion on the exchange time courses shown in figure 1. The concentrations of the triose phosphates and FDP and their rate of breakdown in these lysate preparations is known. At any instant during depletion of these metabolites their observed concentrations are the expected equilibrium concentrations (see table 4, chapter 3). From the measured dependencies of the equilibrium velocities of these enzymes on

Table 1

The added FDP concentration in the model was $500\mu\text{M}$. This gives an equilibrium DHAP concentration at $t=0$ of approximately $600\mu\text{M}$. The rate of DHAP breakdown in the lysate was measured at $10\mu\text{M min}^{-1}$ (fig. 1). The specific equilibrium velocities of the enzymes at different FDP, DHAP and GAP concentrations (only the DHAP concentration is shown here) were estimated from the results shown in chapter 3. The total equilibrium velocities were calculated by multiplying the specific equilibrium velocities by the expected enzyme activities in the lysate. These were estimated from the measured activities of these enzymes in the erythrocyte i.e. aldolase, 1.56 ± 0.09 units/ml cell water (5 determinations); glyceraldehydephosphate dehydrogenase (GAPDH), 84 ± 15 units/ml cell water (8 determinations); lactate dehydrogenase, 78 ± 8 units/ml cell water (17 determinations). All of these determinations were performed on different samples of blood. Details of the assays were given in chapter 2. The triosephosphate isomerase (TIM) activity was estimated, from the data of Beutler (1975), to be 830 units/ml cell water. The activities of the enzymes in the diluted lysate were estimated to be 0.3 units/ml aldolase, 17 units/ml glyceraldehydephosphate dehydrogenase, 17 units/ml lactate dehydrogenase and 170 units/ml triosephosphate isomerase. The initial rate of C-2 exchange in the presence of $490\mu\text{M}$ FDP was estimated to be 0.1mM/min (fig. 1). This known rate of V_{C2X} at $t=0$ was used to calculate the lactate dehydrogenase equilibrium velocity from the predicted values of the equilibrium velocities of the other enzymes using the double reciprocal relationship described in the text. The total lactate dehydrogenase equilibrium velocity was estimated to be 0.4mM/min which gives a specific equilibrium velocity of $0.024\mu\text{mol/min/unit}$. The lactate dehydrogenase equilibrium velocity was assumed to remain constant during triose phosphate depletion and V_{C2X} was calculated from the expected equilibrium velocities of the other enzymes.

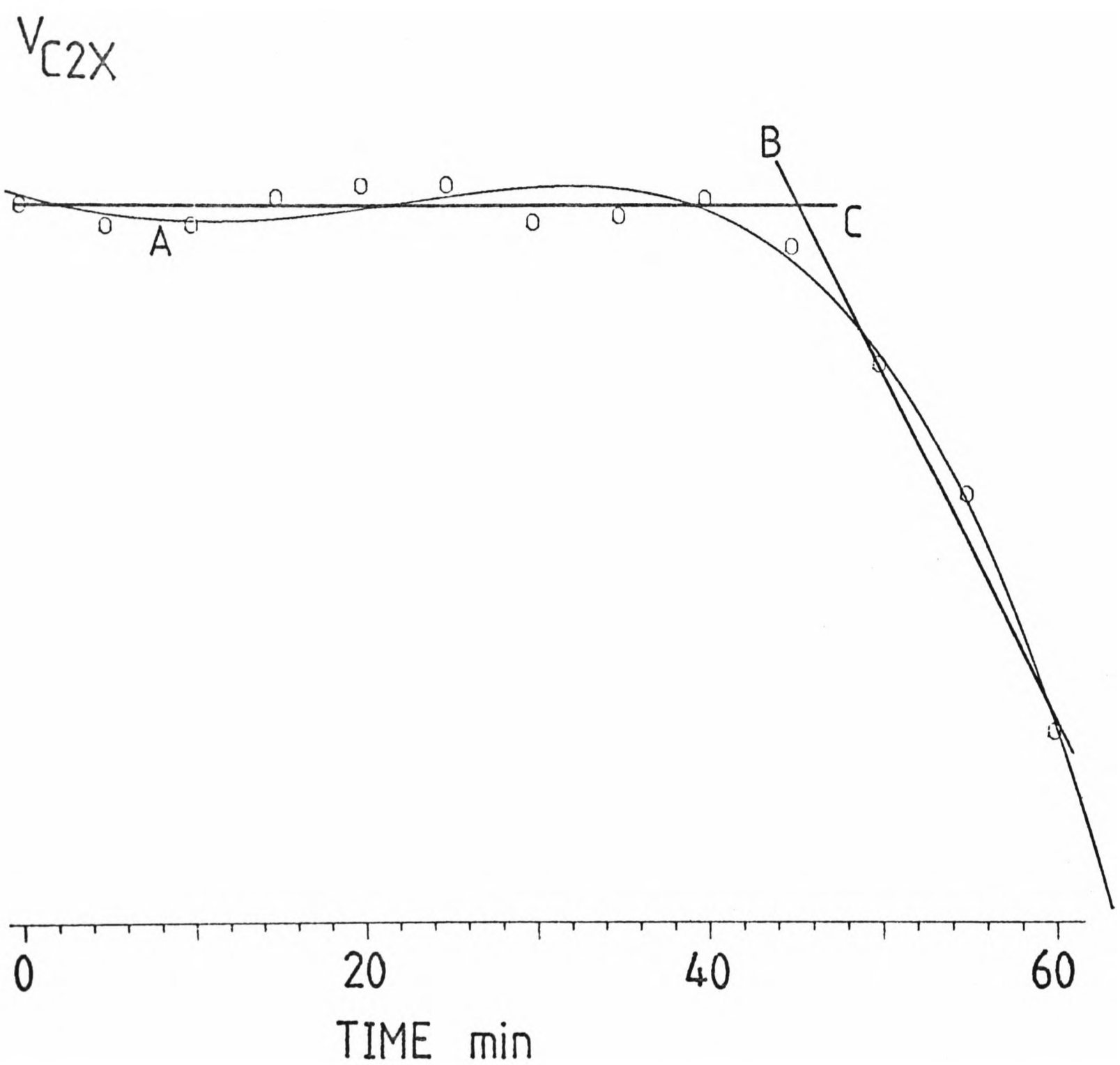


Figure 3

The time dependent changes in V_{C2X} predicted by the in vitro model (shown in table 1) in the dilute erythrocyte lysate system (shown in figure 1).

The figure shows a plot of the predicted value for V_{C2X} versus time. The curve marked A was drawn from a least squares polynomial fit of the data points. A routine available in the Nicolet 1180 computer software was used to fit the data to the polynomial function. The lines marked B and C are simple linear fits of the data points (see text).

the concentrations of the triose phosphates and FDP (shown in chapter 3) and from their known activities (measured spectrophotometrically) in the lysate, the total equilibrium velocities of the individual enzymes at any point in time in the lysate can be estimated. Using the double reciprocal relationship between V_{C2X} and the equilibrium velocities of the enzymes, these individual equilibrium velocities can then be used to calculate a predicted value for V_{C2X} as a function of time. The results of these calculations (shown in table 1) show that the assumption, used in the model presented above, that the aldolase sensitivity coefficient is close to unity is invalid. It does however have the highest sensitivity coefficient of the three enzymes over the range of DHAP, GAP and FDP concentrations shown. The predicted values for V_{C2X} as a function of time, following the addition of approximately 500 μ M FDP to a lysate are presented graphically in figure 3. The points are the calculated values. The curve marked A is a polynomial fit to these data points. Integration of the polynomial allows prediction of the exchange time course which is shown in figure 4 (see appendix 2). An alternative way to describe the changes in V_{C2X} is to represent the changes in two linear phases (lines marked B and C in figure 3). Integration of this linear fit again allows prediction of the exchange time course (see appendix 2). A combination of linear and polynomial fits should allow description of any changes in V_{C2X} which occur as a function of time. Subsequent integration of this system of data fits allows prediction of the resulting exchange time course.

The exchange time courses predicted by the aldolase "Km model" and the "in vitro models" are compared in figure 4 with the time course observed experimentally following the addition of 490 μ M FDP to a lysate preparation. The time courses predicted by the aldolase and in vitro

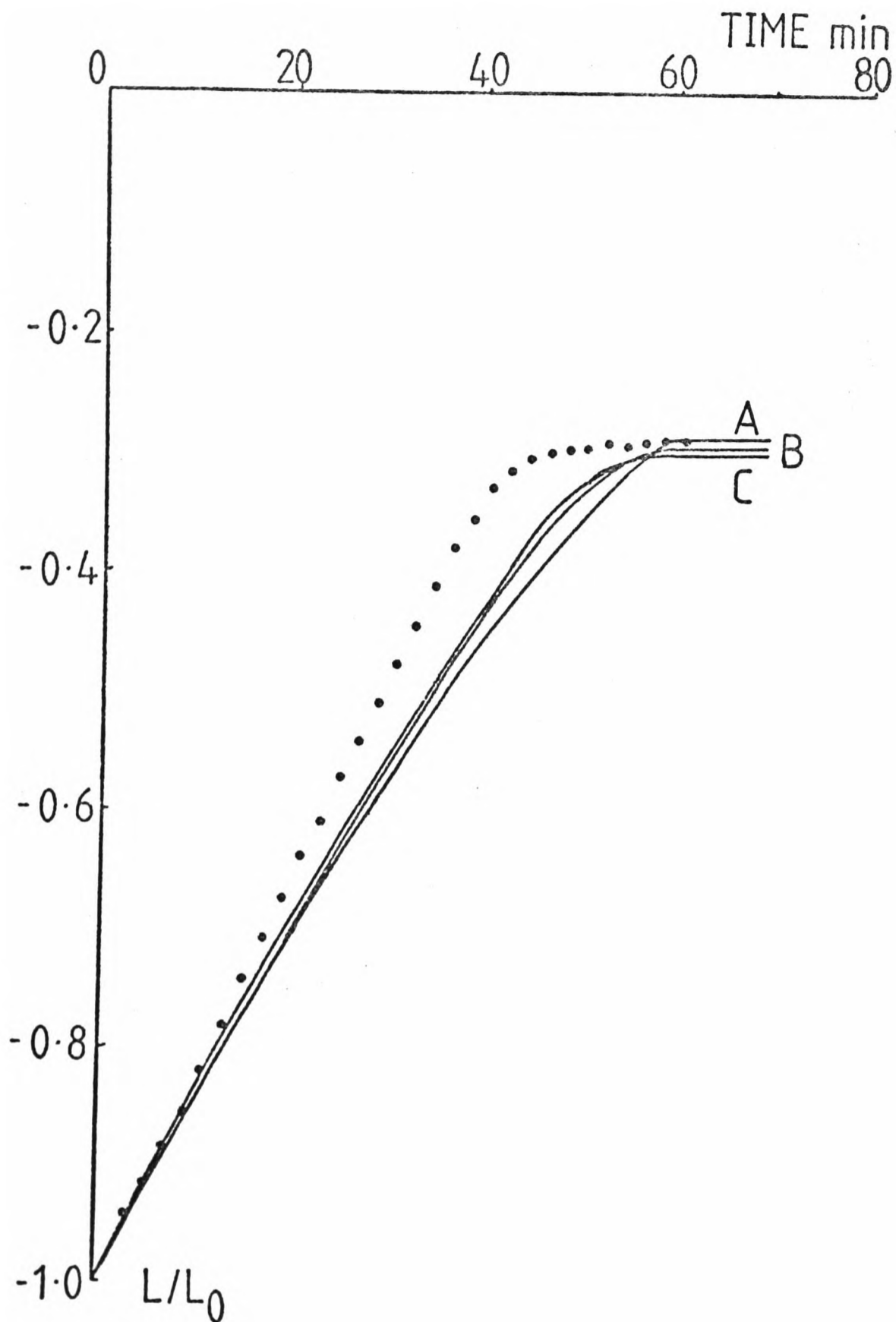


Figure 4

The exchange time courses predicted by the in vitro model of the lysate exchange system shown in figure 1.

The curves marked A and B are drawn from the polynomial and linear fits of the exchange data predicted by the model (see table 1) and shown in figure 3. The method by which these theoretical exchange time courses are obtained is described in appendix 2. The figure also shows the theoretical exchange time course predicted by the aldolase model (curve C). The curve marked D is the exchange time course observed experimentally following the addition of 490 μ M FDP and 12mM lactate to the lysate system shown in figure 1.

The lactate peak height is expressed as the ratio L/L_0 , where L is peak height at time t and L_0 is peak height at $t=0$.

models are very similar showing that although the sensitivity coefficient of aldolase is not equal to one it is nevertheless of prime importance in determining V_{C2X} . The extent of the exchange predicted by the aldolase model, as shown in figure 1, is dependent on the apparent K_m of aldolase for DHAP. The K_m used in the model is similar to the measured K_d for DHAP under similar conditions of pH and ionic strength (Grazi & Trombetta, 1974). The predictions of both models however differ significantly from the experimentally observed time course since they fail to predict an acceleration in the exchange velocity as the FDP and triose phosphate concentrations decline. The aldolase model is intrinsically incapable of predicting an increase in V_{C2X} as the DHAP concentration falls. The in vitro model however would predict this effect if the sensitivity coefficient of aldolase were higher and/or the increase in its equilibrium velocity at lower triose phosphate and FDP concentrations were greater. Further in vitro data would obviously clarify this point. The in vitro model also provides an explanation for the observed insensitivity of the exchange in situ to the concentrations of the triose phosphates and FDP which was demonstrated in chapter 2.

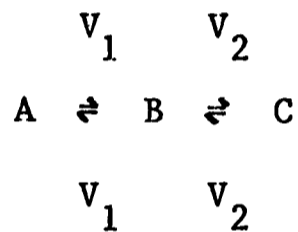
Modelling of this sort cannot of course be used to obtain quantitative information about the exchange properties of an individual enzyme in situ. In order to do this a specific perturbation must be applied to the enzyme (see chapters 5 and 6) or the exchange catalysed by the individual enzyme must be studied directly (see chapter 6). However the in vitro model can be used to make some semi-quantitative predictions about the behaviour of the exchange system in situ. The model in its current form, however, is incapable of predicting the effect of net chemical flux on isotopic flux. Furthermore it is based on an equation which, although experimentally verified in vitro, was

derived for trace isotope exchange (Yagil & Hoberman, 1969). In the next section the validity of this double reciprocal relationship between the enzyme equilibrium velocities and V_{C2X} is established theoretically using a comprehensive model which also permits simulation of the effect of glycolytic or chemical flux on isotopic flux. This model is used in the next chapter to investigate the effect of glycolytic flux on estimates of V_{C2X} in the erythrocyte.

4.4 A comprehensive model of the C-2 exchange system

Isotope Flux

Consider the following system;



where A, B and C are three different interconverting chemical species at chemical equilibrium. A can be converted to B and B to A at rate V_1 and B can be converted to C and C to B at rate V_2 . These rates of interconversion can be measured by isotopically labelling the chemical species. The Vs are then equilibrium velocities for the exchange of isotope. Flux of isotope within this system can be described by a set of differential equations which describe changes in the fractional labelling, X, of the different chemical species as a function of time i.e.

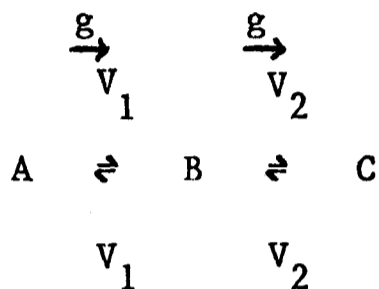
$$(A) dX_A/dt = V_1 (X_B - X_A)$$

$$(B) dX_B/dt = V_1 (X_A - X_B) + V_2 (X_C - X_B)$$

$$(C) dX_C/dt = V_2 (X_B - X_C)$$

Chemical Flux

If there is chemical flux (as opposed to equilibrium chemical interconversion) then these equations describing isotopic flux must be modified to include this flux. In the following example there is net chemical flux from A to C. There is a loss of A to give B at rate g and loss of B, also at rate g , to give C. The concentration of A decreases and C increases, both at rate g , and B remains in a steady state.



The equations describing fractional labelling of A, B and C now become

$$\begin{aligned} ((A_0) - gt) \frac{dX_A}{dt} &= V_1 (X_B - X_A) - gX_A \\ (B) \frac{dX_B}{dt} &= V_1 (X_A - X_B) + V_2 (X_C - X_B) + g(X_A - X_B) \\ ((C_0) + gt) \frac{dX_C}{dt} &= V_2 (X_B - X_C) + gX_B \end{aligned}$$

where (A_0) is the concentration of A at $t=0$ and (C_0) the concentration of C at $t=0$.

Chemical Flux in the C-2 Exchange System

In an in vitro exchange system the exchanging intermediates are at chemical equilibrium. In the intact cell, however, there is also chemical flux in addition to isotope flux. It has been shown (see chapter 5) that during measurement of the overall equilibrium velocity of the system (V_{C2X}) lactate accumulates and FDP declines at equivalent rates. This equivalence indicates that there can be no accumulation of the intermediates involved in the glycolytic pathway between FDP and lactate and furthermore that there can be no net input of material into this section of glycolysis from intermediates above FDP in the glycolytic sequence (see chapter 5 for a discussion of this result).

This section of glycolysis between FDP and lactate, which encompasses the C-2 exchange system, can thus be considered analogous to the A,B,C system described above. There is chemical flux from FDP to lactate with the intermediates assuming a near equilibrium chemical steady state. This system can be considered therefore to be chemically closed. It is not necessarily, however, isotopically closed. Although phosphofructokinase is an essentially irreversible enzyme, there is present in the human erythrocyte, fructose bisphosphatase (Freidemann & Rapoport, 1974). Isotope can escape, therefore, from FDP to glycolytic intermediates higher up the glycolytic sequence toward glucose. It will be shown however that this isotope "leak" from the C-2 exchange system, like that involving the pentose phosphate pathway described in chapter 2, does not affect any of the conclusions reached here.

Double Labelling

Consider the following system where A and B react to give C and Z.

V



A and B are singly labelled, C is labelled at two positions in the molecule and Z carries no label. Three labelled species of C exist i.e.

$C_{(*,0)}$, $C_{(*,*)}$ and $C_{(0,*)}$. $C_{(*,*)}$ represents the doubly labelled molecule, $C_{(*,0)}$ represents the species which derived its label from the A molecule and $C_{(0,*)}$ the species which derived its label from the B molecule. $C_{(*,*)}$ is produced by reaction of labelled A and labelled B. This is a situation rarely observed in radioactive trace labelling studies where the probability of two labelled species reacting is negligibly small.

This exchange system can be described by the following set of

equations:

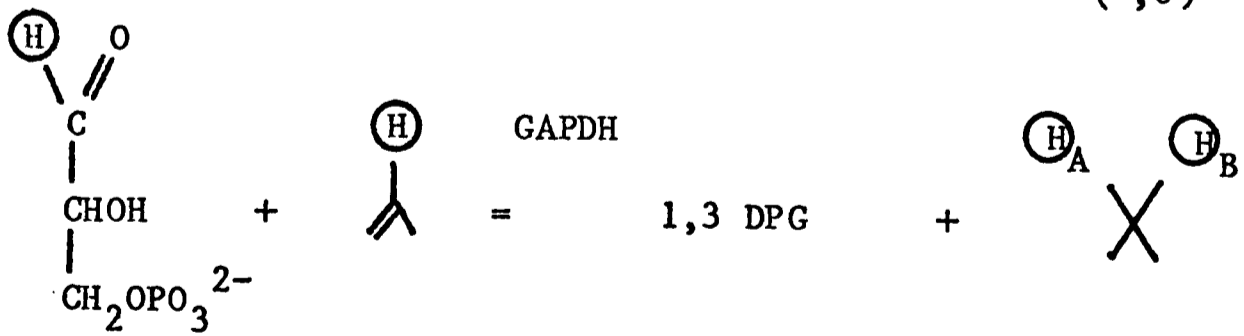
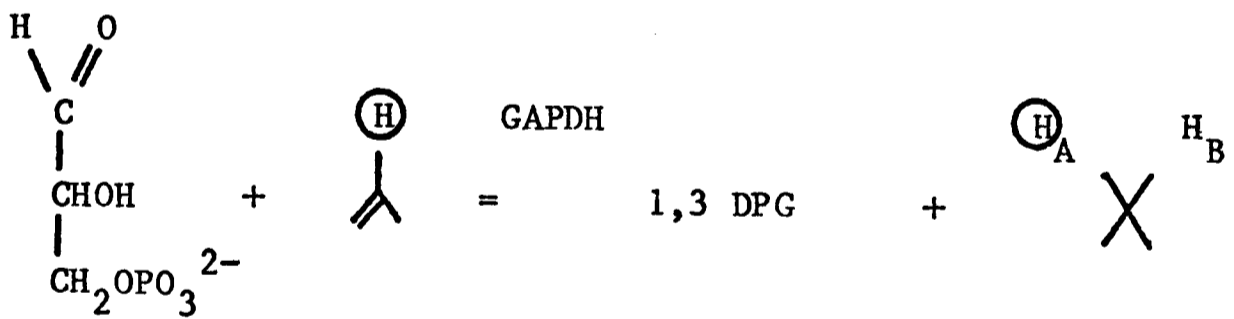
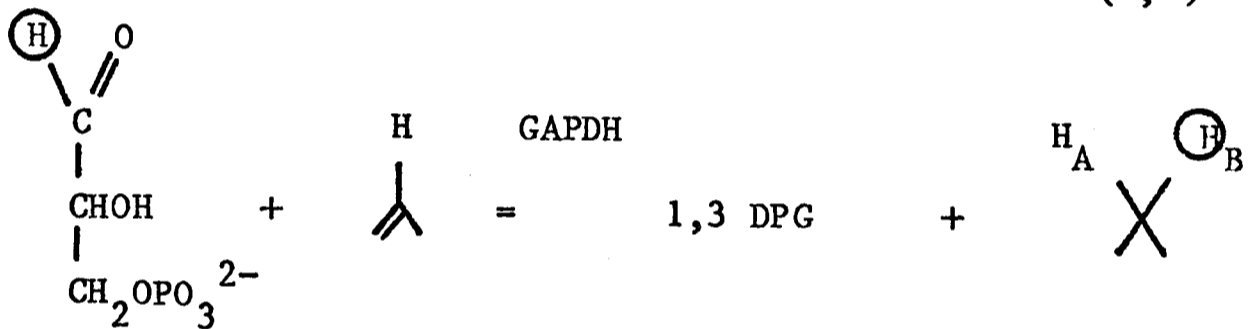
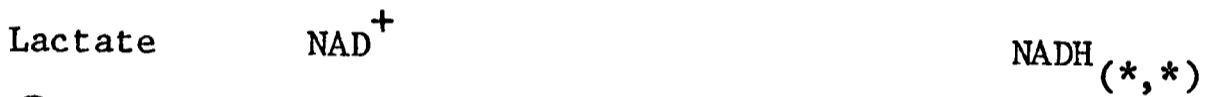
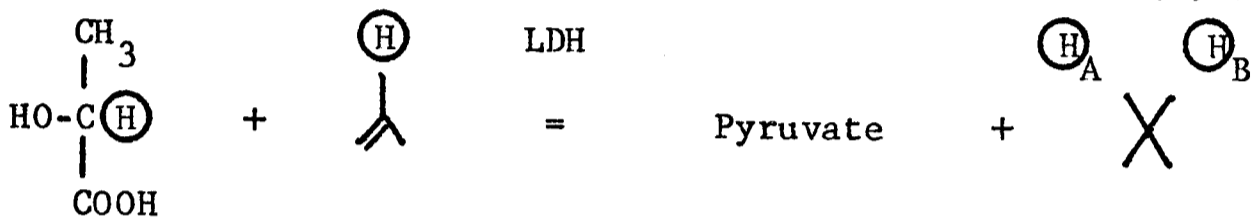
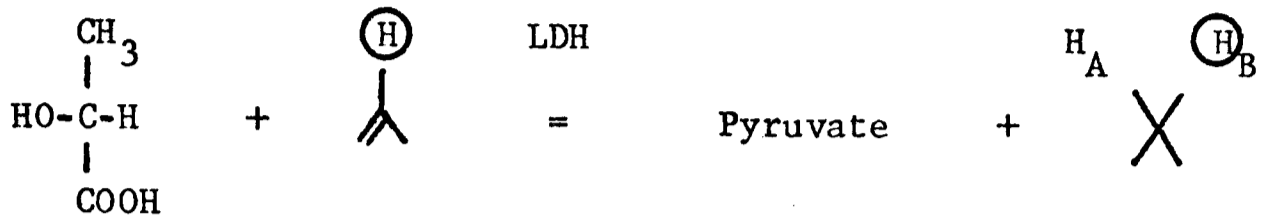
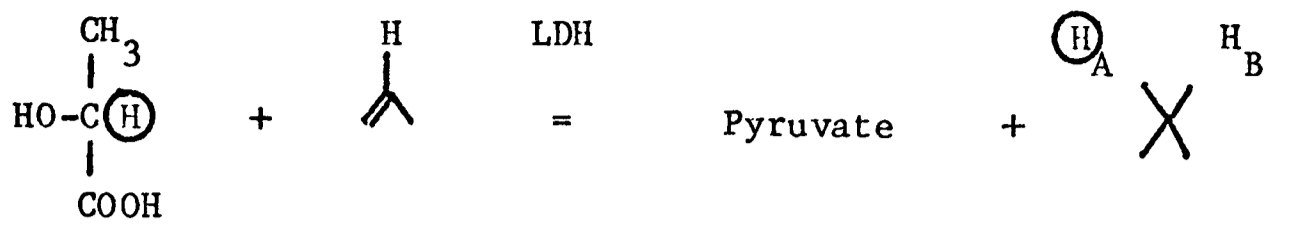
$$(C_{(*,0)})dX_{C(*,0)}/dt = v (X_A(1 - X_B) - X_{C(*,0)})$$

$$(C_{(*,*)})dX_{C(*,*)}/dt = v (X_A X_B - X_{C(*,*)})$$

$$(C_{(0,*)})dX_{C(0,*)}/dt = v (X_B(1 - X_A) - X_{C(0,*)})$$

Double Labelling in the C-2 Exchange System

Double labelling occurs in the C-2 exchange system for NADH. This molecule carries two hydrogens at the C-4 position of the nicotinamide ring both of which can exchange during lactate C-2 hydrogen-solvent exchange. Double labelling occurs because of the opposite stereospecificities of the two dehydrogenases involved. The label at the C-2 position of lactate is exchanged with the A face hydrogen at the C-4 position of the nicotinamide ring in the reaction catalysed by lactate dehydrogenase. This singly labelled NADH species carrying label on the A face of the nicotinamide ring at the C-4 position is denoted as $NADH_{(*,0)}$ in the following equations. NADH labelled on the B face at the C-4 position ($NADH_{(0,*)}$ in the following equations) is produced by exchange of label between GAP and NADH in the reaction catalysed by glyceraldehydophosphate dehydrogenase. Reaction of B face labelled NADH with pyruvate in the reaction catalysed by lactate dehydrogenase (A face stereospecificity) results in a labelled NAD^+ molecule. Labelled NAD^+ is also produced by the reaction of A face labelled NADH with 1,3-DPG in the reaction catalysed by glyceraldehydophosphate dehydrogenase (B face stereospecificity). Labelled NAD^+ would not be produced if the two dehydrogenases had the same stereospecificity with regard to the coenzyme. Reaction of labelled NAD^+ with labelled GAP or labelled lactate results in double labelled NADH. These reactions are illustrated below, the hydrogen label is ringed.

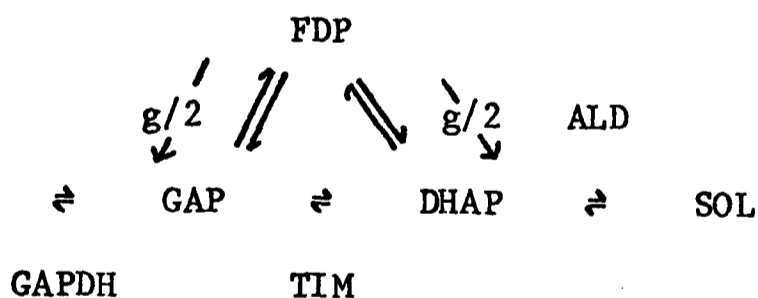


4.4.1 Derivation of the rate equations

In the following equations g represents the rate of lactate production or rate of chemical flux through the C-2 exchange system in 3 carbon equivalents. The V terms represent the isotope exchange equilibrium velocities of the denoted enzymes and the X terms the fractional labelling of denoted metabolites. The enzymes and metabolites are represented by subscripted abbreviations. The abbreviations are as follows; LDH, lactate dehydrogenase; GAPDH, glyceraldehydophosphate dehydrogenase; TIM, triosephosphate isomerase; ALD, aldolase; ALD(RECON), the recondensation reaction between DHAP and GAP catalysed by aldolase which results in labelling at the 4 position of the FDP molecule (see below); SOL, solvent ($^1\text{H}_2\text{O}$ or $^2\text{H}_2\text{O}$); FDP, fructose-1,6-diphosphate; DHAP, dihydroxyacetone-phosphate; GAP, glyceraldehyde-3-phosphate; 1,3-DPG, 1,3-diphosphoglyceric acid; NAD^+ and NADH, nicotinamide adenine dinucleotide, oxidized and reduced forms respectively; PYR, pyruvate and LAC, lactate.

The FDP-DHAP-GAP System

This part of the C-2 exchange system is shown schematically below:-

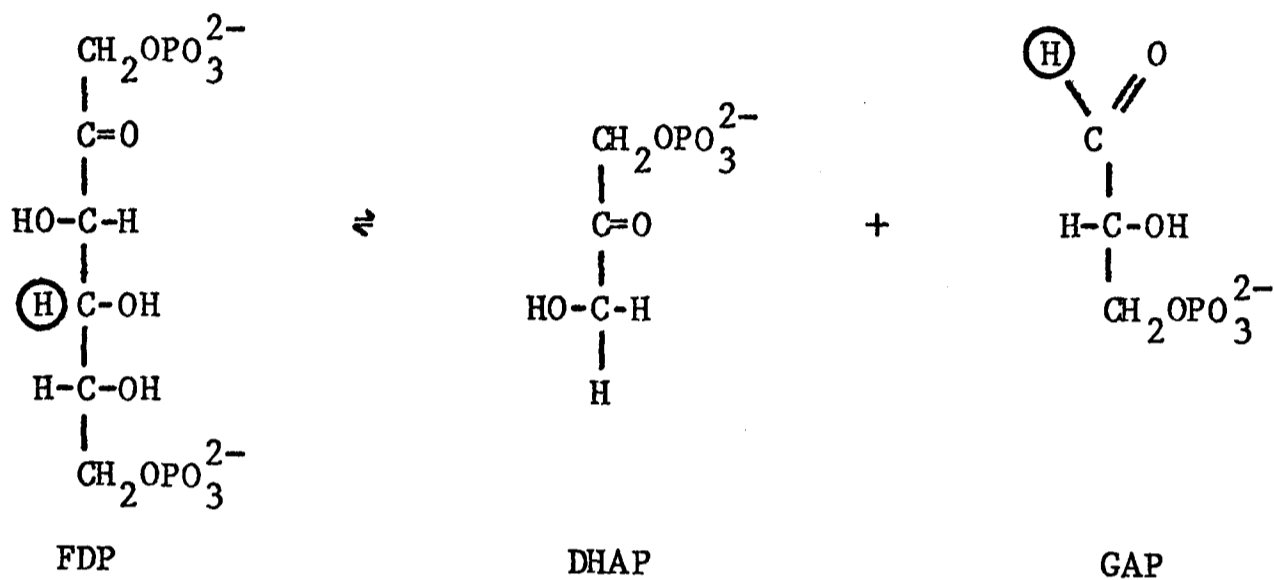


g is the rate of lactate production, the rate of FDP breakdown has been shown to be half this (see chapter 5, one molecule of FDP gives rise to two molecules of lactate).

Aldolase catalyses the exchange of hydrogen between the pro-S C-3 position of DHAP and solvent (Rose, 1958). Triosephosphate isomerase

catalyses the exchange of this label between DHAP and the aldehydic hydrogen of GAP (Rieder & Rose, 1959).

ALD(RECON) represents the recondensation reaction, catalysed by aldolase, between DHAP and GAP. This reaction results in exchange of the aldehydic hydrogen of GAP with the hydrogen at the C-4 position of FDP i.e.



The hydrogen labels are ringed. The label on DHAP is lost to the solvent. The following equations can be written, on the basis of this scheme, to describe the changes in fractional labelling of FDP and DHAP:

$$((\text{FDP})_0 - g t / 2) \frac{dX_{\text{FDP}}}{dt} = V_{\text{ALD(RECON)}} (X_{\text{GAP}} - X_{\text{FDP}}) - g X_{\text{FDP}} / 2$$

$$(\text{DHAP}) \frac{dX_{\text{DHAP}}}{dt} = V_{\text{TIM}} (X_{\text{GAP}} - X_{\text{DHAP}}) + V_{\text{ALD}} (X_{\text{SOL}} - X_{\text{DHAP}}) + g X_{\text{SOL}} / 2 - g X_{\text{DHAP}} / 2$$

The equations describing GAP labelling must also consider NAD(H) labelling (see above section on double labelling).

$$\begin{aligned}
 (\text{GAP}) \frac{dX_{\text{GAP}}}{dt} = & V_{\text{TIM}} (X_{\text{DHAP}} - X_{\text{GAP}}) + V_{\text{GAPDH}} (X_{\text{NADH}}(*,*) + X_{\text{NADH}}(0,*) - X_{\text{GAP}}) \\
 & + V_{\text{ALD(RECON)}} (X_{\text{FDP}} - X_{\text{GAP}}) \\
 & + g X_{\text{DHAP}} / 2 + g X_{\text{FDP}} / 2 - g X_{\text{GAP}}
 \end{aligned}$$

The exchange in solvent can be described by the following equation:

$$(SOL) \quad dX_{SOL}/dt = V_{ALD} (X_{DHAP} - X_{SOL})$$

The NAD⁺-NADH System

The basic scheme of this part of the C-2 exchange system was shown in the section above on double labelling. However this scheme must be extended to include the effects of glycolytic flux through the system. This will lead to the loss of NAD⁺ and the production of NADH in the reaction catalysed by GAPDH and the loss of NADH and the production of NAD⁺ in the reaction catalysed by LDH. The concentrations of NAD⁺ and NADH are assumed to remain constant. The equations describing NAD⁺ and NADH labelling are as follows:

$$(NAD) \quad dX_{NAD}/dt = V_{LDH} (X_{NADH(0,*)} + X_{NADH(*,*)} - X_{NAD}) \\ + V_{GAPDH} (X_{NADH(*,0)} + X_{NADH(*,*)} - X_{NAD}) \\ + g (X_{NADH(*,*)} + X_{NADH(0,*)} - X_{NAD})$$

$$(NADH) \quad dX_{NADH(*,0)}/dt = V_{LDH} (X_{LAC}(1 - X_{NAD}) - X_{NADH(*,0)}) \\ + V_{GAPDH} (X_{NAD}(1 - X_{GAP}) - X_{NADH(*,0)}) \\ + g (X_{NAD}(1 - X_{GAP}) - X_{NADH(*,0)})$$

$$(NADH) \quad dX_{NADH(*,*)}/dt = V_{LDH} (X_{LAC} X_{NAD} - X_{NADH(*,*)}) \\ + V_{GAPDH} (X_{NAD} X_{GAP} - X_{NADH(*,*)}) \\ + g (X_{NAD} X_{GAP} - X_{NADH(*,*)})$$

$$(NADH) \quad dX_{NADH(0,*)}/dt = V_{LDH} (X_{NAD}(1 - X_{LAC}) - X_{NADH(0,*)}) \\ + V_{GAPDH} (X_{GAP}(1 - X_{NAD}) - X_{NADH(0,*)}) \\ + g (X_{GAP}(1 - X_{NAD}) - X_{NADH(0,*)})$$

Table 2

Model simulation of the effect of changing the glyceraldehydephosphate dehydrogenase equilibrium velocity on the overall equilibrium velocity of the C-2 exchange system, V_{C2X} . Verification of the double reciprocal relationship between V_{C2X} and the equilibrium velocity of an individual enzyme.

GAPDH equilibrium (mM/min)	Model predicted $t_{1/2}$ (min)	$t_{1/2}$ predicted by equation relating V_{C2X} to the equilibrium velocities of the enzymes
10	22	22
5	23	23
2	28	28
1	37	37
0.75	42	42
0.50	53	53
0.25	86	86

The model is described in the text and in appendix 4. The conditions used in the model were as follows; 110M solvent, 1mM DHAP, 45uM GAP, 10uM NAD^+ , 10uM NADH, 3mM FDP and 12mM lactate. The enzyme equilibrium velocities were; V_{ALD} , 1.0mM/min; $V_{ALD(RECON)}$, 0.0mM/min; V_{TIM} , 15.0mM/min; V_{LDH} , 1.5mM/min; lactate production, 0.0mM/min. The glyceraldehydephosphate dehydrogenase equilibrium velocity was varied as described in the table. These enzyme equilibrium velocities and substrate concentrations simulate the conditions found in the erythrocyte, see chapter 5.

Solution of the non-linear simultaneous differential equations

The exchange system can be described, as shown above, by a set of non-linear simultaneous differential equations. These can be solved, that is the values of X can be calculated at time t, using computer orientated numerical methods (see for example McCalla, 1967). The principle of these methods is illustrated in appendix 3 by application of the "Euler predictor-corrector method" to the solution of the equations describing C-2 exchange. The limitations of this method when applied to the C-2 exchange system are discussed and another method, a variable step, variable order Gear method is introduced which is much better suited to the particular problems presented by this system (Curtis & Chance, 1972; Garfinkel et al, 1977).

4.5 Uses of the kinetic model

4.5.1 Validation of the double reciprocal relationship

The model can be used to show that a double reciprocal relationship exists between V_{C2X} and the individual enzyme equilibrium velocities at the enzyme and substrate concentrations encountered in these studies. This is demonstrated in table 2 which shows the predicted effects on V_{C2X} of changing the glyceraldehydophosphate dehydrogenase equilibrium velocity in the exchange system. The substrate concentrations used in the model are those normally found in the erythrocyte (see chapters 5 and 6). The enzyme equilibrium velocities are those expected in situ on the basis of the in vitro results shown in chapter 3 and the results of equilibrium velocity determinations shown in chapter 5. The results in table 2 show that the apparent $t_{1/2}$ or point of 50% labelling (null point in the exchange time course) predicted by the model is the same as that predicted by the double reciprocal relationship. This

Table 3

Model simulations of aldolase equilibrium velocity determinations.

A - V_{ALD} was set equal to 1.0 $\mu\text{mol}/\text{min}/\text{unit}$. The aldolase activity in the model was varied between 0.2 and 1.5 units/ml. The equilibrium velocities of the other enzymes were given the following values; V_{GAPDH} 2.5mM/min, V_{TIM} 1.5mM/min, V_{LDH} 1.5mM/min.

V_{ALD} (mM/min)	$V_{ALD}(\text{RECON})$ (mM/min)	V_{ALD} calculated from the exchange time courses predicted by the model ($\mu\text{mol}/\text{min}/\text{unit}$)
-----------------------	-------------------------------------	--

1.0	0.0	1.0
1.0	0.1	1.2
1.0	1.0	1.3

B - As in A except that the equilibrium velocities of the other enzymes were given the following values; V_{GAPDH} 5.0 mM/min, V_{TIM} 3.0 mM/min, V_{LDH} 3.0 mM/min.

V_{ALD} (mM/min)	$V_{ALD}(\text{RECON})$ (mM/min)	V_{ALD} calculated from the exchange time courses predicted by the model ($\mu\text{mol}/\text{min}/\text{unit}$)
-----------------------	-------------------------------------	--

1.0	0.1	1.2
1.0	0.5	1.3

The other conditions used in the model were as follows; 110M solvent, 1.9mM DHAP, 2.0mM FDP, 90 μM GAP, 10 μM NAD⁺, 10 μM NADH, 12mM lactate. These enzyme equilibrium velocities and substrate concentrations are similar to the conditions often used in the in vitro C-2 exchange system.

correspondence breaks down however if the lactate concentration is lowered to levels comparable with those of the other intermediates involved in the exchange.

Table 3 shows the results of a simulated in vitro aldolase equilibrium velocity determination. It will be remembered from the above that aldolase catalyses the exchange of isotope between the pro-S C-3 position of DHAP and solvent and also between the aldehydic hydrogen of GAP and the C-4 position of FDP. It was expected that the equilibrium velocity measured would reflect primarily the exchange of isotope between DHAP and solvent. The results shown in table 3 show this to be the case. Even when the recondensation reaction is set equal in rate to the solvent exchange reaction the equilibrium velocity determined is only slightly greater than the velocity of the solvent exchange reaction. It might be thought that the effect of the recondensation reaction on GAP labelling, if it occurred to any significant extent, could affect glyceraldehydophosphate dehydrogenase equilibrium velocity determinations. However the results in table 4, which are from a simulated glyceraldehydophosphate dehydrogenase equilibrium velocity determination, show that in fact the recondensation reaction has no effect. Of course this is only a simulation of bulk isotope flux, it makes no predictions about mechanistic effects on rate unless these are supplied with the equilibrium velocities input into the program. For example it is unlikely, see above, that the recondensation reaction would take place to any significant extent in the presence of triosephosphate isomerase and at the substrate concentrations found here.

Table 4

Model simulation of the effect of the recondensation reaction catalysed by aldolase ($V_{\text{ALD(RECON)}}$) on glyceraldehydephosphate dehydrogenase equilibrium velocity determinations.

V_{GAPDH} was set equal to $0.10 \mu\text{mol}/\text{min}/\text{unit}$. The other conditions used in the model were the same as those described in part B of table 3. The glyceraldehydephosphate dehydrogenase activity was varied between 2 and 15 units/ml.

V_{ALD} (mM/min)	$V_{\text{ALD(RECON)}}$ (mM/min)	V_{GAPDH} ($\mu\text{mol}/\text{min}/\text{unit}$) calculated from the exchange time courses predicted by the model
1.0	0.0	0.10
1.0	0.1	0.10
1.0	0.5	0.10
15.0	1.5	0.10
15.0	7.5	0.10

4.5.2 Simulation of the effects of chemical flux on isotopic flux

The model can be used to predict the effect of glycolytic or chemical flux on isotopic flux through the C-2 exchange system in situ. It was shown in chapter 2 that under normal circumstances, where the isotope flux is approximately five times greater than the rate of lactate production, that glycolytic flux has little effect on estimates of V_{C2X} . In the next chapter the model is used to examine the consequences of changing the ratio of these fluxes on measurements of V_{C2X} .

4.5.3 Isotope leaks - the effect of side reactions on the exchange

The model shows that under the conditions encountered in these studies changing the activity or concentration of a particular enzyme produces a change in V_{C2X} consistent with that expected from the double reciprocal relationship. Changes in the activities of the other enzymes involved in the exchange will change the sensitivity coefficient of the enzyme but its relationship with V_{C2X} will remain hyperbolic. This holds for C-2 exchange because it is, in the form described, an essentially linear system of exchange reactions. Additional pathways for exchange however can change this situation. For example consider the exchange pathway, mentioned in chapter 2, which involves the pentose phosphate pathway enzymes transaldolase, transketolase and ribulosephosphate 3-epimerase. Since this pathway can exchange the aldehydic hydrogen of GAP with solvent it can bypass the reactions catalysed by aldolase and triosephosphate isomerase. The overall equilibrium velocity for a set of parallel pathways is simply the sum of the equilibrium velocities for the individual pathways (Yagil & Hoberman, 1969). Under these circumstances there would no longer be a

double reciprocal relationship between the aldolase and triosephosphate isomerase equilibrium velocities and V_{C2X} unless the exchange catalysed by the pentose phosphate pathway enzymes were vanishingly small. The pathway would not however affect the double reciprocal relationship between the dehydrogenase equilibrium velocities and V_{C2X} . These would however be affected by another pathway which could introduce solvent label into NADH. The existence of such a pathway is ruled out by the data presented in the next chapter.

The existence of a pentose phosphate pathway, active in the exchange, will clearly affect the predictions of the in vitro model. However it is unlikely that this pathway makes a significant contribution to C-2 exchange. Although there is a large amount of transaldolase activity in the human erythrocyte, transketolase is present in only low activity (Friedemann & Rapoport, 1974). In the assay system used here (see Experimental section) the epimerase has also been shown to be present, although again in low activity. Increasing the epimerase activity in a concentrated lysate from 1.2 to 1.6 units/ml by adding an enzyme preparation from yeast had no detectable effect on V_{C2X} . This does not prove that the epimerase pathway is unimportant, for example transketolase may be the rate limiting step. Addition of transketolase may clarify this point. Experiments in vitro with the isolated enzymes would also provide additional information on the relative importance of the pathway. The reaction catalysed by fructose biphosphatase represents another possible isotope leak. Label transferred from GAP to FDP would subsequently exchange with glycolytic intermediates above FDP in the glycolytic sequence. However the recondensation reaction catalysed by aldolase is unlikely to result in significant FDP labelling and therefore this leak is not expected to be

large. the capability of the in vitro model, shown above, to describe the properties of the exchange system in situ suggest that the contribution of both these pathways is unlikely to be significant. Furthermore they are of no consequence to the equilibrium velocity determinations, shown in the next chapter, on glyceraldehydophosphate dehydrogenase in the intact erythrocyte.

4.6 Summary and conclusions

Models which predict the exchange behaviour of the C-2 exchange system from the individual isotope exchange properties of the enzymes have been demonstrated. These models can be used to provide semi-quantitative explanations of the behaviour of the exchange system in situ. In this respect they are similar to computer models of metabolism. Although of no direct use in determining the in situ kinetic properties of an enzyme, the comprehensive model described can be used to investigate the effect of chemical, in this case glycolytic flux, on measurements of isotopic flux. In general the measurement of the in situ kinetic properties of an enzyme, which are observed by measuring the exchange properties of a system of enzymes, will require modelling of the entire exchange system in vitro in order to determine the possible effects of chemical flux. Such models will, because of changes in the concentrations of the labelled intermediates, be characterised by a set of non-linear differential equations. A method suited to the solution of such equations is described in appendix 3.

In the next chapter a direct method for obtaining the in situ equilibrium velocity of glyceraldehydophosphate dehydrogenase is described. The model is used to determine the effect of glycolytic flux on these in situ equilibrium velocity determinations which involve changing the ratio of the rates of chemical and isotopic flux.

4.7 References

- Curtis, A.R. & Chance, E.M. (1972) "Eighth FEBS Meeting" Vol. 25, "Analysis and Simulation of Biochemical Systems" pp 39-57
- Friedemann, H. & Rapoport, S.M. (1974) in "Cellular and Molecular Biology of Erythrocytes", (Yoshikawa, H. & Rapoport, S.M., eds.) pp 181-259, Urban & Schwarzenberg, München, Berlin & Wien.
- Garfinkel, D., Marbach, C.B. & Shapiro, N.Z. (1977) Ann. Rev. Biophys. Bioeng. 6, 525-542
- Grazi, E. & Trombetta, G. (1974) Biochim. Biophys. Acta 364, 120-127
- Horecker, B.L., Smyrniotis, P.Z. & Hurwitz, J. (1956) J. Biol. Chem. 223, 1009-1019
- McCalla, T.R. (1967) "Introduction to Numerical Methods and Fortran Programming" J. Wiley & Sons Inc. New York London Sydney.
- Rieder, S.V. & Rose, I.A. (1959) J. Biol. Chem. 234, 1007-1010
- Rose, I.A. (1958) J. Am. Chem. Soc. 80, 5835-5836
- Yagil, G. & Hoberman, H.D. (1969) Biochemistry 8, 352-360

4.8 Appendix 1

A kinetic model to describe the effects of DHAP depletion on V_{C2X} .

The model assumes that the overall equilibrium velocity for the C-2 exchange system, V_{C2X} , is wholly determined by the equilibrium velocity of aldolase i.e. $V_{C2X} = V_{ALD}$. It also assumes that the equilibrium velocity of this enzyme is a simple Michaelis-Menten function of the DHAP concentration.

The first order rate constant for the exchange (k) can be described by the following equation;

$$k = \frac{V_{C2X} (D_0 - k_D t)}{L_0 (K_m + D_0 - k_D t)}$$

where D_0 is the DHAP concentration at $t=0$, K_m is the apparent K_m of aldolase for DHAP, k_D is the rate of DHAP breakdown and L_0 is the non-exchanged lactate concentration present at $t=0$. The rate of change of lactate labelling is described by the following equation;

$$\frac{dX_L}{X_L} = \frac{-V_{C2X} (D_0 - k_D t) dt}{L_0 (K_m + D_0 - k_D t)}$$

where X_L is the fractional labelling of the lactate. Integrating both sides of this equation we obtain;

$$X_L = \exp \left(\frac{V_{C2X}}{L_0 k_D} (-k_D t + K_m \ln(K_m + D_0 / K_m + D_0 - k_D t)) \right)$$

If the equation is used to describe changes in lactate methyl peak height in the n.m.r. experiment then it becomes;

$$L/L_0 = 1 - 2X_L$$

where L is the peak height at time t and L_0 is the peak height at $t=0$.

4.9 Appendix 2

Integration of polynomial and linear equations describing changes in V_{C2X} .

It was shown in the text that changes in V_{C2X} could be described by linear or polynomial equations or by a combination of the two. Integration of these equations permits calculation of the exchange time course.

The effect of a linear change in V_{C2X} on the exchange time course

The fractional labelling of the lactate, X_L , can be described by the following equation;

$$\frac{dX_L}{dt} = \frac{-(V - kt)}{L_0 + L_e} X_L$$

where V is V_{C2X} , L_0 is the unlabelled lactate concentration at $t=0$, L_e is the concentration of solvent labelled lactate present at $t=0$ and k is the rate of change in V_{C2X} .

As shown in the text, the changes in V_{C2X} may occur in one or more linear phases. If L_e is assigned the concentration of solvent labelled lactate at the beginning of each new phase and L_0 the concentration of non-solvent labelled lactate. Then each phase, whether it is described by a polynomial or linear equation, can be integrated separately.

Rearranging the above equation;

$$\frac{dX_L}{X_L} = \frac{-(V - kt)}{L_0 + L_e} dt$$

and integrating both sides gives the following equation which describes the fractional labelling of the lactate at time t during a linear phase in which V_{C2X} is changing at a constant rate k.

$$X_L = \frac{L_0 \exp\left(\frac{t(kt - 2V)}{2(L_0 + L_e)}\right)}{L_0 + L_e}$$

For C-2 exchange;

$$L/L_0 = 1 - 2X_L$$

where L is the lactate peak height at time t and L_0 is the peak height at t=0.

The effect of a non linear change in V_{C2X} on the exchange time course

If V_{C2X} changes in a non linear fashion as a function of time then these changes may be described by a polynomial function. In the example given in the text the changes in V_{C2X} were fitted to a polynomial function of the form;

$$V = A + Tt + Wt^2 + Ut^3 + Vt^4$$

where t is time, V is V_{C2X} and A, T, W, U and V are the coefficients of the

function which were varied in order to obtain a fit to the changes in V_{C2X} . The equation describing changes in the fractional labelling of the lactate is thus;

$$\frac{dX_L}{X_L} = \frac{-1}{L_0 + L_e} (A + Tt + Wt^2 + Ut^3 + Vt^4) dt$$

X_L , L_0 and L_e have the same meaning as described above. Integrating both sides of this equation we obtain:

$$X_L = \frac{L_0}{L_0 + L_e} \exp \left(\frac{-1}{(L_0 + L_e)} (At + Tt^2/2 + Wt^3/3 + Ut^4/4 + Vt^5/5) \right)$$

The equation describes the fractional labelling of the lactate at time t where V_{C2X} is changing as a function of time and its value at time t is given by the polynomial function described above.

Thus changes in V_{C2X} may be described by linear or polynomial functions or by a combination of the two. The changes in V_{C2X} can be divided into several phases, each described by a separate function. These phases are integrated separately in order to calculate the exchange time course.

4.10 Appendix 3

Computer programs for numerical integration of the equations describing

C-2 exchange

Euler method

The Euler method is a simple iterative method based on the following equations. Euler's formula can be written as

$$y_{n+1}^P = y_n + hf_n$$

where y_{n+1}^P denotes a predicted value approximating $y(x_{n+1})$, computed by a linear Taylor algorithm. The term f_n is the derivative of the integral curve $y(x)$. If it is assumed that f_n is constant over small intervals (x_n, x_{n+1}) then the value of y at x_{n+1} can be calculated from its value at x_n from the above equation where h is the abscissa increment; $x_{n+1} = x_n + h$. This is called the step size of the numerical method. The above equation is the Taylor-series expansion of first degree for the solution function $y(x)$. Truncation of this expansion, as in the above equation, results in a truncation error which occurs in each step of the solution and is propagated through successive steps. A better approximation of y_{n+1}^P is obtained if higher order terms of the Taylor series are used. This can be difficult however because of the involved form of the derivatives. For this reason methods were developed which indirectly use the Taylor series expansion without computing the higher order derivatives of $f(x,y)$, (see McCalla, 1967). In the predictor corrector method the predicted value y_{n+1}^P is substituted into the following equation which is derived from a second order Runge-Kutta method which itself is equivalent to the second order

Taylor algorithm.

$$y_{n+1}^c = y_n + h/2(f_n + f(x_{n+1}, y_{n+1}^p))$$

where y_{n+1}^c denotes a corrected approximation of $y(x_{n+1})$. If this corrected value is now substituted into the right hand side of the equation as y_{n+1}^p , then the calculation can be repeated to obtain the corrected value. This iterative procedure can be repeated a number of times until convergence for a particular step is obtained. Convergence can be tested by comparing $|y_{n+1}^c - y_{n+1}^p|$ with some positive convergence term, y_{n+1}^c is the current value of the predicted solution, y_{n+1}^p was its value during the previous iteration. When the corrector formula converges the step index is incremented, x_n is increased to give x_{n+1} , and the entire procedure is repeated. The predictor formula is used only once for each step, whereas the corrector is iterated until it converges for each step. Under the conditions found in the erythrocyte there will be very rapid changes, following a pulse of label, in the fractional labelling of those intermediates which have relatively low total concentrations and which are turned over by enzymes with high equilibrium velocities. In order to calculate, using the Euler method, the changes in labelling of these intermediates following a label pulse, a step size (h) must be used which is comparable with the shortest time constants for the transients observed in the fractional labelling of the intermediates following the label pulse. Simulation of the behaviour of the system over a much longer time interval (these initial transients will decay very rapidly) is uneconomic if time steps comparable to the shortest time constants are used since this may involve evaluation of the equations describing fractional labelling as many as 10^6 or even 10^8 times (see Curtis & Chance, 1972). As well as being uneconomic in

computer time the method also becomes inaccurate due to both roundoff error which is propagated through successive calculations and the intrinsic inaccuracy of the predictor-corrector approximation which results from truncation of the Taylor series expansion on which the formulae are based. The equations under these conditions are said to be "stiff".

Gear method

The property of stiffness can be characterised by the Jacobian matrix of the system (for the C-2 exchange system this is given by the subroutine PEDERV in the computer program shown below). The set of equations describing the C-2 exchange system have the general form;

$$(\text{CONC})_i \frac{dX_i}{dt} = V_j(X_1, X_2, \dots, X_i), \quad i=1 \text{ to } 9 \text{ and } j=1 \text{ to } 6$$

where $(\text{CONC})_i$ represents the concentration of the intermediate i , V_j represents the isotope exchange equilibrium velocity or the chemical or glycolytic flux rate (g in the model) for the reaction j and X_i represents the fractional labelling of the intermediate i . This equation can be rewritten in the form;

$$dC_i/dt = k_j(C_1, C_2, \dots, C_i) \quad i = 1 \text{ to } 9 \text{ and } j = 1 \text{ to } 6 \dots \dots \dots 1$$

where C_i represents the concentration of the labelled intermediate i and k_j the rate constant for the reaction j . The Jacobian matrix for this system has the components $\partial k_j / \partial C_i$. Since some of the equations are non-linear this is a time dependent matrix. If the matrix were constant then the equations would represent a set of linear differential equations with constant coefficients. In this case the solutions are

combinations of exponentials of the form $\exp(\alpha_k t)$ where the numbers α_k are the eigenvalues of the matrix of coefficients. Under these circumstances an iterative method for numerical integration is unnecessary. The non-linearity arises because of double labelling (in the case of NADH) and because of changes in the concentrations of the labelled intermediates (in the case of FDP and lactate).

Consider equation 1 and suppose a slightly varied solution is obtained representing a perturbation on the concentrations $C_i(t)$. The concentration of the i th variable in the solution is denoted as $(C_i + n_i)$, where n_i is in general expected to be small. The differential equations satisfied by the varied solution are therefore;

$$\begin{aligned} dC_i/dt + dn_i/dt &= k_j (C_1 + n_1, \dots, C_i + n_i) \\ &\approx k_j (C_1, C_2, \dots, C_i) \\ &+ \sum_{i=1}^9 n_i \partial k_j / \partial C_i + 0(n^2) \quad j=1 \text{ to } 6 \text{ and } i=1 \text{ to } 9 \end{aligned}$$

The right hand term has been expanded in a Taylor series as far as the first derivative term. This gives the variational equation which describes the behaviour of small fluctuations about the solution;

$$dn_i/dt = \sum_{i=1}^9 n_i \partial k_j / \partial C_i, \quad j=1 \text{ to } 6 \text{ and } i=1 \text{ to } 9$$

where $\partial k_j / \partial C_i$ is given by the Jacobian matrix. In the Euler method it is assumed that these fluctuations are negligibly small and thus that the first derivative, y' , of the function $y(x)$ is constant over the time step h . For a very stiff system where the solutions are changing very rapidly this may not be the case and y'' may not equal 0. For a system

of differential equations the second derivative, y'' , of the solutions can be calculated using the following equation where the derivatives are written in vector notation and J is the Jacobian matrix.

$$\underline{y}'' = J \underline{y}'$$

In the variable step, variable order Gear method this equation is used initially to estimate the truncation error obtained with a first order algorithm. Both the order of the algorithm for integration and the time step appropriate to the current stiffness of the system are then selected. These are adjusted throughout the integration process. During simulation of the isotope exchange system the order will increase rapidly during the initial transients obtained following the label pulse. As these die away the order will decrease as a steady state is obtained and the time step will increase. The time step can reach values of the order of 10^6 times the shortest time constant in the system (Curtis & Chance, 1972). The method is thus very economical in terms of computation time, much of the work being done in the simulation of the initial transients, and also more accurate since fewer iterations are required. Under "non-stiff" conditions the Euler and Gear methods gave similar results.

A computer program for numerical integration of the equations describing C-2 exchange using the Euler method.

The program was written in Fortran IV and was run on the Oxford University ICL 2980 computer. The following is a brief outline of the program. A listing of the program is shown on a following page.

At lines 7 and 8 the elements of the A matrix are assigned values representing the total micromolar concentrations of the labelled intermediates involved in the exchange. The elements 1 to 8 contain the concentrations of lactate, NAD^+ , GAP, DHAP, solvent and the three NADH species respectively. At lines 9 and 10 the elements of the B matrix are assigned values representing the micromolar concentrations of the labelled intermediates. In this model the label is regarded as being deuterium and at $t=0$ the lactate is totally deuterated at the C-2 position, the other substrates contain no deuterium. Although the solvent concentration has been set at 1M, instead of 110 M, this has no effect on the predictions of the model since it is still much greater than the concentrations of the other intermediates involved in the exchange. At lines 11 and 12 externally supplied values for the equilibrium velocities (V matrix) and time step (H) are read into the program. The time step was typically 0.01 minutes. The elements of the V matrix represent the equilibrium velocities (input with units of mM/min) of the enzymes lactate dehydrogenase, glyceraldehydophosphate dehydrogenase, triosephosphate isomerase and aldolase respectively. It will be noted that this is a shortened version of the model described in the text which contains terms describing the labelling of FDP and the rate of lactate production. At lines 13,14 and 15 time values (in minutes) at which solution values are to be output are assigned to elements of the T matrix.

From lines 26 to 61 the concentrations of the intermediates used in the program are output as are the values for their fractional labelling at $t=0$. The equilibrium velocities and time step which were read into the program are also output. At lines 58 to 61 the concentration of deuterated lactate and its apparent concentration (in

terms of peak height) in the C-2 exchange experiment are output.

Line 62 marks the start of the predictor section. The elements of the P matrix are assigned the values of the Y matrix which were assigned, at line 24, the values of the B matrix, the concentrations of the deuterated intermediates. U1 is assigned the value of U (which represents time) which was set to zero at line 22.

The subroutine called DERIV is then called. This subroutine is listed at the end of the program. The elements of the R matrix are assigned values representing the fractional labelling of the intermediates. The elements of the D matrix are assigned the calculated values for the deuterium concentrations of the intermediates. The derivation of these equations is shown in the text. On return to the main program the E matrix is assigned the values of the D matrix. The X matrix is then assigned the values of the D matrix plus the values of the E matrix multiplied by the time step H, (line 72). This represents the predictor equation shown above. A flag is set at line 75, which marks the start of the corrector section, and the elements of the P matrix are given the predicted values calculated at line 72. The time value is incremented by the time step H at line 79 and the subroutine DERIV is called again. This calculates new values for the concentrations of deuterated intermediates using the predicted values, contained in the P matrix, as starting values. On return to the main program these new values are assigned to elements of the F matrix. At line 85 the elements of the W matrix are assigned the values of the E matrix (the solution values calculated in the predictor section) plus the values of the F matrix. At line 89 the values of the W matrix are reassigned with values of the Y matrix (the initial solution values used

at the start of the predictor section) plus the values of the W matrix multiplied by half the value for the time step. This line represents the corrector equation. At lines 93 and 94 the computed solution values are tested against a convergence term set at 0.1. If the current values for the solutions differ by less than 0.1 from the initial values or the values computed in the previous iteration then control is transferred to line 102. If the solution values have satisfied the convergence test then the flag (L) set at line 75 will equal zero and control is transferred to line 103. If the value of U (the time value) is greater than the Nth value of the time matrix T then control is transferred to line 110 and the current solution values are output. If the solution values do satisfy the convergence term but the value of U does not exceed the current Nth value of the time matrix T then the value of the Y matrix is set to the value of the W matrix at line 105 i.e. the elements of the Y matrix are assigned the current solution values. The time (U) is incremented by the time step (H). Control is then transferred to line 62 and a new predictor calculation is performed. If the solution values do not satisfy the convergence test then control is transferred to line 96. The values of the X matrix are assigned the values of the W matrix, i.e. the old corrector (W) becomes the new predictor (X). The flag L is set to 1 which results in transfer of control at line 102 to line 75 and the corrector section is reiterated.

Storage and output of solution values begins at line 110. The values of the Z matrix are assigned the current time value (U) and the concentrations of the deuterated intermediates (W). At line 115 the current time value, the concentration of the deuterated lactate and the value of the lactate peak height in the n.m.r. experiment are output. The time is then incremented by the time step (H). N, which defines the

current value of the time matrix (T) at which solution values are to be output, is also incremented. The Y matrix is assigned the values of the W matrix and control is transferred to the start of the predictor section. If N is greater than 13, the total number of values in the time matrix, then the stored solution values for the deuterated concentrations of the other intermediates involved in the exchange are output and the program run terminated.

A computer program for the numerical integration of the equations describing C-2 exchange using the Gear method

The program was written in Fortran IV and calls the NAG library routine D02EBF (NAG library, Mk 7) which is a routine which integrates a stiff system of differential equations using a variable order, variable step Gear method. A brief description of the operation of this program is given in the following, a full description of the NAG library routine is available from NAG Ltd. 7 Banbury Rd. Oxford. The program was run on an Oxford University VAX computer. A program listing is shown on a following page.

Assignment of parameters; the elements of the CONC matrix are assigned the initial millimolar concentrations of the intermediates. The elements 1 to 8 represent solvent, DHAP, GAP, NAD^+ , NADH, FDP and lactate respectively. The elements of the Y matrix are assigned the initial millimolar concentrations of the deuterated intermediates. At $t=0$ only the lactate is deuterated. The enzyme equilibrium velocities are assigned to elements of the VEL matrix. The elements 1 to 5 represent the equilibrium velocities (mM/min) of aldolase, the recondensation reaction catalysed by aldolase (see text),

triosephosphate isomerase, glyceraldehydophosphate dehydrogenase and lactate dehydrogenase respectively. VEL(6) represents the rate of lactate production. The values NUM, XEND and J, also read in from the external file, represent the number of points at which solution values are to be output, the total time over which the integration is to be performed and a convergence term which is described in the NAG documentation. The program initially calls the DISPLAY subroutine which outputs all of the above parameters thus enabling the user to check that the correct values have been input. The NAG library routine is then called which itself calls the following routines during program operation.

Subroutine FCN; this is equivalent to the DERIV subroutine shown in the Euler program. The derivation of the equations is described in the text. The elements of the P matrix are assigned values representing the fractional labelling of the intermediates. The calculated concentrations of the deuterated intermediates are assigned to the elements of the F matrix, the numbering scheme is the same as that described for the CONC matrix.

Subroutine PERDERV; this calculates values for the Jacobian matrix; PW. The matrix element PW(i,j) contains the value for the derivative $\partial F_i / \partial Y_j$.

Subroutine OUT; this stores the calculated solution values at a time point (specified by X in the program) in the matrix RES. The time at which output is next required is then calculated and assigned to X. When all the time points at which solution values are required are passed the subroutine RESULTS is called. This outputs the stored

solution values.

References

Curtis, A.R. & Chance, E.M. (1972) "Eighth FEBS Meeting" Vol. 25,
"Analysis and Simulation of Biochemical Systems" pp39-57

McCalla, T.R. (1967) "Introduction to Numerical Methods and Fortran
Programming" J. Wiley & Sons Inc. New York London Sydney

```

1      PROGRAM C2XMOD
2      DIMENSION A(8),B(8),T(12)
3      DIMENSION R(8),P(8),D(8),E(8),F(8),W(8),X(8),Y(8)
4      DIMENSION Z(12,9),V(4),TT(8),STATE(8)
5      COMMON D,V,R,P,A
6      C*****INPUT SUBROUTINE
7      DATA A(1),A(2),A(3),A(4),A(5),A(6),A(7),A(8)/
8      1 6000.0,90.0,50.0,500.0,1000000.0,50.0,50.0,50.0/
9      DATA B(1),E(2),B(3),B(4),E(5),B(6),B(7),B(8)/
10     1 6000.0,0.0,0.0,0.0,0.0,0.0,0.0,0.0/
11     READ(1,*) V(1),V(2),V(3),V(4)
12     READ(1,*) H
13     DATA T(1),T(2),T(3),T(4),T(5),T(6),T(7),T(8),T(9),T(10),
14     1 T(11),T(12)/
15     2 2.,4.,6.,8.,10.,12.,14.,16.,18.,20.,22.,24. /
16     DO 400 I=1,4
17     V(I)=V(I)*1000.
18     400 CONTINUE
19     ZERO=0.0
20     C*****INITIALIZE
21     N=1
22     U=0.
23     DO 450 I=1,8
24     Y(I)=B(I)
25     450 CONTINUE
26     DATA TT(1),TT(2),TT(3),TT(4),TT(5),TT(6)
27     1 /7HLACTATE,3HNAD,3HGAP,4HHDHAP,7HSOLVENT,4HNADH/
28     WRITE(2,500)
29     500 FORMAT(1X,'SUBSTANCE TOTAL CONC./UM
30     1 ' INITIAL DEUTERIUM CONC./UM')
31     DO 600 I=1,6
32     WRITE(2,501) TT(I),A(I),B(I)
33     501 FORMAT(1X,A10,5X,F12.4,10X,F12.4)
34     600 CONTINUE
35     WRITE(2,550)
36     550 FORMAT(//)
37     WRITE(2,650)
38     650 FORMAT(1X,'ISOTOPE STATE INITIAL DEUTERIUM CONC./UM')
39     DATA STATE(6),STATE(7),STATE(8)
40     1 /3HD 0,3H* 0,3HD */
41     DO 750 I=6,8
42     WRITE(2,700) STATE(I),B(I)
43     700 FORMAT(1X,A4,10X,F12.4)
44     750 CONTINUE
45     WRITE(2,550)
46     WRITE(2,800)
47     800 FORMAT(1X,'EQUILIBRIUM VELOCITIES')
48     WRITE(2,850)
49     850 FORMAT(1X,' LDH GAPDH TIM*
50     1 ' ALDOLASE')
51     WRITE(2,900) V(1),V(2),V(3),V(4)
52     900 FORMAT(1X,5(F12.4,5X))
53     WRITE(2,550)
54     WRITE(2,1000) H
55     1000 FORMAT(1X,'TIME STEP =',F12.4)
56     WRITE(2,550)
57     WRITE(2,1050)
58     1050 FORMAT(1X,' TIME LACTATE VC2X')
59     XX=-1.0*(A(1)-2.*B(1))
60     WRITE (2,1100) ZERO,B(1),XX
61     1100 FORMAT(1X,3(F12.4,5X))
62     1110 DO 1120 I=1,8
63     C*****PREDICTOR SECTION
64     P(I)=Y(I)
65     1120 CONTINUE
66     U1=U
67     CALL DERIV
68     DO 1300 I=1,8
69     E(I)=D(I)
70     1300 CONTINUE
71     DO 1400 I=1,8
72     X(I)=Y(I)+H*E(I)
73     1400 CONTINUE
74     C*****CORRECTOR SECTION
75     1401 L=C
76     DO 1500 I=1,8
77     P(I)=X(I)
78     1500 CONTINUE
79     U1=U+H
80     CALL DERIV
81     DO 1600 I=1,8
82     F(I)=D(I)
83     1600 CONTINUE
84     DO 1700 I=1,8
85     W(I)=E(I)+F(I)
86     1700 CONTINUE
87     H1=H/2.
88     DO 1800 I=1,8
89     W(I)=Y(I)+H1*W(I)
90     1800 CONTINUE

```

91	C*****TEST FOR CONVERGENCE	91
92	DO 1910 I=1,6,2	92
93	IF(ABS(W(I)-X(I)).GT.0.1) GOTO 1850	93
94	IF(ABS(W(I+1)-X(I+1)).LT.0.1) GOTO 1910	94
95	1850 DO 1900 J=1,6	95
96	X(J)=W(J)	96
97	1900 CONTINUE	97
98	GOTO 1920-	98
99	1910 CONTINUE	99
100	GOTO 1930	100
101	1920 L=1	101
102	1930 IF(L.EQ.1.0) GOTO 1401	102
103	IF(U.GT.T(N)) GO TO 2000	103
104	DO 1940 I=1,8	104
105	Y(I)=W(I)	105
106	1940 CONTINUE	106
107	U=U+H	107
108	GOTO 1110	108
109	C*****STORAGE AND OUTPUT OF SOLUTIONS	109
110	2000 Z(N,1)=U	110
111	DO 2100 I=1,8	111
112	Z(N,I+1)=W(I)	112
113	2100 CONTINUE	113
114	YY=-1.0*(A(1)-2.*W(1))	114
115	WRITE (2,2200) U,W(1),YY	115
116	2200 FORMAT (1X,3(F12.4,5X))	116
117	DO 2250 I=1,8	117
118	Y(I)=W(I)	118
119	2250 CONTINUE	119
120	U=U+H	120
121	N=N+1	121
122	IF(N.EQ.13.) GOTO 2300	122
123	GOTO 1110	123
124	C*****OUTPUT OF SOLUTIONS	124
125	2300 WRITE(2,2310)	125
126	2310 FORMAT(1X," TIME NAD NADH(**)"	126
127	1 " NADH(0*) NADH(*0)"	127
128	WRITE (2,550)	128
129	WRITE (2,2350) ZERO,B(2),B(6),B(7),B(8)	129
130	2350 FORMAT(1X,5(F12.4,5X))	130
131	DO 2400 I=1,12	131
132	WRITE (2,2350) Z(I,1),Z(I,3),Z(I,7),Z(I,8),Z(I,9)	132
133	2400 CONTINUE	133
134	WRITE (2,550)	134
135	WRITE (2,2450)	135
136	2450 FORMAT(1X," TIME GAP DHAP"	136
137	1 " SOLVENT"	137
138	WRITE (2,2500) ZERO, B(3),B(4),B(5)	138
139	2500 FORMAT(1X,4(F12.4,5X))	139
140	DO 2600 I=1,12	140
141	WRITE (2,2500) Z(I,1),Z(I,4),Z(I,5),Z(I,6)	141
142	2600 CONTINUE	142
143	STOP	143
144	END	144
145	SUEROUTINE DERIV	145
146	DIMENSION D(8),R(8),V(4),P(8),A(8)	146
147	COMMON D,V,R,P,A	147
148	DO 1200 I=1,8	148
149	R(I)=P(I)/A(I)	149
150	1200 CONTINUE	150
151	D(1)=V(1)*(R(8)+R(6)-R(1))	151
152	D(2)=V(1)*(R(6)+R(7))+V(2)*(R(6)+R(8))-(V(1)+V(2))*R(2)	152
153	D(3)=V(2)*(R(6)+R(7)-R(3))-V(3)*(R(3)-R(4))	153
154	D(4)=V(3)*(R(3)-R(4))-V(4)*(R(4)-R(5))	154
155	D(5)=V(4)*(R(4)-R(5))	155
156	D(6)=V(1)*(R(1)+R(2)-R(6))-V(2)*(R(6)-R(2)+R(3))	156
157	D(7)=V(1)*((1-R(1))*R(2)-R(7))-V(2)*(R(7)-R(3)+(1-R(2)))	157
158	D(8)=V(1)*((1-R(2))*R(1)-R(8))-V(2)*(R(8)-R(2)+(1-R(3)))	158
159	RETURN	159
160	END	160

```

PROGRAM C2XMOD
DOUBLE PRECISION CCNC(9),VEL(6),H,XEND,TOL,X
DOUBLE PRECISION W(9,30),Y(9)
INTEGER I,IFAIL,IR,IW,J,MPED,N,NOUT,NIN,NUM
EXTERNAL FCN,OUT,PEDERV
COMMON XEND,H,I,CCNC,VEL,NUM
C.....INITIALISATION OF PROGRAM
DATA NOLT/6/
DATA NIN/5/
N=9
IW=30
IR=1
MPED=1
C.....ASSIGNMENT OF PARAMETERS
DATA CCNC(1),CCNC(2),CCNC(3)/ 110000.0,1.0,0.045/
DATA CCNC(4),CCNC(5),CCNC(6)/ 0.01,0.01,0.01/
DATA CCNC(7),CCNC(8),CCNC(9)/ 0.01,3.0,13.0/
DATA Y(1),Y(2),Y(3),Y(4),Y(5)/ 0.0,0.0,0.0,0.0,0.0/
DATA Y(6),Y(7),Y(8)/ 0.0,0.0,0.0/
DATA Y(9)/ 12.0/
READ(NIN,*) VEL(1),VEL(2),VEL(3),VEL(4),VEL(5),VEL(6),
+ NUM,XEND,J
TOL=10.**(-J)
WRITE(NOUT,100) TOL
X=C.C
H=(XEND-X)/NUM
I=NUM-1
IFAIL=1
CALL DISPLAY(Y)
CALL DC2EBF(X,XEND,N,Y,TOL,IR,FCN,MPED,PEDERV,
+ OUT,IW,IFAIL)
WRITE(NOUT,200) IFAIL

STOP
100 FORMAT(22H0CALCULATION WITH TOL=,E8.1)
200 FORMAT(8H IFAIL=,I1)
300 FORMAT(1X,E8.1)
END
C.....SUBROUTINES
SUBROUTINE FCN(T,Y,
INTEGER I,J,NUM
DOUBLE PRECISION H,XEND,VEL(6),P(9)
DOUBLE PRECISION F(9),Y(9),SUBCCNC(2),T,CCNC(9)
COMMON XEND,H,I,CCNC,VEL,NUM
SUBCCNC(1)=CCNC(8)-(VEL(6)/2.)*T
SUBCCNC(2)=CCNC(9)+VEL(6)*T
DO 2000 J=1,7
F(J)=Y(J)/CCNC(J)
2000 CONTINUE
DO 3000 J=8,9
F(J)=Y(J)/SUBCCNC(J-7)
3000 CONTINUE
F(1)=VEL(1)*(P(2)-P(1))
F(2)=VEL(3)*(P(3)-P(2))+VEL(1)+VEL(6)/2.)*(P(1)-P(2))
F(3)=VEL(3)*(P(2)-P(3))+VEL(4)*(P(6)+P(7)-P(3))
+VEL(2)+(P(3)-P(3))+VEL(6)/2.)*(P(2)+P(8))-VEL(6)*P(3)
F(4)=(VEL(5)+VEL(6))*(P(7)+P(6)-P(4))+VEL(4)*(P(5)+P(6)-P(4))
F(5)=VEL(5)*(P(9)*(1-P(4))-P(5))
+VEL(4)+VEL(6))*(P(4)*(1-P(3))-P(5))
F(6)=VEL(5)*(P(9)*P(4)-P(6))+VEL(4)+VEL(6))*(P(3)*P(4)-P(6))
F(7)=VEL(5)*(P(4)*(1-P(9))-P(7))
+VEL(4)+VEL(6))*(P(3)*(1-P(4))-P(7))
F(8)=VEL(2)*(P(3)-P(8))-(VEL(6)/2.)*P(8)
F(9)=(VEL(5)+VEL(6))*(P(5)+P(6))-VEL(5)*P(9)
RETURN
END
C.....
SUBROUTINE PEDERV(T,Y,PW)
DOUBLE PRECISION Y(9),PW(9,9),VEL(6),T,P(9)
DOUBLE PRECISION XEND,H,CCNC(9),SUBCCNC(2)
INTEGER I,J,N,NUM
COMMON XEND,H,I,CCNC,VEL,NUM
SUBCCNC(1)=CCNC(8)-(VEL(6)/2.)*T
SUBCCNC(2)=CCNC(9)+VEL(6)*T
DO 300 J=1,7
P(J)=Y(J)/CCNC(J)
300 CONTINUE
DO 400 J=8,9
P(J)=Y(J)/SUBCCNC(J-7)
400 CONTINUE
PW(1,1)=-VEL(1)/CCNC(1)
PW(1,2)=VEL(1)/CCNC(7)
PW(2,1)=(VEL(1)+(VEL(6)/2.))/CCNC(1)
PW(2,2)=(-VEL(3)-VEL(1)-(VEL(6)/2.))/CCNC(2)
PW(2,3)=VEL(7)/CCNC(7)
PW(3,2)=(VEL(3)+(VEL(6)/2.))/CCNC(2)
PW(3,3)=(-VEL(3)-VEL(4)-VEL(2)-VEL(6))/CCNC(3)
PW(3,6)=VEL(4)/CCNC(6)
PW(3,7)=VEL(4)/CCNC(7)
PW(3,8)=(VEL(2)+(VEL(6)/2.))/SUBCCNC(1)
PW(4,4)=(-VEL(7)-VEL(4)-VEL(6))/CCNC(4)
PW(4,5)=VEL(4)/CCNC(5)
PW(4,6)=(VEL(5)+VEL(4)+VEL(6))/CCNC(6)
PW(4,7)=(VEL(5)+VEL(6))/CCNC(7)

```

```

PW(5,3)=(-VEL(4)*P(4)-VEL(6)*P(4))/CONC(3)
PW(5,4)=(-VEL(5)*P(9)+VEL(4)-VEL(4)*P(3)+VEL(6)
+ -VEL(6)*P(3))/CONC(4)
PW(5,5)=(-VEL(5)-VEL(4)-VEL(6))/CONC(5)
PW(5,9)=(VEL(5)-VEL(5)*P(4))/SUBCONC(2)
PW(6,3)=(VEL(4)*P(4)+VEL(6)*P(4))/CONC(3)
PW(6,4)=(VEL(5)*P(9)+VEL(4)*P(3)+VEL(6)*P(3))/CONC(4)
PW(6,6)=(-VEL(5)-VEL(4)-VEL(6))/CONC(6)
PW(6,9)=(VEL(5)*P(4))/SUBCONC(2)
PW(7,3)=(VEL(4)-VEL(4)*P(4)+VEL(6)-VEL(6)*P(4))/CONC(3)
PW(7,4)=(VEL(5)-VEL(5)*P(9)-VEL(4)*P(3)-VEL(6)*P(3))/CONC(4)
PW(7,7)=(-VEL(5)-VEL(4)-VEL(6))/CONC(7)
PW(7,9)=(-VEL(5)+P(4))/SUBCONC(2)
PW(8,3)=VEL(2)/CONC(3)
PW(8,8)=(-VEL(2)-(VEL(6)/2.))/SUBCONC(1)
PW(9,5)=(VEL(5)+VEL(6))/CONC(5)
PW(9,6)=(VEL(5)+VEL(6))/CONC(6)
PW(9,9)=-VEL(5)/SUBCONC(2)
RETURN
END

```

```

C.....
SUBROUTINE CUT(X,Y)
COMMON XEND,H,I,CONC,VEL,NUM
INTEGER I,J,NCUT,NUM
DOUBLE PRECISION VEL(6),Y(9),CONC(9)
DOUBLE PRECISION X,F,XEND
REAL RES(50,13)
DATA NCUT/6/
DO 1000 J=1,9
RES(NUM-I,J)=Y(J)
1000 CONTINUE
RES(NUM-I,10)=CONC(8)-(VEL(6)/2.)*X
RES(NUM-I,11)=CONC(9)+VEL(6)*X
RES(NUM-I,12)=X
RES(NUM-I,13)=-1.0*(RES(NUM-I,11)-2.0*RES(NUM-I,9))
IF(I.EQ.0) CALL RESULTS(NUM,RES)
X=XEND-FLOAT(I)*H
I=I-1
RETURN
END

```

```

C.....
SUBROUTINE DISPLAY(Y)
INTEGER I,NCUT,NUM
DOUBLE PRECISION Y(9),CONC(9),VEL(6)
DOUBLE PRECISION XEND,H
COMMON XEND,H,I,CONC,VEL,NUM
DATA NCUT/6/
WRITE (NCUT,555)
WRITE(NCUT,400) CONC(1),Y(1)
WRITE(NCUT,401) CONC(2),Y(2)
WRITE(NCUT,402) CONC(3),Y(3)
WRITE(NCUT,403) CONC(4),Y(4)
WRITE(NCUT,404) CONC(5),Y(5)
WRITE(NCUT,405) CONC(8),Y(8)
WRITE(NCUT,406) CONC(9),Y(9)
WRITE (NCUT,553)
WRITE(NCUT,552)
WRITE(NCUT,551) VEL(1),VEL(2),VEL(3)
WRITE(NCUT,550)
WRITE(NCUT,551) VEL(4),VEL(5),VEL(6)
RETURN

```

```

400 FORMAT(1X,'SOLVENT',9X,E12.4,10X,F12.4)
401 FORMAT(1X,'DHAP',11X,F12.4,10X,F12.4)
402 FORMAT(1X,'GAP',12X,F12.4,10X,F12.4)
403 FORMAT(1X,'NAD',12X,F12.4,10X,F12.4)
404 FORMAT(1X,'NADH',11X,F12.4,10X,F12.4)
405 FORMAT(1X,'FDP',12X,F12.4,10X,F12.4)
406 FORMAT(1X,'LACTATE',9X,F12.4,10X,F12.4)
555 FORMAT(1X,'SUBSTANCE' TOTAL CONC./MM
+ INITIAL DEUTERIUM CONC./MM)
554 FORMAT(1X,A10,3X,F12.4,10X,F12.4)
553 FORMAT(31HC EQUILIBRIUM VELOCITIES MM/MIN)
552 FORMAT(1X,' ALDOLASE ALD(RECON) TIM')
551 FORMAT(1X,3(F12.4,5X))
550 FORMAT('0', GAPDH LDH
+ LACTATE GROWTH')
END

```

```

C.....
SUBROUTINE RESULTS(NUM,RES)
INTEGER J,NCUT,NUM
REAL RES(50,13)
DATA NCUT/6/
WRITE(NCUT,99999)
DO 100 J=1,NUM
WRITE(NCUT,99998) RES(J,12),RES(J,11),RES(J,9),RES(J,13)
100 CONTINUE
WRITE(NCUT,99997)
DO 200 J=1,NUM
WRITE(NCUT,99996) RES(J,12),RES(J,1),RES(J,2),RES(J,3),RES(J,4)
200 CONTINUE
WRITE(NCUT,99995)
DO 300 J=1,NUM
WRITE(NCUT,99994) RES(J,12),RES(J,5),RES(J,6),RES(J,7)
300 CONTINUE
WRITE(NCUT,99993)
DO 400 J=1,NUM
WRITE(NCUT,99992) RES(J,12),RES(J,10),RES(J,8)
400 CONTINUE
RETURN
99999 FORMAT('0',/,' TIME LACTATE CONC DEUTERATED LACTATE VC2X')
99998 FORMAT(1X,F7.2,F12.4,2F16.4)
99997 FORMAT('0',/,' TIME SOLVENT DHAP. GAP
+ NAD')
99996 FORMAT(1X,F7.2,E12.4,3F12.8)
99995 FORMAT('0',/,' TIME NADH(*O) NADH(**) NADH(C*)')
99994 FORMAT(1X,F7.2,3F12.8)
99993 FORMAT('0',/,' TIME FDP CONC FDP')
99992 FORMAT(1X,F7.2,2F12.4)
END

```

5 A comparison of the kinetic properties expressed
by glyceraldehydephosphate dehydrogenase in the
intact erythrocyte and in vitro

5.1 Introduction

In chapter 2 the properties of the C-2 exchange system in the intact erythrocyte were demonstrated. A method for obtaining, in vitro, the individual isotope exchange equilibrium velocities of the enzymes involved in the exchange was described. In chapter 3 the properties of this in vitro system and its suitability as a model for the in situ system were examined. Kinetic models which relate the isotope exchange properties of the individual enzymes to the overall exchange catalysed by the system of enzymes were described in chapter 4. These models can be used to provide semi-quantitative explanations of the behaviour of the exchange system in situ based on the properties the enzymes display in vitro. However they do not provide any direct information on the properties displayed by an individual enzyme in situ. In this chapter a method is described for obtaining the isotope exchange equilibrium velocity of glyceraldehydephosphate dehydrogenase (GAPDH) in the intact erythrocyte. The kinetic properties displayed by the enzyme are compared with the properties it displays in the in vitro exchange system.

Human erythrocyte GAPDH continues to attract considerable interest, both as a possible regulatory enzyme in erythrocyte glycolysis and perhaps more importantly as an enzyme which will, under certain conditions, bind to the erythrocyte membrane. Binding of enzymes to membranes and the possible significance of this binding to the control of metabolism were discussed in chapter 1.

Conventional steady state kinetic studies employing spectrophotometric techniques have been used to examine the kinetic properties of human erythrocyte GAPDH in vitro (Mills & Hill, 1971; Oguchi, 1970; Maretzki et al, 1973; Schrier et al, 1975a; Wrigglesworth et al, 1976; Eby & Kirtley, 1979; Wang & Alaupovic, 1980). The kinetic constants derived from these studies show a wide range of values depending on the conditions under which they were obtained. For example the observed kinetic parameters can be affected by various substrate interactions. Assays employing arsenate as a substitute for phosphate may produce artefactual results (Duggleby & Dennis, 1974). The values obtained for the K_m for GAP at pHs between 7.2 and 7.4 range from $5\mu\text{M}$ (Maretzki et al, 1973) to $21\mu\text{M}$ (Mills & Hill, 1971), $95\mu\text{M}$ (Wang & Alaupovic, 1980), $120\mu\text{M}$ (Wrigglesworth et al, 1976) and $230\mu\text{M}$ (Schrier et al, 1975a). From the results of assays performed under conditions thought to simulate the in situ environment, Maretzki et al (1973) calculated that the "velocity of the enzyme approaches within one order of magnitude of the glycolytic flux". Mills and Hill (1971) and Wang and Alaupovic (1980), on the basis of their results, suggested that GAPDH may be rate limiting for glycolytic flux in the erythrocyte under certain conditions; for example, when there are elevated concentrations of the triose phosphates and FDP.

GAPDH binding to the erythrocyte membrane has been studied by measuring the binding of the enzyme to isolated membranes and membrane vesicles. The concentrations of free and bound enzyme were usually measured in these studies by separating the two forms by centrifugation. A single high affinity binding site has been identified and shown to be located on the cytoplasmic pole of the band 3 protein

(Yu & Steck, 1975). Aldolase (Strapazon & Steck, 1977), phosphofructokinase (Higashi et al, 1979) and haemoglobin (Salhany et al, 1980) also bind to this site although they have a lower affinity. Competition studies have revealed a complex set of interactions between these proteins at the band 3 site. Binding of both GAPDH and aldolase cause release of phosphofructokinase. Haemoglobin competes with GAPDH for binding but not with aldolase or phosphofructokinase (Higashi et al, 1979 and references cited therein). The binding of aldolase and GAPDH is mutually competitive but GAPDH is bound more tightly and will elute aldolase from the membrane (Solti & Friedrich, 1976). There are more than enough band 3 sites for all three enzymes to be bound, for example it has been estimated that GAPDH, which is the most tightly bound, could maximally occupy only 7-24% of the available sites (Higashi et al, 1979).

The enzymes can be selectively eluted from the membrane by incubation in the presence of their substrates, for example millimolar concentrations of FDP and NADH will selectively elute aldolase (Strapazon & Steck, 1977) and GAPDH (Kant & Steck, 1973) respectively. Binding of these enzymes results in inhibition of their activities (Strapazon & Steck, 1977; Solti & Friedrich, 1976). Binding of phosphofructokinase on the other hand is enhanced in the presence of FDP and this results in a change in its allosteric properties (Higashi et al, 1979; Karadsheh & Uyeda, 1977). Inhibition of GAPDH following binding is not a universal finding, for example Eby and Kirtley (1979) reported an increase in specific activity of the bound enzyme although no experimental results were shown. Wrigglesworth et al (1976) reported that binding resulted in an increase in the K_m for GAP and an "activation" of the enzyme. Schrier et al (1975b) however found no

effect of membrane binding on the kinetic properties of the enzyme. Observations such as these have lead to speculation that membrane binding of these enzymes may be important to the control of erythrocyte metabolism (Higashi et al, 1979). However a consistent observation with the binding of all these proteins to the band 3 site is their almost total elution at physiological ionic strengths. This has lead some workers to suggest that membrane binding is simply an artefact of the hypotonic conditions used to prepare the membranes (Maretzki et al, 1974). Recently catalase has also been shown to bind to the erythrocyte membrane. This binding is inhibited by aldolase, GAPDH and haemoglobin. The enzyme is eluted from the membrane at physiological ionic strengths and is inhibited in the bound state (Aviram & Shaklai, 1981). In order to better assess the physiological relevance of membrane binding a number of studies have been undertaken to try to determine the amount of GAPDH which is bound to the membrane in the intact erythrocyte.

Kliman and Steck (1980) lysed erythrocytes with the detergent saponin and rapidly filtered the resulting lysate. The GAPDH activity was then assayed in the filtrate and in the membrane fraction left on the filter. In this way the concentration of free and bound forms of the enzyme could be measured and the kinetics of enzyme release studied. By extrapolation of the time course of enzyme release to $t=0$ they estimated the fractions of free and bound enzyme in the intact cell. A value of 66_{-12}^{+12} % bound was calculated. This, it was argued, was not inconsistent with the binding constant observed with the isolated enzyme and membranes at physiological ionic strength if the high concentration of binding sites in the cell is taken into account. Changing the metabolite conditions in these cells was found not to

affect the estimated fraction of enzyme bound. Keokitichai and Wrigglesworth (1980) attempted to measure the fraction of GAPDH bound to the membrane in the intact cell by treating the cells with very low concentrations of glutaraldehyde. This, it was hoped, would result in covalent cross-linking of the bound enzyme to the band 3 site in situ. After washing and subsequent lysis approximately 50% of the GAPDH activity was found associated with the membrane and this could not be eluted by salt treatment. Under conditions designed to increase the intracellular NADH concentration a smaller fraction of the enzyme was found associated with the membrane. This experiment has been criticised on the grounds that cross-linking of the enzyme to the membrane could occur in the hypotonic hemolysate since coupling by glutaraldehyde may take place in two discrete steps (Solti et al, 1981). Wrigglesworth et al (1976) reported that staining for the enzyme in unfixed sections of human erythrocytes resulted in heavy deposition of stain around the perimeter of the cell. In a similar type of study Solti et al (1981) treated erythrocytes with tritiated iodoacetate under conditions in which approximately 50% of the GAPDH became labelled. After fixation, the cells were subjected to electron microscopic autoradiography. The results of this study, it was suggested, supported the view that GAPDH is located near the membrane.

In the studies of the in situ activity of GAPDH described in this chapter the role of the enzyme as a possible regulatory enzyme in erythrocyte glycolysis and the likelihood of a membrane bound location in the cell are assessed.

5.2 Experimental

Titration of GAPDH activity in the erythrocyte

Packed cells in Krebs-Ringer buffer containing 10mM glucose were prepared as described in chapter 2. Titrations were performed by adding iodoacetate (20-100 μ M) to three ml aliquots of these cells and incubating them at 37°C for times ranging up to 15 min. Incubations were terminated by diluting the cells to 10 ml with ice cold Krebs-Ringer buffer containing 1mM 2-mercaptoethanol. This washing procedure was repeated 3-4 times. The cells were then stored in Krebs-Ringer buffer (plus 10mM glucose) for 3 to 4 days at 4°C before use in n.m.r. experiments. Assays of the cells for GAPDH activity at the completion of each n.m.r. experiment showed that there had been no further loss of activity during cold storage. The variable conditions required to obtain the same level of inhibition are probably due to accumulation of triose phosphates in the cells (which were stored on ice) during the course of the titration experiments. An increase in the concentrations of the triose phosphates will protect the enzyme from iodoacetate inactivation by the formation of the acyl-enzyme.

Titration of GAPDH activity in vitro

Complete in vitro exchange systems (complete except for lactate) containing 15 units/ml of GAPDH were incubated for 1hr at 37°C with iodoacetate concentrations in the range 1-10 μ M. Control incubations lasting 3hrs showed that there was no further loss of activity after 1hr. By this method in vitro systems were prepared containing GAPDH activities in the range 2-15 units/ml. Equilibrium velocity determinations with these systems were performed as described in previous chapters.

5.3 The Method

In an in vitro system the equilibrium velocity of an enzyme is determined by changing its concentration and measuring the dependence of V_{C2X} on the concentration of the enzyme. A similar experiment can be performed in the intact erythrocyte if the active concentration of the enzyme is changed by specific irreversible inhibition. In the case of GAPDH the concentration of the active enzyme in the human erythrocyte can be varied by incubation of the cells for various periods of time with low concentrations (20-100 μ M) of iodoacetate. Preparation of the erythrocytes and titration of their GAPDH activity is described in the Experimental section. Cell populations were prepared containing a range of GAPDH activities and which had elevated levels of the triose phosphates and FDP. Assays of the other enzymes involved in the exchange showed that iodoacetate treatment only inhibited GAPDH. This is consistent with the results of previous studies of this metabolic inhibitor (Webb, 1966). Lactate transport across the cell membrane has been shown not to be inhibited by iodoacetate (Deuticke et al, 1978).

5.4 Determinations of the equilibrium velocity of glycerinaldehydophosphate dehydrogenase in situ

Tables 1 to 3 show the results of three separate equilibrium velocity determinations performed on different cell preparations.

The results in parts A of the tables show the results of triose phosphate and FDP assays on cell populations possessing different levels of GAPDH activity. They show that during incubation at 37^oC over a period similar to that required for isotope exchange measurements the concentrations of DHAP, and therefore of GAP, remain relatively constant, (triosephosphate isomerase is thought to catalyse a reaction at equilibrium in the human erythrocyte (Veech et al, 1979)). Pyruvate

Table 1

Part A

Triose phosphate and FDP concentrations in erythrocyte preparations possessing different levels of GAPDH activity.

GAPDH Activity (units/ml solvent water)	Total triose phosphate concentrations at t=0 (μ moles/ml cell water)	Total triose phosphate concentrations following incubation for 40 min at 37°C (μ moles/ml cell water)	FDP concentration at t=0 (μ moles/ml cell water)	FDP concentration following incubation for 40 min at 37°C (μ moles/ml cell water)
1.4	0.8	1.1	3.1	1.7
4	0.7	0.9	3.1	1.2
5	0.7	0.8	2.6	1.0
9	0.8	0.9	2.9	1.7
33	0.8	0.9	3.6	1.7

Part B

Estimated overall equilibrium velocity, V_{C2X} , in the cell preparations described in part A of the table.

V_{C2X} was calculated by measuring the exchange in 12mM L-(2-²H)lactate added to the erythrocyte preparations.

GAPDH activity (units/ml solvent water)	Observed t_{null} (min)	Estimated total triose phosphate concentration at t_{null} ($\mu\text{mols/ml}$ cell water)	Endogenous solvent Labelled lactate (L_e) present at $t=0$ ($\mu\text{mols/ml}$ solvent water)	Rate of lactate production (k_L) ($\mu\text{mols/min/ml}$ solvent water)	Estimated V_{C2X} corrected for the effect of L_e ($\mu\text{mols/min/ml}$ solvent water)	Estimated V_{C2X} corrected for the effect of L_e and k_L ($\mu\text{mols/min/ml}$ solvent water)
1.4	95		1.3	0.065	0.083	0.035
4	39	0.9	1.5	-	0.199	0.153
5	37	0.8	0.8	0.063	0.218	0.174
9	27	0.8	0.9	0.060	0.297	0.255
33	21	0.9	0.8	-	0.383	0.340

The estimated equilibrium velocity for GAPDH, using the values for V_{C2X} corrected for the effect of L_e (see text), is
 $0.160 \pm 0.018 \mu\text{mols/min/unit}$

Exchange time courses were initiated by the addition of 12mM L-(2-²H)lactate to an erythrocyte suspension prewarmed to 37°C.

The concentration of endogenous solvent labelled lactate present at $t=0$ was estimated by accumulating a spectrum prior to

addition of the labelled lactate. The exchange was monitored for 60 min by accumulating successive 112 scan, 2 min spectra.

The rate of lactate production was measured by monitoring the growth in the lactate peak height in cells to which no labelled

lactate had been added. The peak intensity was calibrated in terms of lactate concentration by adding a known concentration of

L-(U-¹H)lactate. Growth in the lactate peak height, which was observed to be linear, was monitored before and after addition

of the standard lactate solution. Triose phosphate and FDP assays were performed on parallel incubations as described in

the Experimental section in chapter 2. Apart from the triose phosphate and FDP concentrations, the concentrations of lactate and

the rates and activities shown are quoted per ml of solvent water. This was calculated by assuming that 72% of the erythrocyte

volume is solvent water (Ellam & Stein, 1974). The haematocrit of these cell preparations was 70%.

Table 2

Part A

Triose phosphate and FDP concentrations in erythrocyte preparations possessing different levels of GAPDH activity.

GAPDH Activity (units/ml solvent water)	Total triose phosphate concentration at t=0 (μ moles/ml cell water)	Total triose phosphate concentration following incubation for 40 min at 37°C (μ moles/ml cell water)	FDP concentration at t=0 (μ moles/ml cell water)	FDP concentration following incubation for 40 min at 37°C (μ moles/ml cell water)
6	0.93	1.03 (1.93)	3.76	1.74 (1.29)
11	0.82	0.82 (1.61)	3.29	1.29 (0.90)
20	0.90	0.90 (1.29)	2.70	0.77 (0.58)
64	0.77	0.52 (0.82)	1.93	0.39 (0.23)

GAPDH Activity (units/ml solvent water)	Rate of lactate production (μ moles/min/ml solvent water)	Rate of FDP breakdown (lactate equivalents) (μ moles/min/ml solvent water)
6	0.066	0.064
11	0.063	0.064
20	0.058	0.063
64	0.058	0.050

Part B

Estimated overall equilibrium velocity, V_{C2X} , in the cell preparations described in part A of the table. V_{C2X} was calculated by measuring the exchange in 6 mM L-(2-²H)lactate added to the erythrocyte preparations.

GAPDH activity (units/ml solvent water)	Observed t_{null} (min)	Estimated total triose phosphate concentration at t_{null} (μ moles/ml cell water)	Endogenous solvent labelled lactate (L_e) present at $t=0$ (μ moles/ml solvent water)	Rate of lactate production (k_L) (μ moles/min/ml solvent water)	Estimated V_{C2X} corrected for the effect of L_e (μ moles/min/ml solvent water)	Estimated V_{C2X} corrected for the effect of L_e and k_L (μ moles/min/ml solvent water)
6	13	0.9	1.5	0.066	0.273	0.222
11	11	0.8	1.0	0.063	0.342	0.295
20	9.5	0.9	1.2	0.058	0.390	0.347
64	7.5	0.6	1.4	0.058	0.478	0.434

The estimated equilibrium velocity for GAPDH, using the values for V_{C2X} corrected for the effect of L_e (see text), is 0.204 ± 0.020 μ moles/min/unit

Exchange velocities, rates of lactate production and triose phosphate and FDP concentrations were measured as described in the legend to table 1. The haematocrit of these cell preparations was 71%.

The values in parentheses in part A of the table represent the calculated equilibrium concentrations of these metabolites assuming an equilibrium constant for the aldolase reaction at 37 °C of 1.2×10^{-4} (Herbert *et al*, 1940) and an equilibrium constant for the triosephosphate isomerase reaction of 22 (Veech *et al*, 1969).

Table 3

Part A

Triose phosphate and FDP concentrations in erythrocyte preparations possessing different levels of GAPDH activity.

GAPDH Activity (units/ml solvent water)	Total triose phosphate concentration at t=0 (μ moles/ml cell water)	FDP concentration at at t=0 (μ moles/ml cell water)	Time of Incubation at 37°C (min)	Total triose phosphate concentration following Incubation for the specified time at 37°C (μ moles/ml cell water)	FDP concentration following incubation for the specified time at 37°C (μ moles/ml cell water)
5	0.42	1.49	72	0.15	0.07
6	0.73	2.28	50	0.47	0.68
13	0.68	1.97	60	0.63	0.29
14	0.63	1.86	40	0.48	0.32
56	0.42	1.39	60	0.06	0.03

The effect of adding 1mM pyruvate to these cell preparations.

13	0.68	1.97	60	0.19	0.04
14	0.63	1.86	60	0.11	0.04
56	0.42	1.39	40	0.06	0.08

Part B

Estimated overall equilibrium velocity, V_{C2X} , in the cell preparations described in part A of the table. V_{C2X} was calculated by measuring the exchange in 12 mM L-(2-²H)lactate added to the erythrocyte preparations.

GAPDH activity (units/ml solvent water)	Observed t_{null} (min)	Estimated total triose phosphate concentration at t_{null} (μ moles/ml cell water)	Endogenous solvent labelled lactate (L_e) present at $t=0$ (μ moles/ml solvent water)	Rate of lactate production (k_L) (μ moles/min/ml solvent water)	Estimated V_{C2X} corrected for the effect of L_e (μ moles/min/ml solvent water)	Estimated V_{C2X} corrected for the effect of L_e and k_L (μ moles/min/ml solvent water)
5	78	0.2	1.8	0.073	0.098	0.046
6	41	0.4	1.2	-	0.214	0.163
13	27	0.5	1.3	-	0.315	0.265
14	25	0.5	1.1	-	0.360	0.310
56	19	0.5	1.4	0.068	0.459	0.409

The effect of adding 1mM pyruvate.

6	94	0.0	1.6	-	0.082	0.030
13	58	0.0	1.3	-	0.135	0.084
14	49	0.0	1.2	-	0.161	0.111
56	32	0.0	1.5	-	0.243	0.192

The estimated equilibrium velocity for GAPDH, using the values for V_{C2X} corrected for the effect of L_e (see text), is 0.110 ± 0.017 μ moles/min/unit. In the presence of 1mM pyruvate the observed equilibrium velocity is 0.032 ± 0.007 μ moles/min/unit.

Exchange velocities, rates of lactate production and triose phosphate and FDP concentrations were measured as described in the legend to table 1. The haematocrit of these cell preparations was 74%.

addition to these cells results in acceleration of the breakdown of FDP and the triose phosphates (table 3). This has been observed previously and is the result of an increased flux into the 2,3-DPG pathway due to an elevation of the level of 1,3-DPG (Rose & Warms, 1966 & 1970).

The results in parts B of tables 1 to 3 show the results of equilibrium velocity determinations performed on cell populations possessing the specified GAPDH activity and containing the concentrations of DHAP and FDP shown in parts A. A notable feature of these results is that despite a considerable decrease in the GAPDH activity following iodoacetate titration there is no significant effect on the glycolytic flux as determined by the rate of lactate production. This indicates that under these conditions GAPDH cannot be catalysing a rate limiting reaction for erythrocyte glycolysis.

5.4.1 Effect of lactate production on estimates of V_{C2X}

Parts B of tables 1 to 3 show; 1) the rate of lactate production; 2) the time, following lactate addition, at which peak inversion occurred and 3) the estimated DHAP concentration at this point (t_{null}). Also shown is the endogenous, solvent labelled lactate, present at $t=0$ and estimates of V_{C2X} obtained using the corrections defined by equations 4 and 5 in chapter 2. Equation 4 corrects only for endogenous lactate present at $t=0$. Equation 5 corrects both for endogenous lactate present at $t=0$ and for lactate production occurring between $t=0$ and t_{null} . This latter equation over-corrects for the effect of lactate production since it assumes that this will be totally solvent labelled. The state of labelling will, in fact, depend on the fractional labelling of the other glycolytic intermediates involved in the exchange.

In order to investigate the effect of lactate production on estimates of the overall exchange velocity, equations 4 and 5 were used

Table 4

Model simulations of the effect of lactate production on the observed t_{null} in an exchange time course.

V_{GAPDH} mM/min	Observed t_{null} (min) without lactate production	Observed t_{null} (min) with lactate production	t_{null} corrected for the effects of endogenous solvent labelled lactate present at $t=0$ (L_e)	t_{null} corrected for the effects of L_e and lactate production occurring at rate k_L
10	21	20	21	23
5	22	21	22	25
2	27	25	26	30
1	35	32	33	40
0.75	40	37	39	48
0.50	51	45	47	62
0.25	82	66	69	106

The corrections for L_e and L_e plus k_L were described in chapter 2, (see text). The corrections were applied to the observed t_{null} in the presence of lactate production.

The conditions used in the model were as follows: solvent, 110M; DHAP, 1mM; GAP, 45 μ M; NAD^+ , 10 μ M; NADH, 10 μ M; FDP, 3mM and lactate 13mM. The initial concentrations of the deuterated intermediates were all zero apart from the lactate, of which 12mM was deuterated. The equilibrium velocities were given the following values: V_{ALD} , 1.0mM/min; $V_{ALD(RECON)}$, 0.0mM/min; V_{TM} , 15.0mM/min; V_{LDH} , 1.5mM/min. The rate of lactate production was set at 0.06mM/min and V_{GAPDH} was varied as shown in the table.

to calculate V_{C2X} from simulated exchange time courses generated using the computer program shown in the previous chapter. The results of these simulations are shown in table 4. The conditions used in the model (shown in the legend to table 4) were designed to correspond as closely as possible to the substrate conditions found in these erythrocytes. The concentrations assigned to NAD^+ and $NADH$ are discussed in the next chapter. In fact the levels assigned to these intermediates do not radically affect the predictions of the model. The values for the equilibrium velocities were assigned on the basis of the in vitro results shown in the previous chapter. The equilibrium velocity for the recondensation reaction catalysed by aldolase ($V_{ALD(RECON)}$) was varied between 0 and 1.0mM/min with no effect on the predicted t_{null} . The endogenous solvent labelled lactate was given a value of 1mM and the rate of lactate production a value of 0.06mM/min. These are similar to the values found in the experiments shown in tables 1 to 3. The GAPDH equilibrium velocity in the model was varied between 0.25 and 10mM/min. The results in table 4 show the effect of changing V_{GAPDH} on the observed t_{null} with and without endogenous lactate production. Lactate production significantly decreases the observed t_{null} , particularly at low GAPDH equilibrium velocities. Also shown are values for t_{null} corrected for the effect of endogenous solvent labelled lactate present at $t=0$ (L_e) and for endogenous lactate present at $t=0$ and lactate production (L_e and k_L). Ideally a correction for lactate production should transform the observed t_{null} to the value that would be observed in its absence. In fact the correction for L_e and k_L over-corrects for lactate production since it is an approximation which becomes better when the rate of chemical flux far exceeds that of isotopic flux. On the other hand the correction for L_e alone, which makes no assumptions about the mechanism of the exchange, gives a much

better estimate of the t_{null} .

These results demonstrate that even when the ratio of isotopic flux to chemical flux is lowered by lowering the GAPDH equilibrium velocity the effects of chemical flux on isotope flux measurements are minimal. It is only when the rate of isotope flux becomes very low compared to the rate of chemical flux, as demonstrated in the last line of table 4, that this has a significant effect. The correction for L_e was therefore the correction which was applied in the analysis of the data shown in tables 1 to 3.

5.4.2 Maintenance of a near equilibrium steady state during isotope exchange measurements

The results in tables 1 to 3 show that in the absence of added pyruvate the level of DHAP, and thus the level of GAP, is relatively constant between $t=0$ and the observed t_{null} . Thus in this time interval the equilibrium velocities of GAPDH and of aldolase and triose phosphate isomerase are expected to remain constant. It has already been shown that the exchanges catalysed by all three enzymes are relatively insensitive to the concentrations of the triose phosphates and FDP in this concentration range.

When performing these equilibrium velocity determinations it is preferable to use a relatively high concentration of labelled lactate since this gives better time resolution in the observed t_{null} s. Too large a concentration, however, results in significant DHAP breakdown before a null point is obtained. A balance must be struck, therefore, in choosing the lactate concentration. In these experiments 12mM was thought to represent the optimal lactate concentration and therefore the results shown in table 1 are taken to represent the best estimate of the in situ equilibrium velocity of GAPDH. This yields a value for the

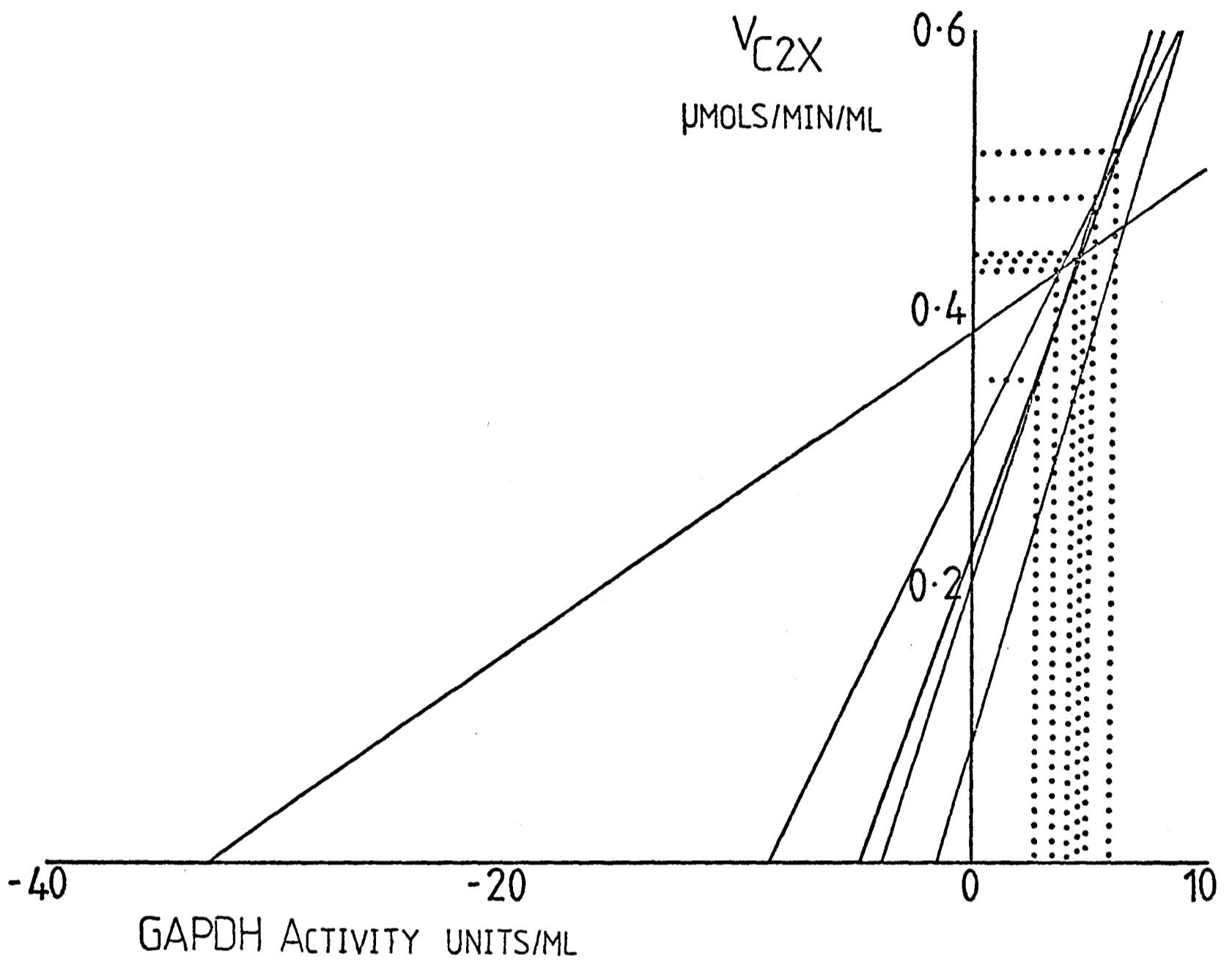


Figure 1

Direct plot of V_{C2X} versus GAPDH activity in the intact erythrocyte.

The exchange data was taken from table 1. The point obtained at the lowest GAPDH activity is an outlier.

specific equilibrium velocity of 0.160 ± 0.018 $\mu\text{mols}/\text{min}/\text{unit}$, where the average measured DHAP plus GAP concentration in these cells during equilibrium velocity determinations was $0.9 \mu\text{mols}/\text{ml}$ cell water. Figure 1 shows a direct plot of the exchange data. The point obtained at the lowest GAPDH activity is clearly an outlier. This is to be expected since the GAP concentration declined significantly in the time required to obtain a null point. Furthermore the correction for L_e is now a much poorer correction since V_{C2X} and the rate of lactate production are of comparable magnitude. The results shown in table 2 show a higher specific equilibrium velocity for GAPDH but this is probably a less reliable estimate in view of the lower labelled lactate concentration employed. The results in table 3 show a lower equilibrium velocity which may be the result of the lower steady state DHAP plus GAP concentrations observed in these cells i.e. $0.5 \mu\text{mols}/\text{ml}$ cell water. Addition of pyruvate results in a marked decrease in the observed GAPDH equilibrium velocity. However this result is complicated by the fact that there is severe depletion of the triose phosphates during measurements of isotope exchange. A decrease in the equilibrium velocity of the enzyme is expected due to both a lowering of the intracellular NADH concentration and the concentrations of the triose phosphates (see below).

It has been stressed that the equilibrium velocities of the enzymes should remain constant during an equilibrium velocity determination. Changes in the concentrations of substrates involved in the exchange, other than the triose phosphates, should also be considered.

The lactate concentration shows a small increase during exchange measurements. This however should not seriously affect the equilibrium velocity of lactate dehydrogenase since it has a small elasticity coefficient for concentrations of lactate in the range shown (chapters 2

Table 5

Lactate and pyruvate assays on cells used for C-2 exchange experiments.

Time (min)	Lactate concentration ($\mu\text{mol/ml}$ solvent water)	Pyruvate concentration (nmol/ml solvent water)	Lactate/pyruvate ratio	NAD^+/NADH ratio
10	10.5	9	1170	3.1
20	11.1	12	930	3.9
30	10.9	12	910	3.9
40	13.6	14	970	3.7

Lactate (10mM) was added to packed cells (80% haematocrit) in Krebs-Ringer buffer, pH 7.4 at 37°C. The cells had been previously incubated at 4°C in order to raise the concentrations of the triose phosphates. At the specified times, following lactate addition, the metabolites were assayed in cell free supernatants. These were prepared by diluting a sample of the cells with Krebs-Ringer buffer at room temperature and then centrifuging for 2min at 15,000g on an Eppendorf 5412 centrifuge. The assays were performed as described in the Experimental sections of chapters 2 and 6. The concentrations quoted are the average of two determinations and were corrected for the excluded volume in the erythrocyte suspension by assuming that 72% of the erythrocyte volume is solvent water (Eilam & Stein, 1974). The NAD^+/NADH ratio was calculated by assuming that lactate dehydrogenase catalyses a reaction at equilibrium in the human erythrocyte with an equilibrium constant of 1.11×10^{11} (Williamson *et al*, 1967).

and 3 and predictions of the kinetic model shown in appendix 1 of chapter 2 for lactate dehydrogenase). An increase in the pyruvate concentration in the concentration range shown in table 5 could lead to a small increase in the equilibrium velocity of this enzyme (predictions of the kinetic model shown in appendix 1 of chapter 2; see also the next chapter). Since the sensitivity coefficient of this enzyme is expected to be relatively high in the cell it was important to establish that fluctuations in its equilibrium velocity did not seriously affect GAPDH equilibrium velocity determinations. This was achieved by varying V_{LDH} as a function of time in the computer model of the exchange system. Increasing or decreasing its value at a rate of 0.01mM/min/min (its value at $t=0$ was 1.5mM/min) had no significant effect on GAPDH equilibrium velocities calculated from the predicted exchange time courses (see table 7). This rate of change in V_{LDH} was calculated from the changes in pyruvate concentration observed in table 5 and the predicted dependence of the enzyme's equilibrium velocity on pyruvate concentration.

Changes in the concentrations of NAD^+ and $NADH$ could affect the equilibrium velocities of both GAPDH and lactate dehydrogenase. The results of lactate and pyruvate assays on cells with elevated levels of the triose phosphates are shown in table 5. Also shown is the $NAD^+/NADH$ ratio calculated by assuming that lactate dehydrogenase catalyses a reaction at equilibrium in the human erythrocyte and which has an equilibrium constant of 1.11×10^{-11} (Williamson et al, 1967). Since the turnover of these coenzymes is slow in the erythrocyte (Tsuboi et al, 1966) their free concentrations in the cell can be calculated from this ratio and from estimates of the total free concentrations of these nucleotides (see below and next chapter). High lactate/pyruvate ratios in cells with elevated levels of the triose phosphates have been

Table 6

Net pyruvate reduction in a lysate.

Time (min)	Pyruvate concentration (mM)
2	6.0
10	4.7
20	4.4
30	4.0

The lysate was prepared by freeze thawing packed cells twice in liquid nitrogen. Nicotinamide, 20mM and NAD^+ , 1mM were then added and the lysate warmed to 37°C . At $t=0$ 8mM pyruvate and 5mM FDP were added. The pyruvate assays were performed as described in the Experimental section of chapter 6.

observed previously (Minikami & Yoshikawa, 1966; Rose & Warms, 1970; Eckel et al, 1966). The increased lactate/pyruvate ratio parallels the rise in the triose phosphates as expected if these are in equilibrium. Changes in this ratio will be suppressed therefore by the triose phosphate pool. Since this remains relatively constant during isotope exchange measurements the lactate/pyruvate ratio and consequently the NAD^+/NADH ratio is not expected to fluctuate significantly. That this is indeed the case is shown by the results in table 5. This "buffering" effect of the triose phosphate pool on the lactate/pyruvate ratio is demonstrated by the addition of pyruvate to cells with high triose phosphate levels. This results in rapid loss of the triose phosphates (as shown in table 3) an increase in the 2,3-DPG concentration and net pyruvate reduction to lactate (Rose & Warms, 1966 & 1970; Eckel et al, 1966). Flux into the 2,3-DPG pool allows net pyruvate reduction to occur. Net pyruvate reduction in a lysate, to which FDP has been added, is demonstrated by the results of pyruvate assays shown in table 6. This buffering of the NAD^+/NADH ratio by the triose phosphate pool explains the effects on C-2 exchange of adding pyruvate to an erythrocyte suspension (figure 17, chapter 2). The addition of pyruvate concentrations which would severely inhibit the exchange in vitro, by increasing the NAD^+/NADH ratio (see below), produced no significant decrease in the exchange velocity in situ. This is presumably because the lactate/pyruvate ratio is restored by pyruvate reduction and triose phosphate oxidation. At relatively low added pyruvate concentrations the loss of the triose phosphates will be insufficient to affect the equilibrium velocities of the enzymes for which they are substrates.

5.4.3 Is the kinetic model an adequate description

of the exchange system in situ?

Endogenous lactate production was simulated in the computer model of the exchange system by assuming that FDP declines and lactate increases at equivalent rates. The solvent label introduced into the C-2 exchange system by glycolytic or chemical flux is determined by the fractional labelling of FDP at the C-4 position and by the fractional labelling of the solvent. The label at the C-4 position of FDP, following FDP degradation, is found in GAP. The label found at the pro-S C-3 position of DHAP following FDP degradation will be solely determined by the fractional labelling of the solvent. In the absence of the recondensation reaction the FDP will be totally solvent labelled and breakdown of one FDP molecule will lead to the production of one solvent labelled GAP molecule and one solvent labelled DHAP molecule. In the presence of the recondensation reaction, where the FDP can become labelled, FDP breakdown will not always result in solvent labelling of GAP. However the effect of this is negligible (see table 7). Thus the assumptions made in the model which were based on experimental observation, i.e. an equivalence in the rate of breakdown of FDP and lactate production (see below), are not critical in a simulation of the effect of glycolytic flux.

In the previous chapter it was shown that undefined isotope "leaks" which affect the labelling of the triose phosphates will have a negligible effect on V_{GAPDH} determinations. Isotope "leaks" which affect the labelling of NAD^+ and NADH , however, could seriously affect the calculated equilibrium velocity for the enzyme. The presence of such leaks can be ruled out on the basis of the following; a) there is no glycerol-3-phosphate dehydrogenase in the human erythrocyte (Rose & Warms, 1970; Friedrich et al, 1977) which could catalyse the exchange of

Table 7

Model simulations of the effect of the recondensation reaction catalysed by aldolase and the effect of time dependent changes in V_{LDH} on V_{GAPDH} determinations in situ

Values calculated for V_{GAPDH} ($\mu\text{mols}/\text{min}/\text{unit enzyme}$) from simulated exchange time courses under the specified conditions.

$V_{ALD(RECON)}$ = 0.0 mM/min	$V_{ALD(RECON)}$ = 1.0 mM/min	$V_{ALD(RECON)} = 1.0 \text{ mM/min}$ and V_{LDH} decreases at a rate of 0.01 mM/min	$V_{ALD(RECON)} = 1.0 \text{ mM/min}$ and V_{LDH} increases at a rate of 0.01 mM/min
0.233	0.234	0.223	0.230

The true value for V_{GAPDH} was set at $0.2 \mu\text{mols}/\text{min}/\text{unit enzyme}$ and the GAPDH activity in the model was varied between 50 and 1.25 units/ml. The conditions used in the model were similar to those described in the legend to table 4. The rate of lactate production was $0.06 \text{ mM}/\text{min}$ and V_{LDH} at $t=0$ was $1.5 \text{ mM}/\text{min}$. The observed t_{nulls} in the simulations were used to calculate V_{C2X} using a correction for L_e only (see text and table 4). The specific equilibrium velocity for GAPDH was estimated using the direct plot analysis.

label between DHAP and lactate; b) a decline in the triose phosphate and FDP concentrations results in loss of the exchange and c) complete iodoacetate inactivation of GAPDH results in total inhibition of the exchange. These observations support the conclusions of Rose and Warms (1969) regarding the pathway for the exchange.

The values for V_{GAPDH} calculated from the predicted exchange time courses of the model under simulated in situ conditions, with and without the recondensation reaction, and with V_{LDH} increasing and decreasing as a function of time, are shown in table 7. It was assumed that V_{GAPDH} has a value of 0.2 $\mu\text{mol}/\text{min}/\text{unit}$. Although the recondensation reaction and changes in V_{LDH} have a negligible effect on the values for V_{GAPDH} calculated from the model these values are approximately 16% higher than the true value. This represents the effect of lactate production. GAPDH equilibrium velocity determinations in situ are expected, therefore, to be an overestimate of the true value.

5.5 Apparent disequilibrium in the reaction catalysed by aldolase

The results shown in parts B of tables 1 to 3 show that the DHAP concentration remains almost constant as a function of time while the FDP concentration declines. Furthermore the ratio of the FDP concentration to the concentrations of DHAP plus GAP is considerably higher than that expected if aldolase and triose phosphate isomerase are catalysing reactions at equilibrium at 37°C (Veech et al, 1969; Herbert et al, 1940). There are two possible reasons for this apparent disequilibrium; a) under these conditions, with high levels of the triose phosphates and FDP, the aldolase reaction is rate limiting for glycolytic flux and there is true disequilibrium in the reaction and b) there is binding of FDP resulting in an apparent disequilibrium.

The evidence for these two postulates is summarised below.

Saito and Minikami (1967) observed disequilibrium in the aldolase reaction in human erythrocytes with elevated triose phosphate levels and attributed this to rate limitation of glycolytic flux by this enzyme. They showed that if GAPDH was completely inhibited by iodoacetate (2.5mM) then there was a slow relaxation of the aldolase substrates towards equilibrium concentrations over a period of 3-4 hrs. The results shown here which show a correspondence between the rate of lactate production and FDP degradation (table 2) support the conclusion that the aldolase reaction is rate limiting for glycolytic flux. Correspondence between the rate of lactate production and total triose phosphate degradation has been observed previously in the human erythrocyte by Eckel et al, (1966). However these observations were made in the absence of added glucose. The results obtained here in the presence of glucose suggest that either flux from glucose into the triose phosphate pool is severely inhibited or that there is considerable flux into the 2,3-DPG pool under these conditions. Disequilibrium in the aldolase reaction has been observed in other tissues. These include guinea pig cerebral cortex (Rolleston & Newsholme, 1967), mouse brain (Lowry & Passoneau, 1964), rat liver and rat muscle (Veech et al, 1969).

Flux limitation in the aldolase reaction in human erythrocytes is unlikely in view of the results of Rose and Warms (1970) who measured an isotope exchange velocity for a ^{14}C label of approximately 0.46 $\mu\text{mol}/\text{min}/\text{ml}$ cells between FDP and 2,3-DPG in cells with elevated FDP levels. This is in considerable excess of the rate of glycolytic flux. Binding of FDP would therefore seem to be a more likely explanation for the observed disequilibrium. This would explain not only the apparent disequilibrium but also the constancy of the DHAP

concentrations observed in these studies, the triose phosphate pool being effectively "buffered" by the bound FDP pool. That binding is responsible for the apparent disequilibrium is suggested by triose phosphate and FDP assays on a dilute lysate to which FDP had been added. The results were shown in the previous chapter. In this case the concentrations of the aldolase substrates were much closer to the expected equilibrium values. In rabbit muscle and liver it has been proposed (Veech et al, 1969) that the observed disequilibrium in the aldolase reaction is the result of FDP binding to the enzyme. This is only possible in these tissues because the aldolase concentration is relatively high and comparable to the observed substrate concentrations. This is not a feasible explanation in the erythrocyte where the observed substrate concentrations are in the millimolar range and the enzyme concentration in the micromolar range (Ottaway & Mowbray, 1977). Furthermore even in muscle and liver binding of FDP to aldolase alone would be insufficient to explain the observed disequilibrium.

FDP can form a Schiff-base with the NH_2 -terminal valine of the β chain of haemoglobin (Bunn et al, 1978). This will decompose following acid treatment to give free FDP. If it is assumed that the bound FDP concentration is approximately 1mM (see table 2) and that the initial rate of breakdown of this complex is approximately half of the rate of lactate production then the first order rate constant for the decomposition of this complex will be approximately 0.03 min^{-1} . If the on rate is diffusion controlled, i.e. approximately $10^8 \text{ M}^{-1} \text{ s}^{-1}$ then the dissociation constant for FDP binding will be approximately 2×10^{-8} . Such tight binding could be the result of Schiff-base formation. In addition to FDP however, DHAP and GAP can also bind at this site. If FDP binding is to explain the apparent disequilibrium then it must be more tightly bound as a Schiff-base than either DHAP or GAP.

Alternatively there may be a prebinding step prior to Schiff-base formation in which FDP has a higher affinity than either DHAP or GAP. Other sugars will also bind at this site, for example glucose, however this reacts much more slowly. Glycosylation can also take place at a number of other sites in haemoglobin and in other proteins (see Schapiro et al, 1980 and references cited therein). This type of binding seems therefore to be a good candidate for the apparent disequilibrium observed in the aldolase reaction in other tissues. It also underlines the difficulty of identifying possible rate limiting enzymes in a metabolic sequence from mass action ratio data alone.

5.6 Conclusions

A method has been demonstrated for obtaining the in situ equilibrium velocity of GAPDH in the human erythrocyte. The experimental results presented in tables 1-3 show that the GAPDH activity can be selectively titrated with iodoacetate in the intact erythrocyte and that this results in a decrease in the velocity of isotope exchange. It does not, however, result in any inhibition of lactate production over the range of GAPDH activities obtained. Thus under these conditions GAPDH is not rate limiting for glycolytic flux. This is in agreement with the conclusions of Rose and Warms (1970).

In the next half of this chapter the results of GAPDH equilibrium velocity determinations in vitro are presented. The aim of this study was to simulate the expected intracellular environment of the enzyme in vitro and compare the equilibrium velocities obtained with those measured in situ.

5.7 Determinations of the equilibrium velocity of glyceraldehydephosphate dehydrogenase in vitro

The method by which these equilibrium velocities were obtained was described in the previous chapter. Table 8 shows the effect on the GAPDH equilibrium velocity of a) changing the added NAD^+ concentration; b) changing the ionic strength; c) changing the solvent from $^2\text{H}_2\text{O}$ to $^1\text{H}_2\text{O}$; d) adding pyruvate to the exchange system; e) adding NADH to the exchange system and f) prolonged incubation at 37°C before initiation of an exchange time course by the addition of lactate. The results of these investigations can be summarised as follows; a) changing the NAD^+ concentration over a wide range has a negligible effect on the observed equilibrium velocity in contrast to the marked effect that the concentration of this coenzyme has on the lactate dehydrogenase equilibrium velocity; b) increasing the ionic strength by adding 80mM KCl resulted in a small decrease in the equilibrium velocity. This effect of ionic strength is also evident if the results of tables 8 and 9 are compared; c) changing the solvent has no effect. This indicates that there are no kinetic isotope effects and also no non-specific solvent effects, although there is the possibility that a fortuitous combination of the two could result in no net observed effect; d) adding pyruvate results in a marked inhibition of the exchange. The most likely explanation of this is a loss of NADH. Adding NADH to the system (e) resulted in an equally marked increase in the equilibrium velocity; f) preincubation at 37°C (45 min) caused no appreciable change in the observed equilibrium velocity indicating that there had been no significant degradation of the substrates. Such degradation is possible, it is known for example that GAPDH catalyses the formation of NADH-X, a covalently modified coenzyme (Oppenheimer & Kaplan, 1974) which is a potent inhibitor of the

Table 8

GAPDH equilibrium velocity determinations in vitro.

d) The effect of adding pyruvate to the exchange system.

Added NAD ⁺ concentration (μM)	V_{GAPDH} ($\mu\text{moles/min/unit enzyme}$)	Added pyruvate concentration (μM)	V_{GAPDH} ($\mu\text{moles/min/unit enzyme}$)
16	0.056 ± 0.009	0	0.118 ± 0.003
40	0.056 ± 0.012	100	0.042 ± 0.001
80	0.055 ± 0.010		

e) The effect of adding NADH to the exchange system.

Added KCl concentration (mM)	V_{GAPDH} ($\mu\text{moles/min/unit enzyme}$)	Added NAD ⁺ concentration (μM)	Added NADH concentration (μM)	V_{GAPDH} ($\mu\text{moles/min/unit enzyme}$)
0	0.104 ± 0.020	20	-	0.104 ± 0.020
80	0.079 ± 0.012	10	10	0.176 ± 0.034

b) The effect of changing the ionic strength.

c) The effect of changing solvent from $^2\text{H}_2\text{O}$ to $^1\text{H}_2\text{O}$.

Solvent	V_{GAPDH} ($\mu\text{moles/min/unit enzyme}$)
$^2\text{H}_2\text{O}$	0.118 ± 0.003
$^1\text{H}_2\text{O}$	0.108 ± 0.026
$^1\text{H}_2\text{O}$	0.111 ± 0.021

f) The effect of preincubation of the exchange system before the initiation of an exchange time course by the addition of lactate.

Time of preincubation at 37°C (min)	V_{GAPDH} ($\mu\text{moles/min/unit enzyme}$)
0	0.118 ± 0.003
45	0.125 ± 0.005

Table 8

The in vitro exchange system contained 100mM Tris-HCl, pH 7.4, (pH 7.4* in $^2\text{H}_2\text{O}$) 0.5mM EDTA, 3 mM dithiothreitol. The systems employed differed with respect to the solvent, the ionic strength and the added concentrations of lactate, NAD(H) and FDP. The differences are detailed in the following: System a) $^2\text{H}_2\text{O}$; no added KCl; 12mM L-(U- ^1H)lactate; 300uM FDP. System b) $^1\text{H}_2\text{O}$; 6mM L-(2- ^2H)lactate; 20 μM NAD $^+$; 600 μM FDP; 0.5mM Pi and 0.25mM Mg $^{++}$. System c) no added KCl; 12mM L-(U- ^1H) or L-(2- ^2H)lactate; 20 μM NAD $^+$; 600 μM FDP; 0.5mM Pi and 0.25mM Mg $^{++}$. System d) $^2\text{H}_2\text{O}$; no added KCl; 12mM L-(U- ^1H)lactate; 600 μM FDP; 0.5mM Pi and 0.25mM Mg $^{++}$. System e) $^1\text{H}_2\text{O}$; no added KCl; 6mM L-(2- ^2H)lactate; 600 μM FDP; 0.5mM Pi and 0.25mM Mg $^{++}$. System f) the same conditions as in system d).

Equilibrium velocity determinations were performed as described in previous chapters. Where the ionic strength was changed (system b) the pH was adjusted to 7.4 following KCl addition.

Table 9

GAPDH equilibrium velocity determinations in vitro.

a) The effect of NAD(H) concentration.

Added NAD ⁺ concentration (μM)	Added pyruvate concentration (μM)	V_{GAPDH} ($\mu\text{mols/min/unit enzyme}$)
10	-	$0.067_{-}^{+}0.014$
20	-	$0.070_{-}^{+}0.008$
10	15	$0.031_{-}^{+}0.002$

b) The effect of changing the added FDP concentration and aldolase activity.

Added FDP concentration (mM)	Aldolase activity ($\mu\text{units/ml}$)	V_{GAPDH} ($\mu\text{mols/min/unit enzyme}$)
1	1.7	$0.074_{-}^{+}0.008$
2	1.7	$0.074_{-}^{+}0.001$
3	1.0	$0.066_{-}^{+}0.002$
1	1.7	$0.074_{-}^{+}0.008$
1	4.9	$0.084_{-}^{+}0.003$
3	1.0	$0.066_{-}^{+}0.002$
3	3.4	$0.052_{-}^{+}0.003$

Table 9

The in vitro exchange system contained 100mM Tris-HCl pH 7.4, 0.5mM EDTA, 3mM dithiothreitol, 0.5mM Pi and 0.25mM Mg⁺⁺ in ¹H₂O. System a) contained approximately 100 units/ml of triosephosphate isomerase, 30 units/ml of lactate dehydrogenase and 1 unit/ml of aldolase. The added FDP concentration was 700μM and the added lactate concentration 12mM. In system b) there were approximately 100 units/ml of triose phosphate isomerase and 100 units/ml lactate dehydrogenase. The added NAD⁺ concentration was 15μM and the added lactate concentration 12mM.

The system also contained 80 mM KCl.

The equilibrium velocity determinations and enzyme assays were performed as described in previous chapters.

Table 10

Iodoacetate titration of GAPDH activity in vitro

The effect of pH on the GAPDH equilibrium velocity.

pH of the exchange system	V_{GAPDH} ($\mu\text{mol/s/min/unit enzyme}$)
7.2	$0.095^{+0.022}$
7.4	$0.082^{+0.005}$

The exchange system contained 100mM Tris-HCl, pH 7.4, 0.5mM EDTA, 3mM dithiothreitol, approximately 100 units/ml of triosephosphate isomerase and lactate dehydrogenase and 1 unit/ml of aldolase. The solvent was $^1\text{H}_2\text{O}$. The added FDP, NAD^+ and lactate concentrations were 1mM, 15 μM and 12mM respectively. Details of the iodoacetate titrations are given in the Experimental section. In all other respects the equilibrium velocity determinations were performed as described previously.

The system also contained 80 mM KCl.

dehydrogenases.

Table 9 shows the results of equilibrium velocity determinations performed on an in vitro system which was designed to simulate the in situ environment. All of these determinations were performed in $^1\text{H}_2\text{O}$. Again it is shown that the equilibrium velocity of the enzyme is insensitive to the concentration of NAD^+ plus NADH although it is clearly dependent on the ratio of these two coenzymes. Lowering the NADH concentration by adding pyruvate results in a marked decrease in the equilibrium velocity. Changing the added FDP concentration between 1 and 3mM and changing the aldolase activity present has no significant effect on the observed equilibrium velocity. This supports the predictions of the model which suggested that the recondensation reaction catalysed by aldolase, if present, would have a negligible effect on GAPDH equilibrium velocity determinations. The results also show that the elasticity coefficient of the enzyme for GAP is small in this concentration range.

In table 10 are shown the results of equilibrium velocity determinations performed at pH 7.4 and pH 7.2. Unlike previous determinations, where the enzyme concentration was varied by addition, the active enzyme concentration was varied, in this case, by titrating with iodoacetate in a manner analogous to that performed with the intact cells. The results of these determinations show that in the pH range of interest the equilibrium velocity is not particularly sensitive to pH and that the results obtained are similar to those obtained by varying the added enzyme concentration. This observation rules out the possibility that iodoacetate modification at one site in the tetrameric GAPDH molecule affects the kinetic properties of the remaining

non-modified sites. All of the enzyme's active sites can be modified by iodoacetate; there is no half of the sites reactivity (Eby & Kirtley, 1979).

5.7.1 The effect of membrane binding

Erythrocyte membranes containing bound GAPDH were prepared by lysing the cells under hypotonic conditions as described in the Experimental section in chapter 3. Aldolase was selectively eluted from these membranes by treating them with FDP. Table 11 shows the results of GAPDH equilibrium velocity determinations performed on this membrane preparation in an in vitro exchange system which had a low ionic strength. Binding of GAPDH to the membranes was assessed by separating the free and bound forms by centrifugation. There was considerable binding of GAPDH under these conditions but negligible binding of rabbit muscle aldolase which was added to the system with 1mM FDP. Part A of the table shows that the overall exchange velocity observed in this system was increased tenfold by the addition of 80mM KCl. Concomittant with this increase was an increase in the fraction of unbound GAPDH. This suggested that the enzyme is inhibited in the bound state. This was confirmed by the results shown in part B which show the effect of varying the amount of membrane preparation in the exchange system. The table shows the concentrations (in units) of free and bound enzyme observed when the amount of added membrane preparation was changed. The fraction bound remains constant. Also shown are the values for V_{C2X} measured in the presence of different concentrations of free and bound enzyme. If it is assumed that the bound enzyme shows no activity and the measured V_{C2X} is plotted against the free enzyme concentration then the direct plot analysis yields a value for the specific equilibrium velocity of $0.057 \pm 0.009 \mu\text{mols}/\text{min}/\text{unit}$ of free enzyme. The data conform

Table 11

The effect of membrane binding on V_{GAPDH}

Part A

The effect of increasing the ionic strength on membrane binding and V_{C2X} in an in vitro exchange system containing an erythrocyte membrane preparation.

Added KCl concentration (mM)	GAPDH Activity (units/ml)		V_{C2X} ($\mu\text{mol s/min/ml}$)
	Free	Bound	
-	1.3	6.8	0.018
80	6.5	0.3	0.205
-	3.3	11.9	0.061
80	15.0	0.0	0.223

Part B

The effect on V_{C2X} of changing the amount of an erythrocyte membrane preparation added to the in vitro exchange system. The added NAD^+ concentration was 15 μM .

GAPDH Activity (units/ml)		Fraction bound	V_{C2X} ($\mu\text{mol s/min/ml}$)
Free	Bound		
1.3	3.8	0.75	0.029
2.2	8.9	0.80	0.049
3.5	12.1	0.78	0.067
4.3	15.5	0.78	0.070

Part C

The effect on V_{C2X} of changing the amount of an erythrocyte membrane preparation added to an in vitro exchange system. $10\mu\text{M NAD}^+$ and NADH were added to the exchange system.

GAPDH Activity (units/ml)		Fraction bound	V_{C2X} ($\mu\text{mols/min/ml}$)
Free	Bound		
2.4	2.7	0.47	0.083
5.6	5.6	0.50	0.108 *
9.9	9.9	0.50	0.120

* The fractions of enzyme free and bound were in this case estimated from the volume of membrane preparation added to the exchange system and the results of the other two assays.

The membranes, depleted of aldolase activity, were prepared as described in the Experimental section of chapter 3. The membranes were washed in the exchange system buffer before use. This buffer had the following composition; 30mM imidazole pH 7.2, 3mM dithiothreitol and 1.5mM EDTA in $^1\text{H}_2\text{O}$. The exchange system contained this buffer plus approximately 1 unit/ml of aldolase, 100 units/ml triosephosphate isomerase, 100 units/ml lactate dehydrogenase, 20mM nicotinamide and 1mM FDP. Exchange time courses were initiated by the addition of 12mM L-(2- ^2H)lactate and equilibrium velocity determinations were performed as described previously. The fractions of enzyme free and bound were assessed, following an exchange measurement, by separating the free and bound forms by centrifugation for 5 min at 37°C in an Eppendorf 5412 micro-centrifuge. The GAPDH activity measured in the supernatant was taken to represent the concentration of free enzyme. The concentration of bound enzyme was assessed by resuspending the membrane pellet, assaying the total activity present and subtracting from this the activity measured in the supernatant.

to a hyperbolic relationship and the calculated equilibrium velocity is similar to that measured for the free enzyme under identical conditions in the absence of membranes i.e. $0.065_{-0.021}^{+}$ $\mu\text{mol}/\text{min}/\text{unit}$. This suggests that the assumption made was correct, i.e. that the enzyme is totally inhibited when bound to the membrane. If NADH is added to the system (part C of the table) the fraction of unbound enzyme is increased and an equilibrium velocity determination under these conditions, which again assumes that the bound enzyme is inactive, yields an equilibrium velocity for the free enzyme of $0.170_{-0.001}^{+}$ $\mu\text{mol}/\text{min}/\text{unit}$. Elution of the enzyme by NADH suggests that inhibition on membrane binding is the result of occlusion of the NADH binding site.

5.8 Conclusions

The equilibrium velocity of the enzyme is decreased very slightly by raising the ionic strength but is largely independent of the GAP and hydrogen ion concentrations expected in erythrocytes with elevated triose phosphate levels. A dependence on the NAD^{+} and NADH concentrations has been demonstrated but in the absence of detailed kinetic analyses, such as those available for lactate dehydrogenase and triose phosphate isomerase, explanations for the observed dependence can only be speculative.

The rabbit muscle enzyme binds NAD^{+} and NADH with similar affinity and displays negative cooperativity in binding (Bell & Dalziel, 1975). Since the NAD^{+} concentration in situ is normally greater than the NADH concentration this suggests that the enzyme will exist in a predominantly NAD^{+} bound form. In the presence of its other substrates, however, the enzyme exists in a largely acylated form which has a lowered affinity for NAD^{+} ; its affinity for NADH is unchanged (Bloch et

al, 1971). Under these conditions NADH will compete more strongly for binding to the enzyme.

The results presented here indicate that both the NAD^+/NADH ratio and the absolute concentrations of these coenzymes are important. It is tentatively proposed that the limiting factor determining the observed equilibrium velocity is the NADH concentration and that its effective concentration is modified by competition with NAD^+ for binding to the enzyme. The equilibrium constant for the enzyme catalysed reaction suggests that the reverse flux will be rate limiting. In this exchange we are studying a partial reaction, the equilibrium constant for which can be represented by the following;

$$K = \frac{(\text{R}-\overset{\text{O}}{\underset{\parallel}{\text{C}}}-\text{E}) (\text{NADH})(\text{H}^+)}{(\text{RCHO}) (\text{E}) (\text{NAD}^+)}$$

where $(\text{R}-\overset{\text{O}}{\underset{\parallel}{\text{C}}}-\text{E})$ is the concentration of acyl-enzyme, (E) is the free enzyme concentration and (RCHO) is the GAP concentration. The equilibrium constant for this reaction has been estimated at 10^{-5} (Velick & Hayes, 1953). Under the conditions used here the acyl-enzyme will be the predominant enzyme form. Changing the NAD^+/NADH ratio over the concentration ranges shown should have little effect on its concentration.

Increasing the added NAD^+ concentration in the in vitro system from 10 to 100 μM results in the NADH concentration increasing from 4 to 17 μM . This increase however does not result in an increase in the equilibrium velocity presumably because there is a much greater increase in the NAD^+ concentration. In contrast the addition of NADH results in

an increase in the NADH concentration with no increase in the NAD^+ concentration. Under these circumstances there is a marked increase in the equilibrium velocity. Addition of pyruvate on the other hand results in loss of NADH, an increase in NAD^+ concentration and a decrease in the equilibrium velocity.

Rose and Warms (1970) measured lactate/pyruvate ratios of 500-800 and Minikami and Yoshikawa (1966) show results indicating a lactate/pyruvate ratio of approximately 1000 in erythrocytes with elevated triose phosphate levels. These results correspond to an NAD^+/NADH ratio of between 3 and 7 (at pH 7.4) and are in good agreement with the results shown in table 5. In the in vitro exchange system at an NAD^+ plus NADH concentration comparable to the estimated free concentration in the erythrocyte (i.e. 10-20 μM ; see next chapter) the NAD^+/NADH ratio has been varied between 0.75 and 5.0. The GAPDH equilibrium velocity measured in this system with an NAD^+/NADH ratio of 5, which was obtained by adding pyruvate, is approximately 25% of that observed in situ. In general the GAPDH equilibrium velocities observed in vitro tend to be lower than those observed in situ.

There are a number of factors which could explain this discrepancy i.e.

- a) the reaction catalysed by lactate dehydrogenase is not at equilibrium and thus the lactate/pyruvate ratio cannot be used as a measure of the free NAD^+/NADH ratio. This is unlikely in view of the results obtained in previous studies (Marshall & Omachi, 1974; Veech et al, 1979) and also from the results shown in the next chapter which demonstrate that flux across the reaction catalysed by the enzyme is in considerable excess of the glycolytic flux;
- b) the pyruvate assays are in error. The pyruvate was assayed in cell

supernatants in order to determine the free cellular concentration. Extraction with perchloric acid was avoided since this has been shown to result in a loss of pyruvate (see next chapter) and would also give the total concentration of the pyruvate present. At such low pyruvate concentrations this may be greater than the free concentration. Error in these assays, however, cannot be ruled out.

c) the in situ equilibrium velocity determinations are in error. It has been shown that the concentrations of the intermediates involved in the exchange are expected to remain constant during exchange measurements and that if they do change they will have only a very small effect on the equilibrium velocities of the enzymes and, ultimately, on V_{GAPDH} determinations. Model simulations show the effect of glycolytic flux to be small although it will lead to a slight overestimate of the in situ equilibrium velocity. Systematic errors in this analysis, however, cannot be rigorously excluded;

d) iodoacetate treatment results in alteration of the kinetic properties of non-modified sites in the tetrameric GAPDH molecule. The titration of enzyme activity with iodoacetate, performed in vitro, shows that in fact there is no such alteration in the enzyme's properties. Another possibility is that in the intact cell the iodoacetate modified enzyme might show a different affinity for the membrane binding site and that this could affect the observed equilibrium velocity. The iodoacetate modified enzyme however has been shown to bind with the same affinity as the non-modified enzyme to the membrane (Kant & Steck, 1973; Solti & Friedrich, 1976);

e) Although relatively homogeneous, erythrocyte suspensions are composed of a population of cells which show a normal distribution with respect to cell age (Piomelli et al, 1968). Cell aging has been shown to result in the decrease of activity of certain enzymes; for example,

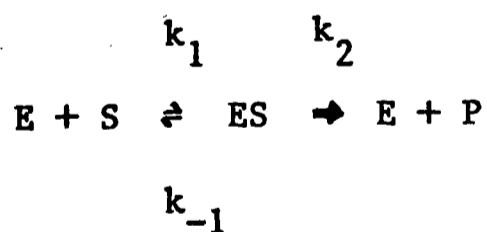
pyruvate kinase and glucose-6-phosphate dehydrogenase (Piomelli et al, 1968; Galbraith & Watts, 1980) and in changes in membrane composition (see for example Galbraith & Watts, 1981). Of the enzymes involved in C-2 exchange, GAPDH and lactate dehydrogenase show no significant changes in activity with increasing cell age (Chapman & Schaumburg, 1967; Lohr & Waller, 1962). This is not, however, a universal conclusion, see for example Fornaini (1967). Aldolase activity decreases by a factor of four between young and old cells (Chapman & Schaumburg, 1967). The ratio of aldolase activity to that of the other enzymes involved in C-2 exchange will vary therefore in different cells according to their age. The effect of this on the observed exchange properties of a cell population will however be moderated by the fact that the cells show a normal distribution with respect to cell age and because the sensitivity coefficient of aldolase is less than 1. The concentrations of adenine and pyridine nucleotides when calculated on a cell water basis do not appear to vary significantly with cell age (Hjelm, 1968).

f) potential "mutual depletion" conditions (Griffiths, 1979) exist for the enzyme and NADH both in vitro and in situ. Such conditions arise when a substrate is tightly bound to an enzyme and both are present at similar concentrations. Under these conditions the formation of the enzyme-substrate complex significantly depletes the concentrations of both enzyme and substrate. For an enzyme catalysing a reaction at equilibrium and which is present in relatively high concentration, the total concentrations of its substrates will deviate significantly from the expected equilibrium concentrations. This has been shown for liver alcohol dehydrogenase (Theorell & Bonnichsen, 1951) where the apparent equilibrium constant for the reaction catalysed by the enzyme was shown to vary as the enzyme concentration was changed. This was shown to be

due to a higher affinity of the enzyme for NADH than NAD^+ . Similar observations have been made with lactate dehydrogenase (Neilands, 1952). The equilibrium constant for the reaction catalysed by GAPDH, on the other hand, shows no significant dependence on enzyme concentration at relatively high GAP concentrations and low NAD^+ and NADH concentrations (Velick & Hayes, 1953). This was interpreted as indicating that the two coenzymes have similar affinities for the enzyme. The effect of enzyme concentration on the concentrations of the substrates for the lactate dehydrogenase reaction and the effect mutual depletion has on the equilibrium velocity displayed by this enzyme are considered in the following chapter. The effect of mutual depletion on reaction velocity v can be described by the following equation;

$$v = \frac{k_2 \left((E_0) + (S_0) + K_m \right) - \sqrt{\left((E_0) + (S_0) + K_m \right)^2 - 4(E_0)(S_0)}}{2}$$

where (S_0) and (E_0) represent the total substrate and enzyme concentrations respectively and K_m is the Michaelis constant for the substrate. This is for the reaction scheme;



where S and P represent substrate and product respectively. If it is assumed that the GAPDH equilibrium velocity is rate limited by the reverse reaction of NADH with the acyl-enzyme then E may be equated with the acyl-enzyme and S with NADH. The above equation can then be used to crudely assess the likelihood that mutual depletion affects the observed

equilibrium velocity of GAPDH in situ or in vitro. From the data provided by Marshall and Omachi (1974) the calculated change in enzyme concentration on changing the enzyme activity between 1 and 10 units/ml in the in vitro system is between 0.1 and 1 μM enzyme active sites. Using a K_m of $8.3\mu\text{M}$ for NADH (Maretzki et al, 1973) $v/(E_0)$ can be calculated in the in vitro system in terms of k_2 . It can be shown that $v/(E_0)$ does not change appreciably in this concentration range and thus that the equilibrium velocity of the enzyme is linearly related to the enzyme concentration. This is consistent with the results of the iodoacetate titration experiment performed in vitro. In the cell where the enzyme active site concentration is approximately $12\mu\text{M}$, then an approximately 40% decrease in the specific equilibrium velocity is to be expected on the basis of the above equation. This is only a rough approximation; for example, the apparent isotope exchange K_m may be larger than estimated due to competition for binding between NAD^+ and NADH. The important point, however, is that the specific equilibrium velocity of the enzyme might be expected to be lower in situ whereas in fact it is consistently observed to be greater than the equilibrium velocity measured in vitro.

If it is accepted that the free concentrations of NAD^+ and NADH in the erythrocyte can be predicted from the lactate/pyruvate ratio and estimates of the total free concentration of these nucleotides (see next chapter) and, if it is accepted that the equilibrium velocity determinations for GAPDH in situ are free from experimental error or artefact, then the discrepancy observed between the equilibrium velocities in situ and in vitro indicate that the enzyme displays a higher affinity for NADH in situ than in vitro. Further equilibrium velocity determinations, however, both in vitro and in situ would be

required to confirm this conclusion and to investigate the origin of this effect. One explanation for this apparent higher affinity of the enzyme for NADH in situ, which can be ruled out immediately, is the effect of membrane binding. This appears to result in total inhibition of enzyme exchange activity. In view of the conditions required to obtain membrane binding in vitro and the fact that the equilibrium velocity of the enzyme is actually greater in situ than expected, little if any of the enzyme can be bound to the membrane in the intact cell.

To summarise the conclusions of this chapter; a) GAPDH is not rate limiting for glycolytic flux in the human erythrocyte; b) it is unlikely that a significant fraction of the enzyme is bound to the membrane in the human erythrocyte under the conditions found here, i.e. elevated levels of the triose phosphates and a high lactate /pyruvate ratio.

5.9 References

- Aviram, I. & Shaklai, N. (1981) Arch. Biochem. Biophys. 212, 329-337
- Bell, J.E., & Dalziel, K. (1975) Biochim. Biophys. Acta 391, 249-258
- Bloch, W., MacQuarrie, R.A., & Bernhard, S.A. (1971) J. Biol. Chem. 246, 780-790
- Bunn, H.F., Gabbay, K.H., & Gallop, P.M. (1978) Science 200, 21-27
- Chapman, R.G. & Schaumburg L. (1967) Br. J. Haematol. 13, 665-678
- Deuticke, B., Rickert, I., & Beyer, E. (1978) Biochim. Biophys. Acta 507, 137-155
- Duggleby, R.G. & Dennis, D.T. (1974) J. Biol. Chem. 249, 167-174
- Eby, D., & Kirtley, M.E. (1979) Arch. Biochem. Biophys. 198, 608-613
- Eckel, R.E., Rizzo, S.C., Lodish, H., & Berggren, A.B. (1966) Amer. J. Physiol. 210, 737-743
- Fornaini, G. (1967) Ital. J. Biochem. 16, 257-330
- Freidrich, P., Aprókovács, V.A., & Solti, M. (1977) FEBS Lett. 84, 183-186
- Galbraith, D.A. & Watts, D.C. (1980) Biochem. J. 191, 63-70

- Galbraith, D.A. & Watts, D.C. (1981) *Biochem. J.* 195, 221-228
- Griffiths, J.R. (1979) *Biochem. Soc. Trans.* 7, 429-439
- Herbert, D., Gordon, H., Subramanyan, V. & Green, D.E. (1940)
Biochem. J. 115, 837-842
- Hjelm, M. (1968) *Folia Haematol.* 89, 392-399
- Higashi, T., Richards, C.S., & Uyeda, K. (1979) *J. Biol. Chem.* 254,
9542-9550
- Kant, J.A. & Steck, T.L. (1973) *J. Biol. Chem.* 248, 8457-8464
- Karadsheh, N.S. & Uyeda, K. (1977) *J. Biol. Chem.* 252, 7418-7420
- Keokitichai, S., & Wrigglesworth, J.M. (1980) *Biochem. J.* 187, 837-841
- Kliman, H.J., & Steck, T.L. (1980) *J. Biol. Chem.* 255, 6314-6321
- Lohr, G.W. & Waller, H.D. (1962) *Folia Haematol.* 78, 385-402
- Lowry, O.H., & Passoneau, J.V. (1964) *J. Biol. Chem.* 239, 31-42
- Maretzki, D., Tsamaloukas, A.G., Küttner, G., Krüger, S., Groth,
J. & Rapoport, S. (1973) VII th International Symposium on the
Structure and Function of Erythrocytes. pp 61-72

Maretzki, D., Groth, J., Tsamaloukas, A.G., Gründel, M., Krüger, S., & Rapoport, S. (1974) FEBS Lett. 39, 83-87

Marshall, W.E., & Omachi, A. (1974) Biochim. Biophys. Acta 354, 1-10

Mills, G.C., & Hill, F.L. (1971) Arch. Biochem. Biophys. 146, 306-311

Minikami, S., & Yoshikawa, H. (1966) J. Biochem. (Tokyo) 59, 145-150

Neilands, J.B. (1952) J. Biol. Chem. 199, 373-381

Oguchi, M. (1970) J. Biochem. (Tokyo) 68, 427-439

Oppenheimer, N.J. & Kaplan, N.O. (1974) Biochemistry 13, 4685-4694

Ottaway, J.H., & Mowbray, J. (1977) Curr. Top. Cell. Regul. 12, 107-208

Piomelli, S., Corash, L.M., Davenport, D.D., Miraglia, J. & Amorosi, E.L. (1968) J. Clin. Invest. 47, 940-948

Rolleston, F.S., & Newsholme, E.A. (1967) Biochem. J. 104, 524-533

Rose, I.A. & Warms, J.V.B. (1966) J. Biol. Chem. 241, 4848-4854

Rose, I.A., & Warms, J.V.B. (1969) J. Biol. Chem. 244, 1114-1117

Rose, I.A., & Warms, J.V.B. (1970) J. Biol. Chem. 245, 4009-4015

Saito, T. & Minikami, S. (1967) J. Biochem. (Tokyo) 61, 211-219

Salhany, J.M., Cordes, K.A., & Gaines, E.D. (1980) Biochemistry 19,
1447-1454

Schrier, S.L. Ben-Bassat, I., Junga, I., Seeger, M., & Grummet, F.C.
(1975a) J. Lab. Clin. Med. 85, 797-810

Schrier, S.L., Junga, I. & Johnson, M. (1975b) Life Sci. 17, 735-738

Shapiro, R., McManus, M.J., Zalut, C., & Bunn, H.F. (1980) J. Biol.
Chem. 255, 3120-3127

Solti, M., & Freidrich, P. (1976) Mol. Cell. Biochem. 10, 145-152

Solti, M., Bartha, F., Halász, N., Tóth, G., Sirokmán, F., &
Freidrich, P. (1981) J. Biol. Chem. 256, 9260-9265

Strapazon, E., & Steck, T.L. (1977) Biochemistry 16, 2966-2971

Theorell, H., & Bonnichsen, R. (1951) Acta Chem. Scand. 5, 1105-1126

Tsuboi, K.K., Allan, J.F., & Fukunaga, K. (1966) J. Biol. Chem. 241,
1616-1620

Veech, R.L., Rajman, L., Dalziel, K., & Krebs, H. A. (1969)
Biochem. J. 115, 837-842

Veech, R.L., Lawson, J.W.R., Cornell, N.W., & Krebs, H.A. (1979) J. Biol. Chem. 254, 6538-6547

Velick, S.F., & Hayes, J.E. (1953) J. Biol. Chem. 203, 545-562

Wang, C., & Alaupovic, P. (1980) Arch. Biochem. Biophys. 205, 136-145

Webb, J.L. (1966) "Enzyme & Metabolic Inhibitors", Vol. III pp 1-270
Academic Press New York & London

Williamson, D.H., Lund, P., & Krebs, H.A. (1967) Biochem. J. 103,
514-527

Wrigglesworth, J.M., Keokitichai, S., Wooster, M.S., & Millar, F.A.
(1976) Biochem. Soc. Trans. 4, 637-640

Yu, J. & Steck, T.L. (1975) J. Biol. Chem. 250, 9176-9184

6 A comparison of the kinetic properties expressed by lactate dehydrogenase in the intact erythrocyte and in vitro

6.1 Introduction

In the previous chapter the equilibrium velocity displayed by glyceraldehydophosphate dehydrogenase in the intact erythrocyte was measured by specifically and irreversibly inhibiting the enzyme to varying degrees with iodoacetate. The first part of this chapter describes the measurement of the equilibrium velocity of lactate dehydrogenase in situ by specific and reversible inhibition of the enzyme with oxamate (see chapter 2). The problems involved in making this measurement are discussed and in the second part of the chapter a much better method for measuring the equilibrium velocity of the enzyme is introduced. This involves monitoring an exchange at the lactate C-2 position which is catalysed by lactate dehydrogenase (LDH) alone.

The equilibrium velocities displayed by the enzyme in vitro and in situ are compared and used to estimate the free NAD^+ plus NADH concentration in the intact cell.

6.2 Experimental

Preparation of erythrocytes

Erythrocytes were prepared as described in chapter 2 except that the buffers contained no glucose. The cells were depleted of glucose by washing 4-5 times in 10 volumes of Krebs-Ringer buffer and then incubating at 37°C for 1 hr followed by another 4-5 washes and storage overnight at 4°C. The cells were washed a further 4-5 times prior to use in n.m.r. experiments.

Preparation of L-(3-²H) and L-(U-²H)lactate

Deuteration of the lactate methyl group was obtained by adding 125mg of lactate (L-(2-²H) or L-(U-¹H)) to 10 ml of a solution containing 100mM Tris-²HCl pH 8.0, 0.5mM EDTA and 3mM dithiothreitol in 99.8% ²H₂O. The solution also contained 2.5g of myoglobin, 2mg of rabbit muscle lactate dehydrogenase, 40mM pyruvate and 10mg/ml penicillin and 10mg/ml streptomycin. This solution was incubated for approximately 1 month at room temperature. The lactate was isolated using the method described for L-(2-²H)lactate in chapter 2.

Metabolite assays

Pyruvate

Pyruvate was assayed in cell free supernatants prepared by spinning down 4 ml of a dilute cell suspension (10-15% haematocrit). To the 3 ml of supernatant obtained was added 0.5 ml ice cold 8% perchloric acid. The resulting protein precipitate was spun off by centrifuging the extract on an Eppendorf 5412 centrifuge for 5 min. The extract (0.5 ml) was then added to 0.4 ml of 0.5M imidazole buffer pH 7.0. Following

thorough mixing 0.1 ml of 1mM NADH was added and the absorbance recorded at 340nm. Approximately 10 units of bovine heart lactate dehydrogenase were then added and a second absorbance reading recorded after 5 min incubation at 37°C. The pH of the final assay mixture was between pH 6 and 7. Blank assays were also performed and the assay values were corrected for the loss of absorbance observed with the blank.

NAD⁺

NAD⁺ assays were performed using the enzyme cycling method of Nisselbaum and Green (1969). This involves reduction of NAD⁺ in the reaction catalysed by alcohol dehydrogenase. The NADH produced reduces the dye thiazolyl blue, through the intermediation of phenazine methosulphate. This results in a colour change from yellow to blue which is observed at 556nm. The rate of reduction of thiazolyl blue is proportional to the concentration of the coenzyme.

Preparation of extracts

Boiled extracts were prepared by placing approximately 0.5 ml of a dilute cell suspension (10-15% haematocrit) on a boiling water bath for 10 min. The resulting protein precipitate was then centrifuged off on an Eppendorf 5412 centrifuge and the supernatant assayed for NAD⁺.

Assay

A stock solution containing 65mM diglycine, pH 7.4, 65mM nicotinamide and 350mM ethanol was prepared. To 10 ml of this was added 0.1 ml of a solution containing 10mg/ml of thiazolyl blue and 30 µl of a 20mg/ml suspension of horse liver alcohol dehydrogenase (obtained from Boehringer). This stock solution was maintained in the dark at 4°C. To 0.95 ml aliquots of this solution was added 30 µl of a 10mg/ml solution of phenazine methosulphate. The solution was then allowed to warm to room temperature and the absorbance at 556nm was recorded for 10 min in

in order to obtain a blank rate. This procedure was followed with all samples since this blank rate was found to vary during the day. After 10 min between 5 and 20 μ l of a standard NAD^+ solution or extract was added. The subsequent increase in absorbance was recorded on a chart recorder with a full scale deflection of 0.5 O.D. units for 20-30 min. A calibration curve of rate of increase in absorbance versus NAD^+ concentration was obtained by adding between 12.5 and 75nM NAD^+ to the assay system. The stock NAD^+ solution was assayed spectrophotometrically by measuring the absorbance at 260nm and assuming an extinction coefficient of $17.6 \times 10^6 \text{ cm}^2 \text{ mol}^{-1}$ (Dalziel, 1963). All solutions were prepared fresh each day and stored in the dark at 4°C . Absorbance measurements were made on a Unicam SP800A UV spectrophotometer.

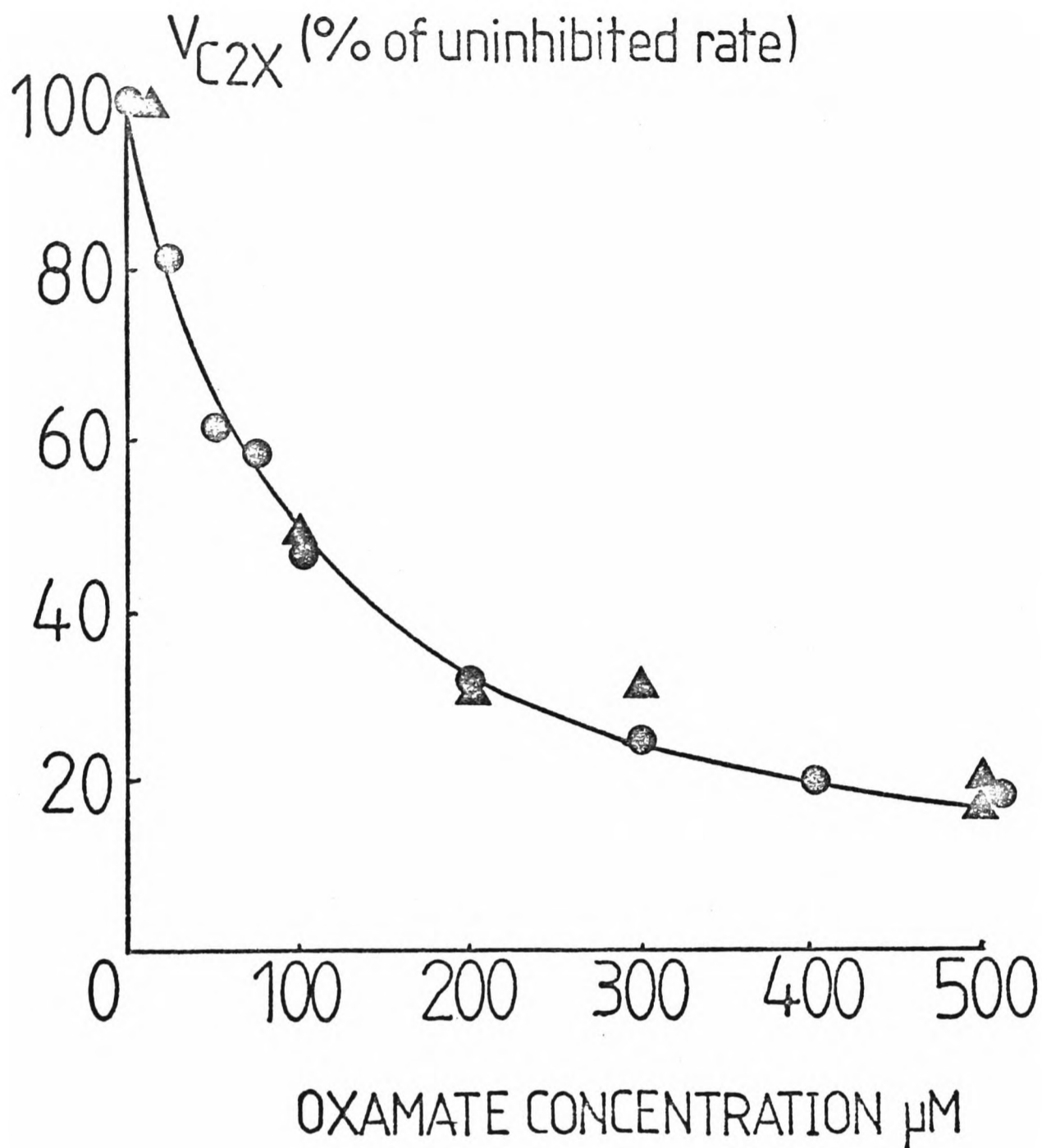


Figure 1

Oxamate inhibition of lactate dehydrogenase in vitro

The inhibition was measured at 10 (▲) and 100μM (●) added NAD⁺.

The in vitro exchange system contained aldolase, triosephosphate isomerase, glyceraldehydephosphate dehydrogenase and lactate dehydrogenase in a buffer solution containing 100mM Tris-HCl pH 7.4, 0.5mM EDTA and 3mM dithiothreitol in ²H₂O. The lactate dehydrogenase activity in the system containing 10μM NAD⁺ was 15 units/ml and 6 units/ml in the system containing 100μM NAD⁺. The lactate concentration was 12mM. The enzymes, obtained as ammonium sulphate suspensions, were dialysed against 0.1% EDTA/lmM 2-mercaptoethanol.

The theoretical curve was calculated as described in appendix 2 chapter 2. The ratio V_{LDH}/V_R for the uninhibited system was calculated using the double reciprocal relationship described in previous chapters. V_{LDH} was calculated from the enzyme activity and its known dependence on the NAD⁺ concentration. V_R was calculated from taking the reciprocal of $1/V_{C2X} - 2/V_{LDH}$.

6.3 Measurement of the in situ equilibrium velocity of lactate dehydrogenase using oxamate inhibition

As shown in chapter 2, the enzyme can be specifically and reversibly inhibited with relatively low concentrations of oxamate. Oxamate is a substrate analogue which competes with pyruvate for binding to the enzyme (Novoa et al, 1959). The extent to which this inhibition is expressed in the overall exchange velocity of the C-2 exchange system is dependent on the sensitivity coefficient of the enzyme. This was demonstrated in figure 15 chapter 2 which is, in part, reproduced here as figure 1. The figure showed the effect of changing, in vitro, the ratio of the lactate dehydrogenase equilibrium velocity (V_{LDH}) to the combined equilibrium velocities of the other enzymes expressed as V_R , the reciprocal of the reciprocal sum of the equilibrium velocities of the other enzymes. As this ratio is increased the overall equilibrium velocity, V_{C2X} , becomes progressively less sensitive to inhibition of LDH. The inhibition or dissociation constant, K_i , for oxamate binding to the enzyme was estimated to be $60\mu\text{M}$. In figure 1 inhibition data obtained in vitro at $10\mu\text{M}$ added NAD^+ is shown in addition to that obtained at $100\mu\text{M}$ added NAD^+ . This shows that oxamate inhibition is the same at 10 and $100\mu\text{M}$ $\text{NAD}(\text{H})$. The oxamate K_i appears therefore to be independent of $\text{NAD}(\text{H})$ concentration. It should be noted that the ratio V_{LDH}/V_R was approximately the same (0.5-0.6) in both of the exchange systems containing 10 and $100\mu\text{M}$ added NAD^+ . Furthermore although the pyruvate concentration was different in the two systems (4 and $17\mu\text{M}$ respectively) this is not expected to significantly affect oxamate inhibition and the theoretical inhibition curves obtained are very similar, (only a single curve is shown in figure 1).

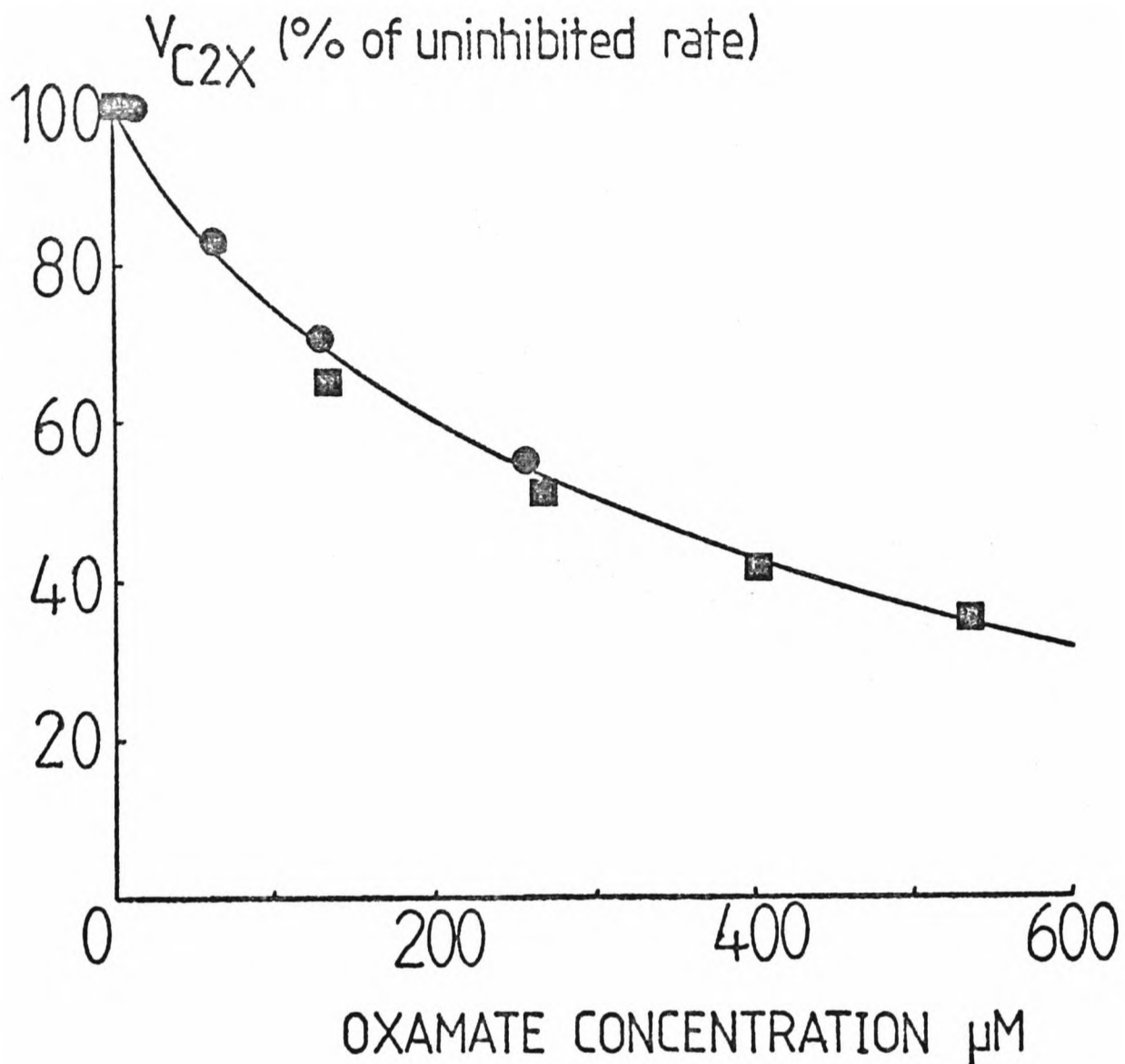


Figure 2

Oxamate inhibition of lactate dehydrogenase in situ

The figure shows results obtained from two different cell preparations, in both the cells were suspended in $^2\text{H}_2\text{O}$ Krebs-Ringer buffer, pH 7.4. In one cell preparation (●) the haematocrit was 78% and the lactate dehydrogenase activity 71 units/ml solvent water. In the other preparation (■) it was 77% and the lactate dehydrogenase activity was 60 units/ml solvent water. The added lactate concentration was 12mM.

The theoretical curve was calculated as described in the text and in the legend to table 1.

This oxamate inhibition experiment can be performed in the intact erythrocyte (figure 2) where it can be used to estimate V_{LDH}/V_R in situ. From this ratio and using the measured V_{C2X} and the double reciprocal relationship between V_{C2X} and the equilibrium velocities of the enzymes a value for V_{LDH} , the total equilibrium velocity for LDH, can be calculated. Dividing this value by the activity of the enzyme assayed spectrophotometrically yields a value for the specific equilibrium velocity of the enzyme in situ. It is crucial however that in these calculations the cellular pyruvate concentration is known. This is demonstrated in table 1 which shows an analysis of the data presented in figure 2. Oxamate inhibition is competitive with pyruvate, the extent of the inhibition is dependent therefore on the pyruvate concentration. Using a K_i value of $60\mu\text{M}$ the in situ inhibition data shown in figure 2 can be fitted with a variety of V_{LDH}/V_R ratios depending on the pyruvate concentration. The value of this ratio determines the calculated V_{LDH} as shown in table 1. This also shows the theoretically expected values for V_{LDH} at the different pyruvate concentrations and at an NAD^+ concentration of $10\mu\text{M}$. Knowledge of the pyruvate concentration is important therefore in two respects; a) the pyruvate concentration will determine the extent of oxamate inhibition and b) its level will determine the uninhibited equilibrium velocity of the enzyme. Simulation of the in situ environment in vitro will require therefore accurate knowledge of the pyruvate concentration. Although the pyruvate concentration must be known for in vitro studies its effect on the inhibition in situ can be avoided by using oxalate, an LDH inhibitor which in this case competes with lactate for binding to the enzyme (Novoa et al, 1959). Since the lactate concentration is relatively high and saturating its modulating effect on oxalate inhibition is less radical and more easily allowed for than that of

Table 1

Estimation of V_{LDH} in situ from oxamate inhibition studies.

The effect of pyruvate.

The experimental data shown in figure 2 can be fitted with a variety of values of V_{LDH}/V_R depending on the pyruvate concentration.

Pyruvate concentration	V_{LDH}/V_R ratio required to obtain a fit to the experimental data	V_{LDH} <u>in situ</u> calculated from the V_{LDH}/V_R ratio ($\mu\text{mols}/\text{min}/\text{unit}$)	Expected V_{LDH} <u>in vitro</u> at 10 μM NAD^+ and the specified pyruvate concentration ($\mu\text{mols}/\text{min}/\text{unit}$)
4	8.0	0.068	0.015
40	4.0	0.041	0.027
100	2.0	0.014	0.019

The specific equilibrium velocity (V_{LDH}) of the enzyme in situ can be calculated from the uninhibited value of V_{C2X} and the estimated V_{LDH}/V_R ratio. The V_{LDH}/V_R ratio was calculated by fitting the experimental data shown in figure 2 using a K_i value for oxamate inhibition of 60 μM . The expected V_{LDH} in vitro was calculated using the kinetic model for lactate dehydrogenase described in chapter 2 for an NAD(H) concentration of 10 μM , a lactate concentration of 12mM and the specified pyruvate concentration.

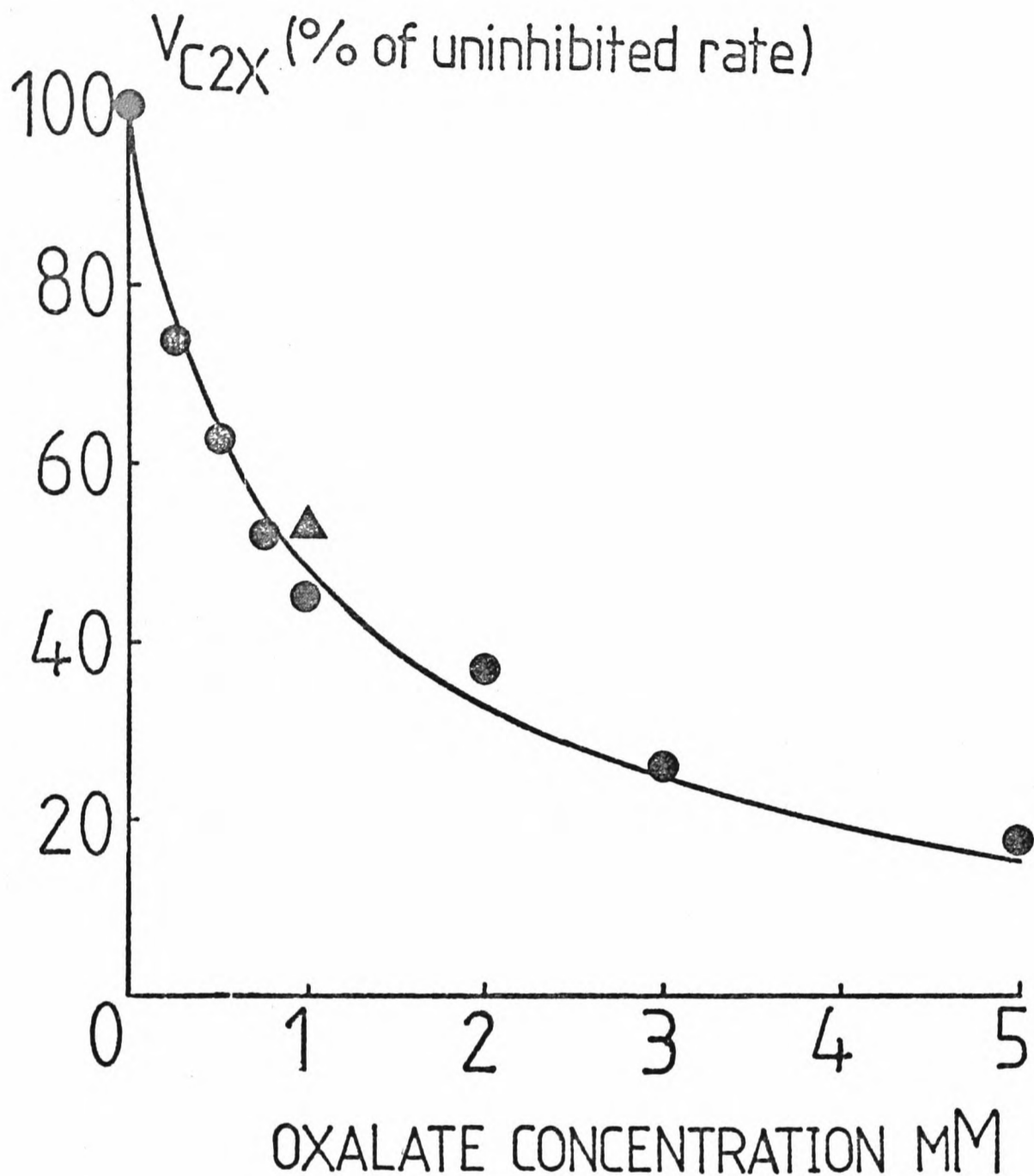


Figure 3

Oxalate inhibition in vitro

The in vitro system had a similar composition to that described in the legend to figure 1. The added lactate and NAD^+ concentrations were 12mM and 100 μM respectively. The system contained 9.5 units/ml of lactate dehydrogenase. The theoretical curve was drawn for a V_{LDH}/V_R ratio of 2.4 and for $K_s = 4.1\text{mM}$ and $K_i = 0.11\text{mM}$ (see text and appendix 2 chapter 2). The point marked (\blacktriangle) was obtained at 18mM added lactate.

pyruvate on oxamate inhibition. Oxalate inhibition in an in vitro system is demonstrated in figure 3. The theoretical curve was calculated in the same way as the curves for oxamate inhibition. The lactate K_s was assumed to be 4.1mM (Everse & Kaplan, 1973) and the experimental data was fitted using a K_i value of 0.11mM. This inhibition constant is similar to that obtained in conventional steady state kinetic studies of the enzyme (Novoa et al, 1959).

With accurate measurement of the cellular pyruvate concentration and further studies of oxalate and oxamate inhibition of the enzyme in vitro, under conditions more similar to those present in situ e.g. at higher ionic strength, these experiments could be used to estimate the in situ equilibrium velocity of LDH. However this line of investigation was not pursued any further when it became apparent that the equilibrium velocity of the enzyme could be measured by studying an exchange catalysed by LDH alone.

6.4 Equilibration of isotope at the lactate C-2 position between methyl labelled lactate molecules

-A direct method for obtaining the equilibrium velocity of lactate dehydrogenase

Simpson (1981) showed that the LDH activity in intact erythrocytes could be measured by measuring the equilibrium velocity for the exchange of $^1\text{H}/^2\text{H}$ label between the methyl groups of lactate and pyruvate. By comparing the equilibrium velocity displayed by the enzyme in vitro and in situ it was concluded that the free NAD(H) concentration in the erythrocyte is approximately 10% of the total extractable concentration of approximately 100 μM . Measurement of this exchange, however, suffers a number of drawbacks when used as a method for measuring V_{LDH} and the

effective NAD(H) concentration in the erythrocyte. The drawbacks are;

a) in vitro the exchange of totally deuterated pyruvate methyls with totally protonated lactate methyls results in a linearly related increase in the pyruvate peak intensity and decrease in the lactate peak intensity in the spin echo spectrum. In situ however the pyruvate methyl can exchange with solvent (Simpson et al, 1981)), this results in the formation of partially deuterated methyl groups. This exchange must be allowed for when estimating the rate of equilibration catalysed by the enzyme. However a further complication is introduced by the fact that partial deuteration of a methyl group affects the n.m.r. relaxation properties of the remaining protons. Under these conditions linearity between the proton composition of the lactate or pyruvate methyl and its peak intensity in the n.m.r. spectrum is lost. These effects can however be allowed for (Simpson, 1981); b) the method requires the use of very high pyruvate concentrations, 10mM was the concentration usually employed. At this pyruvate concentration the enzyme suffers considerable pyruvate inhibition which distorts the expected dependence on NAD^+ concentration. The result of this is that the equilibrium velocity of the enzyme increases very rapidly at low NAD^+ concentrations with little further increase above 20 μM . This reduces the sensitivity of the enzyme as a probe for the intracellular NAD(H) concentration in the range expected in the erythrocyte i.e. up to 100 μM .

A similar experiment to the lactate/pyruvate methyl isotope equilibration experiment can be performed with lactate alone. This involves observing the equilibration of label at the lactate C-2 position between two different lactate species distinguished by their methyl label. The principle of this method is described in figure 4. If LDH plus NAD^+ is added to an equimolar mixture of L-(U-²H)lactate and

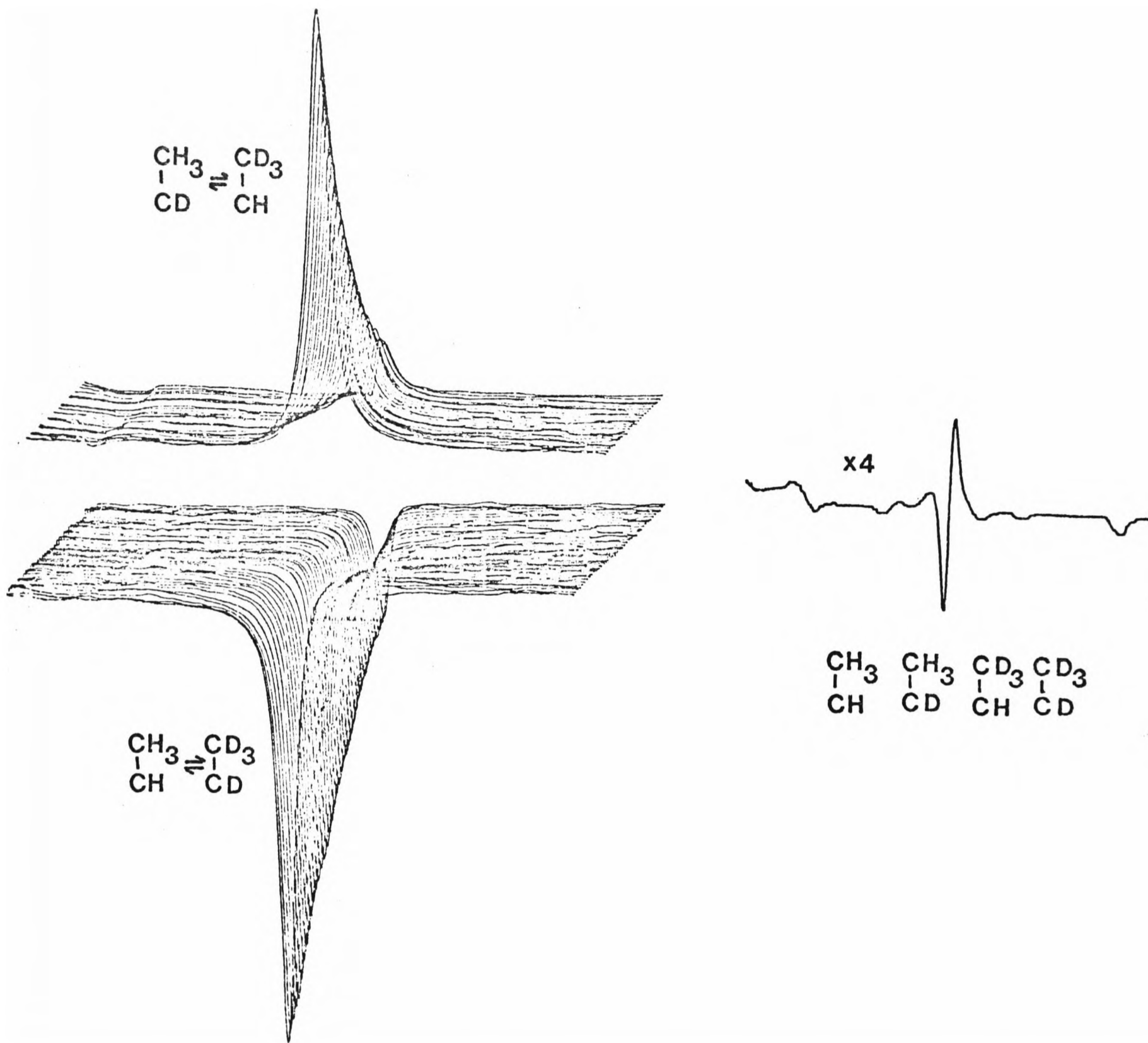


Figure 4

The C-2 equilibration experiment

The figure shows stacked plots of the lactate methyl resonance in ^1H spin echo spectra (2 min accumulation time; 80 scans; $\tau = 68\text{ms}$) for the two different equilibration experiments. The water resonance was suppressed by applying a saturating pulse at the water resonance frequency during the delay between successive acquisitions. A line broadening of 30 Hz was applied.

$L-(U-^1H)$ lactate there is equilibration of $^1H/^2H$ label at the C-2 position of the two lactate species. At equilibrium 4 equimolar species are obtained, i.e. $L-(U-^2H)$ lactate, $L-(U-^1H)$ lactate, $L-(2-^2H)$ lactate and $L-(3-^2H)$ lactate. Only those species with protonated methyls are observed in the p.m.r. experiment. Therefore before equilibration only $L-(U-^1H)$ lactate is observed, this gives an inverted methyl in the spin echo experiment at $\tau = 68ms$. At isotopic equilibrium an equimolar mixture of $L-(U-^1H)$ lactate and $L-(2-^2H)$ lactate gives rise to positive and negative methyl peaks of equal intensity which partially cancel to give a null point. A similar experiment can be performed with $L-(3-^2H)$ lactate and $L-(2-^2H)$ lactate as the starting lactate species (figure 4). This experiment, like the methyl equilibration experiment, can be performed both in situ and in vitro and used to estimate the free intracellular NAD(H) concentration. It has, however, a number of advantages i.e. a) because the pyruvate concentration is very low (10-50 μ M) exchange of isotope with solvent in the pyruvate and consequently lactate methyl groups is minimal; b) with equimolar concentrations of the two lactate species at $t=0$ the net result of the exchange in the spin echo spectrum is the loss of the entire peak intensity due to the C-3 protonated methyl present. In the C-3 equilibration experiment with equimolar lactate and pyruvate concentrations the lactate and pyruvate peaks change by only half of their original intensity at $t=0$. Observation of C-2 equilibration is enhanced therefore in the spin echo experiment compared to C-3 equilibration; c) the equilibrium velocity for C-2 equilibration is much more sensitive to the concentration of NAD^+ in the range 0-100 μ M (see figure 5) because there is no pyruvate inhibition.

6.4.1 Measurement of C-2 equilibration in situ and in vitro

Equilibrium velocity measurements were performed in a manner similar to that employed with C-2 exchange measurements. The in vitro system in this case however contained only LDH and the specified NAD^+ , lactate and pyruvate concentrations. Exchange time courses were initiated by the addition of one of the lactate species to an otherwise complete exchange system prewarmed to 37°C . The system usually contained between 5 and 10 units/ml LDH and 20mM lactate. The exchange was monitored by collecting 2 min spectra (80 scans) for between 60 to 90 minutes until more than 75% of the two lactate species had exchanged. In many cases a spectrum was obtained at a much later time, when isotopic equilibration was complete, in order to check that a true null point was obtained (see figure 4). It is essential that the end point be known with some precision since a discrepancy in this value can radically affect the calculated rate of equilibration. Exchange time courses were fitted to an equation of the following form (using a least squares fitting routine available in the Nicolet 1180 computer software);

$$y = Ae^{(-kt)}$$

where y is peak height at time t , A is the amplitude of the change in peak height and k is the first order rate constant for the exchange. This is equal to the sum of the individual rate constants for the exchange of isotope between lactate species A and B and between species B and A respectively. Since these rate constants are equal the equilibrium velocity for the exchange is obtained by multiplying $k/2$ by the concentration of one of the lactate species (i.e. half the total concentration of lactate). Dividing this value by the

spectrophotometrically assayed activity of the enzyme gives the specific equilibrium velocity of the enzyme. The computed standard deviation in k was never greater than $\pm 5\%$. Measuring the equilibrium velocity of LDH by monitoring C-2 equilibration is considerably easier, less time consuming and less error prone than measuring the equilibrium velocity by C-2 exchange since it requires only a single exchange measurement.

C-2 equilibration experiments with erythrocytes were performed with dilute cell suspensions at haematocrits between 10 and 15%. At these cell dilutions the LDH activity present (per ml of solvent water) is comparable to that found in the in vitro system i.e. approximately 10 units/ml. Exchange measurements on these cell preparations were performed in exactly the same way as on the in vitro system. By measuring the exchange over the same number of half times in situ and in vitro any possible isotope effects on the rate and consequently on a comparison of the results obtained in situ and in vitro can be ignored. The erythrocytes used in these experiments had been stored in citrate/phosphate/glucose for 3-4 weeks in order to deplete them of 2,3-DPG. The breakdown of this metabolite during exchange measurements would lead to pyruvate production (Whittam, 1958). The cells were depleted of other metabolites by washing and incubating them at 37°C in the absence of glucose (see Experimental section). As a consequence of this they showed no endogenous lactate production during exchange measurements. Control incubations with L-(2- ^2H)lactate and L-(3- ^2H)lactate showed that the cells were unable to catalyse the exchange of deuterons with solvent protons at either the C-3 or C-2 positions of the lactate molecule. Addition of 0.5mM iodoacetate to a cell preparation did not affect the observed equilibration rate and calculated equilibrium velocity for the enzyme. All of the C-2

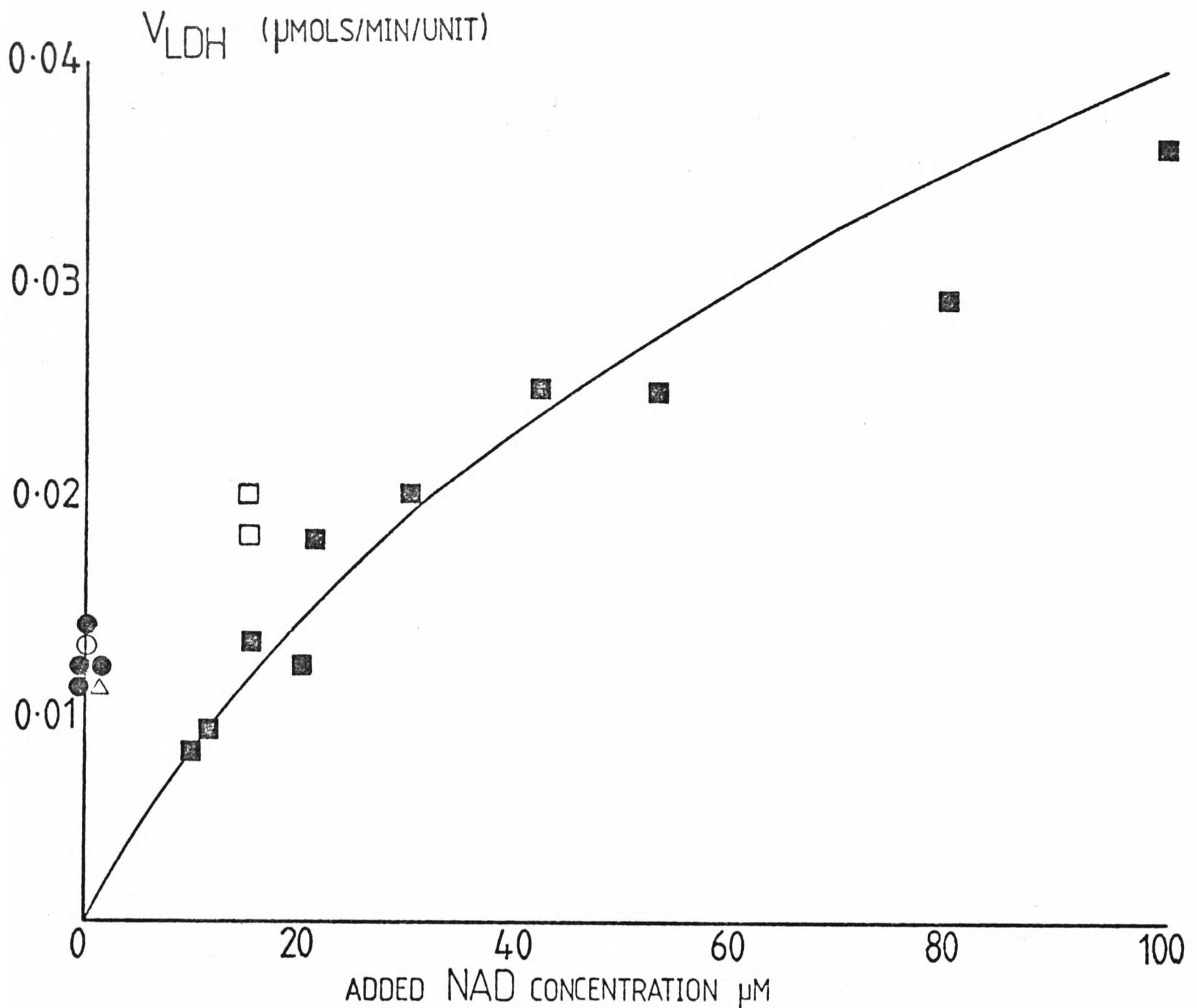


Figure 5

The dependence of the equilibrium velocity for C-2 equilibration on the added NAD^+ concentration in an in vitro system.

Comparison with the observed equilibrium velocity in situ.

Equilibrium velocity measurements were made as described in the text. The in vitro system contained 100mM Tris-HCl pH 7.4, 0.5mM EDTA and 80mM KCl in H_2O . The enzyme activity was between 5 and 10 units/ml and the concentration of the two lactate species (L-(U-¹H) and L-(U-²H) lactate) was 10mM. The lactate dehydrogenase was usually added to the system as an ammonium sulphate suspension. In some cases however the enzyme was dialysed against the in vitro system buffer before use. Both preparations showed the same exchange activity indicating that the ammonium sulphate, at the concentrations present, had no effect on the observed equilibrium velocity. The cell preparations were glucose depleted and suspended in Krebs-Ringer buffer, pH 7.4 at haematocrits between 10 and 15%.

The points marked (■) were obtained in the in vitro system at the specified added NAD^+ concentration. The solid line drawn through these points was calculated using the model ("model 1") described in the appendix. The points marked (□) were obtained in the in vitro system with 50µM added pyruvate. The points marked (●) on the ordinate were obtained from cell preparations. The point marked (○) was obtained from a cell preparation in the presence of 50µM added pyruvate and that marked (△) was obtained in the presence of 0.5mM iodoacetate.

equilibration measurements were performed in $^1\text{H}_2\text{O}$.

6.4.2 The concentrations of free NAD^+ plus NADH in the erythrocyte

Figure 5 shows the dependence of the equilibrium velocity for C-2 equilibration on the added NAD^+ concentration in an in vitro system. The solid line is a theoretical curve derived using the kinetic model described in the appendix. The equilibrium velocities obtained in situ are shown on the ordinate. These results indicate a free intracellular NAD^+ plus NADH concentration of between 10 and 15 μM . However before such a conclusion can be reached the proposed similarity between the in vitro and in situ environments should be examined.

6.4.3 The effect of pyruvate

Table 2 shows the results of pyruvate assays on metabolically depleted cells used for C-2 equilibration experiments. The pyruvate was assayed in the supernatants of centrifuged cell preparations. Extraction of pyruvate with perchloric acid was avoided since this has been shown to result in an apparent loss of pyruvate (Gloster & Harris, 1962). It was suggested that LDH is not totally destroyed during perchloric acid treatment. As a result of this LDH is introduced with pyruvate into an assay system in which pyruvate is assayed by monitoring, spectrophotometrically, NADH oxidation following subsequent addition of LDH. Introduction of the enzyme with pyruvate means that a stable initial absorbance reading cannot be obtained and the pyruvate concentration is consequently underestimated. Acidification of the intracellular medium prior to inactivation of the enzyme or destruction of NADH may also lead to a loss of pyruvate by forcing the equilibrium towards NAD^+ and lactate. Another point which should be noted about these pyruvate assays (which are described in the Experimental section)

Table 2

Pyruvate assays on glucose depleted cells used for C-2 equilibration experiments.

Added lactate concentration (mM)	Added pyruvate concentration (μ M)	Assayed pyruvate concentration (μ M)	Number of determinations
-	-	7	2
-	-	6	3
-	100	94	2
-	-	8	2
20	-	16	2
-	91	98	2
20	91	100	2

The pyruvate was assayed in cell free supernatants. The cells were suspended in Krebs-Ringer buffer at haematocrits between 10 and 15% and incubated for 20 min at 37^oC before being assayed for pyruvate. The assays were performed as described in the Experimental section.

is the pH of the assay system. This was usually between 6 and 7. At higher pHs the equilibrium constant for the reaction makes it impossible to assay all of the pyruvate in the presence of such high lactate concentrations.

The assayed pyruvate concentration in these cells in the presence of added lactate is $16\mu\text{M}$ which is significantly higher than that expected in vitro at $10\mu\text{M}$ added NAD^+ i.e. $5\mu\text{M}$. The effect of this higher pyruvate concentration will be to increase the equilibrium velocity of the enzyme as demonstrated in figure 5. Addition of pyruvate to both the in vitro and in situ systems results in an increase in the observed equilibrium velocity of the enzyme. Since the pyruvate concentration ($50\mu\text{M}$) is very much less than the lactate concentration (20mM) flux of label into the pyruvate will have a negligible effect on the observed exchange of label in the lactate. Addition of pyruvate to a cell preparation results in a smaller increase in the equilibrium velocity than that observed in vitro. This is presumably because the initial pyruvate concentration is higher in the cell. These observations suggest that in the in vitro system, which lacks additional pyruvate, the equilibrium velocity displayed by the enzyme will be slightly less than that observed in situ. The estimated free intracellular NAD(H) concentration is therefore likely to be a slight overestimate and it is probably closer to $10\mu\text{M}$ than to $15\mu\text{M}$. This effect of pyruvate could be avoided by performing both the in vitro and in situ experiments in the presence of $50\text{--}100\mu\text{M}$ pyruvate.

6.4.4 The effect of pH

The results in table 3 show the effect of pH on the equilibrium velocity of the enzyme. Also shown are the theoretically calculated

Table 3

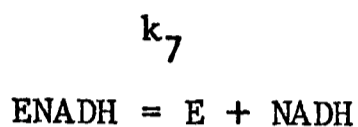
The effect of pH on the equilibrium velocity for C-2 equilibration.

pH	Experimentally observed V _{LDH} (μmoles/min/unit)	V _{LDH} calculated from a theoretical model which	
		assumes that only the substrate concentrations change (μmoles/min/unit)	assumes that there are changes in the substrate concentrations and in the dissociation constant for NADH binding to the enzyme (μmoles/min/unit)
7.0	0.015	0.007	0.008
7.2	0.015	0.009	0.010
7.4	0.015	0.011	0.011
7.6	0.013	0.011	0.013
7.8	0.012	0.017	0.015

The in vitro system contained glycylglycine-imidazole buffer at the specified pH, 0.15M KCl and 0.5mM EDTA. The lactate dehydrogenase was added as an ammonium sulphate suspension to give 5 units enzyme/ml. All samples contained 15μM NAD⁺ and 10mM L-(U-²H)lactate and 10mM L-(U-¹H)lactate.

The theoretical values were calculated as described in the text using "model 1" which is described in the appendix.

values for V_{LDH} assuming that there is only a change in the equilibrium concentrations of the enzymes substrates but no change in its kinetic parameters. There is considerable disparity between the calculated and observed effects of changing the pH. However Schwert et al (1967) have shown that in this pH range there is a significant change in the dissociation constant for NADH. Winer and Schwert (1958) concluded that k_7 is not affected in the pH range 7 to 8 but that k_8 decreases significantly as the pH is raised.



$$k_8$$

From the data of Schwert et al (1967) the effect of pH on the dissociation constant can be calculated (figure 3 in their paper). The change in the ratio k_7/k_8 is estimated to be $+3 \times 10^{-6}$ for an increase of 1 pH unit between pH 7 and 8. By extrapolating to the data of Borgmann et al (1974); the effect of pH on the kinetic parameters in the theoretical model can be calculated. Theoretical calculations for the equilibrium velocity of the enzyme which take into account this effect of pH are shown in the third column of table 3. The result of this change in the rate constants is a much reduced effect of pH on the calculated equilibrium velocity in closer agreement with the experimentally observed values.

Throughout these investigations the intracellular pH of the erythrocyte has been assumed to be 7.4. However as shown for GAPDH in the previous chapter and now for LDH this is not a critical assumption when simulating the intracellular environment in vitro for these enzymes.

Table 4

The effect of buffer composition on the equilibrium velocity for C-2 equilibration.

Buffer	V_{LDH} ($\mu\text{mols}/\text{min}/\text{unit}$)
100mM glycylglycine-imidazole pH 7.4, 0.5mM EDTA, 0.15M KCl	0.015
Krebs-Ringer	0.016
Tris-HCl pH 7.4, 0.5mM EDTA, 80mM KCl	0.013

All three determinations were performed with $15\mu\text{M}$ added NAD^+ , 10mM L-(U-¹H)lactate and 10mM L-(U-²H)lactate.

6.4.5 The effect of buffer composition

Equilibrium velocities measured at pH 7.4 in Tris-HCl, imidazole-glycylglycine and Krebs-Ringer buffers show no significant differences (table 4).

6.4.6 The effect of enzyme concentration

The effect of enzyme concentration on the specific equilibrium velocity of the enzyme has been investigated both experimentally and theoretically (table 5). Increasing the enzyme concentration in the in vitro system in the presence of $2\mu\text{M NAD}^+$ had no significant effect on the experimentally observed specific equilibrium velocity. The absence of an effect was predicted by a kinetic model described in appendix 1. This model also predicts the effect of enzyme concentration on the apparent equilibrium constant of the reaction. These predictions are compared in table 6 with the experimental observations of Neilands (1952).

6.4.7 Isotope effects

Primary and secondary deuterium isotope effects on equilibrium constants for enzyme catalysed reactions have been extensively studied (see for example Cook et al, 1980) and rules have been formulated for predicting their magnitude. The equilibrium constant for lactate oxidation will be decreased by a factor of 0.83 if L-(3-²H)lactate is used (Cook et al, 1980). If L-(2-²H)lactate is used the equilibrium constant will be decreased by a factor of 1/1.19. The rules predicting the effect are multiplicative and therefore the equilibrium constant with L-(U-²H)lactate is expected to be decreased by a factor of $0.83/1.19=0.69$. This relatively large effect will be halved in the equilibration experiment since an equimolar mixture of L-(U-²H) and

Table 5

The effect of enzyme concentration on the specific equilibrium velocity of the enzyme

Experimental observations and theoretical calculations.

A-Experimental observations

Lactate dehydrogenase activity (units/ml)	V_{LDH} ($\mu\text{mols}/\text{min}/\text{unit}$)
50	0.0032
50	0.0032
17	0.0035

B-Theoretical calculations

Lactate dehydrogenase activity (units/ml)	True equilibrium constant	Apparent equilibrium constant	V_{LDH} ($\mu\text{mols}/\text{min}/\text{unit}$)
50	1.57×10^{-4}	2.25×10^{-4}	0.00069
20	"	1.83×10^{-4}	0.00064
10	"	1.69×10^{-4}	0.00075
1	"	1.58×10^{-4}	0.00077

Table 5

A- The in vitro system contained 100mM glycylglycine-imidazole buffer, pH 7.4, 0.5mM EDTA, 0.15M KCl and $2\mu\text{M NAD}^+$. Exchange experiments were performed with 10mM L-(3- ^2H)lactate and 10mM L-(2- ^2H)lactate. The enzyme was dialysed twice against 1000 vol. of the buffer used in the in vitro system. No exchange was observed in the absence of added NAD^+ .

B- The theoretical calculations were performed using "model 2" which is described in the appendix. The true equilibrium constant is calculated from the concentrations of the free substrates. The apparent equilibrium constant is that which would be measured if the system were assayed for the substrates. It includes the concentrations of both the free and enzyme bound forms of the substrates.

Table 6

The effect of enzyme concentration on the apparent equilibrium constant of the reaction.

A comparison of theoretical predictions and experimental observation.

Enzyme active site concentration (M)	Apparent equilibrium constant		Ratio of the apparent equilibrium constant to the true equilibrium constant	
	Predicted	Observed	Predicted	Observed
8.0×10^{-7}	0.640×10^{-4}	0.23×10^{-4}	1	1
2.0×10^{-6}	0.663×10^{-4}	0.23×10^{-4}	1	1
3.8×10^{-5}	1.59×10^{-4}	0.50×10^{-4}	2.5	2.2
7.6×10^{-5}	3.14×10^{-4}	1.4×10^{-4}	4.9	6.1
1.9×10^{-4}	14.9×10^{-4}	4.5×10^{-4}	23.2	19.6

The experimental observations are those of Nelands (1952). The added NAD^+ and lactate concentrations used in these studies were estimated to be 3.0×10^{-4} M and 6.0×10^{-2} M respectively. Nelands showed the dependence of the measured or apparent equilibrium constant of the reaction on the concentration of the bovine heart enzyme. The theoretical predictions were made using a model ("model 2"), which is described in the appendix, under conditions similar to those described by Nelands. The enzyme concentration was multiplied by 4 to give the active site concentration, lactate dehydrogenase is a tetrameric enzyme (Everse & Kaplan, 1973). The rate constants used in the model were calculated for a temperature of 25°C from the data of Borgmann et al (1974).

Table 7

A comparison of the two C-2 equilibration experiments.

Labelléd lactate species added at t=0	Enzyme activity (units/ml)	V _{LDH} (μmols/min/unit)
L-(U- ² H) and L-(U- ¹ H) lactate	10	0.007
" " " "	19	0.008
L-(2- ² H) and L-(3- ² H) lactate	10	0.010
" " " "	19	0.010

The determinations were performed in an in vitro system containing 100mM glycylglycine-imidazole buffer pH 7.4, 0.5mM EDTA and 0.15M KCl. The concentration of each lactate species was 10mM and the concentration of added NAD⁺ 10μM. The enzyme, which was obtained as an ammonium sulphate suspension, was dialysed against the buffer used in the in vitro system.

L-(U-¹H)lactate is employed. Under these circumstances the equilibrium constant for lactate oxidation is expected to be decreased by a factor of 0.85. With the mirror experiment, which employs an equimolar mixture of L-(2-²H) and L-(3-²H)lactate, the calculated perturbation in the equilibrium constant is a decrease by a factor of 0.83. These calculations suggest that there will be no time dependent changes in the equilibrium concentrations of the enzyme's substrates during exchange measurements. Such changes could distort the calculated equilibrium velocity. They also indicate that the equilibrium velocities observed in the two equilibration experiments should be approximately the same. That this is the case is shown by the results in table 7. However, as pointed out above, the absence of a time dependent change in the equilibrium velocity due to isotope effects is not critical in an in situ versus in vitro comparison of the properties of the enzyme.

6.5 The total extractable NAD(H) concentration in the erythrocyte

Previous estimations of the total extractable NAD⁺ plus NADH concentration in the human erythrocyte show a range of values (see Simpson (1981) and references cited therein). The estimated concentrations in the cell water range from 57μM (Hasart et al, 1972) to 201μM (Schulman et al, 1974). These concentrations were calculated by assuming that 0.72 of the erythrocyte volume is solvent water. Loder et al (1967) and Simpson (1981) obtained values in the range 60-100μM. Using the enzyme cycling method (see Experimental section) of Nisselbaum and Green (1969), which was the method used by Simpson (1981), a concentration of 80μM (estimated from two determinations) was obtained. The total extractable concentration was also estimated using the C-2 equilibration experiment by replacing the NAD⁺ normally added to the in vitro system with a sample taken from a boiled extract. The specific

equilibrium velocity of the enzyme was calculated and used, with the data shown in figure 5, to estimate the NAD(H) concentration in the extract. By accounting for the dilution that occurred in the preparation of the extract a total NAD(H) concentration in the cell water of 60 μ M was calculated. These results show good agreement with those of Simpson (1981) and Loder et al (1967) and are in considerable excess of the estimated free NAD(H) concentration. A large fraction of the coenzyme appears, therefore, to be bound in the cell. The location of these binding sites has been considered previously, for example by Marshall and Omachi (1974) and by Simpson (1981).

6.6 Conclusions

The use of the observed in situ lactate dehydrogenase activity as a probe of the free intracellular NAD(H) concentration has been examined by Simpson (1981) and Simpson et al (1982). For example it has been shown that by raising the intracellular NAD(H) concentration the equilibrium velocity for equilibration of isotope between the pyruvate and lactate methyls can be increased. Swelling the cells in hypotonic media resulted in a decrease of the observed equilibrium velocity. These experiments do not rule out the possibility that the enzyme is inhibited by an as yet unknown inhibitor in situ and that in fact the free NAD⁺ concentration is much greater than 10 μ M. Cellular heterogeneity could distort the calculated specific equilibrium velocity although lactate dehydrogenase activity and the concentrations of the pyridine nucleotides have been shown not to vary with cell age (Chapman & Schaumburg, 1967; Hjelm, 1968).

The C-2 equilibration reaction has been shown to be a relatively sensitive probe of the free NAD(H) concentration in the human

erythrocyte. This reaction could also be monitored in other tissues where it could be used in a similar manner to estimate the kinetically and metabolically relevant concentration of the free coenzyme.

Endogenous lactate production and exchanges with solvent isotope at the C-3 and C-2 positions were avoided in the studies described here. Their presence however need not be a serious barrier to application of the technique in other tissues since they can be measured independently of the equilibration reaction. If a model of the exchange system is employed which incorporates these independently measurable exchanges then the observed equilibration data can be fitted to the model in order to obtain an equilibration rate. The computer programs employing the Gear method which are described in chapter 3 and appendix 1 of this chapter would be suitable for such data fitting.

6.7 References

Borgmann, U., Moon, T.W. & Laidler, K.J. (1974) *Biochemistry* 13, 5152-5158

Brown, F.F., Campbell, I.D., Kuchel, P.W. & Rabenstein, D.C. (1977) *FEBS Lett.* 82, 12-16

Chapman, R.G. & Schaumberg, L. (1967) *Br. J. Haematol.* 13, 665-678

Cook, P.F., Blanchard, J.S. & Cleland, W.W. (1980) *Biochemistry* 19, 4853-4858

Dalziel, K. (1963) *J. Biol. Chem.* 238, 1538-1543

Everse, J. & Kaplan, N.O. (1973) *Adv. Enzymol.* 37, 61-133

Gloster, J.A. & Harris, P. (1962) *Clin. Chem. Acta* 7, 206-211

Hasart, E., Jacobasch, G. & Rapoport, S. (1972) *Acta. Biol. Med. Ger.* 28, 603-613

Hjelm, M. (1968) *Folia Haematol.* 89, 392-399

Loder, P.B., Babarczy, G. & de Gruchy, G.C. (1967) *Br. J. Haematol.* 13, 95-105

Marshall, W.E. & Omachi, A. (1974) *Biochim. Biophys. Acta.* 354, 1-10

Neilands, J.B. (1952) J. Biol. Chem. 199, 373-381

Nisselbaum, J.S. & Green, S. (1969) Anal. Biochem. 27, 212-217

Novoa, W.B., Schwert, G.W. & Millar, D.B.S. (1959) J. Biol. Chem. 234, 1143-1148

Schulman, M.P., Gupta, N.K., Omachi, A., Hoffman, G. & Marshall, W.E. (1974) Anal. Biochem. 60, 302-311

Schwert, G.W., Millar, B.R. & Peanasky, R.J. (1967) J. Biol. Chem. 242, 3245-3252

Simpson, R.J. (1981) D. Phil. Thesis, Oxford University

Simpson, R.J., Brindle, K.M., Brown, F.F., Campbell, I.D. & Foxall, D.L. (1981) Biochem. J. 193, 401-406

Simpson, R.J., Brindle, K.M., Brown, F.F., Campbell, I.D. & Foxall, D.L. (1982) Biochem. J. 202, 581-587

Whittam, R. (1958) J. Physiol. (London) 140, 479-497

Winer, A.D. & Schwert, G.W. (1958) J. Biol. Chem. 231, 1065-1083

6.8 Appendix

Kinetic models for predicting the velocity of C-2 equilibration.

Model 1

An analytical expression for the velocity of C-2 equilibration can be obtained using the method of Yagil and Hoberman (1969). This method was described in appendix 1 of chapter 2 where it was used to derive an expression relating the rate constants of the lactate dehydrogenase mechanism to the velocity of C-2 exchange. In the case of C-2 exchange there is exchange of label between the lactate C-2 position and the C-4 position of the nicotinamide ring of free NADH. In the case of C-2 equilibration there is exchange of label between the two starting lactate species via the C-4 position of the nicotinamide ring of NADH. The NADH need not dissociate from the enzyme for this exchange to take place. The expression was derived therefore for the exchange of label via the enzyme bound NADH, the concentration of this species will of course be determined by the free NADH concentration. Since free NADH is not an obligatory intermediate in the exchange the term $1/k_{-4}(R)$ is lost from the first bracket of the equation shown in appendix 1 chapter 2. The equation now describes the velocity for the exchange of label between lactate and bound NADH. The velocity of exchange between the two lactate species via the NADH will be half of this value and the experimentally observed velocity will be halved again because the two equimolar lactate species (at $t=0$) are competing for the same enzyme site.

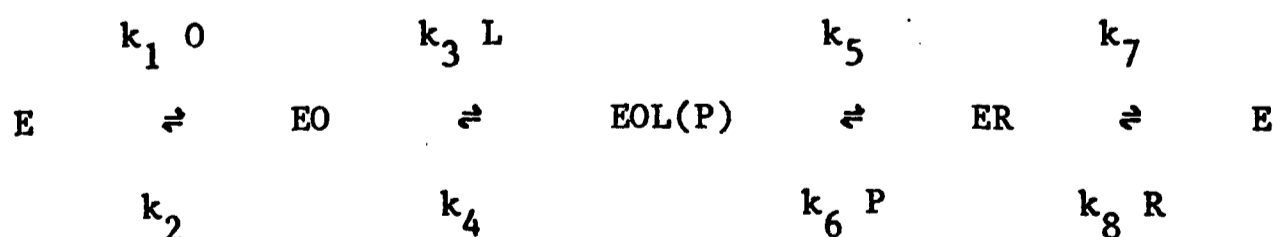
In the model described in chapter 2 an equilibrium constant of 2.79×10^{-4} (at pH 7.4) was used. This is a slightly arbitrary choice since the value obtained from the rate constants used in the model is

1.57×10^{-4} ($k_{+1} k_{+2} k_{+3} k_{+4}/k_{-1} k_{-2} k_{-3} k_{-4}$). It was felt that such a choice is justified in view of the range of values quoted in the literature. However in the model used in this chapter a value of 1.57×10^{-4} is used in order to make the predicted equilibrium velocities consistent with those predicted by "model 2" which is described in the second part of this appendix. The values predicted by this model are shown in figure 5 and table 3 in the main text. These values were however multiplied by a factor of two in order to give a better fit to the experimental data. The values for the rate constants were obtained from the data of Borgmann et al (1974).

Model 2

The equation derived in "model 1" is an approximation which assumes that the total enzyme concentration is much lower than that of the substrates. This equation cannot be used to predict the effect of enzyme concentration on the specific equilibrium velocity. In order to do this an explicit description of the exchange system must be formulated. The differential equations describing chemical and isotopic flux are shown below.

The equations were derived for the following description of the lactate dehydrogenase mechanism.



where E represents the free enzyme concentration, O the NAD^+ concentration, L the lactate concentration, P the pyruvate concentration and R the NADH concentration.

Differential equations describing chemical flux

$$\begin{aligned}dE/dt &= -k_1 E \cdot O - k_8 E \cdot R + k_2 EO + k_7 ER \\dEO/dt &= -k_2 EO - k_3 EO \cdot L + k_1 E \cdot O + k_4 EOL \\dEOL/dt &= -k_4 EOL - k_5 EOL + k_3 EO \cdot L + k_6 ER \cdot P \\dER/dt &= -k_7 ER - k_6 ER \cdot P + k_5 EOL + k_8 E \cdot R\end{aligned}$$

$$\begin{aligned}dO/dt &= -k_1 E \cdot O + k_2 EO \\dL/dt &= -k_3 EO \cdot L + k_4 EOL \\dP/dt &= -k_6 ER \cdot P + k_5 EOL \\dR/dt &= -k_8 E \cdot R + k_7 ER\end{aligned}$$

These equations were solved for different initial values of E, O and L using the Gear method described in chapter 3. A listing of the computer program used, LDHMOD, is shown on a following page. The K matrix contains the rate constants k_1 to k_8 . The Y matrix (Y(1) to Y(8)) contains the concentrations of the intermediates; E, EO, EOL, ER, O, L, P and R respectively.

The program can be used to calculate the rate of relaxation of the system to chemical equilibrium and the final equilibrium concentrations of the substrates and intermediates. For 10 units of enzyme, 20mM lactate and $10\mu\text{M NAD}^+$ the $t_{1/2}$ for relaxation to chemical equilibrium is 19 s, a rate which is orders of magnitude faster than the rate of relaxation to isotopic equilibrium. The final equilibrium concentrations of the free substrates predicted by this model at low enzyme concentration (i.e. 1 unit/ml of enzyme which is equivalent to $3.07 \times 10^{-8} \text{ M}$ active sites) are exactly the same as those predicted by model 1. The enzyme active site concentration/unit enzyme was calculated by assuming that V_{max} is equal to $1 \mu\text{mol/min/ml}$ (which is equivalent to $1.667 \times 10^{-5} \text{ M s}^{-1}$) and dividing this by k_2 . At higher enzyme concentrations there is a discrepancy between the true and

apparent equilibrium constants as shown in tables 5 and 6 in the main text. The true equilibrium constant was calculated using the equilibrium concentrations of the free substrates, at low enzyme concentrations these are equivalent to their total concentrations. The apparent equilibrium constant is that which would be measured if the equilibrium mixture were assayed for each substrate. It includes both the free and enzyme bound substrates.

The program outputs the equilibrium concentrations of all eight species to a file which is then read by program LDHMOD2 which calculates the equilibrium velocity for C-2 equilibration.

The differential equations describing isotopic flux

$$\begin{aligned}
 dX_{L(0,0)}/dt &= k_4 X_{EOL(0,0)} - k_3 X_{L(0,0)} \cdot EO \\
 dX_{L(*,*)}/dt &= k_4 X_{EOL(*,*)} - k_3 X_{L(*,*)} \cdot EO \\
 dX_{L(0,0)}/dt &= k_4 X_{EOL(*,0)} - k_3 X_{L(*,0)} \cdot EO \\
 dX_{L(0,*)}/dt &= k_4 X_{EOL(0,*)} - k_3 X_{L(0,*)} \cdot EO \\
 dX_R/dt &= k_7 X_{ER} - k_8 X_R \cdot E \\
 dX_{ER}/dt &= k_8 X_R \cdot E - k_7 X_{ER} - k_6 X_{ER} \cdot P \\
 &\quad + k_5 (X_{EOL(*,*)} + X_{EOL(*,0)}) \\
 dX_P/dt &= k_5 (X_{EOL(*,*)} + X_{EOL(0,*)}) - k_6 X_P \cdot ER \\
 dX_{EOL(0,0)}/dt &= k_3 X_{L(0,0)} \cdot EO - X_{EOL(0,0)} (k_4 + k_5) \\
 &\quad + k_6 (ER - X_{ER}) (P - X_P) \\
 dX_{EOL(*,*)}/dt &= k_3 X_{L(*,*)} \cdot EO - X_{EOL(*,*)} (k_4 + k_5) \\
 &\quad + k_6 X_{ER} X_P \\
 dX_{EOL(*,0)}/dt &= k_3 X_{L(*,0)} \cdot EO - X_{EOL(*,0)} (k_4 + k_5) \\
 &\quad + k_6 X_{ER} (P - X_P) \\
 dX_{EOL(0,*)}/dt &= k_3 X_{L(0,*)} \cdot EO - X_{EOL(0,*)} (k_4 + k_5) \\
 &\quad + k_6 X_P (ER - X_{ER})
 \end{aligned}$$

X represents in this case not fractional labelling of an intermediate

but instead its concentration. The K and C matrices in LDHMOD2 have the same numbering scheme as the K and Y matrices respectively in LDHMOD. The Y matrix (Y(1) to Y(11)) contains the concentrations of the labelled intermediates; L(0,0), L(*,*), L(*,0), L(0,*), R, ER, P, EOL(0,0), EOL(*,*), EOL(*,0) and EOL(0,*) respectively. The symbol * represents label, either ^1H or ^2H , the first argument in parentheses denotes the labelling at the C-2 position of the lactate molecule (free or bound) and the second argument the labelling at the C-3 position.

The program returns the time dependent changes in the concentrations of the labelled substrates plus the calculated specific equilibrium velocity of the enzyme.

References

Yagil, G. & Hoberman, H.D. (1969) *Biochemistry* 8, 352-360

Borgmann, U., Moon, T.W. & Laidler, K.J. (1974) *Biochemistry* 13, 5152-5158

```

PROGRAM LDHMOD
DOUBLE PRECISION Y(8),K(8),X,XEND,H,TOL,W(8,30),XEN
INTEGER I,IFAIL,IR,IW,J,MPED,N,NCUT,NIN,NPART,NLM,NU,JJ
EXTERNAL FCN,CUT,PEDERV
COMMON XEND,H,I,K,NLM
C.....INITIALISATION OF PROGRAM
DATA NCUT/6/
DATA NIN/5/
DATA NPART/4/
N=8
IW=30
IR=1
MPED=1
C.....ASSIGNMENT OF PARAMETERS
DATA K/1.08E6,5.43E2,4.71E5,2.91E3,8.58E2,4.34E6,1.33E2,5.41E7/
DATA Y(2),Y(3),Y(4)/0.0,0.0,0.0/
READ (NIN,*) Y(1),Y(5),Y(6),Y(7),Y(8),NLM,XEND,J,
+ NL,XEN,JJ
TOL=10.**(-J)
WRITE(NCUT,100) TOL
X=0.0
H=(XEND-X)/NUM
I=NUM-1
IFAIL=1
CALL DISPLAY(Y)
CALL DD2EBF(X,XEND,N,Y,TOL,IR,FCN,MPED,PEDERV,
+ CUT,W,IW,IFAIL)
WRITE(NCUT,200) IFAIL
WRITE(NPART,300) NL,XEN,JJ
STOP
100 FORMAT(22H0CALCULATION WITH TOL=,E8.1)
200 FORMAT(3H IFAIL=,I1)

300 FORMAT(1X,I4,F12.1,I4)
END
C.....SUBROUTINES
SUBROUTINE FCN(T,Y,F)
INTEGER I,J,NUM
DOUBLE PRECISION H,XEND,K(8),F(8),Y(8),T
COMMON XEND,H,I,K,NLM
F(1)=K(2)*Y(2)+K(7)*Y(4)-Y(1)*(K(1)+Y(5)+K(8)+Y(8))
F(2)=K(1)*Y(1)+Y(5)+K(4)+Y(3)-Y(2)*(K(2)+K(3)+Y(6))
F(3)=K(3)*Y(2)+Y(6)+K(6)*Y(4)-Y(7)-Y(3)*(K(4)+K(5))
F(4)=K(5)*Y(7)+K(8)*Y(1)+Y(8)-Y(4)*(K(7)+K(6)+Y(7))
F(5)=K(2)*Y(2)-K(1)*Y(1)+Y(5)
F(6)=K(4)*Y(3)-K(3)*Y(2)+Y(6)
F(7)=K(5)*Y(3)-K(6)*Y(4)+Y(7)
F(8)=K(7)*Y(4)-K(8)*Y(1)+Y(8)
RETURN
END
C.....
SUBROUTINE PEDERV(T,Y,PW)
DOUBLE PRECISION XEND,H,K(8),Y(8),PW(8,8),T
INTEGER I,NUM
COMMON XEND,H,I,K,NLM
PW(1,1)=-K(1)*Y(5)-K(8)*Y(8)
PW(1,2)=K(2)
PW(1,4)=K(7)
PW(1,5)=-K(1)*Y(1)
PW(1,8)=-K(8)*Y(1)
PW(2,1)=K(1)*Y(5)
PW(2,2)=-K(2)-K(3)+Y(6)
PW(2,3)=K(4)
PW(2,5)=K(1)+Y(1)
PW(2,6)=-K(3)+Y(2)
PW(3,2)=K(3)+Y(6)
PW(3,3)=-K(4)-K(5)
PW(3,4)=K(6)+Y(7)
PW(3,6)=K(3)+Y(2)
PW(3,7)=K(6)+Y(4)
PW(4,1)=K(8)+Y(8)
PW(4,3)=K(5)
PW(4,4)=-K(7)-K(6)+Y(7)
PW(4,7)=-Y(4)+K(6)
PW(4,8)=K(8)+Y(1)
PW(5,1)=-K(1)*Y(5)
PW(5,2)=K(2)
PW(5,5)=-K(1)+Y(1)
PW(6,2)=-K(3)+Y(6)
PW(6,3)=K(4)
PW(6,6)=-K(3)+Y(2)
PW(7,3)=K(5)
PW(7,4)=-K(6)+Y(7)
PW(7,7)=-K(6)+Y(4)
PW(8,1)=-K(8)+Y(8)
PW(8,4)=K(7)
PW(8,6)=-K(8)+Y(1)
RETURN
END
C.....
SUBROUTINE CUT(X,Y)
DOUBLE PRECISION XEND,H,X,K(8),Y(8)
INTEGER I,J,NUM,NPART
COMMON XEND,H,I,K,NLM

```

```

REAL RES(60,9)
DATA NPART/4/
DO 1000 J=1,8
RES(NUM-I,J)=Y(J)
1000 CONTINUE
RES(NUM-I,9)=X
IF(I.EQ.0) CALL RESULTS(NUM,RES)
IF(I.EQ.0) WRITE(NPART,2000) (RES(NUM,J), J=1,8)
X=XEND-FLOAT(I)*H
I=I-1
2000 FORMAT(1X,8E12.4)
RETURN
END
.....
SUBROUTINE DISPLAY(Y)
DOUBLE PRECISION XEND,H,K(8),Y(8)
INTEGER I,NUM,NCUT
COMMON XEND,H,I,K,NUM
DATA NCUT/6/
WRITE(NCUT,100)
WRITE(NCUT,200)
WRITE(NCUT,300) Y(6),Y(7),Y(5),Y(8)
WRITE(NCUT,400)
WRITE(NCUT,500) Y(1)
RETURN
100 FORMAT(1X,' INITIAL SUBSTRATE CONCENTRATIONS')
200 FORMAT('0',' LACTATE PYRUVATE NAD
NADH')
300 FORMAT(1X,4E12.4)
400 FORMAT('0',' ENZYME CONCENTRATION')
500 FORMAT(1X,8E12.4)
END
.....
SUBROUTINE RESULTS(NUM,RES)
INTEGER J,NCUT,NUM
REAL RES(60,9)
DATA NCUT/6/
WRITE(NCUT,1000)
WRITE(NCUT,2000)
DO 100 J=1,NUM
WRITE(NCUT,3000) RES(J,9),RES(J,6),RES(J,7),RES(J,5),RES(J,8)
100 CONTINUE
WRITE(NCUT,4000)
DO 200 J=1,NUM
WRITE(NCUT,5000) RES(J,9),RES(J,1),RES(J,2),RES(J,3),RES(J,4)
200 CONTINUE
WRITE(NCUT,7000) ((RES(NUM,7)+RES(NUM,8))/(RES(NUM,6)+RES(NUM,5)))
WRITE(NCUT,8000) (((RES(NUM,7)+RES(NUM,3))*(RES(NUM,8)+RES(NUM,4))))
+ /(((RES(NUM,6)+RES(NUM,3))*(RES(NUM,5)+RES(NUM,2))))
RETURN
1000 FORMAT('0',' CONCENTRATIONS OF SUBSTRATES AND ENZYME SPECIES')
2000 FORMAT('0',' TIME LACTATE PYRUVATE NAD
NADH')
3000 FORMAT(1X,F7.2,4E12.4)
4000 FORMAT('0',' TIME E EO EOL
ER')
5000 FORMAT(1X,F7.2,4E10.4)
7000 FORMAT(29HC TRUE EQUILIBRIUM CONSTANT=, E12.4)
8000 FORMAT(33HC APPARENT EQUILIPRIUM CONSTANT=, E12.4)
END

```

```

PROGRAM LDHMOD2
DOUBLE PRECISION Y(11),K(8),X,XEND,H,TOL,C(8),W(11,30)
INTEGER I,IFAIL,IR,IW,J,MPED,N,NCUT,NIN,NUM
EXTERNAL FCN,OUT,PEDERV
COMMON XEND,H,I,K,NLM,C
C.....INITIALISATION OF PROGRAM
DATA NCUT/6/
DATA NIN/5/
N=11
IW=30
IR=1
MPED=1
C.....ASSIGNMENT OF PARAMETERS
DATA K/1.08E6,5.43E2,4.71E5,2.91E3,8.58E2,4.34E6,1.33E2,5.41E7/
READ(NIN,*) C,NUM,XEND,J
XEND=XEND*6C
DATA Y(3),Y(4),Y(5),Y(6),Y(7),Y(8),Y(9),Y(10),Y(11)/
+ 0.0,0.0,0.0,0.0,0.0,0.0,0.0,0.0,0.0/
Y(1)=C(6)/2.0
Y(2)=Y(1)
TOL=10.**(-J)
WRITE(NCUT,100) TOL
X=C.0
H=(XEND-X)/NUM
I=NUM-1
IFAIL=1
CALL DISPLAY(Y)
CALL DD2E3F(X,XEND,N,Y,TOL,IP,FCN,MPED,PEDERV,
+ OUT,IW,IFAIL)
WRITE(NCUT,200) IFAIL
STOP
100 FORMAT(22H0CALCULATION WITH TOL=,E8.1)

200 FORMAT(8H IFAIL=,I1)
END
C.....SUBROUTINES
SUBROUTINE FCN(T,Y,F)
DOUBLE PRECISION H,XEND,K(8),F(11),Y(11),T,C(8)
INTEGER I,J,NUM
COMMON XEND,H,I,K,NLM,C
F(1)=K(4)*Y(8)-K(3)*Y(1)*C(2)
F(2)=K(4)*Y(9)-K(3)*Y(2)*C(2)
F(3)=K(4)*Y(10)-K(3)*Y(3)*C(2)
F(4)=K(4)*Y(11)-K(3)*Y(4)*C(2)
F(5)=K(7)*Y(6)-K(8)*C(1)*Y(5)
F(6)=K(8)*C(1)*Y(5)-K(7)*Y(6)+K(5)*(Y(9)+Y(10))
+ -K(6)*C(7)*Y(6)
F(7)=K(5)*(Y(9)+Y(11))-K(6)*C(4)*Y(7)
F(8)=K(3)*C(2)*Y(1)-Y(8)*(K(4)+K(5))
+ +K(6)*(C(4)-Y(8))*(C(7)-Y(7))
F(9)=K(3)*C(2)*Y(2)-Y(9)*(K(4)+K(5))
+ +K(6)*Y(6)*Y(7)
F(10)=K(3)*C(2)*Y(3)-Y(10)*(K(4)+K(5))
+ +K(6)*Y(6)*(C(7)-Y(7))
F(11)=K(3)*C(2)*Y(4)-Y(11)*(K(4)+K(5))
+ +K(6)*Y(7)*(C(4)-Y(6))
RETURN
END
C.....
SUBROUTINE PEDERV(T,Y,PW)
DOUBLE PRECISION XEND,H,K(8),C(8)
DOUBLE PRECISION T,Y(11),PW(11,11)
INTEGER I,NLM,J,L
COMMON XEND,H,I,K,NLM,C
DO 100 J=1,11
DO 200 L=1,11
PW(J,L)=0.0
200 CONTINUE
100 CONTINUE
PW(1,1)=-K(3)*C(2)
PW(1,8)=K(4)
PW(2,2)=-K(3)*C(2)
PW(2,9)=K(4)
PW(3,3)=-K(3)*C(2)
PW(3,10)=K(4)
PW(4,4)=-K(3)*C(2)
PW(4,11)=K(4)
PW(5,5)=-K(8)*C(1)
PW(5,6)=K(7)
PW(6,5)=K(8)*C(1)
PW(6,6)=-K(7)-K(6)*C(7)
PW(6,9)=K(5)
PW(6,10)=K(5)
PW(7,7)=-K(5)*C(4)
PW(7,9)=K(5)
PW(7,11)=K(5)
PW(8,1)=K(7)*C(2)
PW(8,6)=-K(6)*C(7)+K(5)*Y(7)
PW(8,7)=-K(6)*C(4)+K(6)*Y(6)
PW(8,8)=-K(4)-K(5)
PW(9,2)=K(3)*C(2)
PW(9,5)=K(6)+Y(7)
PW(9,7)=K(6)+Y(6)
PW(9,9)=-K(4)-K(5)

```

```

Pw(10,3)=K(3)*C(2)
Pw(10,6)=K(6)*C(7)-K(6)*Y(7)
Pw(10,7)=-K(6)*Y(6)
Pw(10,10)=-K(4)-K(5)
Pw(11,4)=K(3)*C(2)
Pw(11,6)=-K(6)*Y(7)
Pw(11,7)=K(6)*C(4)-K(6)*Y(6)
Pw(11,11)=-K(4)-K(5)
RETURN
END

```

```

C.....
SUBROUTINE CUT(X,Y)
DOUBLE PRECISION XEND,H,X,K(8),Y(11),C(8)
INTEGER I,J,NUM
COMMON XEND,H,I,K,NUM,C
REAL RES(60,13)
DO 1000 J=1,11
RES(NUM-I,J)=Y(J)
1000 CONTINUE
RES(NUM-I,12)=X/60
RES(NUM-I,13)=DLOG(Y(1)-Y(3))
IF(I.EQ.0) CALL RESULTS(NUM,RES,C)
X=XEND-FLOAT(I)*H
I=I-1
RETURN
END

```

```

C.....
SUBROUTINE DISPLAY(Y)
DOUBLE PRECISION XEND,H,K(8),Y(11),C(8)
INTEGER I,J,NUM,NCLT
COMMON XEND,H,I,K,NUM,C
DATA NCLT/6/
WRITE(NCUT,100)
WRITE(NCUT,200)
WRITE(NCUT,300) C(6),C(7),C(5),C(8)
WRITE(NCUT,400)
WRITE(NCUT,500)
WRITE(NCUT,300) (C(J),J=1,4)
RETURN
100 FORMAT(1X,' SUBSTRATE CONCENTRATIONS')
200 FORMAT('0',' LACTATE PYFUVATE NAD NADH')
300 FORMAT(1X,4E12.4)
400 FORMAT('0',' CONCENTRATIONS OF ENZYME SPECIES')
500 FORMAT('0',' E EO ECL
ER')
END

```

```

C.....
SUBROUTINE RESULTS(NUM,RES,C)
INTEGER J,NCUT,NUM
DOUBLE PRECISION C(8)
REAL RES(60,13),VLDH
DATA NCUT/6/
IF(NUM.GT.30) GOTO 350
WRITE(NCUT,1000)
WRITE(NCUT,2000)
DO 100 J=1,NUM
WRITE(NCUT,3000) RES(J,12),RES(J,1),RES(J,13)
100 CONTINUE
WRITE(NCUT,4000)
DO 200 J=1,NUM
WRITE(NCUT,5000) RES(J,12),RES(J,1),RES(J,2),RES(J,3),RES(J,4)

200 CONTINUE
WRITE(NCUT,6000)
DO 300 J=1,NUM
WRITE(NCUT,7000) RES(J,12),RES(J,5),RES(J,7)
300 CONTINUE
350 DO 400 J=1,NUM
IF(RES(J,13).LT.DLOG(C(6)/4.0)) GOTO 500
400 CONTINUE
500 VLDH=((RES(J-1,13)-RES(J+1,13))/(RES(J+1,12)-RES(J-1,12)))
+ *250.0*C(6)/((C(1)+C(2)+C(3)+C(4))/3.07E-8)
WRITE(NCUT,8000)
WRITE(NCUT,9999)
WRITE(NCUT,9000) VLDH
RETURN
1000 FORMAT('0',' CONCENTRATIONS OF LABELLED
+ SPECIES')
2000 FORMAT('0',' TIME LACTATE(0,0) LOG X LACTATE(0,0)')
3000 FORMAT(1X,F7.2,E12.4,5X,F10.4)
4000 FORMAT('0',' TIME LAC(0,0) LAC(*,+) LAC(*,0)
+ LAC(0,+)' )
5000 FORMAT(1X,F7.2,4E12.4)
6000 FORMAT('0',' TIME NADH PYRUVATE')
7000 FORMAT(1X,F7.2,3E12.4)
8000 FORMAT('0',' SPECIFIC EQUILIBRIUM VELOCITY')
9000 FORMAT('+',F12.6)
9999 FORMAT('0',' UMOLS/MIN/UNIT')
END

```

7 Some general comments on the application of ^1H n.m.r.

to the study of isotope exchange

and the kinetic properties expressed by enzymes in intact cells

Fractional labelling - the effect of chemical flux

During measurement of C-2 exchange a unique point is observed, the null point, which represents the point at which 50% of the lactate present is labelled at the C-2 position. At a single point in time the fractional labelling is known. With C-2 equilibration, and with C-2 exchange at any other point during the exchange time course, the fractional labelling can only be calculated retrospectively when the amplitude of the exchange is known. This can be complicated if there is endogenous lactate production. In the case of C-2 equilibration lactate production will necessitate fitting of the equilibration data to a kinetic model of the exchange system. With C-2 exchange, where there are two points at which the fractional labelling is known i.e. at $t=0$ and t_{null} , this is unnecessary in order to obtain an exchange velocity. The C-2 exchange experiment has therefore a significant advantage over the C-2 equilibration experiment when allowing for the effect of chemical flux. However a problem with this experiment is that in order to observe this point the exchange system may require prolonged incubation. During this time changes in metabolite concentrations may occur which affect the apparent equilibrium velocity. This problem could be avoided if an exchange were monitored which gave continuously the fractional labelling of the observed metabolite. Such an exchange is illustrated in figure 1.

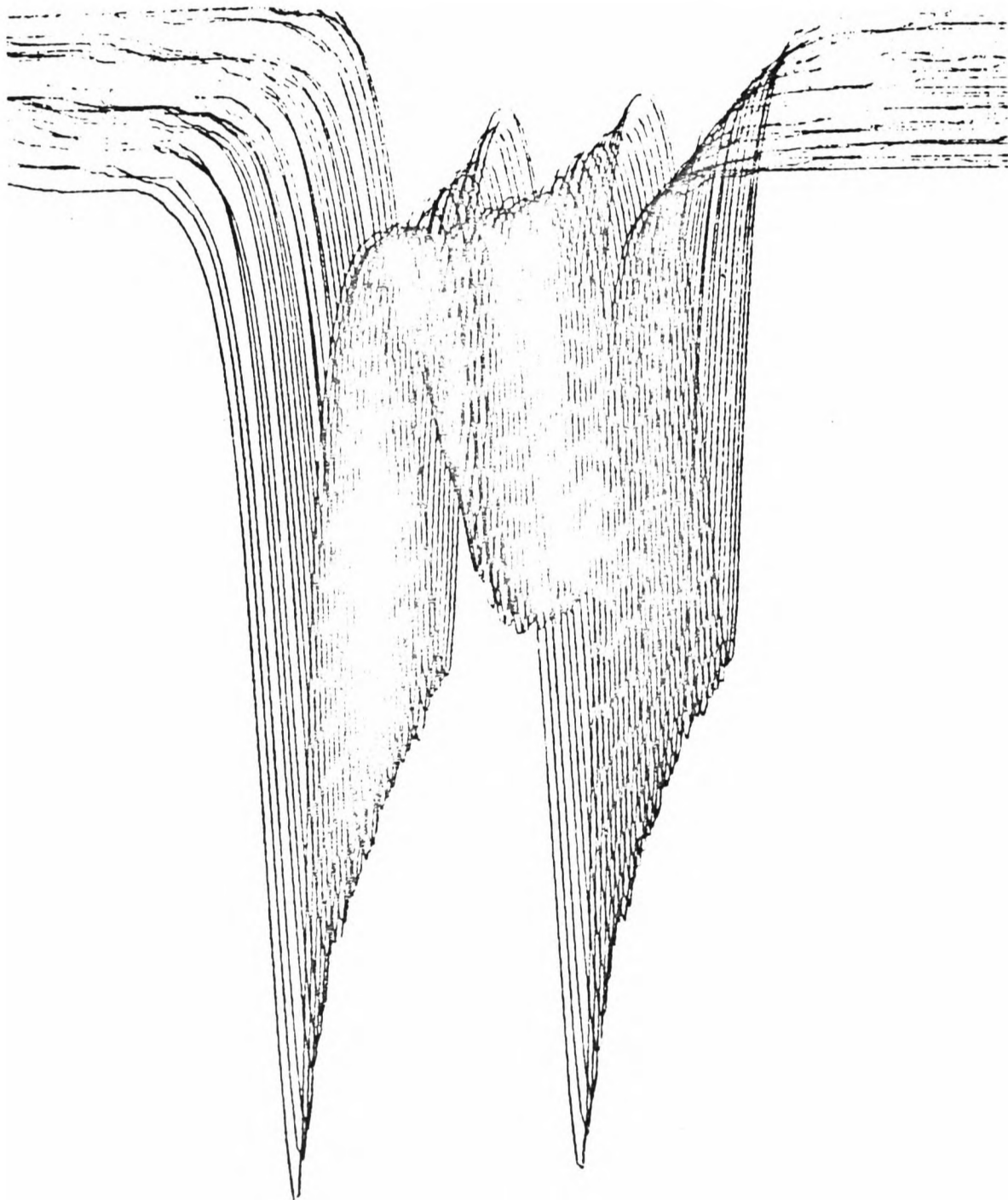
The exchange shown in figure 1 is that of ^{13}C between the methyl groups of alanine and pyruvate catalysed by the enzyme alanine

Figure 1

Equilibration of a ^{13}C label between the methyl groups of alanine and pyruvate catalysed by the enzyme alanine aminotransferase.

The figure shows a stacked plot of the alanine methyl resonance in successive spin echo p.m.r. spectra ($\tau=68\text{ms}$). Spectra were accumulated at 2 min intervals. The water resonance was suppressed by applying a saturating pulse at the water resonance frequency between successive repetitions of the $90^\circ-\tau-180^\circ-\tau$ pulse sequence.

The in vitro system initially contained 10mM DL-(3- ^{13}C)alanine and 10mM pyruvate in a buffer solution composed of 100mM Tris-HCl, pH 7.4 (in H_2O) 0.5mM EDTA and 3mM dithiothreitol. There were approximately 0.2 units of enzyme present.



aminotransferase. This exchange has been studied previously using a ^{14}C label (Saier & Jenkins, 1967). The figure shows a stacked plot of successive spin echo p.m.r. spectra of the alanine methyl resonance obtained during an exchange time course. An equimolar mixture of DL-(3- ^{13}C)alanine and (3- ^{12}C)pyruvate was added to a solution containing the isolated enzyme. The alanine methyl resonance (a homonuclear coupled doublet) is initially split by the ^{13}C label to give a doublet (of doublets) with a coupling constant of 130Hz. Flux of ^{12}C into, and ^{13}C out of, the alanine methyl in the reaction catalysed by the enzyme results in the growth of a central unsplit alanine methyl resonance. The ratio of the central peak height to that of the two satellites gives the fractional labelling of the alanine. It will be noted that at equilibrium the peak heights of the centre peak and satellites are equal. This was because DL-alanine was used and the enzyme is stereospecific for the L form. If the L form were used then at equilibrium the peak height of the centre peak would be double that of the satellites. A reciprocal peak splitting is observed in the pyruvate methyl peak.

An exchange experiment therefore which employs a ^{13}C label and which is observed by its effect on the ^1H n.m.r. spectrum enables the fractional labelling of the metabolite to be monitored continuously. This type of exchange experiment should be a valuable complement to those already described.

To summarise the studies described here. Isotope exchange at the C-2 position of lactate has been monitored using a spin echo p.m.r. technique that permits continuous and non-invasive assessment of the rate and extent of the exchange. The enzyme catalysed exchange has been

used to compare the properties expressed by the enzymes lactate dehydrogenase (LDH) and glyceraldehydophosphate dehydrogenase (GAPDH) in vitro and in situ in the human erythrocyte. These studies showed that, in the case of GAPDH, the enzyme is unlikely to be bound to the erythrocyte membrane in situ and that the reaction it catalyses is not rate limiting for glycolytic flux. In the case of LDH it was shown that the activity it expresses in situ is consistent with a free intracellular NAD(H) concentration of about 10 μ M.

The technique offers significant advantages over conventional radioactive labelling techniques since it avoids the requirement for repeated sampling extraction and separation of labelled compounds. Although lacking the sensitivity of tracer methods it has been shown that with a coupled exchange system isotope exchange can be measured in metabolites present in micromolar amounts. In the case of GAPDH between the metabolites NADH and GAP. To study the exchange catalysed by this enzyme in the erythrocyte directly would be difficult if not impossible to do. Direct assays of NADH in the erythrocyte yield widely varying values (see previous chapter). Furthermore some of these studies suggest that a considerable fraction of the NADH is bound. A tracer labelling study would involve extraction, separation and determination of the counts in both NADH and GAP. The lability of these compounds and their low concentration will ensure considerable error in these measurements. The C-2 equilibration experiment would be impossible to perform using conventional radiolabel techniques although it could be performed using mass spectroscopy. Here again though the technique requires discrete sampling and extraction of the labelled lactate.

In an investigation of the control of metabolism the aim must be

to relate the observed in vitro properties of the enzymes involved in a particular metabolic pathway to the fluxes and metabolite levels observed within it. Simple extrapolation of the observed in vitro steady state kinetic properties of an enzyme to the properties it expresses in situ can be misleading, as was shown for GAPDH. Furthermore such an extrapolation presupposes that the intracellular environment is accurately defined. The occurrence of protein-protein interactions and metabolite binding could modify this environment. Metabolite binding in situ can result in a significant discrepancy between the total extractable concentration of a metabolite and the kinetically and metabolically relevant free form. The observation of apparently non-equilibrium levels of FDP in the human erythrocyte was taken to indicate that the reaction catalysed by aldolase is not at equilibrium in this tissue (Saito & Minikami, 1967). Isotope exchange studies however, which give an indication of the actual in situ activity of an enzyme, showed that this was not the case (Rose & Warms, 1970). It has been shown that the n.m.r. technique can be used to obtain precise measurements of isotope exchange. These allow the investigation of the in situ kinetic properties of an enzyme and permit a comparison of the of the properties displayed by the enzyme in situ and in vitro.

The human erythrocyte is an extensively studied and well characterised system which has proved to be a convenient "test bed" for the techniques described. It is hoped that in the future these techniques can be applied to other tissues.

7.1 References

Rose, I.A. & Warms, J.V.B. (1970) J. Biol. Chem. 245, 4009-4015

Saier, M.H. & Jenkins, W.T. (1967) J. Biol. Chem. 242, 91-100

Saito, T. & Minikami, S. (1967) J. Biochem. (Tokyo) 61, 211-219